66–10,368

OUBRE, Carroll Lee, 1933–

THE TOTAL HEMISPHERICAL THERMAL EMITTANCE OF (100), (110), AND (111) SINGLE CRYSTALS OF NICKEL AS A FUNCTION OF OXIDE THICKNESS TEMPERATURE RANGE 300–900°C.

Rice University, Ph.D., 1966
Engineering, chemical

University Microfilms, Inc., Ann Arbor, Michigan

RICE UNIVERSITY

THE TOTAL HEMISPHERICAL THERMAL EMITTANCE OF (100), (110), AND (111) SINGLE CRYSTALS OF NICKEL AS A FUNCTION OF OXIDE THICKNESS TEMPERATURE RANGE 300-900°C

BY

CARROLL L. OUBRE

A THESIS SUBMITTED
IN PARTIAL FULFILLMENT OF THE
REQUIREMENTS FOR THE DEGREE OF

DOCTOR OF PHILOSOPHY
IN
CHEMICAL ENGINEERING

Thesis Director's signature:

Houston, Texas

September 1965

ACKNOWLEDGMENTS

The author would like to express his gratitude to the following persons and organizations:

Dr. W. W. Akers for his advice and assistance as director of the thesis committee,

Dr. Jack L. Shelton for his tremendous help while learning the experimental procedures and also for use of much of the equipment he built to determine emittances,

Mr. Robert Herring and Mr. Bill Loesch for their help with metallurgical techniques and equipment,

Mr. John Rusk for preparing many of the single crystal samples,

The National Aeronautics and Space Administration for financial support,

My wife, Margaret, for her encouragement and patience.

TABLE OF CONTENTS

TABLE OF CONTENTS (Continued)

TABLE OF CONTENTS (Continued)

TABLE OF CONTENTS (Continued)

NOMENCLATURE

A	constant in Arrhenius's equation
a	area
c	velocity of light
C.C.	Chromium Corporation
D	diameter
Δ E	voltage drop
H	heat capacity
Δ H	change in distance measured by cathetometer
I	current
J	mechanical equivalence of heat
k	reaction rate constant
k	thermal conductivity
N	microbalance reading with calibrated weight
Δ N	change in microbalance reading
p	surface area per unit length
P/A	power per unit area
poly	polycrystalline
Q	activation energy (kcal/mole)
q_{BB}	black body radiation
$q_{conduction}$	heat transfer by conduction
$q_{convection}$	heat transfer by convection
$q_{radiation}$	heat transfer by radiation
R	gas constant
R	resistance

R_{30}	resistance at $30^{o}C$
R_{RT}	resistance at room temperature
R.C.I.	Research Crystal Inc.
S.E.	Semi-elements
t	time
T	absolute temperature
T_b	temperature within blackbody chamber
T_o	room temperature
V	volts
W	radiant energy emission
x	distance
α	absorptivity
α	resistance adjustment factor
ϵ	emittance
ϵ_o	bare metal emittance for baseline case
ϵ_B	bare metal emittance
ϵ_{ox}	oxidized metal emittance
$\epsilon_{n,\lambda}$	spectral normal emittance
λ	wave length
γ	frequency
Ω	ohms
μ	microns
μg	micrograms
θ	oxidation time
ρ	resistivity

τ	period of electromagnetic radiation
σ	electrical conductivity
σ	Stefan Boltzmann's constant

LIST OF FIGURES

LIST OF FIGURES (Continued)

LIST OF FIGURES (Continued)

LIST OF TABLES

LIST OF TABLES (Continued)

TABLE O

LIST OF SAMPLES

Sample	Type Crystal	Manufacturer	Length of Sample	Width of Sample	Sample Thickness (mils)	Sample (mils) / Heat Sink (mils)
SE#1	(110)	Semi-elements	3" long	.166"	10.4	3.5
SE#2	(110)	"	single	"	7.5	2.5
SE#3	(110)	"	crystal	.162"	9.6	3.2
SE#4	(110)	"	with	.166"	10.8	3.6
SE#5	(100)	"	$1\frac{1}{2}$" long	.169"	9.5	3.2
SE#6	(100)	"	polycrys-	"	7.5	2.5
SE#7	(100)	"	talline	.168"	7.5	2.5
SE#8	(100)	"	heat	.163"	9.75	3.25
SE#9	(111)	"	sinks	.166"	9.0	3.0
SE#10	(111)	"	↓	.174"	6.0	3.0
SE#11	(111)	"		.168"	6.4	2.1
SE#12	(111)	"		.169"	9.5	3.2
OSC#1	(100)	Research Crystal Inc.	same	.194"	7.3	1.5
OSC#2	(110)	"	as	.162"	6.0	1.2
OSC#3	(100)	"	above	.204"	11.8	3.9
OSC#4	(100)	"	↓	.167"	5.4	2.7
OSC#5	(110)	"		.147"	9.6	3.2
OSC#6	(100)	"		.208"	9.6	3.2
OSC#7	(100)	"		.1675"	4.0	4.0
OSC#8	(110)	"		.132"	10.0	3.3
OSC#9	(110)	"		.136"	12.1	2.4

TABLE O
(Continued)

Sample	Type Crystal	Manufacturer	Length of Sample	Width of Sample	Sample Thickness (mils)	Sample (mils) / Heat Sink (mils)
O#1	Polycrystalline	Chromium Corp.	3"	.170"	.45	no heat sinks
O#2	"	"	"	"	"	"
O#3	"	"	"	"	"	"
O#4	"	"	"	"	"	"
O#5	"	"	"	"	"	"
O#16	"	"	6" and 3"	"	"	"
O#21	"	"	"	"	"	"
O#23	"	"	"	"	"	"
O#8-(2-3)c.c.	"	"	6"	"	2.5	"
O-#15-10W1x5	"	Wilkinson	3" sample $1\frac{1}{2}$" heat sinks	"	10	2.0
O-#16-10W2x1	"	"	"	"	10	5.0

ABSTRACT

The total hemispherical emittance of nickel was determined as a function of oxide thickness in the temperature range of 300-900°C. Both polycrystalline nickel and the three principal crystal faces--(100), (110) and (111)--were investigated. Some of the nickel single crystals specimens were prepared with the dimensions of 3" long x 1/6" wide x 5-10 mils thick.

The temperature range for the bare metal emittance of polycrystalline nickel was also extended to 1250°C. A number of observations were also made in the vicinity of the Curie temperature of nickel.

Kinetic data for the oxidation of nickel as a function of temperature was also obtained during the emittance studies. The oxide thickness varied from 3.25 $\mu g/cm^2$ to 120.8 $\mu g/cm^2$. Activation energies were calculated for the three principal faces of nickel.

Colored microphotographs were taken during the various stages of oxidation of the nickel single crystals. The magnification was 50x and 1000x.

SUMMARY OF RESULTS

1. Emittance

No significant difference was noted in the "emittance vs. T curve" for oxidized polycrystalline nickel vs. the (110) and (100) crystal faces of nickel. The (111) crystal face had a slightly higher (ca. 10%) emittance for the same weight of oxide. Microphotographs showed that the (111) oxidized single crystal had a more uniform distribution of oxide nuclei, which would tend to a higher emittance.

A slight minimum was noted in all "emittance vs. T curves" for nickel in the vicinity of the Curie temperature (359°C). This was observed for both the bare metal and oxidized samples and for polycrystalline and single crystals.

The "oxide weight vs. emittance curves" showed an increase in emittance with oxide thickness for all samples. The emittance increased more rapidly at first when the surface was first being covered. As the surface became completely covered with green NiO, the increase in emittance lessened.

2. Nickel Single Crystal Preparation

Nickel single crystals were prepared in the shape of a thin slab 6" x 1/6" x 10 mils thick. These were prepared from a single crystal rod $\frac{1}{2}$" diameter by 6" long. The preparation consisted of spark cutting, mechanical thinning, mechanical grinding and polishing, and chemical polishing. Good back reflection Laue x-ray pictures were obtained for the samples.

3. Oxidation Rate Studies

A difference in oxidation rates was noted for the three crystal faces. The oxidation rate data was split into three regions which gave straight lines when plotting the log of the reaction rate constant vs. 1/T. The three regions were designated "the nuclei-formation region," "the intermediate oxide region," and "the thick oxide region." The (110) face oxidized at the fastest rate and the (100) face at the lowest rate for all three regions.

The activation energy (based on very little data) was initially high, then decreased, and finally increased as the surface became fully covered with a thick oxide.

4. Microphotographs

Colored microphotographs showed the presence of a thin uniform oxide film, nuclei of oxide, and groups of nuclei (polyhedra) all on the same sample. The nuclei distribution was more even on the (111) face.

I. INTRODUCTION

The work described in this thesis follows up earlier work conducted by J. Shelton (30). Previous studies included the investigation of thermal emittances of polycrystalline nickel as affected by oxide thickness. Since polycrystalline nickel contains a random orientation of crystal faces along with grain boundaries, an analysis of oxidation based on polycrystalline material is difficult. Because the different crystal faces oxidize at a different rate, the crystal sample contains an array of different thicknesses of oxide upon oxidation, as shown in the photograph 24-P in Appendix G.

Because of these difficulties with the polycrystalline material, the emittance and oxidation studies were extended to include the three principal single crystal faces of nickel--(100), (110) and (111)--shown in Figure I-1. It was necessary to prepare most of our own samples, since it was very difficult to find the thin polished single crystals needed. During the emittance studies, an attempt was also made to correlate kinetic data obtained during oxidation of the single crystals.

Emittance studies were initiated because of the increasing need for thermal emission data for application to high temperature heat transfer problems in industrial processes and in space science. The experimental approach was decided upon, because of the inadequacy of the theory for predicting thermal properties. Many of the previous experimental studies have also proved useless because of the uncertainty of the surface preparation or condition.

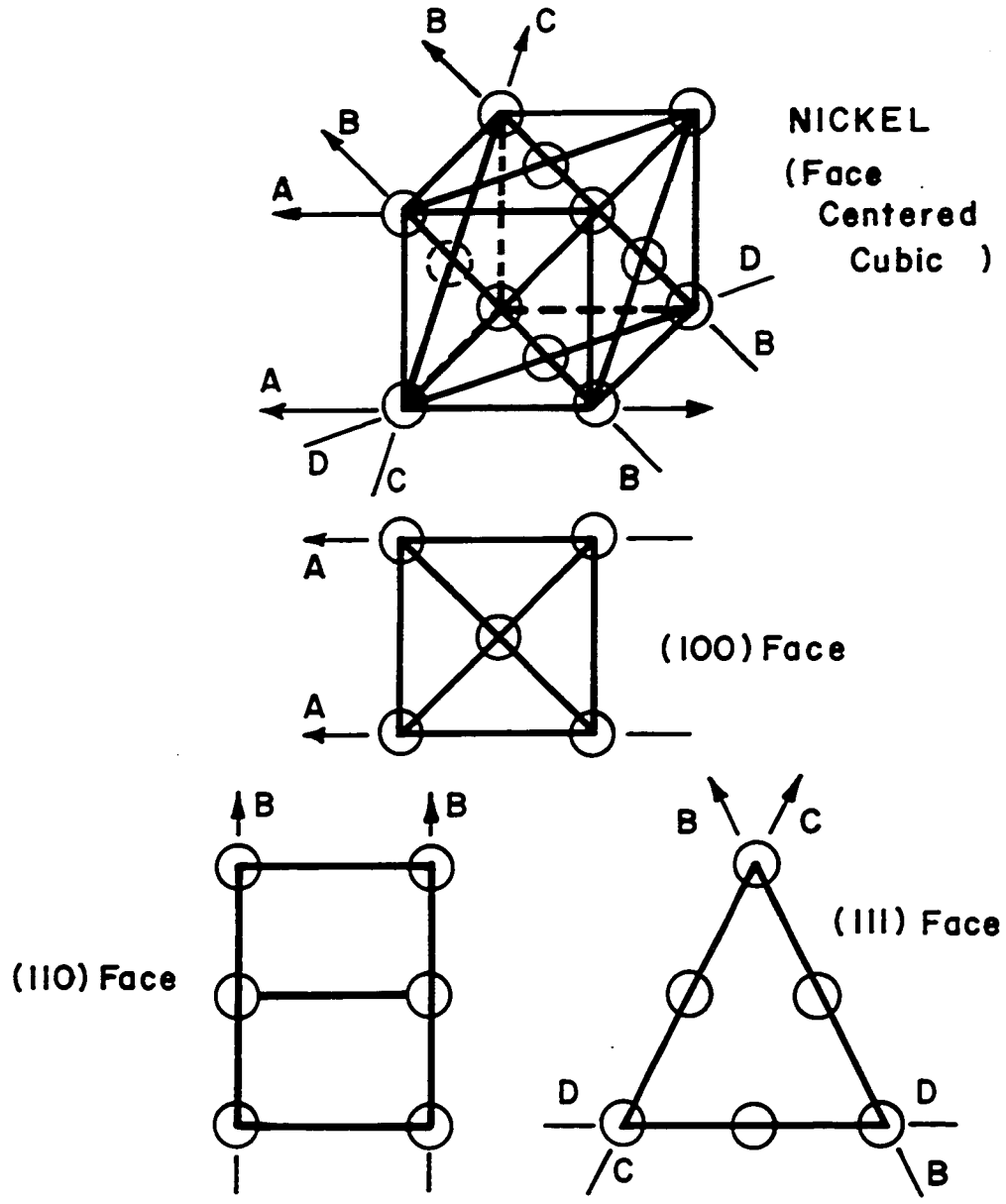

FIGURE I-1 SCHEMATIC DIAGRAM OF PRINCIPAL CRYSTAL FACES OF NICKEL

Most of the previous oxidation studies of nickel have been concerned with either the rapid initial chemisorption with one to several monolayers or with the thick film oxidation. The range between these two extremes is extremely interesting, since the emittance change is the greatest in this "in between region." Many recent studies of nickel have been made in the "monolayer region" using a Low Energy Electron Diffraction (LEED) unit.

Nickel was selected for the oxidation studies because of the following advantages:

(1) A coherent non-volatile film containing only NiO is formed in the region studied, as shown in Figure I-2;

(2) there is little stress set up between the metal and the oxide and flaking doesn't occur;

(3) the thermal expansion coefficients for Ni and NiO are so close that Ni and NiO exhibit only a very small change upon cooling.

The filament-in-vacuum technique was used to obtain the total hemispherical thermal emittances of the bare and oxidized single crystals.

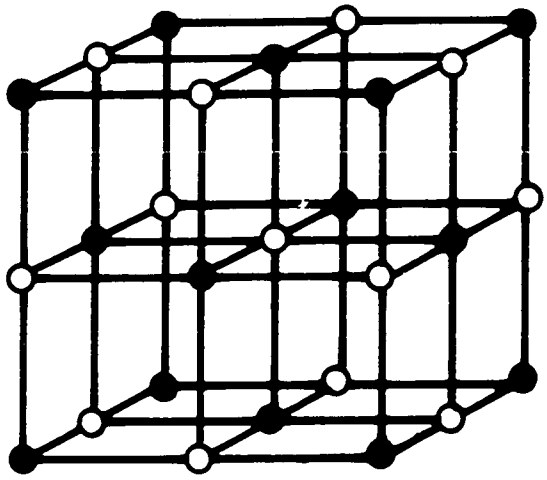

● Nickel Atoms

○ Oxygen Atoms

FIGURE I-2 CRYSTAL STRUCTURE OF NiO (NaCl TYPE)

II. THEORY AND LITERATURE

A. Radiative Heat Transfer

The radiative heat transfer for an ideal thermal emitter or black body was described by Planck and given by the Stefan-Boltzmann equation:

$$W = \sigma T^4 \tag{2-1}$$

W = radiant energy emission

σ = Stefan-Boltzmann constant

T = absolute temperature of radiating body

The equation is adjusted for non-black bodies by inserting the empirical factor ϵ, the emittance, so that

$$W = \epsilon \sigma T^4 \tag{2-2}$$

The emittance is known to be a function of temperature, of the wave length of the emitted energy, and of the physical and chemical characteristics of the material.

There is no satisfactory theory to predict the emissive power of solids throughout the wave length interval commonly encountered.

Drude (1900) derived a theoretical expression between the optical and electrical properties of metals. The Hagen and Rubens (1903) form of the relation is generally given as shown below:

$$\epsilon \propto \sqrt{\nu/\sigma} \tag{2-3}$$

where ϵ = emissivity

ν = frequency

σ = electrical conductivity

The equation has been found to hold for wave lengths greater than 10 microns.

B. Filament-in-vacuum Method

The filament-in-vacuum method for experimentally determining total hemispherical thermal emittances is a power input method in which the sample is heated electrically by the conduction of the sample itself. The steady state power input and sample temperature are measured. The power consumption due to radiation loss from the sample is compared with the radiation of a black body at the same temperature to determine the emittance of the sample.

The method was most successfully utilized to determine the total hemispherical emittances of platinum-rhodium wires. If a wire is mounted between larger diameter main leads and enclosed in a black body container at a uniform temperature T_b, the energy equation is:

$$q_{conduction} + q_{convection} + q_{radiation} + \text{energy input} = \text{heat accumulation} \qquad (2\text{-}4)$$

or for steady state conditions after evacuating the black body:

$$\frac{\partial}{\partial x}\left(k\frac{\partial T}{\partial x}\right) + \frac{4I^2R}{J\pi D^2} - \frac{4\sigma}{D}\left(\epsilon T^4 - \alpha T_b^4\right) = 0 \qquad (2\text{-}5)$$

where T = sample temperature (^{o}K)

x = distance from the end of the wire

k = thermal conductivity of the wire

I = current in the wire

R = electrical resistance of the wire

J = mechanical equivalent of heat

D = wire diameter

σ = Stefan-Boltzmann constant

ϵ = wire emittance

α = wire absorptivity at T to black body radiation from the walls of the container

Boundary conditions are $T = T_L$ at $x = 0$

where T_L = main lead temperature

and $\frac{\partial}{\partial x}\left(k \frac{\partial T}{\partial x}\right) = 0$ near the middle of the wire.

If only the middle portion of the sample is considered, a uniform temperature T_c exists. The first term in Equation (2-5) is then zero and the equation simplifies to

$$\frac{4I^2R_m}{J\pi D^2} - \frac{4\sigma}{D}\left(\epsilon T_m^4 - \alpha T_b^4\right) = 0 \qquad (2\text{-}6)$$

or

$$\epsilon = \frac{I^2R_m}{J\pi D\sigma T_m^4} + \alpha\left(\frac{T_b}{T_m}\right)^4 \qquad (2\text{-}7)$$

The method can be adapted to measuring emittances of thin, rectangular foils. This adaption with necessary assumptions is given in the Sample Calculation Section.

C. Emittance

The total hemispherical emittance of nickel has been investigated by Burgess and Foote (4), Barnes (1), Richmond (27), and Russell (28). Shelton studied the emittance of nickel as a function of oxide thickness

in the temperature range 400-900°C. No emittance data on any type of single crystals were found. Also no emittance data, other than that of Shelton's, were found for nickel oxide.

Shelton has presented a survey of the literature for an overall description of the field of thermal radiation. Shelton also discussed spectral and directional radiations as contrasted to the total hemispherical emittance actually measured. He also discussed radiation from a semi-transparent surface. From a microscopic standpoint, starting with Maxwell's equations for the behavior of electromagnetic radiation in both vacuum and matter, Shelton showed how Hagen and Rubens arrived at their equation

$$e_{n,\lambda} = \frac{2}{(\sigma \tau)^{\frac{1}{2}}} = 2\left(\frac{\rho}{c\lambda}\right)^{\frac{1}{2}} \qquad (2\text{-}8)$$

where

$e_{n,\lambda}$ = spectral normal emissivity
σ = specific electrical conductivity
τ = the period of the electromagnetic radiation in vacuum
ρ = resistivity
λ = free space wave length

The above equation is accurate for metals below 400°C at all wave lengths.

Other equations for insulators and for the emittance of semi-transparent media were discussed by Shelton.

D. Phenomena at the Curie Temperature

Uhlig (33), Pickett and MacNairn conducted studies to investigate the initial oxidation rate of nickel and the effect of the Curie tempera-

ture. They observed a discontinuity in oxide growth at the Curie temperature. Based on control of the initial oxidation rate by electron transfer from metal to oxide, the discontinuity of oxide thickness at the Curie temperature was explained by an observed work function of nickel slightly higher above the Curie temperature than below.

F. Cennamo (6) found a discontinuity or dip in the "emittance vs. temperature" curve for nickel. He, however, measured the total normal radiation.

E. Kinetics of Nickel Oxidation

Nickel oxide is a p-type or metal deficit semi-conductor as shown by both the oxidation dependence on its semi-conductivity and by the Hall effect. It is shown schematically below:

$O^{=}$	Ni^{++}	$O^{=}$	Ni^{3+}	$O^{=}$
Ni^{++}	$O^{=}$	Ni^{++}	$O^{=}$	Ni^{++}
$O^{=}$	Ni^{3+}	$O^{=}$	$\square$	$O^{=}$
Ni^{++}	$O^{=}$	Ni^{++}	$O^{=}$	Ni^{++}

Thus, as seen, there is a stoichiometric excess of $O^{=}$ in the lattice, resulting in defects, namely cation vacancies $Ni_{\square}^{++}$. Electrical neutrality is established by the formation of cations of higher vacancy, Ni^{3+}. Transport through the lattice occurs by diffusion of these species, both of which are formed by the surface reaction at the oxygen gas:oxide interface and are destroyed at the other side of the interface.

Even at temperatures far below ambient, a chemisorbed layer of oxygen rapidly forms on a base nickel surface. The chemisorbed oxygen and Ni^{++} ions then react to form NiO. It is generally agreed that this is accomplished by outward movement of the cations. More oxygen is then chemisorbed on the newly formed NiO and the reaction occurs as before. Initially the electrons for ionization come directly from the metal. As the oxide layer is formed, the electrons may be provided by the oxide, leaving positive holes. These holes, Ni^{3+} serve as conductors to carry positive current across the oxide to the metal surface. Further oxidation is dependent upon the flux of both the cation vacancies and positive holes from the gas interface to the metal.

Besides the chemical potential gradients (due to the concentration gradients), there is an electrical field set up between the negative surface charge and the resultant positive charge in the metal. The region known as the "very thin film" region is distinguished by such fields which may be as high as 10^7 V/cm. These fields can be important in the diffusion process.

When the oxide film becomes thick enough so that the space charge boundary layers no longer have an appreciable effect, the conditions are fulfilled which lead to the familiar parabolic rate equation.

$$W^2 = k_p t + C \qquad (2\text{-}9)$$

Gulbransen and Andrew (14) in their nickel oxidation studies at 400-750°C found large deviations from the parabolic law during the initial stages of reaction. Sartell and Li (29) studied the oxidation

of high-purity nickel in the range 950-1200°C and found a parabolic relationship. Their work, however, was with thick films of oxide. Fueki and Ishibashi (13) also found a parabolic relationship in their nickel alloy oxidation studies at 700-900°C. Baur, Bartlett, Ong and Fussell (2) found a parabolic relation was followed except for a brief initial period during their nickel oxidation studies at 1000-1200°C. Phillips (25) found two consecutive parabolic relationships during nickel oxidation studies below 1000°C and a single parabolic relationship above 1000°C. Hansen (15) found a "near parabolic" relation at 90μg/cm^2 and an absolute parabolic at about 300μ g/cm^2.

Investigators have differed in their findings for the rate expression for nickel oxidation in the region between nucleation and the "thick" oxide region defined by the parabolic equation. Campbell (5) found a logarithmic relation for the oxide thickness region 15-25μg/cm^2, and a quartic relation for the region 25-40μg/cm^2. Hansen found a logarithmic relation to hold up to 90-100μg/cm^2 after which it changed to a quartic law. Hansen operated with O_2 pressures of .13 mm Hg to 10.6 cm Hg pressure. The logarithmic and quartic relationships were obtained at the higher O_2 pressures. The forms of rate equations described are

$$\underline{\text{cubic}} \qquad \frac{dW}{dt} = k\, W^{-2} \tag{2-10}$$

$$\text{or} \qquad W^3 = k_c t + C \tag{2-11}$$

$$\underline{\text{quartic}} \qquad \frac{dW}{dt} = k\, W^{-3} \tag{2-12}$$

$$\text{or} \qquad W^4 = k_q t + C \tag{2-13}$$

$$\underline{\text{logarithmic}} \qquad \frac{dW}{dt} = k_1 e^{-W/k_2} \tag{2-14}$$

$$\text{or} \qquad W = k_2 \ln \left[\frac{k_1}{k_2} (t-t_o) + k_3 \right] \tag{2-15}$$

Most of the other investigators did not divide their findings according to oxide thickness. The variable described was usually oxidation temperature. The temperature which corresponded to this intermediate oxide thickness region usually was 600°C and below. Uhlig, Pickett and MacNairn found a two stage logarithmic curve at 307-442°C. Their studies included oxide films up to 3400 Å (ca. 60 μg/cm^2). Hauffe and Engle (17) and Gulbransen and Andrew found a cubic relation. At temperatures near 200°C, Scheuble and Campbell and Thomas found a logarithmic rate to hold.

The nuclei-formation region is discussed in the next section in conjunction with the discussion of the texture and orientation of oxide layers.

F. Texture and Orientation of Surface Layers

1. Metal Oxidation (19)

The very first stages of metal oxidation under reduced oxygen and sulfur potentials has been extensively studied by Bénard and his school. Generally, they found that at the beginning of the oxidation, the metal is covered by a film the thickness of which increases up to a critical value of several tens of Angstroms. The oxide which continues to form tends to accumulate at certain crystallization centers.

The average number of these centers corresponds, for a given crystallographic orientation, temperature and pressure, to an equilibrium determined by the rate of surface diffusion of the metal and oxygen. The nuclei thus grows laterally until the whole surface is covered. Thus the three stages of oxidation included the formation of

(1) the invisible film

(2) the nuclei

(3) the continuous layer.

The picture of nucleation obtained by Harris, Ball and Gwathmey was similar to that of Bénard except they found nuclei of less than 80 Å diameter and polyhedra of 80-3000 Å diameter.

In most of these cases, it was observed that the number of nuclei was independent of time, but increased with the partial pressure of the reacting non-metal.

The morphology and number of nuclei were found to be particularly strongly affected by the crystallographic orientation of the metal substrate, while their orientation on the same crystal plane was identical.

Some have suggested that the formation of oxide nuclei during the first stages of oxidation was due to dislocations in the metal substrate. Bénard, however, did not think that such an interpretation was compatible with the observations made by his school.

Other investigators have observed nuclei formation in the early stages of nickel oxidation. Campbell considered the region of $< 15 \mu g/cm^2$ as nucleation during initial rate oxidation studies with polycrystalline

nickel. Martius (23) obtained microphotographs (1000x and then enlarged 2.5x) of "crystallites" of oxide formed at very low partial pressures of O_2 at 1100°C on nickel.

Much of the nuclei formation region has been studied with the use of low energy electron diffraction (LEED) while studying the oxidation of single crystals of copper and nickel.

2. Single Crystal Oxidation

Low energy electron diffraction (LEED) was described by MacRae (22) to study adsorption of O_2 and the surface structures formed on single crystals of nickel. The use of LEED allows the study of displacements of surface atoms due to asymmetric forces. With conventional x-ray or electron diffraction, energies on the order of 50 kev are used compared to 50-150 volts for the low energy diffraction. With the high energy source, the measurements are made not only on the surface but also on the bulk material. With the low energy source, the surface itself can be studied.

Studies with LEED of (100) nickel single crystals indicated that the nickel atoms in the topmost layer of the surface had exactly the same arrangement as the atoms in similar planes in the bulk of the crystal. The same was found for nickel atoms on both the (111) and (110) planes.

The three closest packed surfaces of nickel, the (111), the (100), and the (110), have respectively 9, 8 and 7 nearest neighbors rather than the usual 12 in the bulk of the crystal. Because of this,

different chemical effects were observed on these surfaces. Oxidation studies in a vacuum of 5×10^{-9} Torr, for instance, illustrated that the troughs formed by the surface atoms on the (110) surface were important in the adsorption process. The structures formed during the adsorption of oxygen on the (110) surface were found to be a reconstruction of the surface and involved the migration of nickel atoms along the troughs.

In other oxidation studies at 500°C and 10^{-6} Torr O_2 pressure, however, the (100) face of NiO was observed to form on the (1$\bar{1}$0) surface of nickel. The oxide during the initial stage of growth, was observed to form small nucleate patches at what appeared to be random positions, but which could have been surface imperfections. The diffraction spots were initially weak and diffuse, but gradually became more intense and definitive as the individual patches grew larger in size. Gradually the patches covered the entire surface and it was no longer possible to see the diffraction spots characteristic of the nickel substrate.

The oriented growth of NiO was observed to occur also on both the (100) and (111) surfaces. Unlike the (100) surface, however, the most stable oxide on these surfaces was observed to have the same orientation as the substrate nickel crystal. Thus NiO with (100) orientation formed on both the (110) and (100) nickel surfaces, whereas the orientation of the oxide was (111) on the (111) nickel surface.

Other differences were noted with the NiO on the (111) surface. Although the oxide at the surface was constrained to grow with the

same orientation as the nickel, once it started to grow, the most stable plane of oxide was observed to grow in the form of three-sided pyramids with (100) planes on the face of the pyramids.

Rhodin (26) used thin single crystal slices of copper and determined adsorption isotherms and heat of adsorption curves with nitrogen at liquid air temperatures. He studied the (100), (110) and (111) faces of copper by means of a strong but sensitive microbalance. Rhodin observed slightly different characteristics for the different crystal faces, showing specificity for physical adsorption with respect to crystal structure.

Harris, Ball and Gwathmey (16) studied the oxide films formed on the (311), (111) and (100) faces of a single crystal of copper. They found that, not only were there large differences in the rate of oxidation between the faces, but within one face there are large differences in rate of oxidation. They found differences in oxide growth for the nuclei, polyhedra and base films. They believed that the polyhedra were directly associated with the copper and found the number of polyhedra to be independent of time. The number and size of nuclei, on the other hand, were affected mostly by oxidation time and temperature.

Kruger (18) studied the oxide films formed on single crystals of copper immersed in water, containing various amounts of oxygen. Some of his observations were

1. the rate of oxidation varied with the crystallographic plane,
2. the oxide films were not continuous, and

3. the degree of orientation and epitaxy of the oxide films depended on the crystal faces upon which they were grown.

G. Thickness Measurement by Interference Colors (11 and 12)

When white light falls on a film-covered metal, interference of certain wave lengths can occur, depending on the film thickness. The light reaching the eye is colored if the wave lengths subject to interference are within the visible region of the spectrum. The interference occurs between the light reflected from the inner and outer surfaces of the oxide film. It is possible, however, to have a film too thin to cause any visible interference.

As the oxide film thickens, color effects due to interference cease and the appearance becomes that of the specific color of the oxide.

The fact that the color sequence is the same for all metals shows that the color depends on the film thickness and is not a specific property of the oxide. Pioneer work of measuring film thicknesses based on interference colors was conducted by Tammann and his collaborators and is often called Tammann's method. He obtained rough measurements of the thickness by matching the color produced by a film on the metal (viewed by reflected light) with the color produced by an air-film between glass (viewed by transmitted light). The thickness of the air film is divided by the refractive index of the oxide film to obtain the oxide film thickness.

If, for instance, the film is of such a thickness that the green light reflected from one surface is exactly out of phase with that

reflected from the other, the light will have a reddish color, since red is complementary to green. In the case of air films this was found to occur when the thickness became

$$\frac{\lambda_G}{4}, \frac{3\lambda_G}{4}, \frac{5\lambda_G}{4}, \frac{7\lambda_G}{4}$$

λ_G = wave-length of green light in air

The wave-length in the film substance will be 1/n that in air, so that 1st, 2nd, 3rd, and 4th order reds at thickness

$$\frac{1}{4}\frac{\lambda_G}{n}, \frac{3}{4}\frac{\lambda_G}{n}, \frac{5}{4}\frac{\lambda_G}{n}, \frac{7}{4}\frac{\lambda_G}{n}$$

Some inaccuracies occur in this method, however, because of the following:

1. a specific phase-change is known to occur at the metallic surface,
2. the refractive index, n, varies with wave-length, and
3. the color is not determined solely by the position of the wave-length where there is maximal interference, but is influenced by the intensity of wave-lengths on either side of the maximum.

Figure II-2 shows why the "character" of the colors occurring at different "orders" is not quite the same. It also shows why the sequence of colors does not exactly repeat itself. Interference occurs whenever the effective paths travelled by light reflected at the two surfaces differ by an odd number of half wave-lengths. Neglecting the

specific phase-charge, it would occur when the film thickness differed by an odd number of quarter wave lengths.

Table (2-1)

Colors of Films on Metals
(20)

Order	Colors Produced by Oxide on Nickel
"Invisible Range"	Color of Metal Unchanged
First Order	Yellow-Brown Rose-Mauve Blue Silvery or Greenish
Second Order	Yellow-Brown Red Blue Green
Third Order	Yellow Red Trace of Lavender Blue Green
Fourth Order	--- Red Green
Fifth Order	Faint Red Passing into Specific Color of Film Substance

Figure II-2 refers to a film thickening progressively on a metallic surface, viewed by white light. Initially, when the film is very thin, the interference band will be in the ultra-violet and will have no color (Stage A). When a certain thickness is reached, the blue light reflected from one surface will be out of phase with that reflected from

FIGURE II-2

PRODUCTION OF INTERFERENCE COLORS (20)

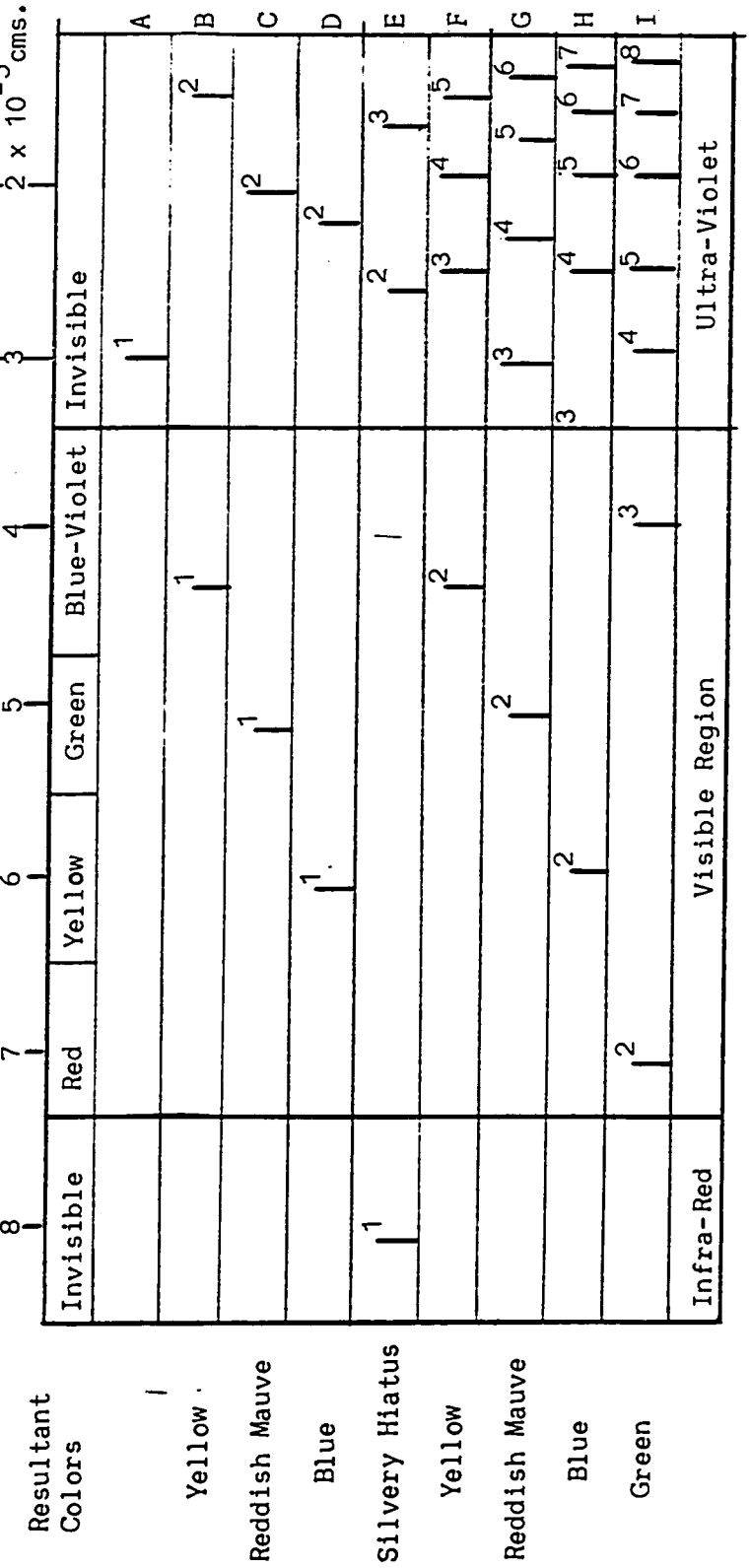

the other surface, thus giving the complementary color of yellow (Stage B). When a greater thickness is reached, the longer green waves suffer interference, producing a reddish mauve (Stage C). This continues until the first interference band passes out of the visible part of the spectrum before the second has entered it, giving a silvery hiatus (Stage E). The second band then enters the visible region, giving second-order colors, as shown in Stages F, G and H. Since, however, the third band follows the second more closely than the second followed the first, the third band will enter the blue-violet region while the second is still in the red, yielding a green at the end of the second-order colors. As noted earlier, there was no green in the first-order colors.

The unequal spacing of bands is the result of interference occurring when the thickness

$$y = \frac{\lambda}{4n} , \frac{3\lambda}{4n} , \frac{5\lambda}{4n} , \frac{7\lambda}{4n} , \text{ etc.} \qquad (2\text{-}16)$$

Thus a given thickness will produce interference of light having wavelengths

$$\lambda = 4ny , \frac{4}{3} ny , \frac{4}{5} ny , \frac{4}{7} ny , \text{ etc.} \qquad (2\text{-}17)$$

so that the values of λ converge.

The various orders of color for an oxide film on nickel are shown in Table (2-1).

When the NiO film is removed from the metal, the color at any point is found to have become roughly complementary to that observed

at the same point when the film was still on the metal. Thus, the place which was originally yellow becomes blue and that which was originally green becomes red and vice versa. The colors of NiO before and after stripping from the metal are shown in Table (4-5).

Constable (8 and 9) made accurate spectroscopial determinations of the wave length corresponding to the middle of an interference band in oxide films of copper, nickel and iron. His initial studies on nickel were with a crushed nickel oxide imbedded in clay which he reduced and then oxidized. The results of these tests are shown in Table (4-7). Other studies were conducted using a nickel cylinder. A spectrophotometric study was made of the light reflected from thin films of oxide of successively increasing thickness formed upon the cylinder. The thicknesses of the films, corresponding to the various colors of the first and second order for nickel oxide, were obtained by using the values of Kundt for the refractive index for various wave lengths. These results are shown in Table (4-6).

III. EXPERIMENTAL APPARATUS AND PROCEDURE

A. The Experimental Apparatus

The experimental apparatus is shown schematically in Figures III-1 and III-3. A more detailed sketch of the emittance chamber is shown in Figure III-2. A sketch of the microbalance system is shown in Figure III-4. A more detailed description is included in Appendix B. The equipment consisted primarily of the emittance chamber, vacuum pumps, current supplies, gas manifold, and oxide measurement apparatus. Other supporting instruments consisted of the Mettler balance, Micro-Projector for measuring sample width, Microscope for measuring distance between potential leads, spark cutter, mechanical polishing wheels, x-ray instrument for obtaining back reflection Laue diagrams of the nickel single crystals and Metallograph for studying oxide textures.

The emittance chamber was a 6" I.D. steel cylinder, 13" tall and fitted with removable flanges, as shown in Figure III-2. Copper electrodes were mounted on the top flange. Clamps on the electrodes were used to hold the sample under light tension. The electrodes were connected by feed-through terminals to the power supply units. Nickel feed-through terminals on the top flange were used to connect the 1 mil diameter nickel potential leads welded to the sample to the L and N Potentiometer. A chromel-alumel thermocouple was attached to the top specimen clamp. The thermocouple leads exited through the top flange via a vacuum seal. The vacuum system, gas manifold and ionization vacuum gauge were connected to the bottom flange.

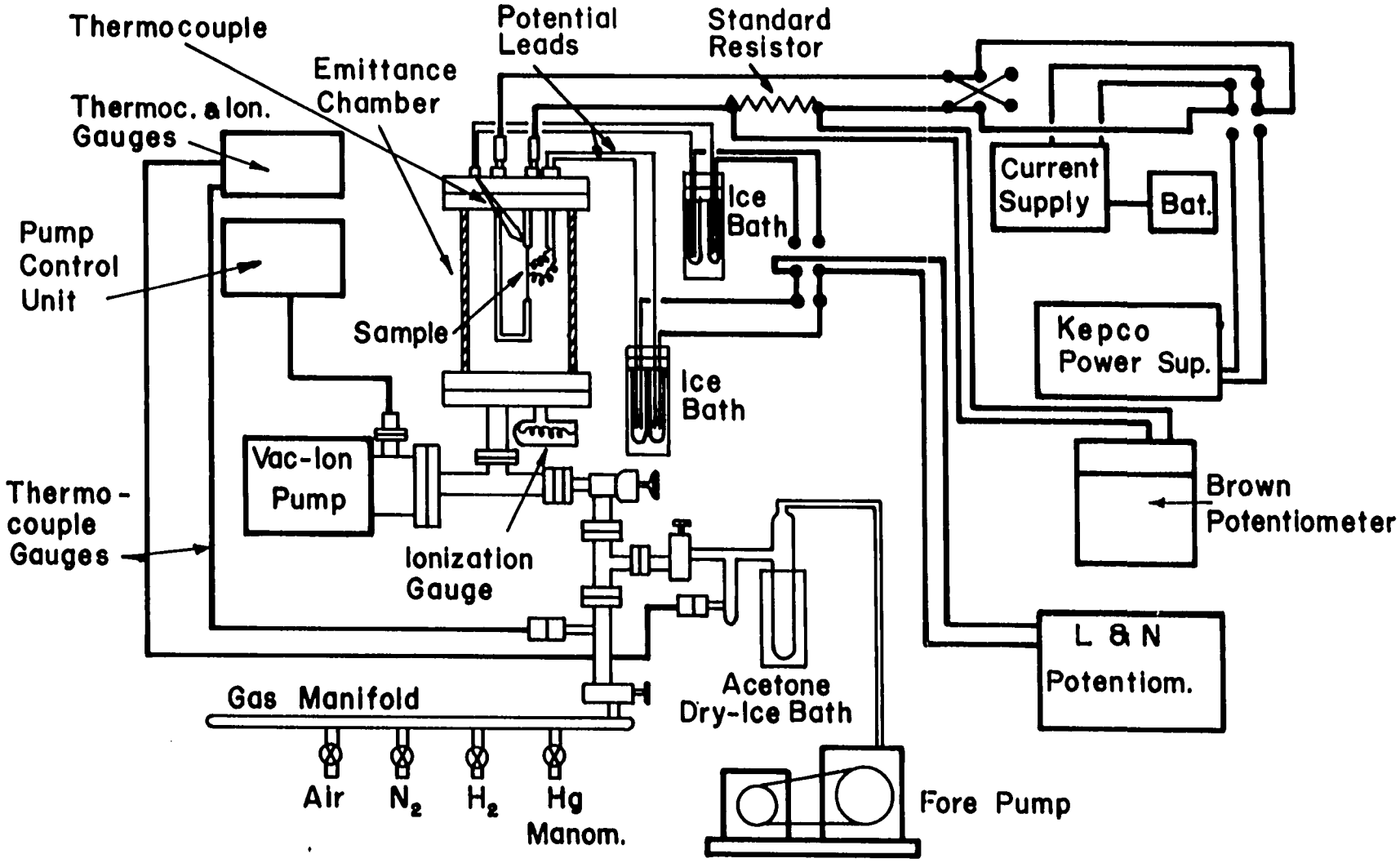

FIGURE III-1 EMITTANCE DETERMINATION SYSTEM

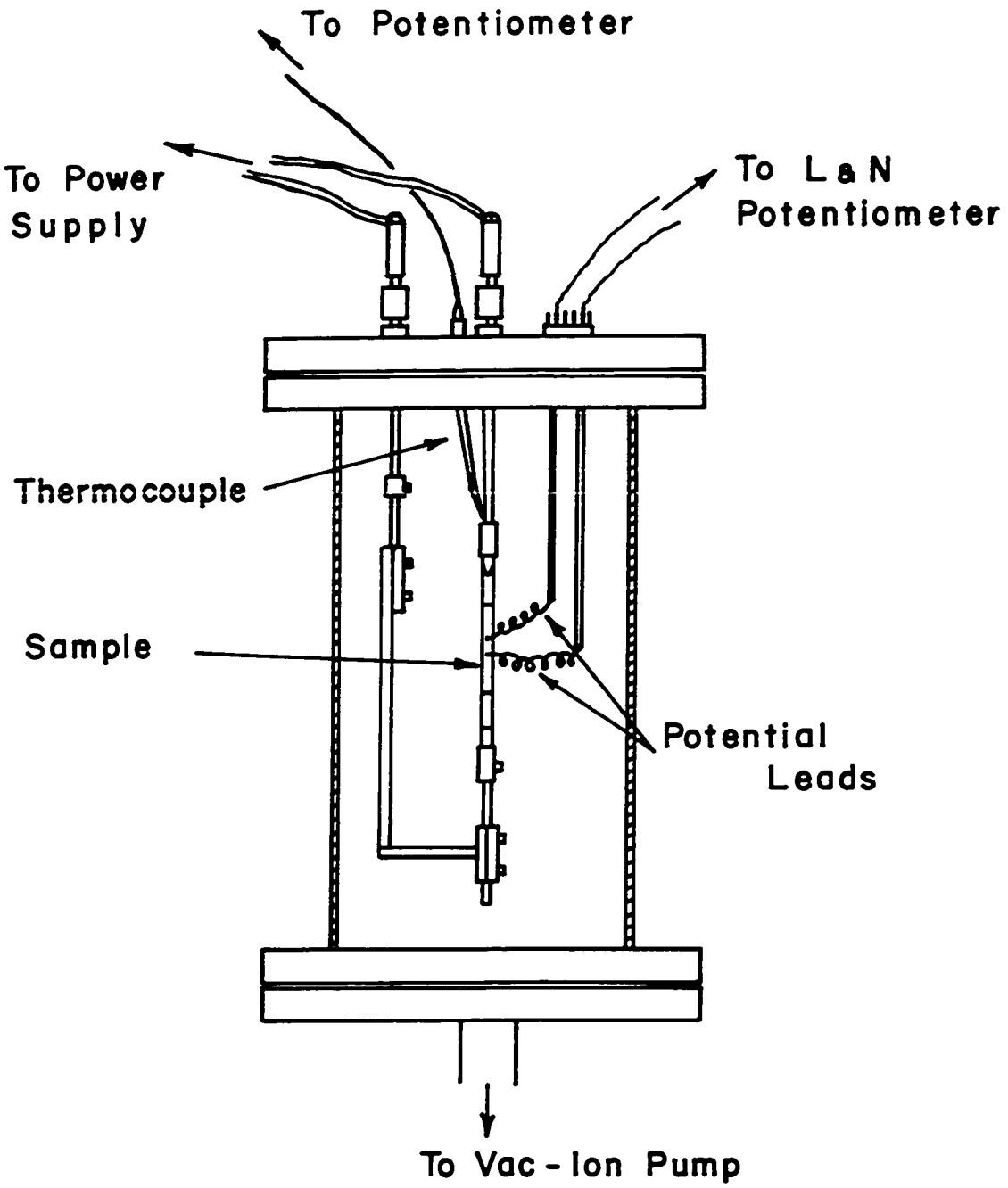

FIGURE III-2 EMITTANCE CHAMBER

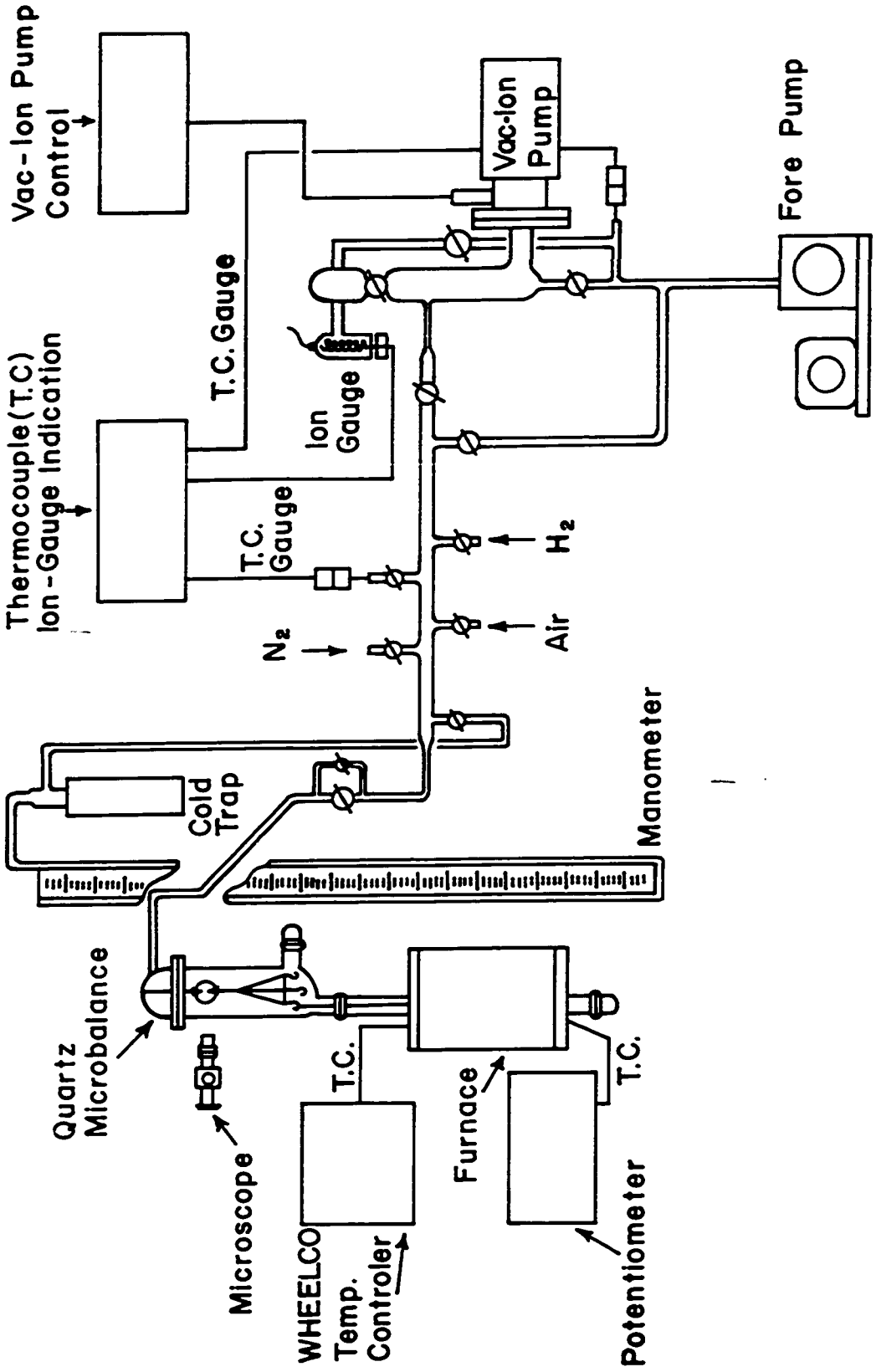

FIGURE III-3 OXIDE DETERMINATION SYSTEM

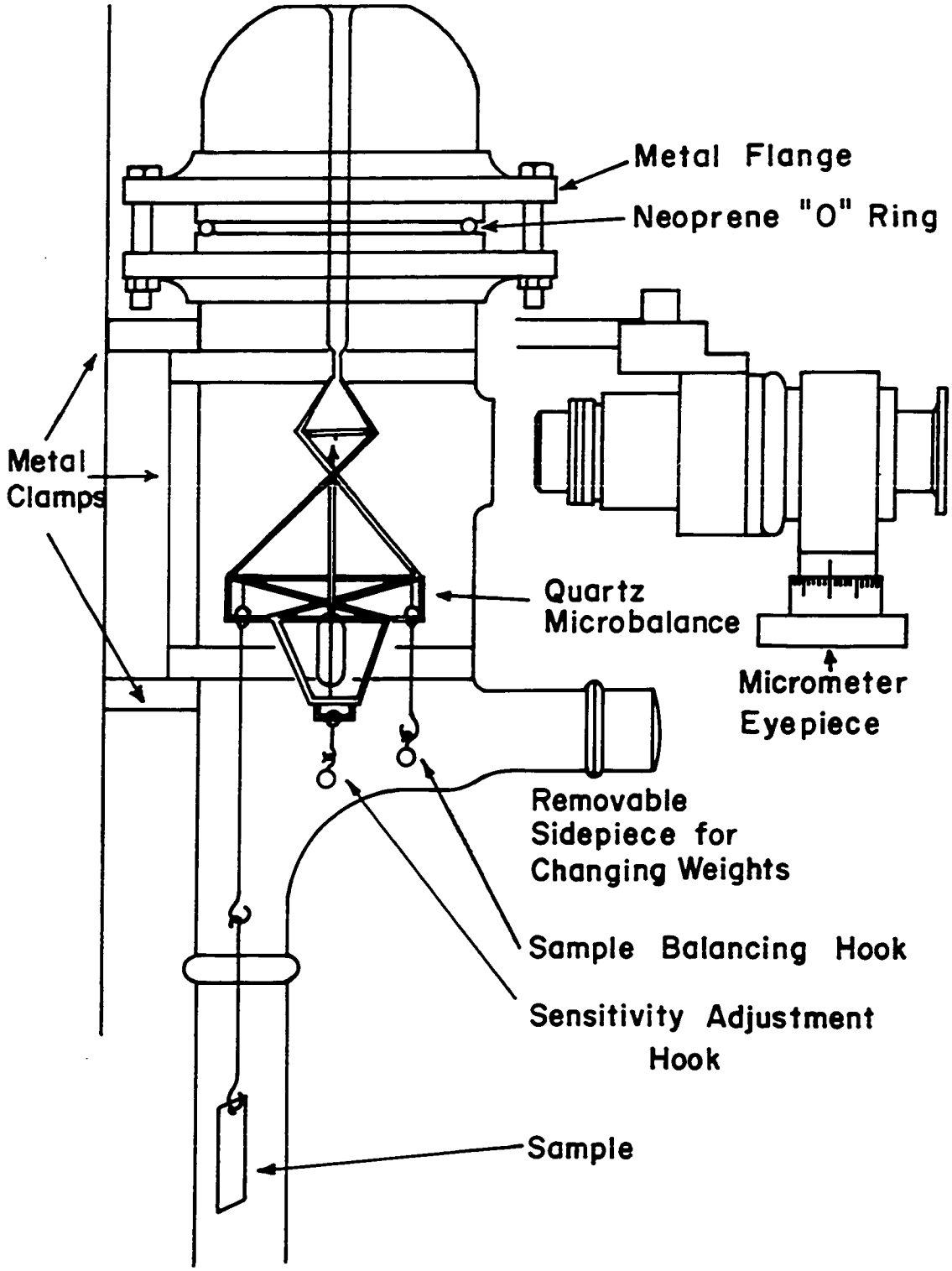

FIGURE III-4 QUARTZ MICROBALANCE SET-UP

The emittance chamber was also used for annealing and oxidizing the metal samples.

The current supply for room temperature resistance measurements consisted of lead storage batteries with a transistor control circuit, shown schematically in Figure B-I in Appendix B. Over 10 amps was available over a continuous current range with a resolution of better than 1/1000. The current supply used for heating the thick polycrystalline samples was a Model No. KS8-50M Kepco with a 0.01% regulation. The output range was 0-8 volts and 0-50 amps.

The current supplies were in series with a four terminal standard resistor. The voltage drop across the resistor was read on a Brown self-balancing potentiometer to obtain the current in the specimen. A polarity reversing switch was between the current supply and the current electrodes on the emittance chamber.

The thermocouple voltage and the voltage drop across the potential leads on the sample were measured on a Type K3 L & N Potentiometer. Since nickel has a high thermal emf against copper, all nickel-copper junctions were kept in an ice bath. The ice bath was also used for the thermocouple reference junction.

A Vac-Ion pump was used to obtain vacuums in the range of 10^{-7} to 10^{-8} Torrs in the emittance chamber. Prior to starting the Vac-Ion pump, it was necessary to obtain a rough vacuum of about 10^{-4} Torr with a Welch type pump. The pressure in the emittance chamber was measured with an ionization gauge. Thermocouple gauges and a mercury manometer were used for other pressure measurements.

The gas manifold system allowed the introduction of H_2, N_2 and air into the emittance chamber. Air for oxidation was allowed to flow through a dry ice-acetone bath to remove any traces of moisture.

The oxide measuring system consisted of a quartz spring for the thin polycrystalline samples and a quartz microbalance for the thicker single crystal samples. The oxidized samples were reduced in a temperature-controlled furnace. The loss in weight was measured with a cathetometer in the case of the quartz spring and a microscope with micrometer when employing the microbalance. Type J (21) microgram standard weights were used to calibrate the microbalance. A type M5 Mettler Microbalance was used as a check for the microbalance.

The thin polycrystalline samples were cut on a milling machine. The single crystal specimens were cut with a Servomet Type SMB spark cutter, shown schematically in Figure F-II in Appendix F. The single crystals were thinned and polished using Buehler-type polishers and grinders.

A Wilder Micro-Projector was used to measure sample widths and sample lengths after cutting for oxide determination. The distance between potential leads was measured with the microscope and measuring apparatus of a Tukon Tester.

Crystal orientation was determined by means of a General Electric X-Ray Corporation diffraction unit. Microphotographs were obtained with an American Optical Company Metallograph.

B. Sample Calculations

1. Emittance

The ability to obtain the emittance using the filament-in-vacuum-method is possible because most of the heat loss terms are negligible. The heat flow equation for a thin foil is shown below:

Figure III-5

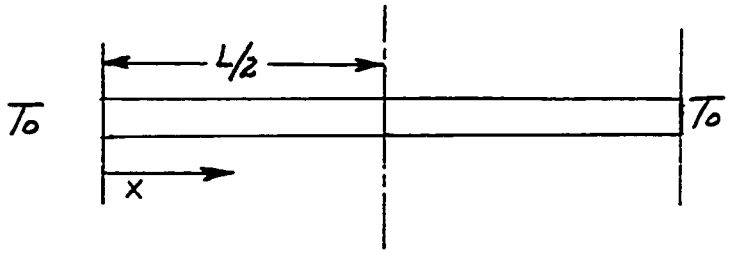

Heat Flow for Thin Foil

Heat flow in other directions for a thin foil can be neglected. Therefore only the x-direction is considered. Heat losses due to convection are negligible because of the high vacuum to which the sample is exposed. Thus Equation (3-1) shown below describes the remaining heat flow.

$$\frac{\partial^2 T}{\partial x^2} + \frac{1}{k}\frac{\partial k}{\partial x}\frac{\partial T}{\partial x} + \frac{I^2\rho}{ka^2} - \frac{p\sigma}{a\,k}\left[\epsilon T^4 - \alpha T_o^4\right] = \frac{H}{k}\frac{\partial T}{\partial t} \qquad (3\text{-}1)$$

The heat accumulation term can be eliminated by waiting for steady state conditions. This required a much longer time for the thick single crystal specimens. Up to five minutes was required in some instances to obtain a steady state voltage drop.

By making the sample long and thin, the ratio of surface area per unit length to cross sectional area, p/a, can be increased. This

allows cancellation of the conduction terms in Equation (2-16), resulting in the following equation:

$$p\sigma(\epsilon T^4 - \alpha T_o^4) = \frac{I^2\rho}{a} \qquad (3\text{-}2)$$

The assumption is made that the radiation from the emittance chamber to the specimen is black. This was accomplished by making the emittance chamber very large in comparison to the specimen.

Since the re-radiation is small in comparison to the specimen radiation, the absorptance α is assumed to have the value of ϵ at the specimen temperature. Therefore the equation is reduced to

$$\epsilon = \frac{\frac{I^2\rho}{pa}}{\sigma(T^4 - T_o^4)} = \frac{EI/area}{\sigma(T^4 - T_o^4)} \qquad (3\text{-}3)$$

Shelton (30) has solved Equation (3-1) numerically to check the validity of Equation (3-3). He has shown that for the temperature range studied, the error due to the temperature difference between potential leads is negligible for the thin polycrystalline specimens.

It was necessary to add heat sinks to each end of the single crystal specimens, as shown in Figure III-6 to eliminate conduction losses from the sample to the electrodes. The sample to heat sink ratio was adjusted to give a curve similar to that obtained when using thin samples with no conduction losses.

The conduction loss was calculated by J. Shelton and shown to be negligible. Also the heat losses due to the potential leads were calculated to be negligible.

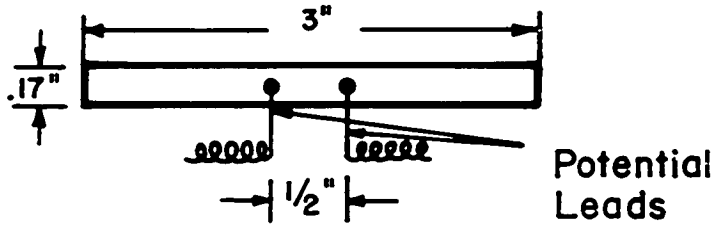

THIN POLYCRYSTALLINE SPECIMEN

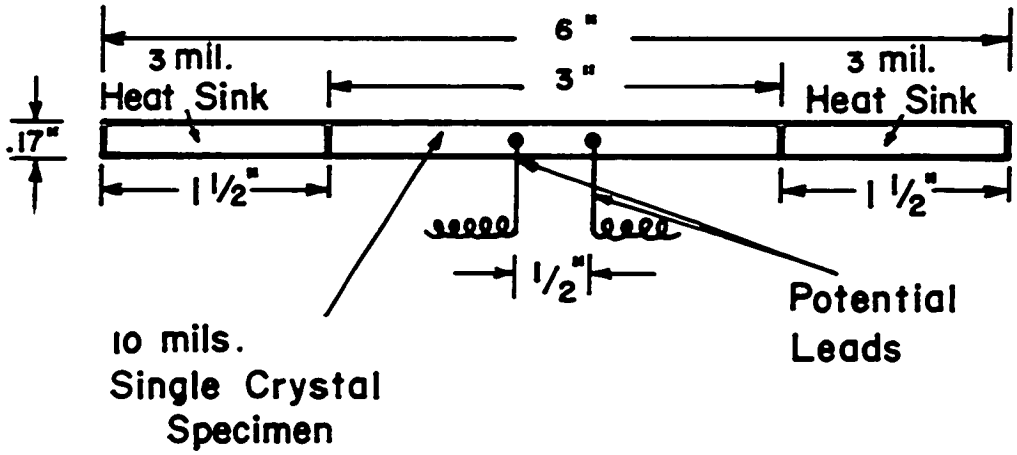

SINGLE CRYSTAL SAMPLE WITH HEAT SINKS

FIGURE III-6 DETAILS OF SPECIMEN CONFIGURATION WITH DIMENSIONS

To determine emittance, as shown in Equation (3-3), it was necessary to obtain the power per unit area required to give a specified surface temperature, T. The voltage, E, was obtained by determining the voltage drop across the potential leads with the L & N Potentiometer. The current I, was obtained by measuring the voltage drop across the standard resistance and calculating the current. The sample area was obtained from the sample measurements as shown below:

$$\text{Area} = 2\left[(\text{distance between potential leads})(\text{width} + \text{thickness})\right] \quad (3\text{-}4)$$

The thickness of the thin polycrystalline samples was assumed neglible. For the thick single crystals, however, the thickness was considered.

The temperature of the sample was determined by resistance thermometry. The ratio of the resistance R at temperature T to the resistance R_{30} at 30°C was determined by J. Shelton and shown in Figure B-IV in Appendix B. Therefore by obtaining R/R_{30}, it was then possible to obtain the sample temperature from the calibration curve. The resistance at 30°C was calculated as follows:

$$R_{30} = \frac{R_{RT}}{1 + (T_{room} - 30)\alpha} \quad (3\text{-}5)$$

The room temperature resistance, R_{RT}, was obtained by measuring the voltage drop across a standard resistance, calculating the current, and in turn calculating the resistance at T_{room} as follows:

$$R_{RT} = \frac{(\Delta E \text{ across sample at } T_{room})}{(I_{\text{standard resistance}})} \quad (3\text{-}6)$$

The value of α was determined by J. Shelton to be 0.00542. A plot of R_{30}/R_T vs. T is shown in Figure B-V in Appendix B.

The denominator of Equation (3-3) is the black body radiation, q_{BB}, and was obtained from a tabulation by M. W. Russell (28).

The emittances of the oxidized sample was calculated in a similar manner.

2. Oxide Determination

After completing the emittance determinations, the sample was cut and reduced in hydrogen so as to determine the amount of oxide. The sample consisted of the center 1" of the specimen. The loss of oxygen due to the reduction was calculated as $\mu g/cm^2$. The area of the sample was calculated as follows:

$$\text{Area} = 2\left[\text{Sample length (width + thickness)}\right] \qquad (3\text{-}7)$$

The quantity of oxygen lost was determined by the calibrated quartz spring in the case of the thin samples and by the quartz microbalance in the case of the thicker single crystals. The quartz spring was calibrated by J. Shelton and shown in Figure B-III in Appendix B. The quartz microbalance was calibrated prior to each run with the 500μg J weight. Thus the amount of oxide was calculated as follows:

quartz spring:

$$\text{Weight of oxide } (\mu g) = \frac{\Delta H}{14.6}\ \mu g/mm \qquad (3\text{-}8)$$

ΔH = length difference measured by a cathetometer

quartz microbalance:

$$\text{Weight of oxide } (\mu g) = \frac{500\,\mu g}{N(\text{divisions})} \times \Delta\, N(\text{divisions}) \quad (3\text{-}9)$$

Δ N = change in reading due to reduction

N = microbalance reading with 500μg "J weight"

C. Experimental Procedure

1. Sample Preparation, Measurement, and Installation--thin foils

The thin polycrystalline specimens were cut from a thin foil sheet of Chromium Corporation nickel foil. The thick polycrystalline samples were cut from Wilkinson nickel foil. Polycrystalline foils were cut either 3" or 6" long as shown in the sample listing in Table 0. Most of the foils were cut with a width of about .17". The foils were cut with a milling operation as described in Appendix A.

The cut specimens were degreased in a three step ultrasonic cleaning process. Washing in benzene was followed by cleaning in acetone and finally by rinsing in warm distilled water.

A capacitive discharge spot welder with hand attachment was used to weld the .001" diameter nickel potential leads to the sample. These were centered about the midpoint of the foil .5" apart, as shown in Figure III-6. The potential leads were wound into helicies from about 5 cm lengths of wire. The spring effect of the helix facilitated handling. The samples were taped to a 5 x 7 card during attachment of potential leads to facilitate the welding operation.

The sample, still attached to the card, was measured with instruments described in Appendix A to determine the width and the distance

between potential leads.

The sample was then removed from the card and installed between the electrode clamps, as shown in Figure III-2. The potential leads were then soldered to the nickel terminals with nickel solder.

The top flange with sample was then replaced into the emittance chamber. A new copper gasket was used every other time.

2. Sample Preparation--single crystals

A detailed description is included in Appendix F.

3. Determination of Room Temperature Resistance

After bolting the top flange in place, the initial room temperature resistance of the sample was determined with one atmosphere of air in the emittance chamber. This was accomplished by allowing a current of 10 mv to flow through the .1Ω standard resistor and sample. The voltage drop across the standard resistor and across the potential leads of the specimen were then determined. Finally, the temperature within the chamber was determined. From these measurements, the room temperature resistance and the resistance at 30^{o}C were calculated as shown in the Sample Calculation Section.

4. Establishing a High Vacuum

The procedure for establishing a high vacuum in the emittance chamber with air in the chamber was to first pump out the system with the fore pump. Since the system design did not allow for preventing air to enter the chamber when down for a sample change, it was sometimes difficult to start the Vac Ion pump because of the moisture

from the air. When this occurred, the pump was baked out with a Glas-Col heating jacket purchased from Varian. This hastened the start up by vaporizing the water and allowing the fore pump to pump out the vapors. Purging the system several times with dry nitrogen also aided start up.

5. Annealing

The polycrystalline samples were annealed in 1000 μ of H_2 for four hours at about 800°C. Annealing was carried out to remove interstitial oxygen and also to obtain some crystal growth. The annealing step also provided a surface which could be more closely reproduced. No annealing was required for the single crystal specimens, since there was no interstitial gases and also since the surface contained a single crystal structure.

Annealing was accomplished by heating the sample to the desired temperature in H_2. After the annealing operation, the system was filled to 1 atmosphere with N_2. After allowing the temperature to equilibrate for several hours, the "room temperature resistance after annealing" was determined.

6. Bare Metal Emittance Measurement

After measuring the room temperature resistance after annealing, the system was evacuated to about 10^{-7} Torr for the emittance run. The current supply was then adjusted to provide a current sufficient to bring the sample to about 600-700°C. After the current supply was switched on, the voltage drop across the standard resistor was measured

along with the voltage drop across the potential leads on the specimen. Only a very short time was required to obtain a steady state temperature with the thin polycrystalline samples. Several minutes were required in the case of the thick single crystals.

The current across the standard resistor was then calculated along with the resistance, temperature and finally the emittance of the sample. These calculations were described in the Sample Calculation Section.

Data were taken at every 50°C in the temperature range of about 275-850°C, starting with the highest temperatures first. The current was turned off immediately after a reading was taken. The current was then adjusted to the approximate position to give the next desired temperature before turning on the current again.

7. Room Temperature Resistance after Annealing

After the last bare metal emittance run, 1 atmosphere of nitrogen was admitted into the emittance chamber. After several hours to reach equilibrium, a room temperature resistance determination was repeated. Normally, the room temperature resistance increased during the emittance determination step. This increase, however, was found to occur during the first "heat up period" and was mostly due to replacing interstitial H_2 with interstitial N_2. Therefore, the first emittance point was calculated with the "room temperature resistance after annealing" whereas subsequent determinations used the "room temperature resistance after bare metal emittance" in the calculation of surface temperature.

8. Oxidation

After determining the room temperature resistance after the bare metal emittance step, the emittance chamber was again evacuated to 10^{-7} Torr. The sample was then oxidized in dry air at a pressure of 1000 microns. The oxidation was accomplished by heating the sample with the amount of current required to give the desired temperature. The oxidation step was allowed to continue until the calculated desired oxide was attained.

During the single crystal studies in which it was desired to obtain the same emittance curve with different oxidized single crystals, it was necessary to oxidize several times. After each oxidation step, the emittance was checked until the desired curve was obtained. The temperature and oxidation times depended upon the extent of oxidation that was desired. The oxidation conditions for the various runs are shown in Tables (D-1) and (D-2) in Appendix D.

9. Room Temperature Resistance after Oxidation

After the oxidation step, the room temperature resistance was again determined. The resistance was observed to increase during the oxidation step as shown in the tables of data in Appendix C. The percentage change in resistance due to oxidation was much greater for the thin samples than for the thick single crystal samples.

10. Oxidized Emittance Determination

After determining the room temperature resistance after oxidation, the emittance chamber was again evacuated to 10^{-7} Torr and the

emittance of the oxidized sample determined. The procedure and calculations for the oxidized emittance was similar to that described for the bare metal emittances.

11. Room Temperature Resistance after Oxidized Emittance

The "room temperature resistance after oxidized emittance determinations" was then measured. Normally there was little change in resistance during this step.

12. Oxide Determination

(a) Quartz spring

At the end of the run, the oxidized sample was removed from the emittance chamber and the center 1" section cut for the oxide determination. The length of the cut sample was determined with the Micro-Projector and microphotographs were taken.

For the thin polycrystalline samples, a quartz spring was used to determine the amount of oxide. The cut sample was hung on the calibrated quartz spring and suspended in the furnace. The sample was degassed at 10^{-7} Torr for one hour at about 200°C. One atmosphere of hydrogen was admitted and a zero reading taken with the cathetometer on the quartz spring. The sample was then reduced for two hours at about 800°C. After the furnace had cooled, the change in spring setting was determined and the amount of oxygen removed was calculated as shown in the Sample Calculation Section.

(b) Quartz microbalance

To obtain the desired accuracy it was necessary to use a quartz

microbalance to determine the amount of oxide on the thick single crystal samples. At the end of the run, the mid section of the single crystal was cut and microphotographed. The oxidized sample was then weighed on the Mettler Microbalance and then hung in the furnace.

Prior to the run, it was necessary to balance the sample on the microbalance. The balance was then calibrated in 1 atmosphere of air with the 500μg J weight. The sensitivity was adjusted so as to attain a full scale reading of about 500μg. The system was then sealed and evacuated to 10^{-7} Torr.

After filling the system with N_2, the microbalance was allowed to settle overnight. On the following morning, a zero reading was taken and the system was filled with 1 atmosphere of H_2.

The sample was then reduced by heating the furnace to about 800°C. The heat up period usually required about $\frac{1}{2}$ hour. It was found that as long as a critical temperature of about 250-275°C was attained, the reduction of the oxide occurred almost instantaneously.

After the furnace cooled, the chamber was evacuated and filled with 1 atmosphere of N_2. After allowing the system to settle overnight, a final microbalance reading was taken and the amount of oxygen in the oxide calculated as shown in the Sample Calculations Section. The sample was then removed and weighed on the Mettler to obtain a check on the amount of oxide.

IV. DISCUSSION OF RESULTS

A. General Observations

1. Sample Preparation Difficulties--thin foils

As described in the Sample Preparation Section in Appendix B, celluloid was used to prevent the thin nickel specimens from sticking to each other during the milling operation. Prior to this, onion skin paper had been used to prevent sticking. In the milling operation the samples were clamped together between brass bars. Wherever the clamps were attached, it was observed that the surface configuration of the onion skin paper was impressed onto the surface of the nickel resulting in numerous tiny pits.

When these samples were annealed, the room temperature resistance was observed to increase sharply instead of decreasing as was expected. Apparently the roughened surface resulted in hot spots on the surface.

Large differences in bare metal emittances previously attributed to measurement errors could have instead been due to the difference in surface roughness when using the onion skin paper.

No such difficulties were encountered when using celluloid to prevent sticking. Other types of paper were also tried, but most resulted in roughened foil edges.

2. Effect of Interstitial Gases on Room Temperature Resistance

A study was carried out to study the emittance of a 6" long sample versus a 3" long sample. During these studies, the effect of

different interstitial gases on the room temperature resistance was observed.

The room temperature resistance of the 6" long sample was determined and the emittance chamber was opened to the atmosphere to cut the sample to 3". Measurements of room temperature resistance made with N_2 in the chamber showed that the resistance of the same sample increased when the chamber was opened to the atmosphere. This was believed to be due to diffusion of oxygen into the pores.

When the same sample was evacuated and flashed in hydrogen, the room temperature resistance decreased to its lowest value. Thus the room temperature resistance was highest with air in the pores and lowest with H_2 in the pores.

3. Time Required to Reach Steady State During Heating

As anticipated, the thicker single crystal samples required a longer time to reach a steady state temperature during heating than the thin polycrystalline samples.

Steady state conditions were usually reached in less than a minute for all thin specimens studied in the temperature range studied.

An example of the times required to reach steady state conditions for various temperatures for a 10 mil thick sample is shown in the following table:

Table (4-1)

Time Required to Reach Steady State

(Bare Metal Emittance Step)

Run 0#15-10W1x5 $p = 1.4 \times 10^{-7}$ Torr

T (^{o}C)	Time required for steady state	T (^{o}C)	Time required for steady state
1011	30 sec.	697	2 1/2 min.
983	40 sec.	630	3 min.
930	1 min.	554	3 1/2 min.
891	1 1/4 min.	464	4 min.
859	1 1/2 min.	421	8 min.
803	1 3/4 min.	319	12 min.
753	2 min.		

4. Annealing of Single Crystals

No change in emittance was observed for the single crystals when comparing the bare metal emittance before and after annealing. Also, there was very little change in the room temperature resistance of the single crystal sample during annealing. This was anticipated since there are essentially no interstitial gases in the single crystals because of the absence of grain boundaries.

The annealing operation was subsequently eliminated from the procedure after demonstrating that it had little or no effect on the emittance results.

5. Emittances with "Thick" Samples

Initial studies with the 10 mil thick polycrystalline samples indicated a broad minimum in the bare metal emittance curve. Shapes of bare metal emittance curves for various sample thicknesses are shown below:

Figure IV-1

Effect of Emittance Vs. Sample Thickness

(3" long samples)

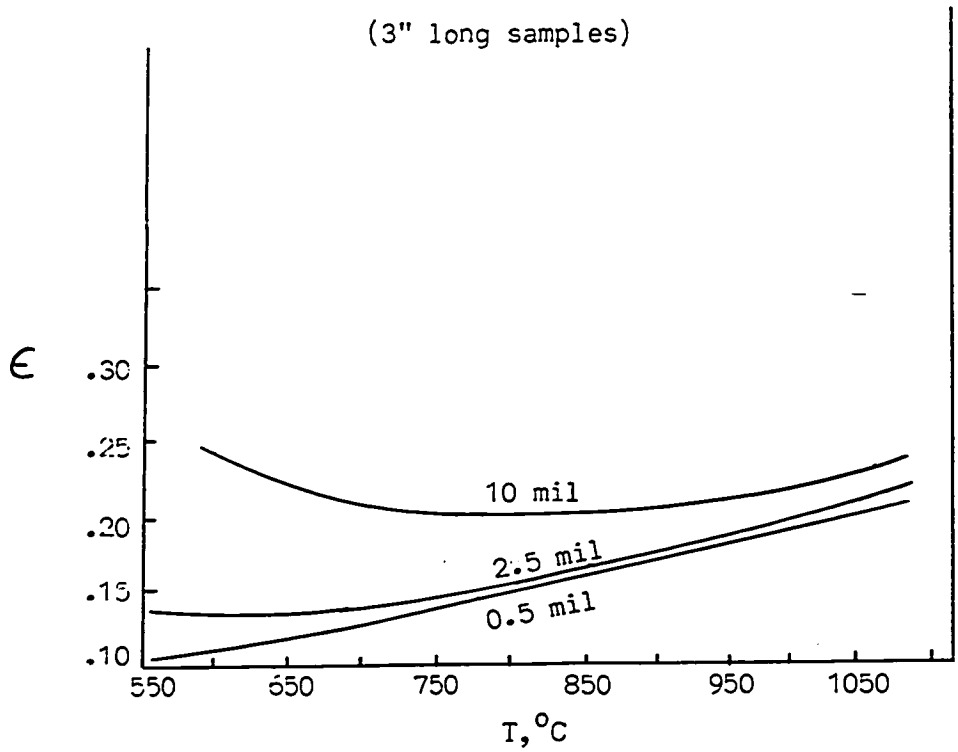

It appeared that the unexpected broad minimum in the thick samples was due to conduction losses from the sample to the copper electrodes. More power was required to attain the same temperature as for the thin foils because of the conduction losses. This resulted in a higher emittance as shown below:

$$\epsilon = \frac{\text{Power}/A}{\sigma (T^4 - T_o^4)} \qquad (4\text{-}1)$$

As the temperature decreased, the ratio of conduction losses to total power increased resulting in the minimum noted in the curve.

This difficulty was overcome by spot welding heat sinks on each end of the nickel specimen, as shown in Figure III-6. By varying the ratio of sample thickness to heat sink thickness, the shape of the emittance curve, especially in the lower temperature region, could be altered. A series of studies were made to determine the ratio which would give the same shape of curve obtained with thin foils. If the ratio were too high (for instance 10 to 1), heat would be conducted from the heat sinks into the sample. This condition resulted in abnormally low emittances. The other extreme (no heat sink) resulted in abnormally high emittances as described earlier. The correct ratio which gave no heat flow in or out was approximately 2.0 to 4.0 . Thus all samples were prepared to fall within this range, as shown in Table 0. Exceptions were samples OSC#1 and OSC#2, in which heat sinks were added after the samples were oxidized.

Since the power required to heat oxidized samples was much greater than for bare samples, the conduction losses when using thick samples was a much smaller percentage of the total power. Thus, the oxidized emittances were less affected by sample thickness or sample to heat sink ratio.

Other investigators indicated a broad minimum in their "emittance vs. T curve" for nickel. They probably encountered the same difficulty with thick samples.

6. Problems with Quartz Microbalance

It was found necessary to calibrate the microbalance prior to each run. The calibrations were accomplished by using a 500μg J weight as described in Table B-2 in Appendix B. On several occasions, the microbalance was calibrated with the 50μg J weight to check linearity in the low range. The calibrations were conducted with the sample in place and with the system opened to the atmosphere.

Occasionally, it was necessary to adjust the sensitivity of the balance to have the full range equal the 500μg calibration weight. The sensitivity was increased by removing weights from the sensitivity hook and vice versa.

Some problems were encountered initially with electrostatic charge build-up on the quartz tube surrounding the sample. Glass wool used to insulate the top of the furnace was the cause of the static problem. The static charges resulted in a gradual fluctuation of the zero point. After eliminating the glass wool and washing the system with ethyl alcohol, the electrostatic problem was eliminated.

It was also found that best results could be obtained by allowing the system to settle overnight before taking a reading. This was especially important after the system had been heated.

Another problem encountered occurred when new quartz weights were added to the quartz hook holding the nickel sample. These quartz weights were used for balancing the sample prior to each run. Apparently, there was enough oxide on the quartz weights to give an erroneously high reading. Consequently, all weights were added to the quartz hook outside of the furnace.

Since an independent check was made with the Mettler Microbalance during each run, these values were used in early runs in which problems were encountered with the microbalance.

7. Reduction of oxide

During the reduction of the nickel oxide, it was found that essentially all of the oxide was reduced in approximately 1 minute when a temperature of about 250°C was attained. The reduction step for two of the runs is shown in Figures IV-2 and IV-3. The data for these studies are shown in Table (E-1) in Appendix E.

B. Emittance

1. Bare Metal Emittance--Polycrystalline Nickel

The emittance of the unoxidized polycrystalline nickel specimens are shown in Figures C-I and C-II. The values of the emittances for each of the runs are very close. Previous larger differences described by Shelton could have been due to surface irregularities caused by using onion skin paper during the milling operation. Also, the distance between potential leads was measured very accurately by a microscope.

High temperature emittances of the bare metal specimens up to 1230°C were also obtained, as shown in Figure IV-4. The larger differences between the runs were due to having used different batches of nickel for the runs.

In all of the bare metal runs, a small minimum was noted in the vicinity of the Curie temperature (359°C) of nickel. Initially it was

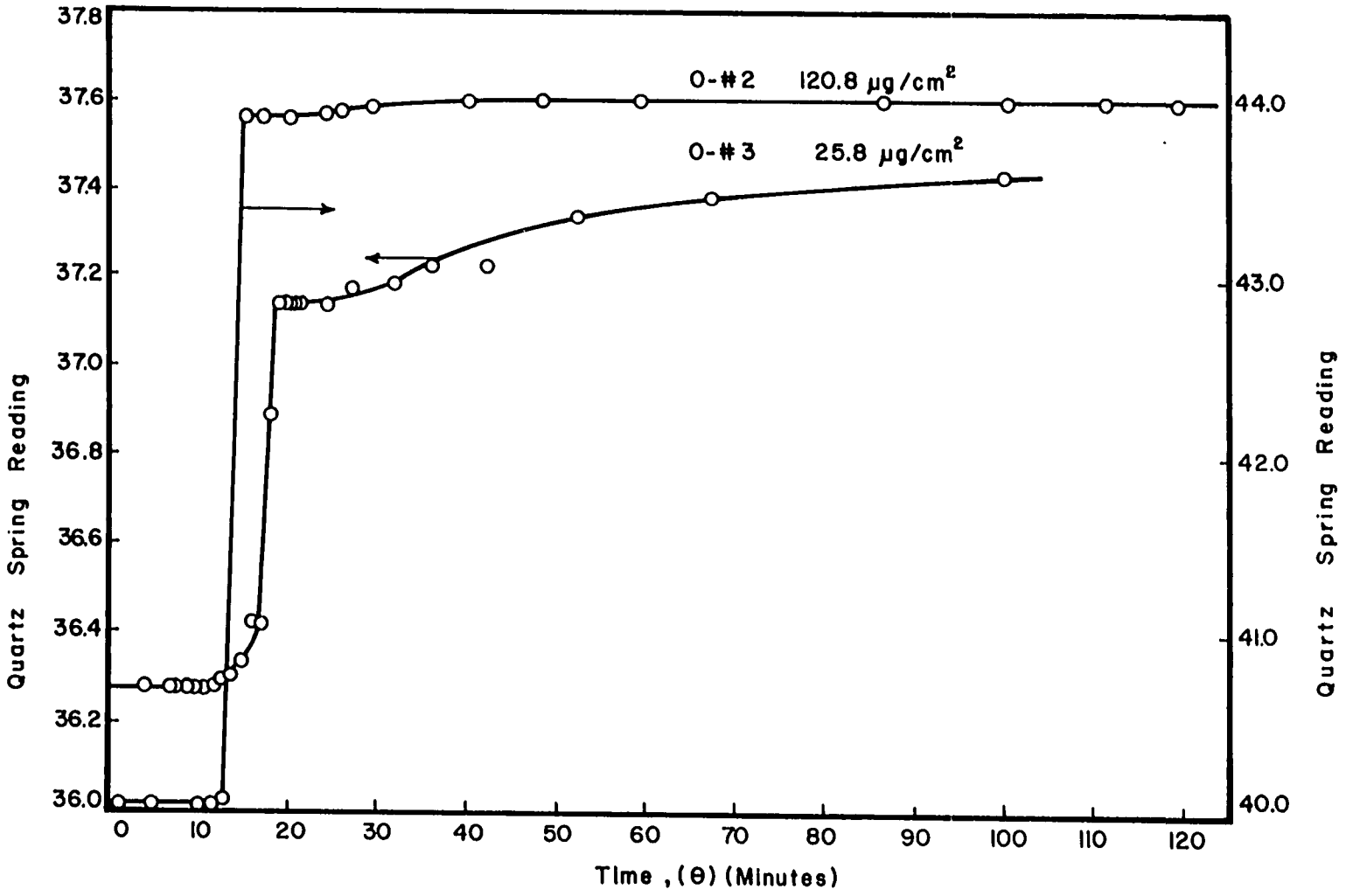

FIGURE Ⅳ-2 REDUCTION OF OXIDE (SPRING READING vs. TIME)

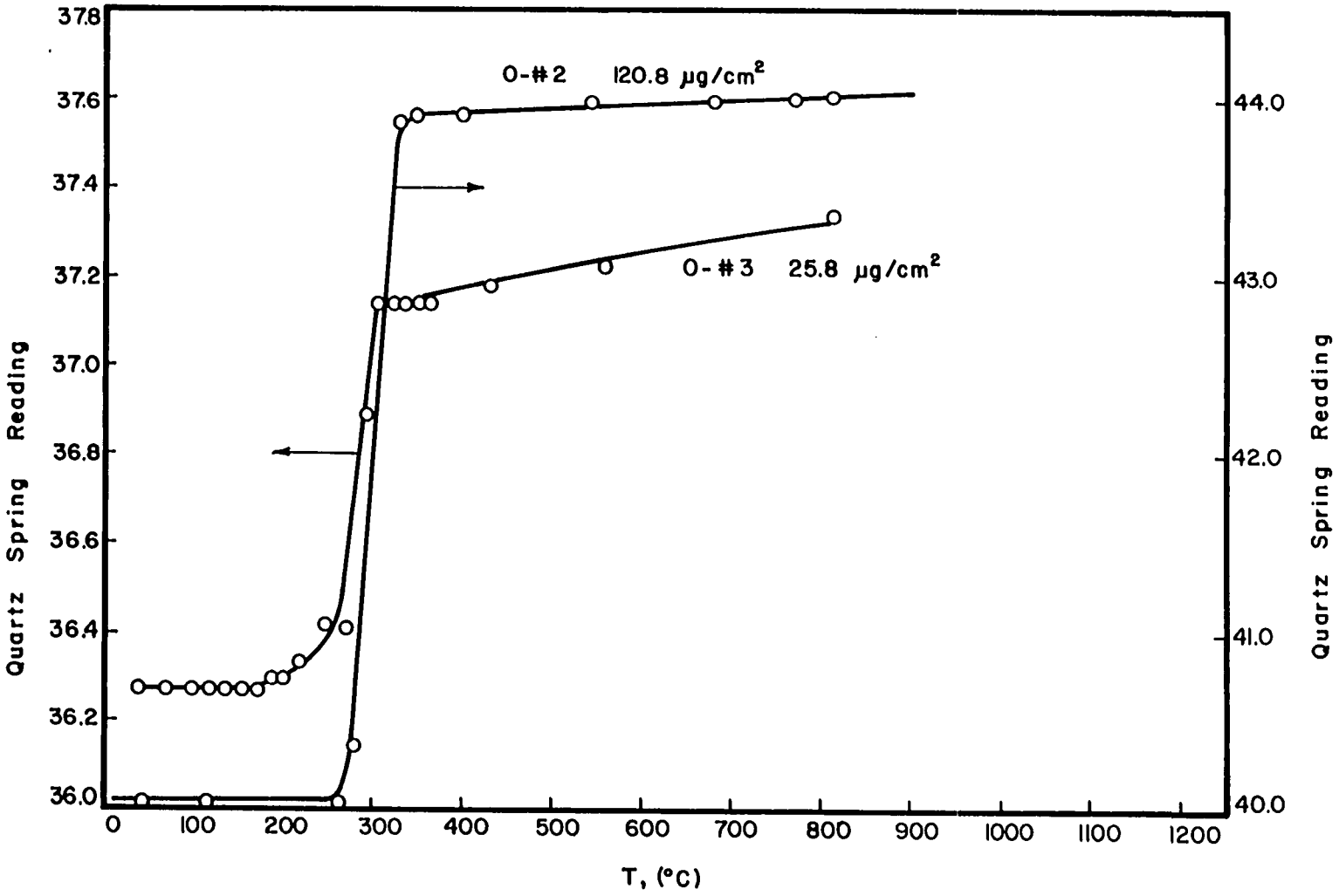

FIGURE IV-3 REDUCTION OF OXIDE (SPRING READING vs. TEMPERATURE)

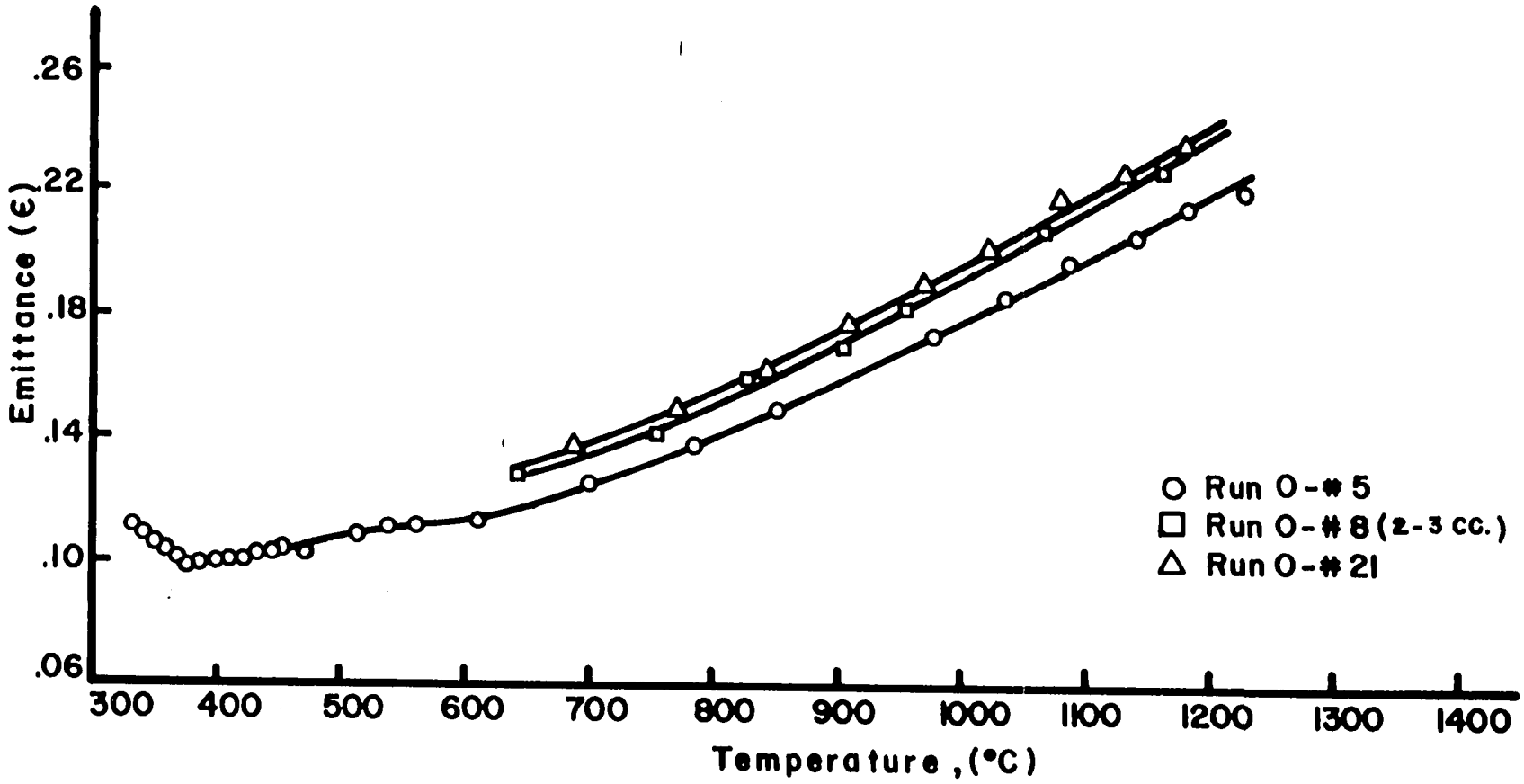

FIGURE IV-4 HIGH TEMPERATURE BARE METAL EMITTANCES FOR POLYCRYSTALLINE NICKEL

thought that the dip was due to conduction losses in the low temperature region with the 3" long samples; however, additional runs with 6" long samples indicated the same shape of curve. Also, other tests were made with the potential lead distance decreased to give a ratio of sample distance to potential lead distance of about 30-40 to 1. In all runs made, the "dip" in the curve appeared.

2. Bare Metal Emittance--Nickel Single Crystals

The shape of the bare metal emittance curves (ϵ vs. T) for the (100), (110) and (111) single crystals did not appear to be significantly different. The bare metal emittance curve for sample SE#3 was used as a baseline for comparing oxidized metal emittances. This curve was the closest to the average for all of the Semi-element samples.

A comparison of the polycrystalline bare metal emittances with the nickel single crystal curve SE#3 is shown in Figure C-I. The single crystal curve falls below the polycrystalline curves, since the single crystals had a highly polished surface on each side. The polycrystalline material from Chromium Corporation was manufactured by depositing nickel on a smooth substrate. Because of this, one side was smooth and polished whereas the other side was rough and dull. The average emittance for the nickel with one rough surface would be expected to be higher than if the nickel had both sides polished, as with the single crystals.

The differences between the bare metal emittance curves for the Semi-element (SE) samples as shown in Figures C-III, C-IV and C-V, are

greater than for the polycrystalline samples. Since each of the single crystal specimens were individually prepared, it was more difficult to obtain an identical surface for each sample.

The differences between the bare metal emittance curves for the samples prepared from the Research Crystal Inc. nickel crystal (Figures C-VI and C-VII) were greater since there were more differences in width and thickness for these samples. The two curves (OSC#4 and #7) which were much higher than the others, had spots from the chemical polishing.

The differences between the bare metal curves for the single crystals were greater in the lower temperature range because of variations in the sample to heat sink ratio. In comparing the oxidized emittances, a separate correction was made for the region below 600°C.

A minimum was also noted in the vicinity of the Curie temperature for all the single crystal runs.

3. Initial Emittance--Single Crystal vs. Polycrystalline

For polycrystalline nickel, an initial small amount of oxygen is merely adsorbed by the crystal internally. This is indicated in Figure C-I in which the curve with 3.25μg/cm^2 oxide is barely higher than the bare metal curve. With polycrystalline nickel, intergranular oxidation also depletes the oxygen internally.

With the nickel single crystals, there are no grains and therefore much less interstitial oxygen. This was indicated experimentally also, by showing there was no effect on bare metal emittances with annealing. Curves IV-9 to IV-12 and Figure C-III in Appendix C show

that a large difference was noted in the oxide emittance even with very low amounts of oxide.

The 0 μ g/cm^2 values shown in Figures IV-9 through 12 are those of the bare metal baseline curve (SE#3).

4. Correction for Comparing Oxides

To compare oxidized emittances, it was necessary to make two corrections as shown below:

(1) a correction for the differences in bare metal emittances and

(2) a correction for the differences in conduction losses due to differences in sample to heat sink ratio.

For the first correction, the ratio of ϵ_o/ϵ_B was obtained for each 40°C increment from 880°C to 600°C, where

ϵ_o = bare metal emittance for baseline curve (SE#3)

ϵ_B = bare metal emittance measured

The ratios of ϵ_o/ϵ_B were then averaged and this average correction ratio $\left(\frac{\epsilon_o}{\epsilon_B}\right)_{av.}$ was assumed for all temperatures. The range of 600-880°C was selected, since the bare metal curves were parallel within this range. Below 600°C, the curves began to differ in shape because of differences in conduction losses. Above about 600°C, the differences in bare metal emittances between runs was assumed to be due to measurement errors or surface differences.

Thus the corrected oxidized emittance data ($\epsilon_{ox.}$) for the range above 600°C was obtained as follows:

$T \geq 600^{\circ}C$:

$$(\epsilon_{ox.})_{corrected} = \left(\frac{\epsilon_o}{\epsilon_B}\right)_{av} \epsilon_{ox.} \qquad (4\text{-}2)$$

The values of this correction or area factor are shown in Tables (C-3) to (C-33) in Appendix C.

For the oxidized emittance values below $600^{\circ}C$, the second correction was also applied. Since this difference was assumed to be due to conduction loss differences, the correction was assumed to be additive. This second correction is shown below:

$T < 600^{\circ}C$:

$$(\epsilon_{ox.})_{corrected} = \epsilon_{ox.} \pm \left[\left(\frac{\epsilon_o}{\epsilon_B}\right)_{av} \epsilon_B - \epsilon_o\right] \qquad (4\text{-}3)$$

(Sample SE#3 was selected as the baseline bare metal emittance, since it was closest to the average for all the bare metal runs.)

5. Polycrystalline Oxidized Emittances

The effect of "oxide thickness" on emittance was initially investigated for thin polycrystalline nickel foils. The amount of oxide was varied from $3.25 \mu g/cm^2$ to $120.8 \mu g/cm^2$. The "as measured" values are shown in Figure C-I in Appendix C and the values adjusted with SE#3 as a baseline are shown in Figure IV-5. Two runs were made with a sample length of 6" instead of 3" as was used in the initial runs. These results are shown in Figure C-II in Appendix C.

The emittances of the polycrystalline foils generally agreed with that obtained by Shelton. The curves in this thesis, however, covered a lower temperature range.

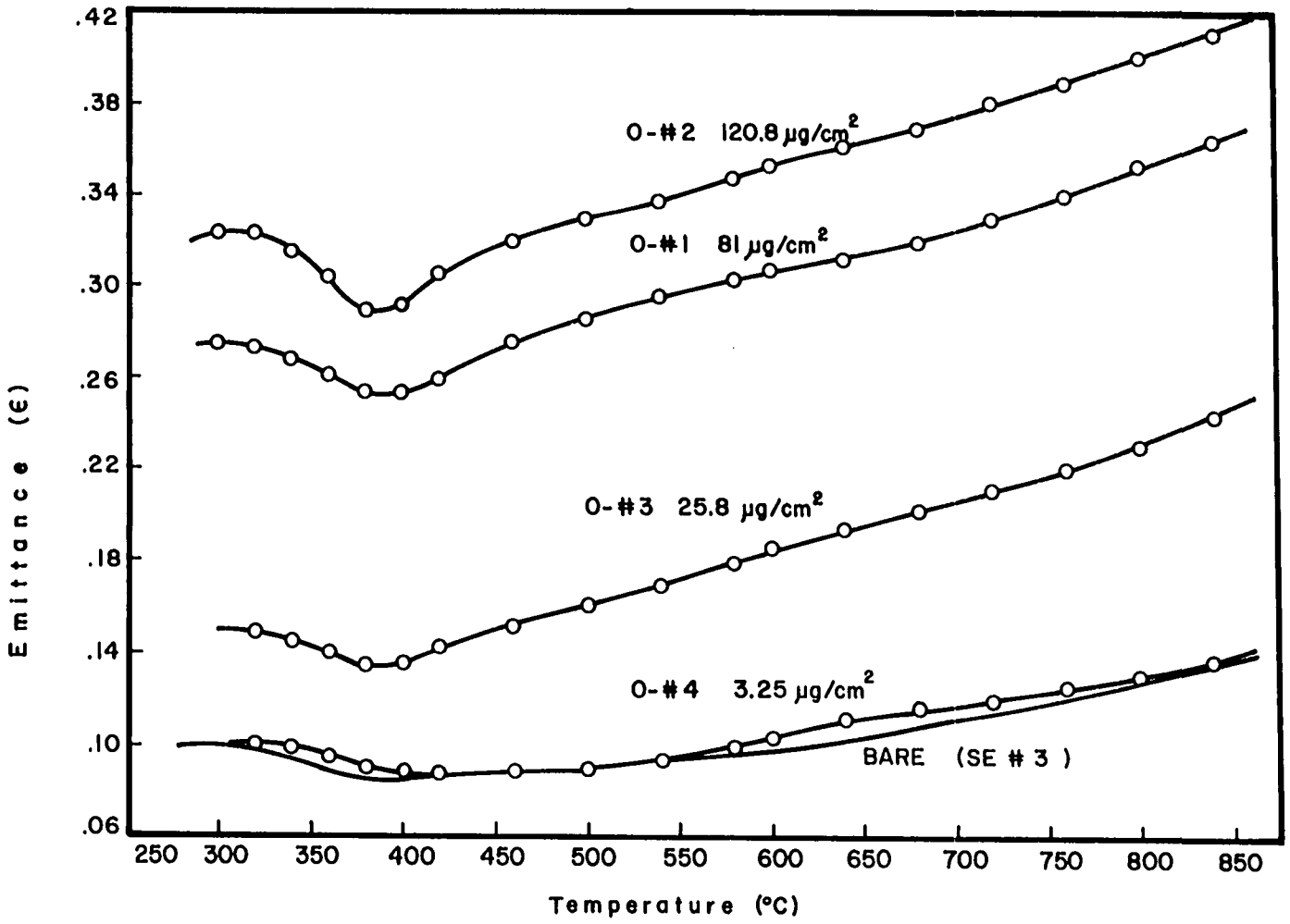

FIGURE IV-5 EMITTANCE vs. TEMPERATURE - EFFECT OF OXIDE THICKNESS FOR POLYCRYSTALLINE NICKEL (SE #3 AS BASELINE)

6. Oxidized Emittances of Nickel Single Crystals

The uncorrected oxidized emittances for the Research Crystal Inc. single crystals are plotted in Figures C-VI and C-VII in Appendix C. Oxide thicknesses from 18.96$\mu g/cm^2$ to 82.8$\mu g/cm^2$ were studied with the (110) oriented crystal face, whereas a thickness range of 13.5-77.2$\mu g/cm^2$ was investigated with the (100) crystals. The corrected curves for these same runs are shown in Figures IV-6 and IV-7. The correction, as previously mentioned, consisted of obtaining an adjustment ratio based on the differences in bare metal emittances.

The unadjusted curves for the (100), (110), and (111) faces of the Semi-element single crystals are shown individually in Figures C-III, C-IV and C-V in Appendix C. The corrected emittance curves for all three crystal planes are plotted in Figure IV-8. While obtaining these data, an effort was made to compare the three faces at several different thicknesses of oxide. For a given amount of oxide, the (111) crystal face appeared to have a higher emittance. The microphotographs taken of the various crystals showed that the oxide on the (111) face was more uniform than the other two faces. Thus for the same amount of oxide, more of the surface of the (111) face appeared to be covered with oxide. The low energy electron diffraction studies with very thin oxide films on nickel single crystals also indicated that the oxide formed differently on the (111) face. Also, it was shown that the same orientation of oxide formed on the (110) and the (100) faces whereas the (111) oxide formed on the (111) face.

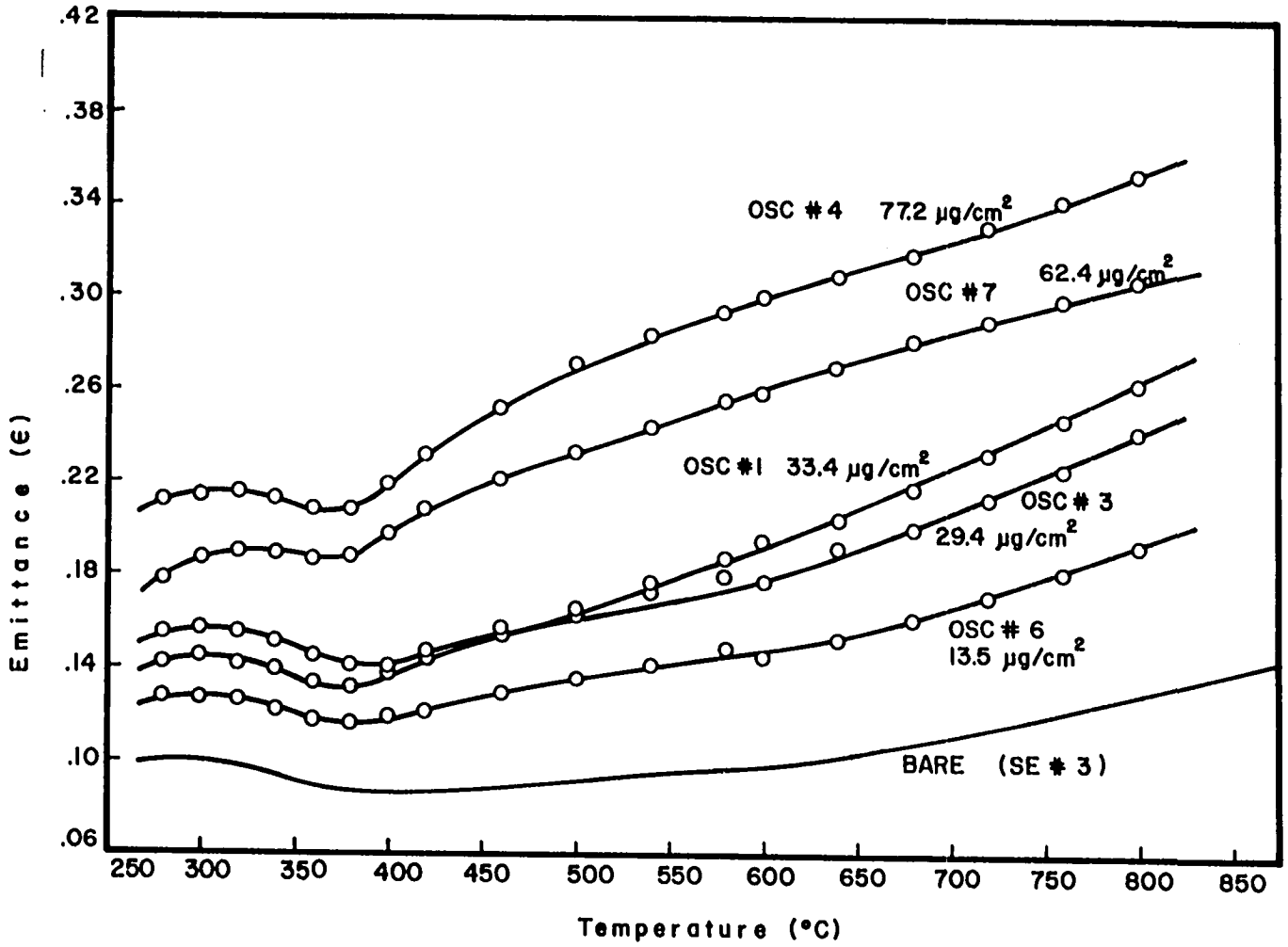

FIGURE IV-6 EMITTANCE vs. TEMPERATURE - EFFECT OF OXIDE THICKNESS FOR (100) R.C.I. SINGLE CRYSTALS OF NICKEL (SE #3 AS BASELINE)

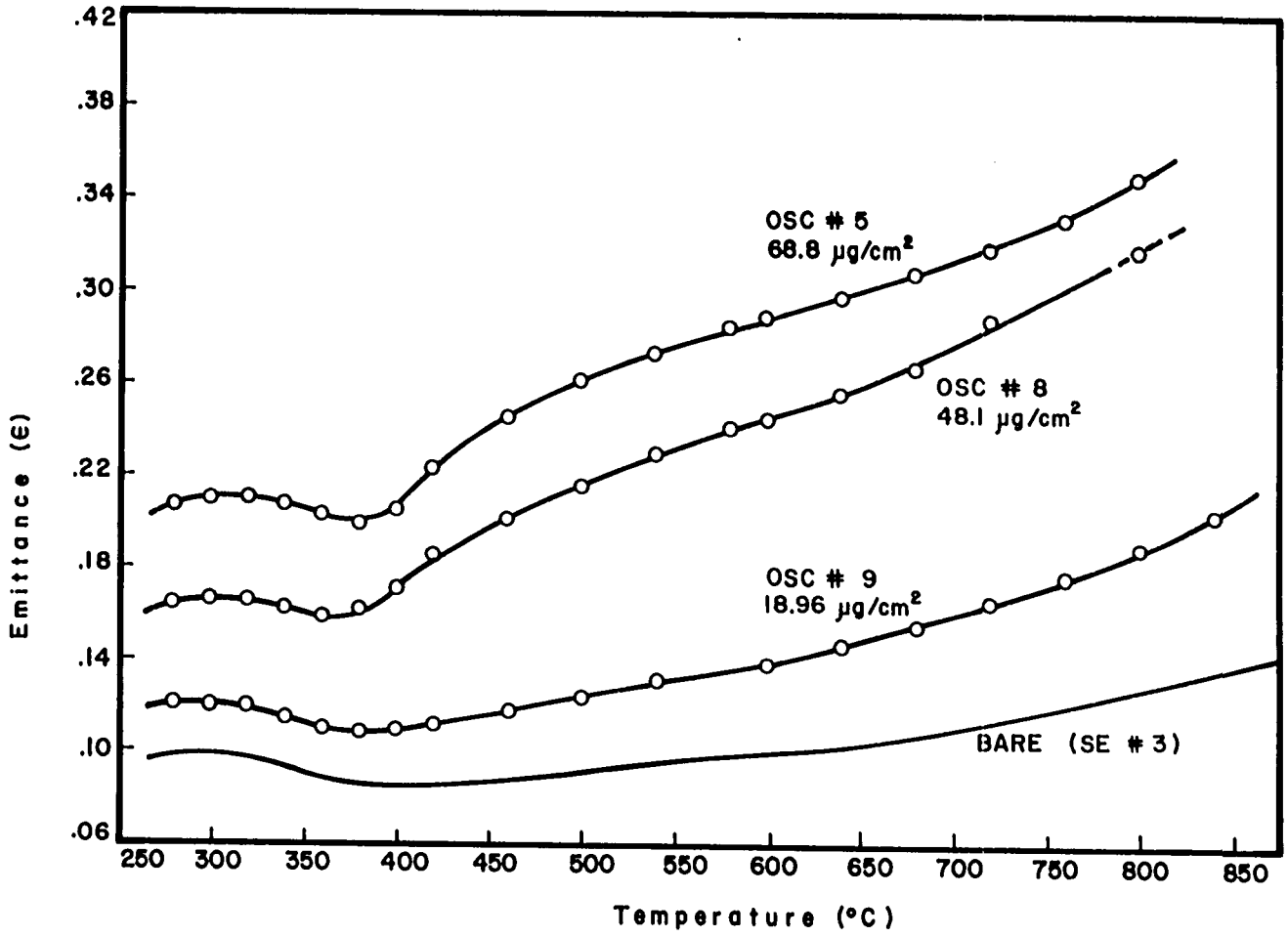

FIGURE IV-7 EMITTANCE vs. TEMPERATURE - EFFECT OF OXIDE THICKNESS FOR (110) R.C.I. SINGLE CRYSTALS OF NICKEL (SE # 3 AS BASELINE)

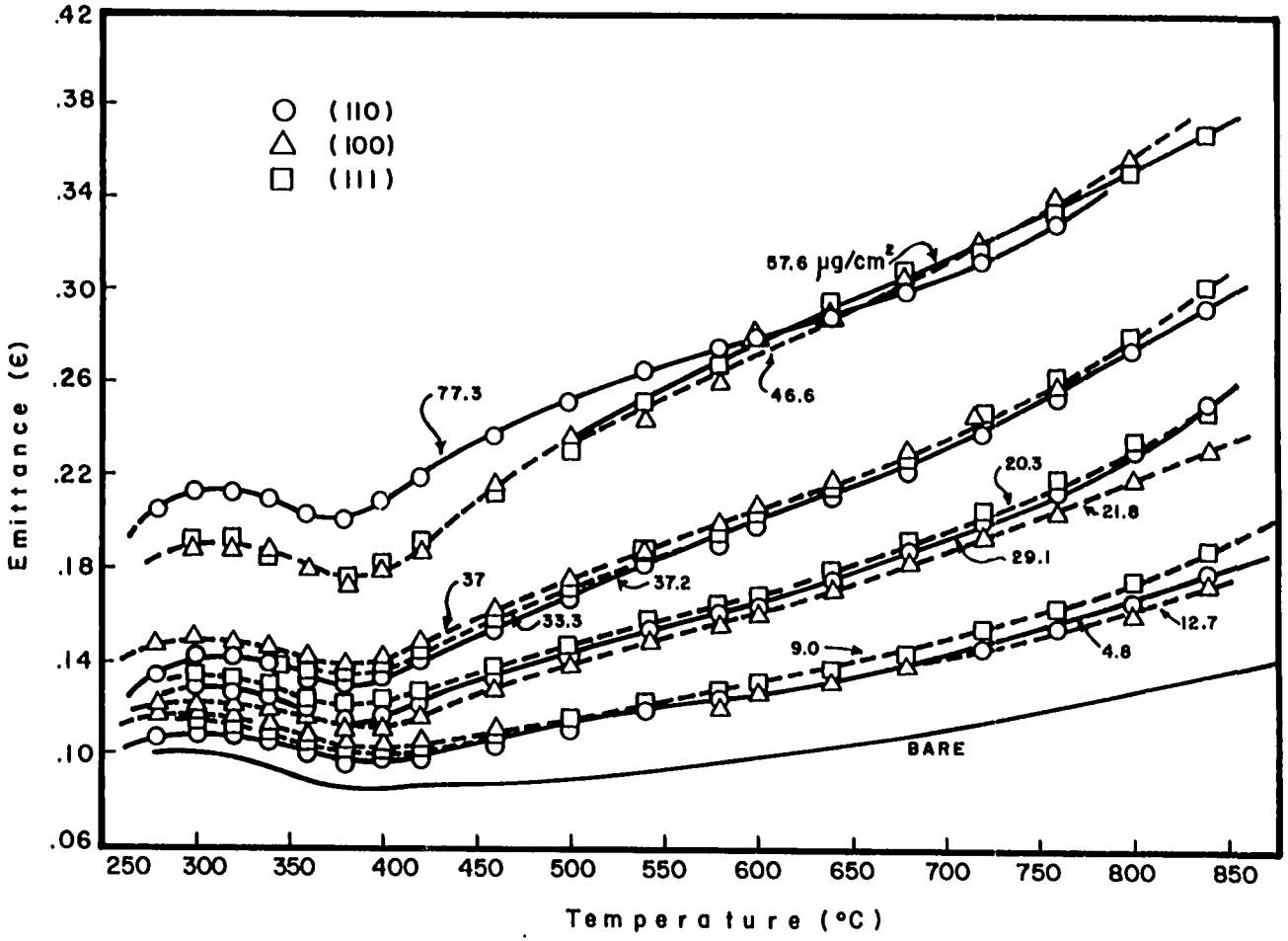

FIGURE IV-8 EFFECT OF OXIDE THICKNESS ON EMITTANCE vs. TEMPERATURE FOR THREE PRINCIPAL CRYSTAL FACES OF NICKEL

(SEMI-ELEMENTS CRYSTALS)(S.E. # 3 AS BASELINE)

Figure IV-12 is a plot of emittance vs. oxygen weight for all the single crystals and also the thick polycrystalline samples. All emittance values were at 800°C. The "zero oxide weight value" was that for the bare metal baseline sample SE#3.

The plot indicates that there was no significant difference between the (100) and (110) faces and the polycrystalline material. The (111) face appeared to be about 10% higher than the rest for a given oxide weight. Sample SE#7, which is a (100) crystal with 46.6 $\mu g/cm^2$ of oxide appeared to be anomalous.

Figures IV-9 to IV-11 are plots of the individual nickel single crystal "emittance vs. oxygen weight." Figures IV-9 and IV-10 include both Semi-element and Research Crystal Inc. crystals. Figure IV-11 includes only Semi-element crystals, since it was impossible to prepare long (111) crystals from the large single crystal purchased from Research Crystals Inc. These correlations shown in Figures IV-9 to IV-11 also show the effect of temperature, since the emittances were at 800°C and 600°C.

The curves show a gradual increase in emittance with oxide weight. It appears that there was a gradual leveling off at about 60 $\mu g/cm^2$. Microphotographs taken in this region indicated that most of the metal had been covered with oxide. The further thickening of the oxide did not greatly change the texture or roughness of the surface.

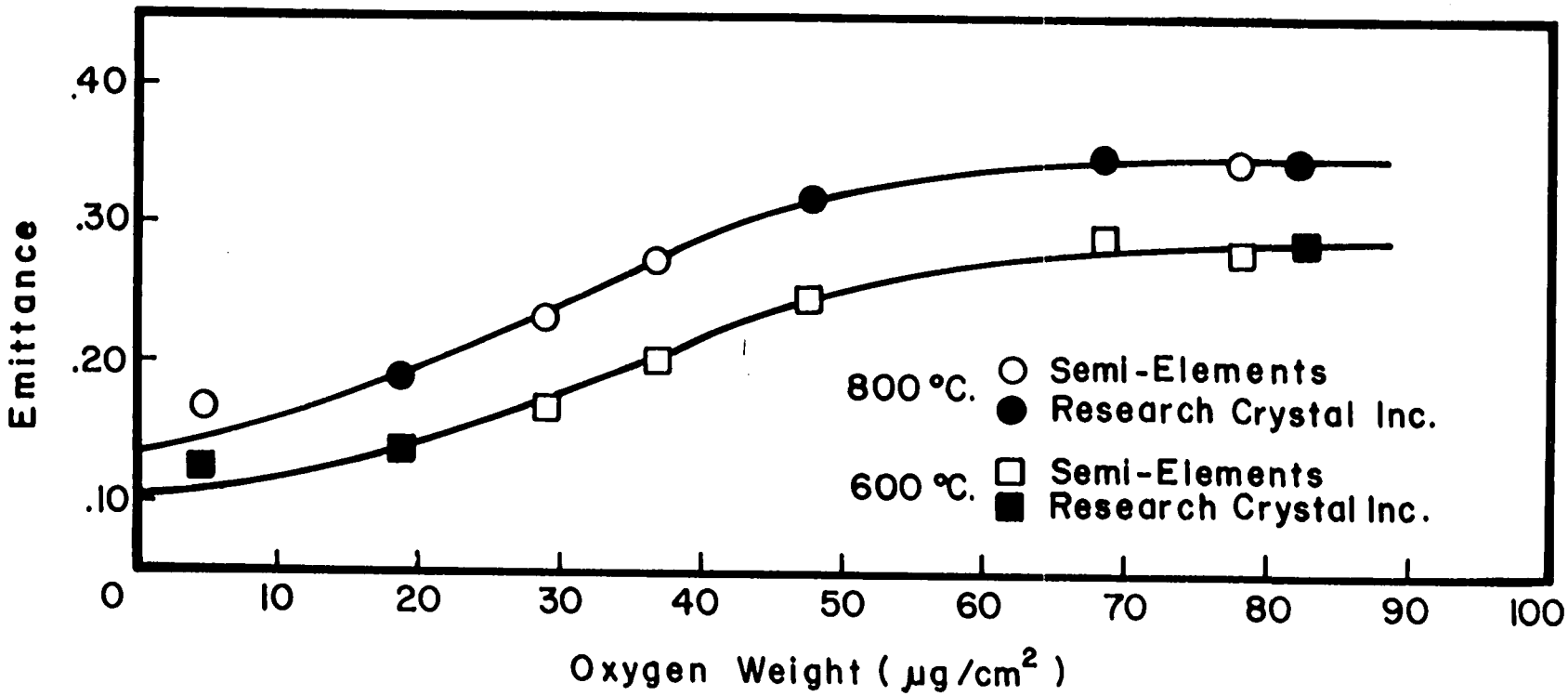

FIGURE IV-9 EMITTANCE vs. OXYGEN WEIGHT FOR COMBINED (R.C.I. & S.E.) (110) NICKEL CRYSTALS AS A FUNCTION OF TEMPERATURE

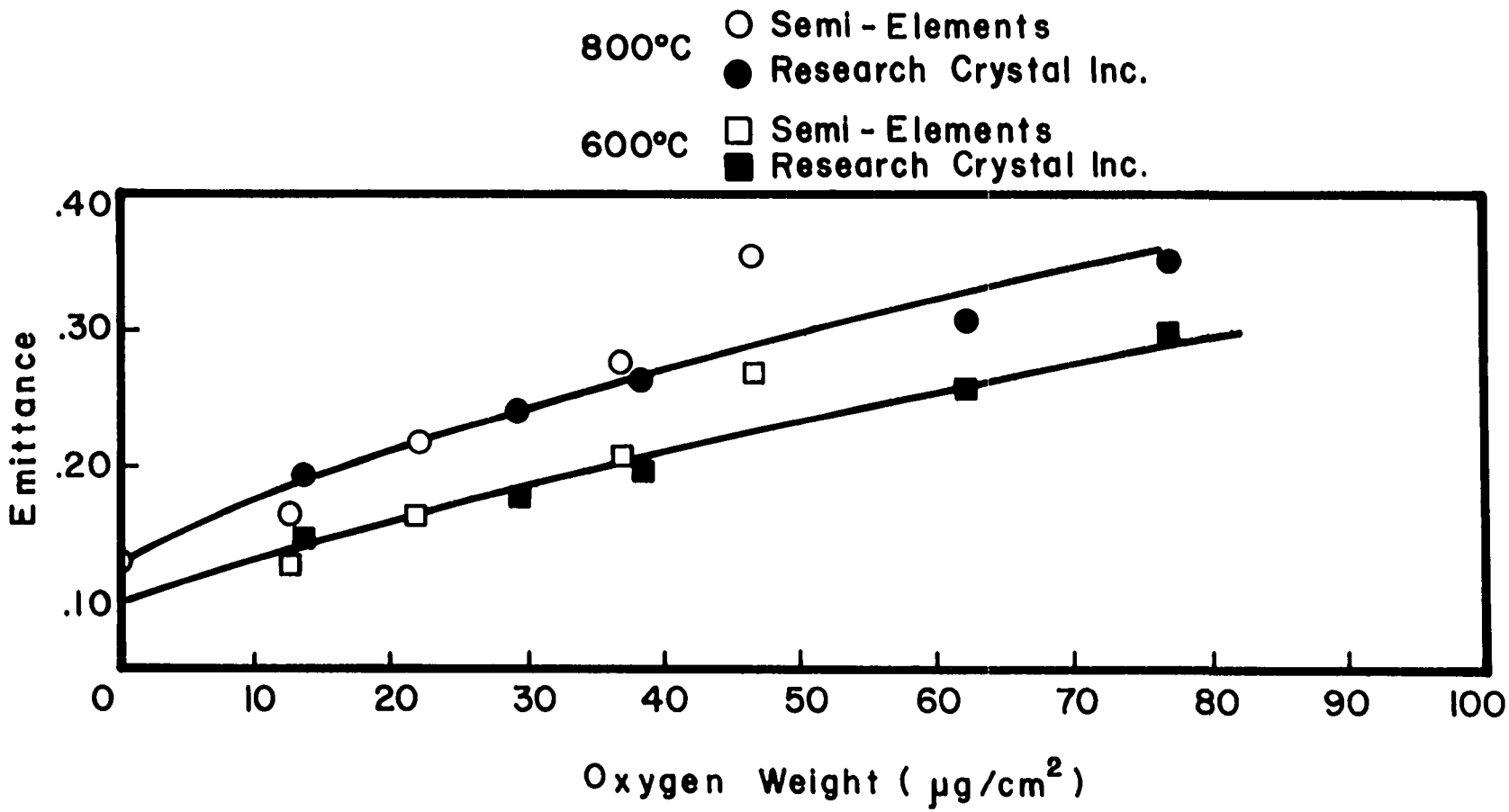

FIGURE IV-10 EMITTANCE vs. OXYGEN WEIGHT FOR COMBINED (RCI & S.E.)(100) NICKEL CRYSTALS AS A FUNCTION OF TEMPERATURE

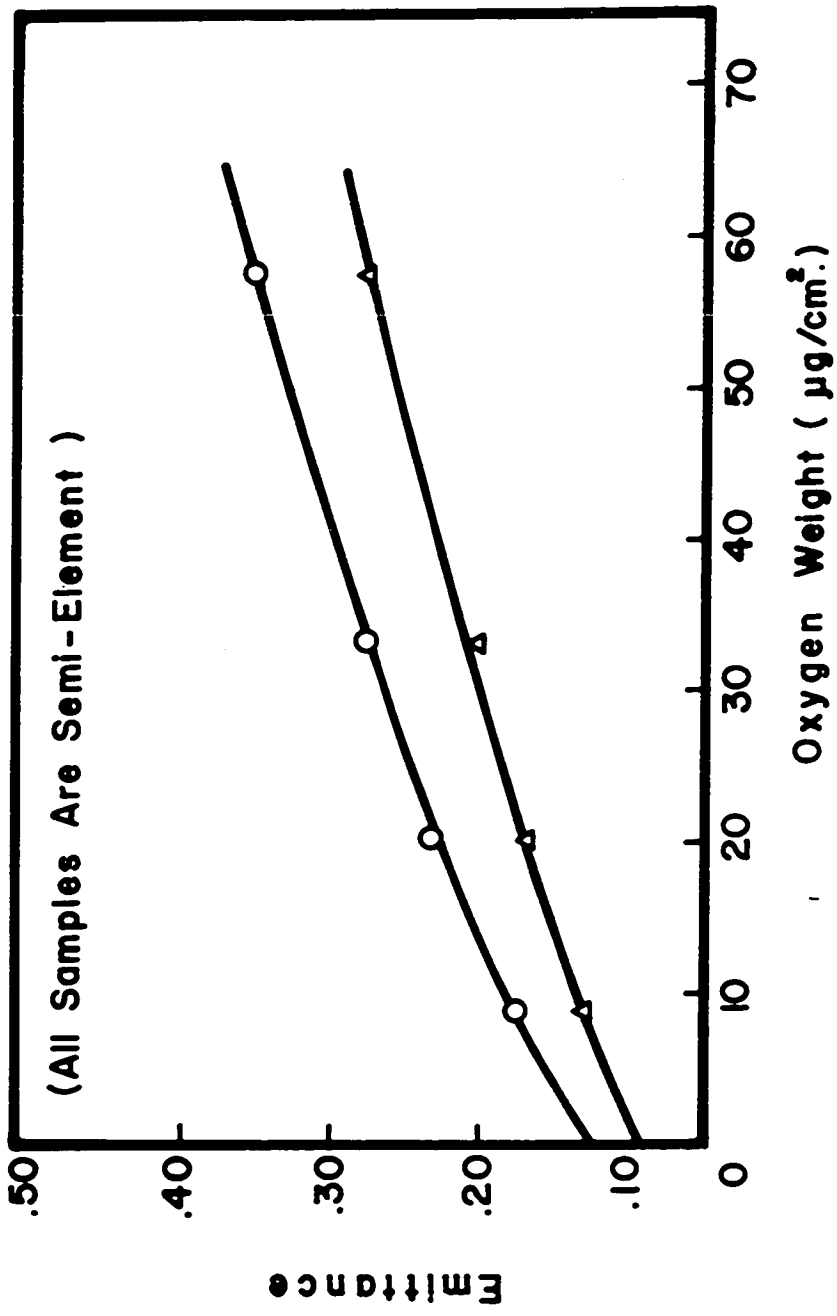

FIGURE IV-11 EMITTANCE vs. OXYGEN WEIGHT FOR (111) NICKEL SINGLE CRYSTALS AS A FUNCTION OF TEMPERATURE

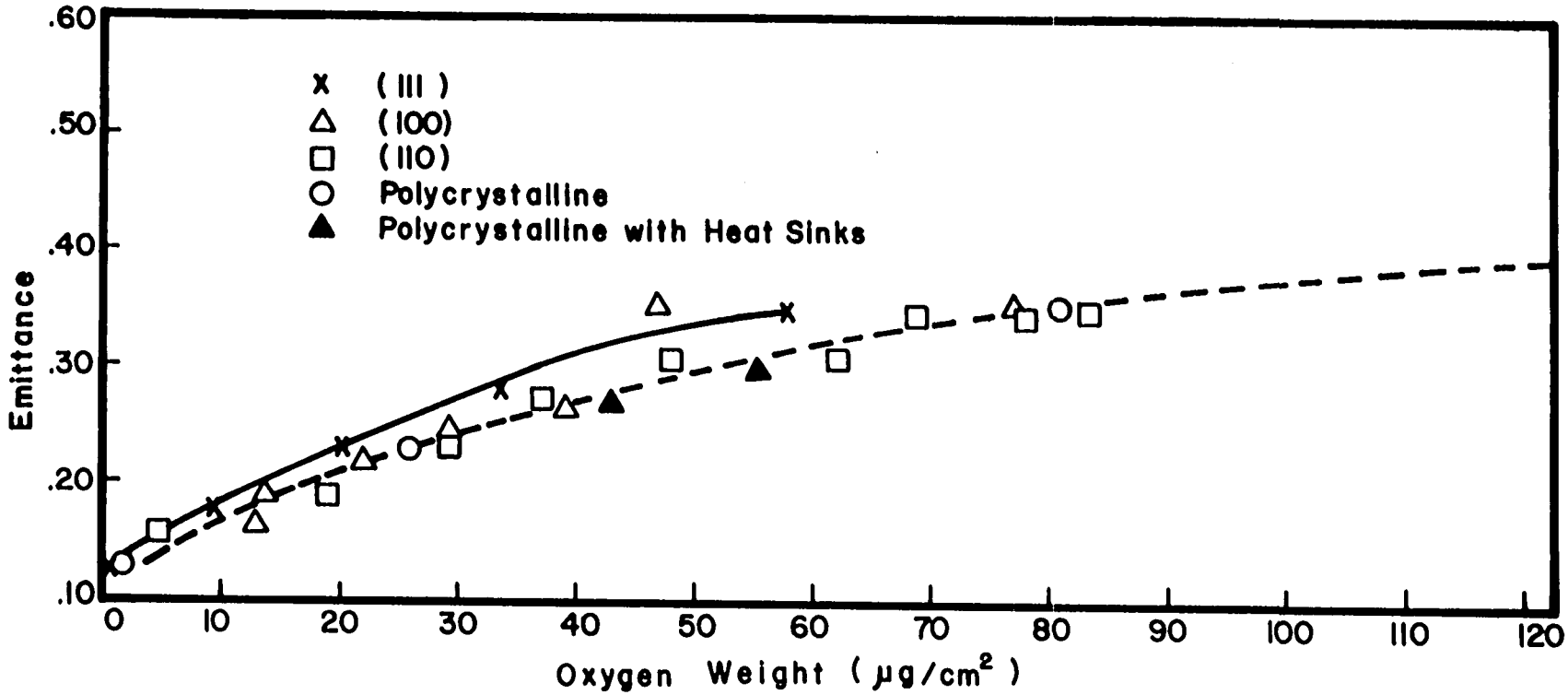

FIGURE IV-12 COMPARISON OF "EMITTANCE vs. OXYGEN WEIGHT" FOR (100),(110),(111) CRYSTAL FACES OF NICKEL vs. POLYCRYSTALLINE
TEMPERATURE 800° C.

C. Oxidation Rates and Activation Energy

1. Oxidation Rate

Although the primary purpose of this study was to obtain emittance data, an attempt was made to collect kinetic data during the process. Because the equipment and experiment were not designed to obtain rate data, it was impossible to obtain isothermal kinetic data. The sample was oxidized in 1000 microns of air in the emittance chamber. As the sample oxidized, the resistance and emittance changed. Because of the resistance increase with oxidation, the sample temperature tended to increase when operating with a constant current. However, because the emittance increased with temperature, the sample temperature tended to decrease during oxidation. The emittance change was much greater than the resistance change and therefore the overall result was a decrease in sample temperature during oxidation.

The oxidation data are summarized in Appendix D. As shown in Table (D-1), the difference between the maximum temperature and the average temperature during oxidation varied from about 5°C for the very thin oxide run to about 75°C for one of the thick oxide runs. A weighted average temperature was used in plots to obtain the activation energy.

The oxidation time for the single crystals varied from 2.5 to 96.5 minutes. Generally, it was observed that temperature was the most important factor in obtaining a specified oxide thickness. It appeared that most of the oxide formed in the first few minutes. This would suggest that the oxidation followed a log law. Thus in order to obtain a thicker oxide film, it was necessary to increase the temperature.

An error occurred in the rate calculations because of the time required to heat the sample to a steady state temperature. In most cases, this heat-up period was excluded from the oxidation time, since the temperatures during this period were outside the range of oxidation temperature. In some instances, however, a correction was added for this period. A steady state temperature was assumed to be reached when the voltage drop across the potential leads increased to a maximum and then slowly decreased.

Some oxidation rate data were taken during certain runs, as shown in Table (D-2). In comparing the emittances of the three nickel single crystal faces, it was necessary to obtain the same emittance curve for each of the faces. This necessitated a trial and error technique in which the sample was oxidized and the emittance checked. If the emittance were too low, additional oxidation was incurred and another emittance check made. This was continued until the desired emittance value was attained. It was possible to use some of this intermediate data to calculate initial oxidation rates. To do this, it was necessary to plot a curve of emittance vs. oxide weight at the temperature at which the emittance check was made. This was done by using other data for the plot. Thus intermediate values for oxide weight was obtained by interpolating from this curve.

Upon observation of Figures IV-13 through IV-15, it appeared that the (110) face oxidized the fastest in all three regions and the (100) face the slowest, although there was some discrepancy in the "nuclei formation region."

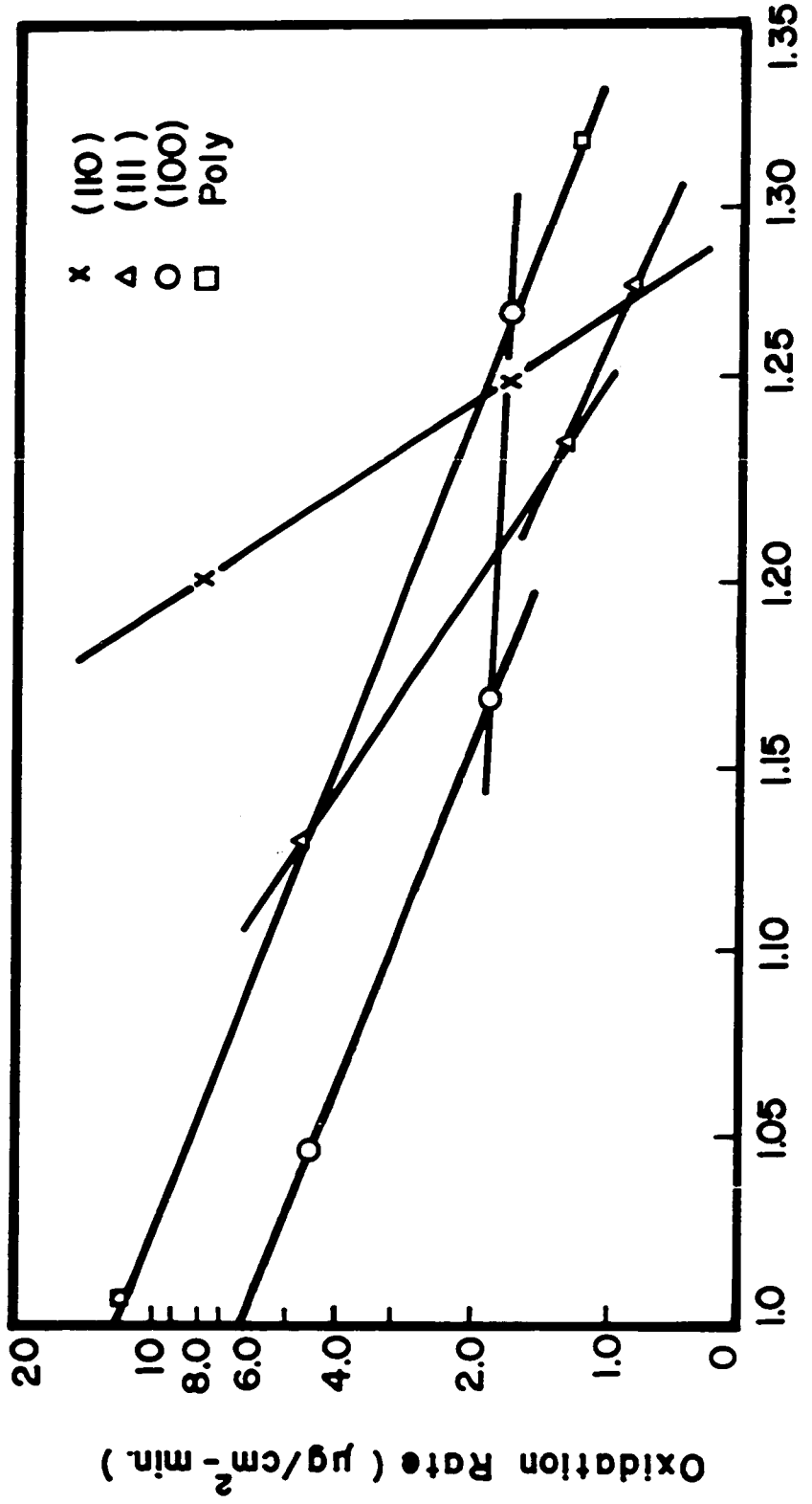

FIGURE IV-13 RATE OF OXIDATION vs. T
"NUCLEI-FORMATION REGION"
(3.25 - 20.4 μg/cm² Oxide)

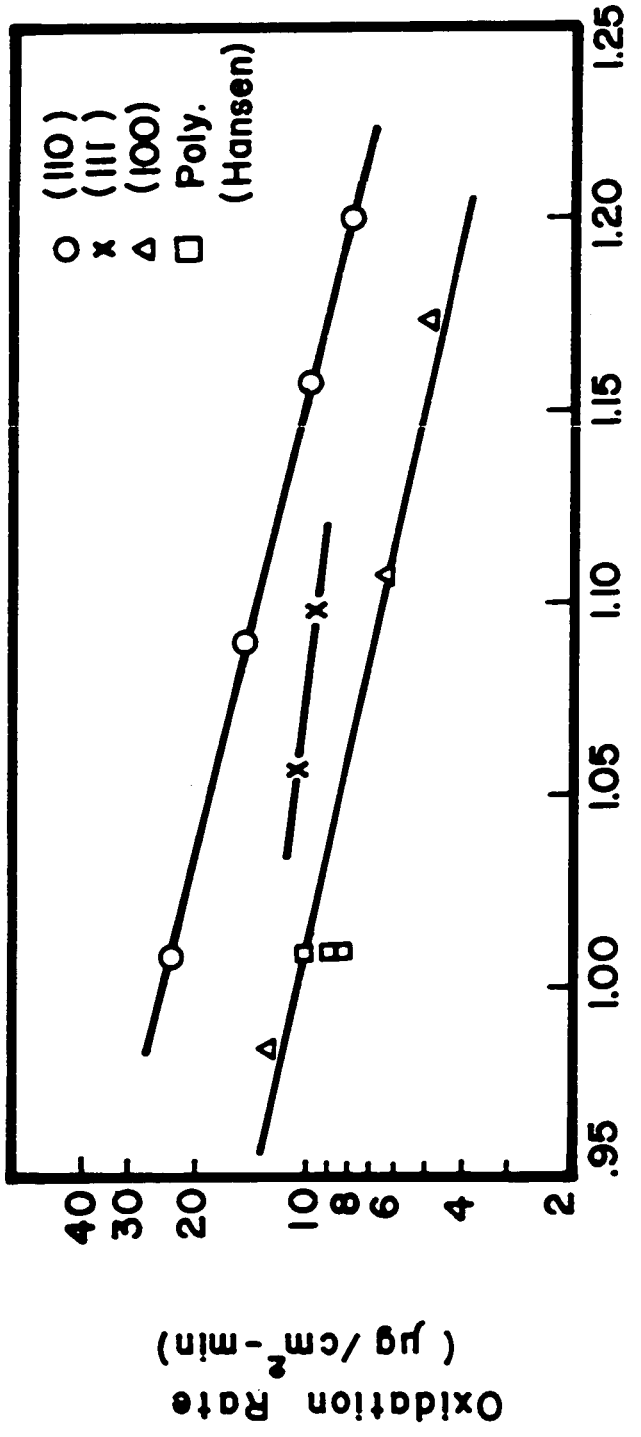

FIGURE IV-14 RATE OF OXIDATION vs. T "INTERMEDIATE OXIDE REGION" (19 - 38.4 μg/cm² Oxide)

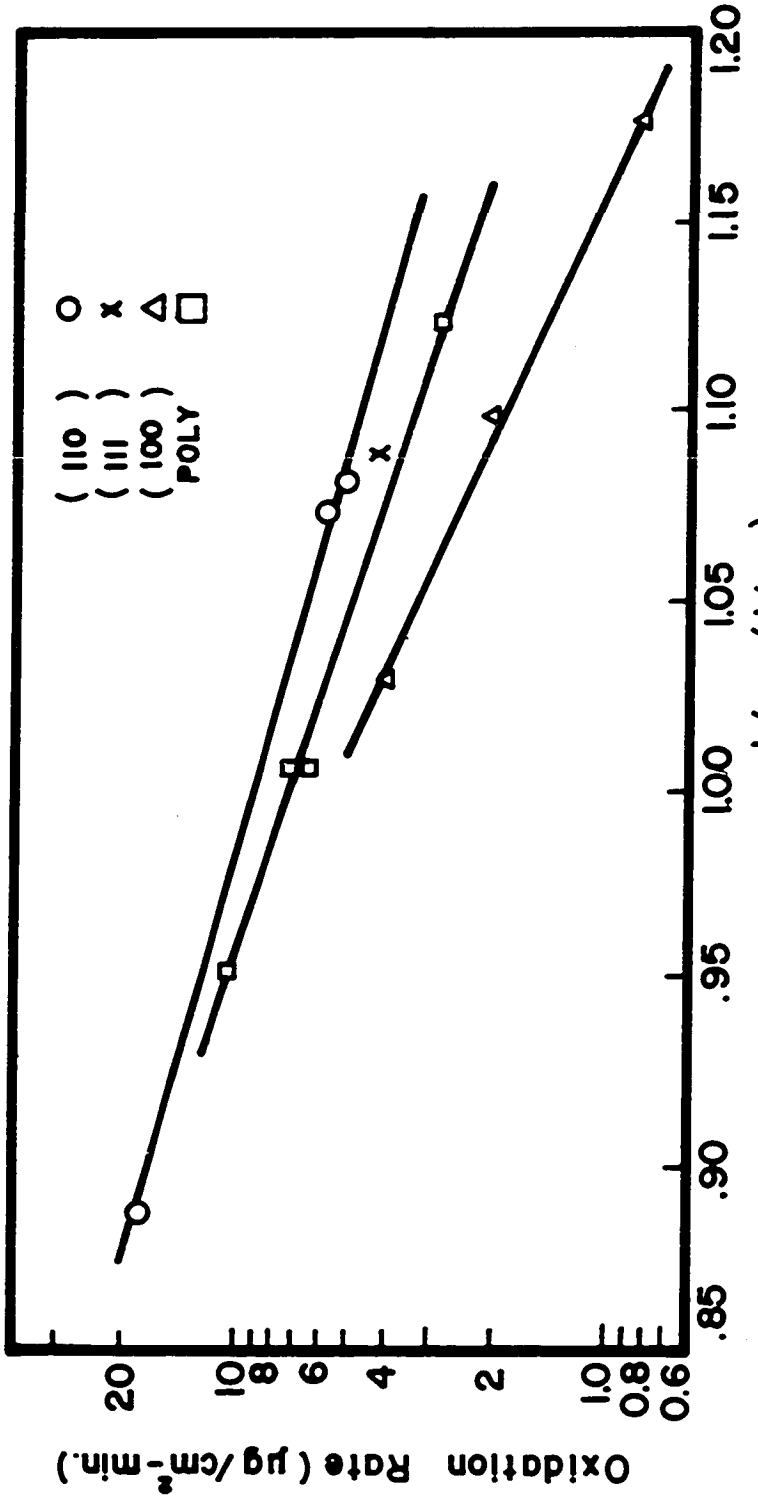

FIGURE IV-15 RATE OF OXIDATION vs. T.-"HEAVY OXIDE" REGION (42.9-82.8 μg/cm²-min.)

The oxidation rate data for the thin polycrystalline foils, as shown in Table (D-6) in Appendix D, were poor because of the large resistance change in the sample during oxidation. Since the surface temperature determination required a knowledge of the room temperature resistance of the sample, it was difficult to obtain a true average oxidation temperature. The polycrystalline rate data used in the plots of log k vs. 1/T were those from Hansen (15) and also included the two thick polycrystalline sample runs, shown in Tables (D-7) and (D-8) in Appendix D.

2. Activation Energy

As can be seen in Figures IV-13 to IV-15, it was necessary to separate the data for plotting log of the rate vs. 1/T into three different regions. These were designated, as shown in Tables (D-3) to (D-5) in Appendix D, as

(1) "the nuclei formation region,"

(2) "the intermediate oxide region," and

(3) "the heavy oxide region."

When the data were separated in this manner, straight lines were obtained.

In the "nuclei formation region," very little data were available, as shown in Figure IV-13. Also, as can be seen in this plot, there were breaks in the curves of the (100) and (111) faces. The "nuclei formation region" included weights of oxygen ranging from 3.25 to 20.4 $\mu g/cm^2$. The "intermediate region" included oxygen weights from

19 - 38.4 $\mu g/cm^2$. The "heavy oxide" covered the range of 42.9 - 82.8 $\mu g/cm^2$. Although this was designated "heavy oxide region," it consisted of essentially complete coverage of the metal with oxide but was still only about 3000 - 5000 Å thick.

The activation energies for the different nickel single crystal faces were calculated by means of Arrhenius's equation

$$k = A \cdot e^{-Q/RT} \qquad (4\text{-}4)$$

where k = rate constant

A = constant with same dimensions as k

Q = activation energy

T = absolute temperature

R = gas constant

By plotting the log of the rate constant vs. 1/T, Q could be calculated by measuring the slope.

The activation energies calculated from the slopes are shown in Table (4-2).

Table (4-2)

Calculated Activation Energies (kcal/mole)
Ni→NiO

	Oxide Thickness		
	"Nucleation" 3.25 - 20.4 $\mu g/cm^2$	"Intermediate" 19 - 38.4 $\mu g/cm^2$	"Heavy" 42.9 - 82.8 $\mu g/cm^2$
(110)	59	11.5	13
(111)	25 17	6	
(100)	15 18.5	10	21
Polycrystalline	15		15.5

As seen in the plots of log k vs. 1/T, there was very little data available. In some instances, a straight line was drawn through two points, which left much to be desired.

As shown in Table (4-2), the activation energies generally fell in the range of 10 - 25 kcal/mole for both polycrystalline nickel and single crystals. The high value of 59 kcal/mole for the (110) face in the "nuclei formation region" and the low value of 6 kcal/mole for the (111) face in the intermediate region were both based on plots with only two points.

Although most of the previous activation energy data for nickel had been calculated from thick oxide film formation following the parabolic rate equation, some data were found for thin films, as shown in Table (4-3).

Table (4-3)

Activation Energies by Other Investigators

Investigator	Conditions		Activation Energy kcal/mole
Campbell (5)	2.5 - 15 $\mu g/cm^2$		25
	15 - 25 $\mu g/cm^2$		25 - 45
	25 - 40 $\mu g/cm^2$		45
Gulbransen and Andrew (14)	Parabolic oxidation		41.2
Moore (24)	"	"	38.4
Fueki and Ishibashi (13)	"	"	28.4
Sartell and Li (29)	Inner oxide layer		20
Uhlig, Pickett and Macnairn (33)	Thin > Curie T		21
	Oxide < Curie T		19.9
Phillips (25)	Thick oxide		38
Benard et al. (3)	Film formed on Cu	(100)	23
		(110)	10
		(111)	8
		(311)	15

The calculated values were generally of the same order of magnitude as the thin-film oxides shown in Table (4-3).

D. Examination of Oxidized Samples

Colored microphotographs were taken of the various oxidized single crystals. These are shown in Figures 1-P to 46-P in Appendix G. Pictures 1-P to 24-P were taken with a magnification of 50 power; the remaining pictures were at 1000x.

Figure 24-P is that of a polycrystalline nickel foil with 43.1 $\mu g/cm^2$ of oxygen. As can be seen in this microphotograph, all the various interference colors were present. Since each exposed crystal orientation oxidized at a different rate, the various faces each exhibited a different thickness of oxide.

Table (4-4) contains a listing of the samples with a description of the colors seen on the microphotographs. As can be seen in the pictures, relatively few contained a single color. Only the samples containing a very thin film of oxide appeared to be uniform enough to exhibit a single characteristic color. All other samples, as expected, had different thicknesses of oxide on the crystal surface.

Thus it appeared that a very thin homogeneous oxide film formed initially, followed by nuclei formation and conglomerations of nuclei or polyhedra. Each of the various forms of oxide were of a different thickness and oxidized at a different rate and therefore exhibited different colors due to interference.

The microphotographs at 1000 power showed the formation of nuclei on the surface. The distribution of oxide nuclei was more uniform for

Table (4-4)

Colors of Oxidized Samples Seen in Microphotographs

Figure	Sample	Crystal	Oxide	Color
4-P	SE#1	(110)	4.9	pinkish-red
8-P	SE#3	(110)	29.1	red-yellow-green
9-P	SE#2	(110)	37.2	orange-green
16-P	SE#4	(110)	77.3	dark brown
2-P	SE#5	(100)	12.7	yellow-gold
7-P	SE#6	(100)	21.8	greenish-orange
12-P	SE#8	(100)	37.0	greenish-orange-brown
14-P	SE#7	(100)	46.6	greenish-dark brown
3-P	SE#9	(111)	9.0	yellowish brown
5-P	SE#12	(111)	20.3	bluish-green
11-P	SE#10	(111)	33.3	orange-brown
15-P	SE#11	(111)	57.6	dark brown
17-P	OSC#6	(100)	13.5	green
18-P	OSC#3	(100)	29.4	red-green
19-P	OSC#1	(100)	38.1	greenish-dark brown
20-P	OSC#4	(100)	77.2	greenish-brown
21-P	OSC#8	(110)	48.1	light brown
22-P	OSC#5	(110)	68.8	greenish-brown
23-P	OSC#2	(110)	82.8	greenish-brown
24-P	O-#15-10W1x5	Polycrystalline	43.1	green-blue-pink-brown

the (111) face. Both the (100) and (110) crystal faces seemed to contain groupings of the nuclei. Thus for a given amount of oxide, the (111) surface would have had more of the metal covered by the oxide. As mentioned earlier, the emittance of the oxidized (111) surface was higher than for the other two crystal faces for a given amount of oxide. Since the emittance of oxide is much greater than that of the bare metal, the microphotographs would tend to predict the higher emittance of the (111) face.

Table (G-1) in Appendix G shows a listing of the microphotographs with the exposure and development time required for each photograph.

Earlier studies to determine the thickness of the oxide film on nickel based on interference colors are shown in Tables (4-5) to (4-7). These studies, however, were made on polycrystalline nickel and as can be seen in photograph 24-P in Appendix G, practically all colors are represented. The same colors and repetition of colors, however, were noted in the microphotographs.

Several back reflection Laue x-ray pictures were made of the single crystals after oxidation and reduction to determine if the single crystal structure still existed. These pictures are shown in Figures G-I to G-III in Appendix G and are described below.

Figure G-I - OSC#1 - (100) - 38.4 $\mu g/cm^2$

Figure G-II - OSC#6 - (100) - 13.5 $\mu g/cm^2$

Figure G-III- OSC#2 - (110) - 82.8 $\mu g/cm^2$

The above listing of oxide was before reduction in H_2. The samples represented a thin, intermediate and thick oxide level.

Table (4-5)

Colors Produced by Oxide Films (Reflected) before and after Stripping from Metal (20)

Colors of Metal	Colors after Transfer
Yellow I	Bluish White
Mauve I	Whitish
Blue I	Yellow
"Silvery Hiatus"	Red
Yellow II	Mauve to Blue
Red II	Green
Blue II	Yellow
Green II	Red
Red III	Green

Table (4-6)

Thickness of Oxide Films on Nickel (20)

Order	Color of Nickel Oxide	°A
First	Dark Brown	380
	Red Brown	420
	Very Dark Purple	450
	Very Dark Violet	480
	Dark Blue	500
	Pale Blue Green	830
Second	Pale Silvery Green	880
	Yellowish Green	970
	Full Yellow	980
	Old Gold	1110
	Orange	1200
	Red	1260

Table (4-7)

Colors Produced by Activated Reduced Nickel (9)

A - Grey nickel

B - Faint brown

C - Light brown

D - Very dark brown

E - Violet

F - Very dark blue

H - Green grey

I - Yellow

J - Full brown

K - Violet

L - Blue

M - Greenish: final color of NiO

As can be seen in the x-ray in Figure G-II which represented the sample that had had the least amount of oxide, an excellent Laue picture still existed. A visual observation of the sample after reduction indicated a very highly polished surface with little or no after effects from oxidation.

A good Laue pattern also existed on the sample in Figure G-I which had had 38.4 $\mu g/cm^2$ of oxide. It appeared that the crystal orientation was a few degrees off; however, it was not known if this existed in the original sample. A visual observation of the surface after

oxidation and reduction showed several white spots on the otherwise polished surface.

The Laue x-ray in Figure G-III represented the single crystal with the heaviest oxide history. Also it was a (110) crystal whereas the other two were (100) crystals. This x-ray indicated considerable damage to the crystal during oxidation and reduction. The spots on the x-ray that were visible were strained and there appeared to be quite a bit of scattering. A visual observation of this crystal after oxidation and reduction indicated that the surface was no longer polished, but contained a whitish-metal appearance.

It must be remembered, however, that the Laue x-ray represented not only the surface, but also some of the bulk metal.

APPENDIX A

DESCRIPTION OF MATERIALS

Appendix A contains a description of the materials used in the studies. Included is an analysis of the polycrystalline nickel used along with a brief description of the purity of the single crystals. The purity of the gases used during the experiments is also discussed.

A. Thin Polycrystalline Foil

The thin polycrystalline nickel foil was electrolytic Grade A Foil manufactured by the Chromium Corporation of America. The analysis is given below.

Table (A-1)

Analysis of Chromium Corporation Nickel Foil

Ni	99.40%	Pb	< 0.001%
Co	0.53%	Sb	< 0.001%
Zn	< 0.001%	Cd	< 0.001%
S	0.015%	C	< 0.001%
Cu	0.009%	Mg	< 0.001%
Fe	0.013%	Mn	< 0.001%
Si	< 0.001%		

Since this foil is electrodeposited, there is one smooth, shiny side and one matte "etched" side.

B. Thick Polycrystalline Foil

The thick polycrystalline nickel was manufactured by the Wilkinson Company. It is an as rolled nickel alloy 270 which is 99.97% pure. The analysis of Nickel 270 is shown below.

Table (A-2)

Analysis of Nickel 270

Ni	99.97%	S	Trace
C	0.02%	Si	Trace
Mn	Trace	Cu	Trace
Fe	Trace	Cr	Trace

C. Nickel Single Crystals

(1) SE Samples

Twelve of the nickel single crystal samples described as "SE Samples" were purchased from Semi-Elements, Inc. These included four (100) oriented samples, four (110) oriented samples and four (111) oriented samples. The samples were received with an as etched satin finish surface. The samples contained 99.99% nickel.

(2) OSC Samples

These single crystal samples were prepared from a large single crystal of nickel purchased from Research Crystals Inc. The single crystal was 1/2"-5/8" diameter by 6" long with a [100] orientation along the axis. The purity listed was Nivac.

D. Gases

Hydrogen used in annealing of the polycrystalline samples and reduction of oxide in the weight determination step was Matheson Ultra Pure Grade hydrogen. The total impurities are reported at less than 10 ppm. The gaseous nitrogen used was Big-3 Pre-Purified grade.

APPENDIX B

DETAILS OF THE EXPERIMENTAL APPARATUS

Appendix B contains details of the experimental apparatus and the methods used to obtain the various measurements. Also included is a schematic of the current supply system assembled by J. Shelton. A detailed drawing of the quartz microbalance manufactured by Worden's is also shown.

Calibration curves including those of

1. the quartz spring microbalance,
2. temperature vs. R/R_{30}, and
3. R_{30}/R_T vs. temperature

are also included. These curves were taken from the thesis of Shelton.

A. Emittance Chamber

The emittance chamber as shown in Figure.III-2 consists of a one foot length of Type 304 welded tubing (6" O.D. x 0.120" wall) with Varian Con-Flat flanges heli-arc welded to each end. One end consisted of a blend flange machined to receive the feed through insulators. The other flange was machined to receive tubulation to the vacuum system. All connections were heli-arc welded in place. The flanges were sealed with 8" copper gaskets.

B. Vacuum Equipment

A Welch Duo-Seal Model 1402B mechanical pump with a capacity of about 100 liters/min. was used for rough vacuum. Higher vacuums were achieved with a Model #911-0002 Vac Ion pump manufactured by Varian Associates. The pump had a 75 liter/second capacity and was controlled with a Model #921-0007 control unit. Vacuum was measured with a Veeco Type RG3-A control panel. Both the thermocouple gauges and the ionization tube gauge were connected to this control unit.

A Varian high vacuum valve was used to separate the high vacuum emittance chamber from the fore pump. Ordinary teflon bulb brass valves were used in the low vacuum portion of the system.

C. Current Supply

Two separate current supply systems were used. The power for heating the thin polycrystalline samples was obtained from three 6-volt Reliable Batteries rated at 336 amp-hours. A transistor regulating circuit was built by J. Shelton to give a continuously variable current

over the range of 0 to 10 amps. The circuit is shown schematically in Figure B-I.

The same current supply unit was used in determining room temperature resistances for the thicker single crystal samples and also for the thick polycrystalline samples. A Model #KS8-50M Kepco Power Supply was used to heat the thicker samples. The D.C. output range was 0-8 volts and 0-50 amps. The unit had a 0.01% regulation and stability and was transistorized.

Beckman Duodial series RB turns-counting dials were used to replace the regular dials on the Kepco unit.

D. Electrical Measurements

Voltages were measured with a Leeds and Northrup 7553-5 Type K-3 Potentiometer and a Minneapolis-Honeywell Self Balancing Microvolt Potentiometer. Leeds and Northrup pinch and rotary switches were used for signal switching and polarity reversing.

The various types of standard resistors used were as shown below:

Table (B-1)

List of Standard Resistors

Resistance	Type of Resistor	E.E. Dept. Designation
.1005 Ω	Constructed	
.010001 Ω	Leeds and Northrup #4222B Reichsanatalt Type D.C.	
.005001 Ω	General Electric Shunt Type (100 amps)	07C
.0016686 Ω	Weston Shunt Type (50 MV; 30 amps)	B3C
.0005009 Ω	Weston Shunt Type (50 MV; 100 amps)	B7E

E. Oxide Weight Measurements

A quartz spring manufactured by Worden Laboratories was used to obtain the weight difference between the oxidized and reduced sample for the thin polycrystalline samples. The calibration curve is shown in Figure B-III.

For the single crystal samples and the thick polycrystalline samples a quartz microbalance was used. The microbalance system, shown in Figures III-4 and B-II, was manufactured and assembled by Worden Laboratories. As shown, the system consisted of the microbalance, the vacuum chamber and the microscope eyepiece. The microscope was a Nikken Ramsden-Okular 10x #3668 type with a micrometer adjustment consisting of 8 turns with 100 divisions turn.

Class J weights manufactured and certified by Voland Corporation were used to calibrate the microbalance before each run. The weights were calibrated against standards calibrated by the National Bureau of Standards under test number 175314 as shown below:

Table (B-2)

Designation	Apparent Mass Vs. Brass	
(0.05 mg.)	0.05 mg.	0.000 mg.
(0.5 mg.)	0.5 mg.	0.000 mg.

A Mettler Micro Balance Model M5 with a $\pm$ 0.002 mg. accuracy was used as an independent check for the oxide weight.

F. Sample Preparation

(1) Spark Cutter

A Metals Research Ltd. Servomet Type SMB spark cutter was used to obtain strain-free cutting of the large nickel single crystal. A schematic drawing of this instrument is shown in Figure F-II.

(2) Grinding and Polishing

A Buehler Ltd. belt grinder was used for thinning single crystals. For fine polishing, a Buehler low speed grinder was used. Fine polishing was accomplished with a Buehler table polishing unit. The sample was held in a hard tool steel holder, shown in Figure F-III-A, to control thickness.

(3) Spot Welder

A Weldmatic Model 1015-C spot welder with hand unit was used to attach the 1 mil diameter nickel potential leads to the nickel samples.

(4) Foil Machining Apparatus

The nickel foil specimens were prepared from large sheets of foil. Milling jigs were made from stress relieved brass bar stock. Both faces of two pieces of annealed bar stock were surface ground and sheets of foil clamped between them. Six sheets of foil were alternated with seven sheets of thin celluloid to prevent sticking. The assembly was then clamped in a milling machine. A sharp milling saw was advanced slowly through the brass and foils. The width of each slice was easily adjusted to produce the desired foil width.

G. Sample Measurements

(1) Width Measurement

A Wilder Micro-Projector with a micrometer adjustment was used to measure the width of the samples.

(2) Potential Lead Distance

The distance between the potential leads was obtained by using the optical and measuring components of a Wilson Tukon Tester. The optical component consisted primarily of a Bausch and Lomb Microscope and the micrometer measuring component was a Wilson Microton.

(3) Sample Length after Cutting for Oxide Determination

The Wilder Micro-Projector was also used to obtain this length measurement.

H. Sample Inspection

(1) Single Crystal Determination

A General Electric X-Ray Corporation diffraction unit was used to observe the crystal structure of the single crystal samples after final preparation. A copper target was used in obtaining the back reflection Laue diagrams.

(2) Microphotographs

An American Optical Company Metallograph was used to take pictures of the bare metal samples and also the oxidized samples. Most of the bare metal pictures were taken with 3000 speed/type 47 black and white Polaroid film. The oxidized samples were taken with Type 48 Polaroid colored film.

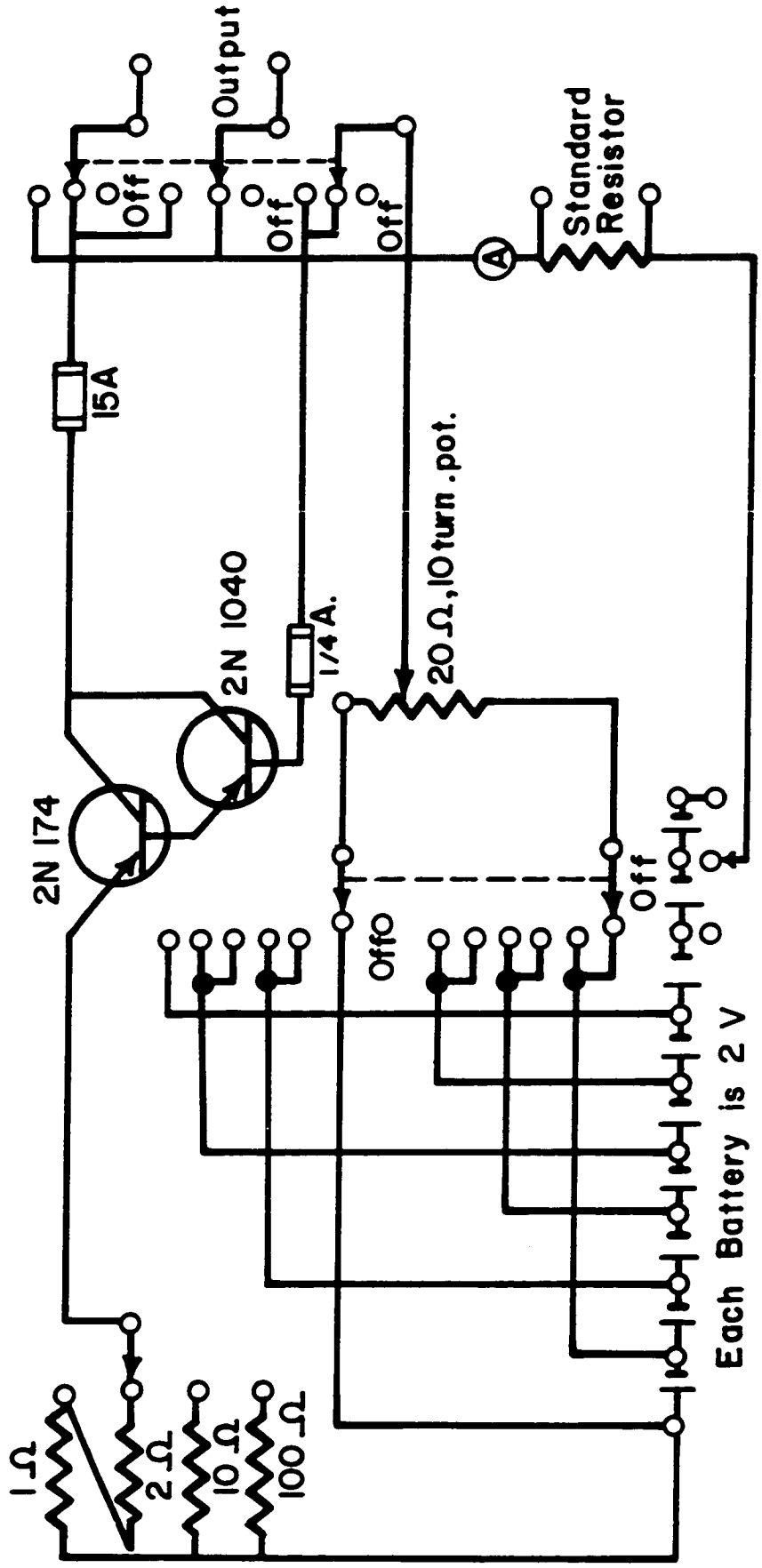

FIGURE B-I CURRENT SUPPLY SCHEMATIC

FIGURE B-II

QUARTZ MICROBALANCE

(from Worden's)

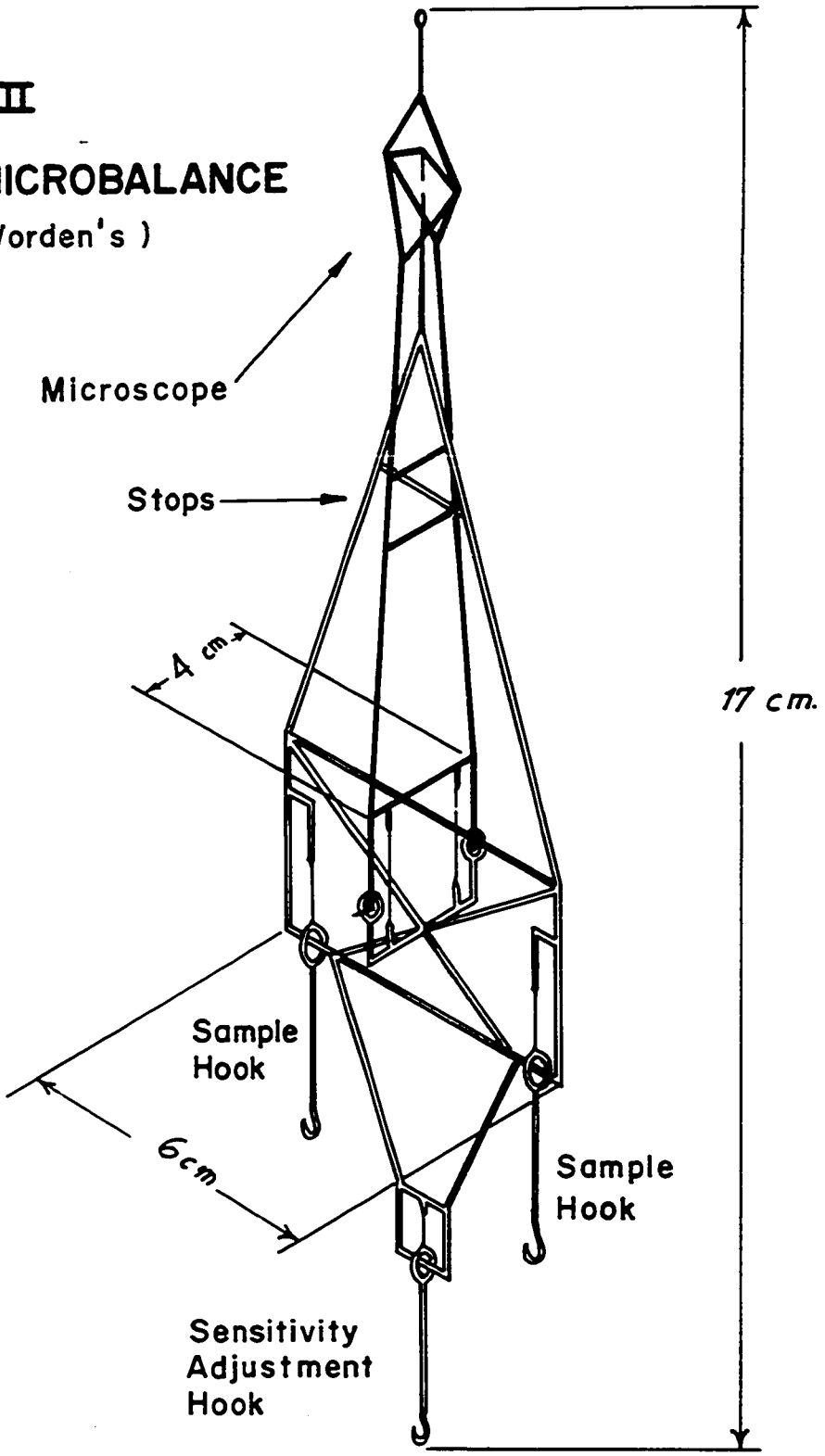

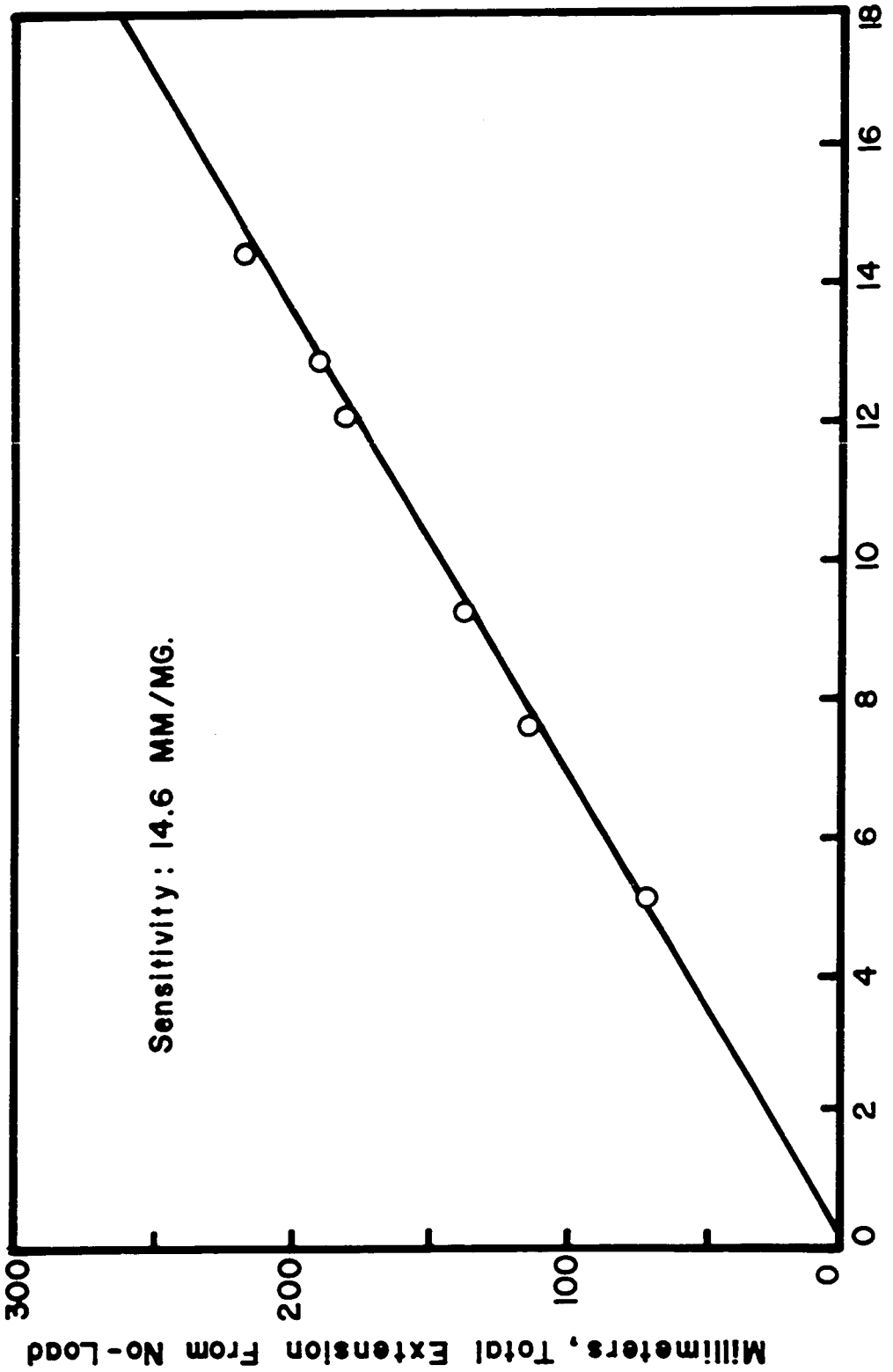

FIGURE B-III QUARTZ SPRING CALIBRATION CURVE

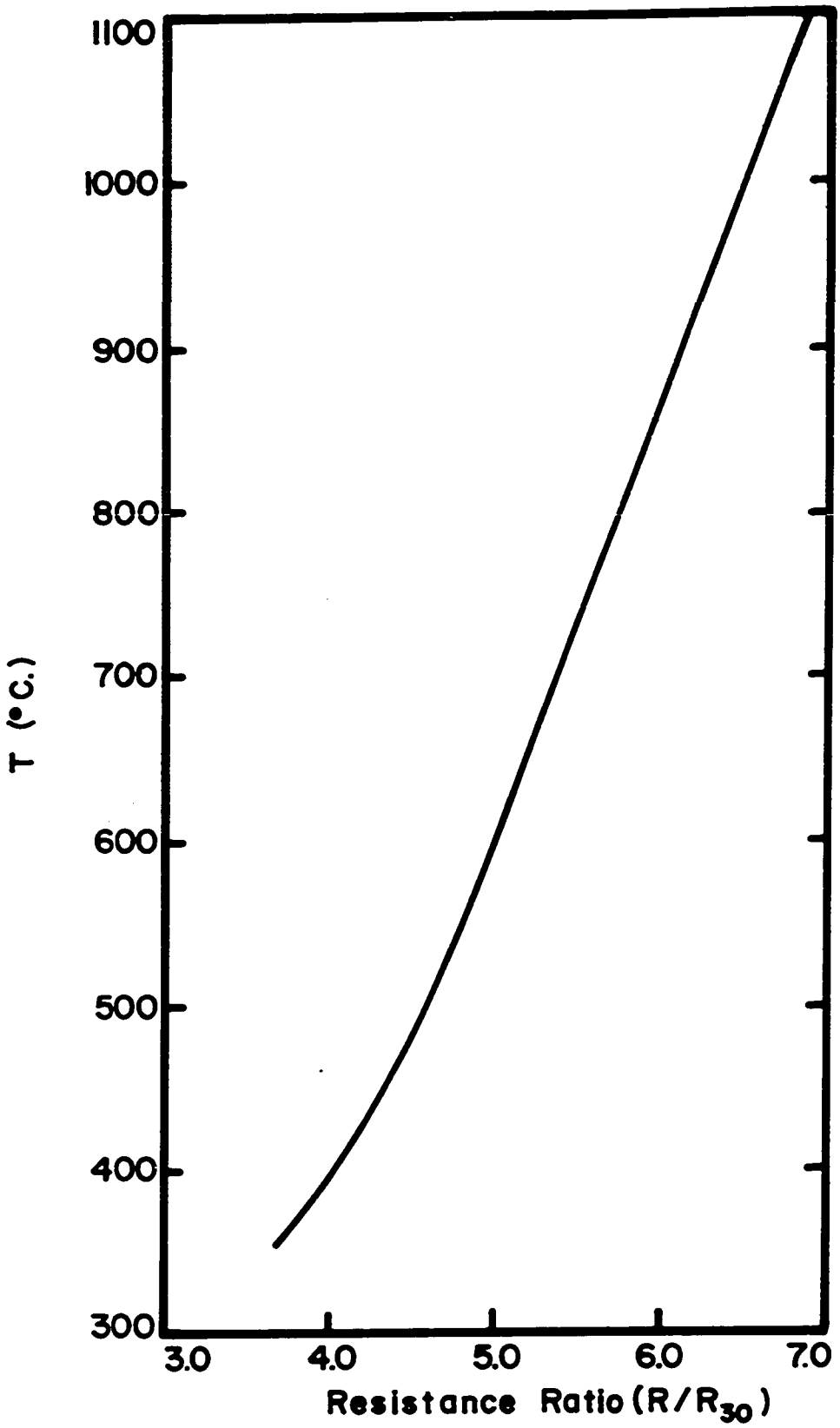

FIGURE B-Ⅳ T vs. R/R_{30} CALIBRATION CURVE

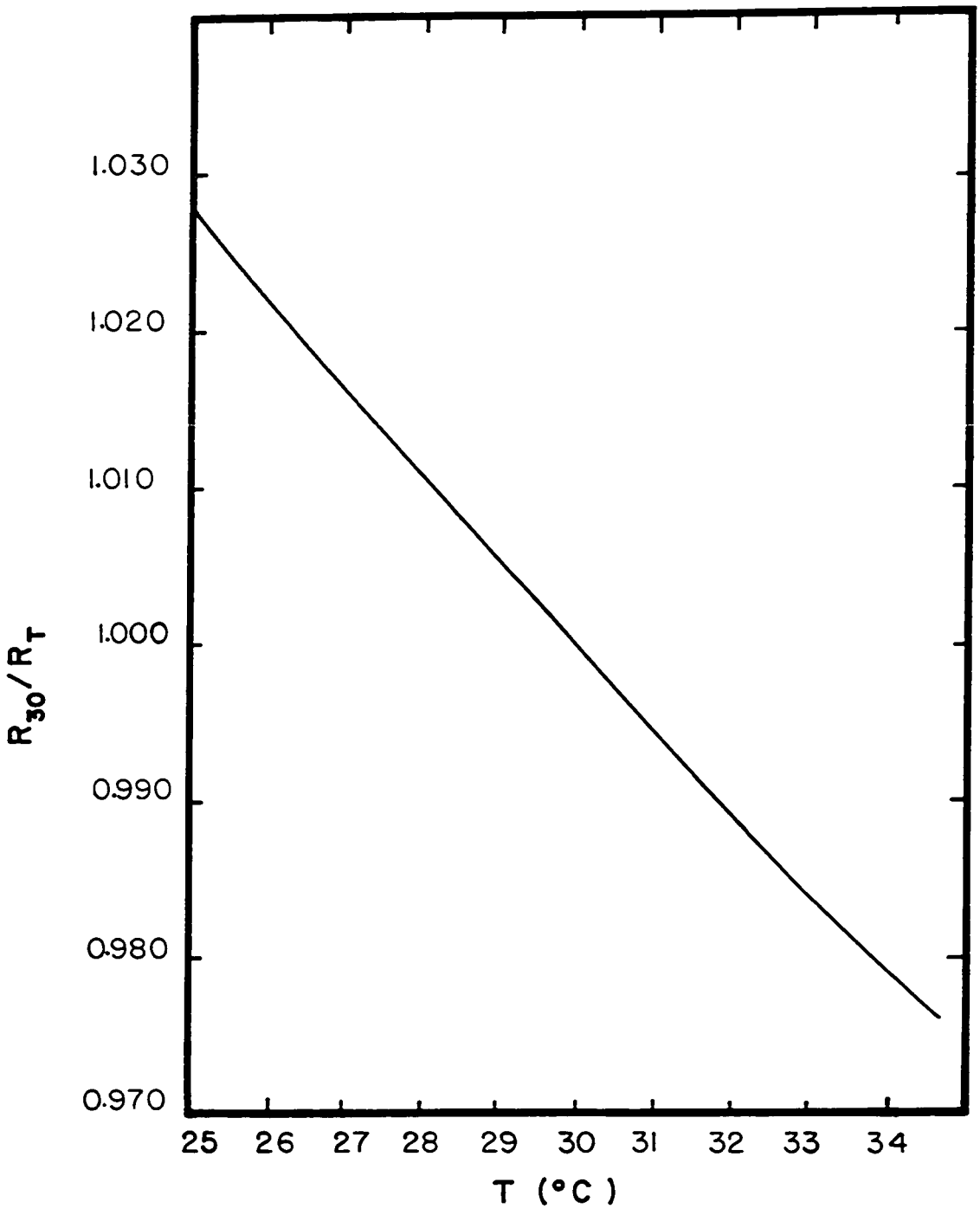

FIGURE B-V R_{30}/R_T vs. TEMPERATURE

APPENDIX C

EMITTANCE DATA AND RESULTS

This appendix contains data and summarized results of the emittance work. Included is a summarized table of adjusted emittance values for the oxidized single crystals.

Following this is a group of curves of emittance vs. temperature for the oxidized single crystals. These include the unadjusted

Emittance vs. temperature for 3" polycrystalline samples
" " " for 6" " "
" " " for (100) Semi-element crystals
" " " for (100) " " "
" " " for (111) " " "
" " " for (100) Research Crystal Inc.
" " " for (110) " " "

Finally this appendix includes all of the emittance data taken. The value for length listed in the sample data is the potential lead distance. The sample to heat sink ratio is the thickness of the sample divided by the thickness of the heat sink. The area factor is the average of the ratio of the baseline bare metal emittance (SE#3) to the bare metal emittance actually measured. This factor was used to compare oxidized emittances.

The resistances at 30°C (R_{30}) listed are the resistances after emittance measurements.

Table (C-1)

Adjusted Emittance Values with SE#3 Bare Metal Curve as Baseline

Run →	SE#1	SE#2	SE#3	SE#4	SE#5	SE#6
Correction Factor →	.9589	1.035	1.000	1.049	1.018	1.007
Temperature ↓ °C	ϵ corrected	ϵ corrected	ϵ corrected	ϵ corrected	ϵ corrected	ϵ corrected
880	.1889					
840	.1793	.2929	.2500		.1741	.2306
800	.1659	.2743	.2300		.1639	.2180
760	.1563	.2546	.2142	.3283	.1548	.2054
720	.1477	.2391	.2010	.3126	.1466	.1938
680	.1390	.2256	.1881	.3000	.1390	.1828
640	.1323	.2132	.1763	.2885	.1334	.1722
600	.1266	.2018	.1680	.2780	.1278	.1626
580	.1246	.1960	.1638	.2752	.1234	.1574
540	.1192	.1823	.1542	.2650	.1179	.1488
500	.1127	.1688	.1442	.2520	.1130	.1387
460	.1059	.1537	.1340	.2377	.1094	.1288
420	.0997	.1404	.1230	.2198	.1059	.1158
400	.0956	.1321	.1165	.2083	.1035	.1119
380	.0962	.1297	.1150	.2012	.1038	.1109
360	.1003	.1342	.1180	.2025	.1068	.1176
340	.1055	.1393	.1235	.2097	.1118	.1192
320	.1086	.1435	.1275	.2132	.1157	.1201
300	.1096	.1417	.1290	.2128	.1168	.1208
280	.1067	.1337		.2050	.1158	.1206

Table (C-1)
(Continued)

Run →	SE#7	SE#8	SE#9	SE#10	SE#11	SE#12
Correction Factor →	1.057	.993	.9755	.9511	.9690	1.031
Temperature ↓ °C	$\epsilon_{corrected}$	$\epsilon_{corrected}$	$\epsilon_{corrected}$	$\epsilon_{corrected}$	$\epsilon_{corrected}$	$\epsilon_{corrected}$
880			.2029			
840			.1878	.3005	.3673	.2505
800	.3552	.2751	.1756	.2787	.3513	.2320
760	.3382	.2582	.1644	.2611	.3353	.2165
720	.3208	.2438	.1546	.2444	.3203	.2031
680	.3034	.2304	.1458	.2287	.3048	.1907
640	.2875	.2170	.1385	.2145	.2946	.1784
600	.2690	.2070	.1322	.2007	.2791	.1696
580	.2602	.1988	.1273	.1919	.2673	.1640
540	.2475	.1868	.1190	.1816	.2515	.1560
500	.2357	.1746	.1145	.1701	.2348	.1469
460	.2154	.1619	.1082	.1570	.2151	.1367
420	.1883	.1489	.1036	.1418	.1915	.1270
400	.1790	.1414	.1011	.1328	.1798	.1226
380	.1780	.1396	.1016	.1324	.1781	.1206
360	.1815	.1421	.1035	.1357	.1820	.1230
340	.1870	.1461	.1083	.1387	.1856	.1296
320	.1895	.1488	.1118		.1896	.1320
300	.1899	.1500	.1145		.1906	.1340
280		.1477				

Table (C-1)
(Continued)

Run →	OSC#1	OSC#2	OSC#3	OSC#4	OSC#5	OSC#6
Correction Factor →	.7104	.7104	.8653	.7486	.7825	.8811
Temperature ↓ °C	ϵ corrected	ϵ corrected	ϵ corrected	ϵ corrected	ϵ corrected	ϵ corrected
880						
840						
800	.2628	.345	.2414	.3533	.3486	.1921
760	.2472	.3339	.2258	.3414	.3310	.1806
720	.2323	.3204	.2120	.3301	.3185	.1709
680	.2174	.3097	.1995	.3189	.3075	.1612
640	.2039	.2991	.1869	.3092	.2977	.1524
600	.1943	.2891	.1765	.2998	.2887	.1454
580	.1871		.1799	.2940	.2844	.1483
540	.1767		.1721	.2826	.2727	.1414
500	.1655		.1630	.2701	.2610	.1353
460	.1538		.1577	.2509	.2450	.1282
420	.1436		.1470	.2316	.2233	.1212
400	.1406		.1375	.2187	.2052	.1181
380	.1404		.1314	.2077	.1986	.1160
360	.1445		.1328	.2073	.2032	.1176
340	.1515		.1394	.2123	.2074	.1217
320	.1548		.1419	.2148	.2103	.1258
300	.1561		.1450	.2137	.2100	.1264
280	.1542		.1419	.2114	.2063	.1272

Table (C-1)
(Continued)

Run →	OSC#7	OSC#8	OSC#9	0-#15-10W1x5	0-#16-10W2x1	0-#1
Correction Factor →	.7104	.7865	.8026	.8142	.8153	.8076
Temperature ↓ °C	$\epsilon_{corrected}$	$\epsilon_{corrected}$	$\epsilon_{corrected}$	$\epsilon_{corrected}$	$\epsilon_{corrected}$	$\epsilon_{corrected}$
880						
840			.2023	.2797		.3630
800	.3069	.3177	.1886	.2662	.2976	.3525
760	.2984		.1766	.2540	.2845	.3392
720	.2895	.2879	.1653	.2426	.2715	.3287
680	.2803	.2674	.1549	.2312	.2593	.3194
640	.2700	.2556	.1461	.2215	.2479	.3117
600	.2586	.2446	.1380	.2133	.2356	.3077
580	.2546	.2410	.1391	.2072	.2327	.3029
540	.2431	.2284	.1312	.1973	.2227	.2946
500	.2322	.2147	.1237	.1857	.2110	.2858
460	.2202	.2010	.1174	.1724	.2020	.2742
420	.2079	.1855	.1120	.1621	.1769	.2588
400	.1970	.1712	.1100	.1575	.1690	.2530
380	.1873	.1615	.1088	.1548	.1618	.2527
360	.1861	.1590	.1101	.1533	.1619	.2606
340	.1891	.1624	.1155	.1547	.1649	.2673
320	.1896	.1665	.1196	.1582	.1636	.2724
300	.1863	.1668	.1205		.1586	.2744
280	.1784	.1648	.1208			

Table (C-1)
(Continued)

Run →	0-#2	0-#3	0-#4	0-#16	0-#23	SE#3
Correction Factor →	.8045	.7773	.8309	.8322	.8410	Bare Metal
Temperature ↓ °C	ϵ corrected	ϵ corrected	ϵ corrected	ϵ corrected	ϵ corrected	ϵ
880						.1440
840	.4113	.2421	.1363	.2688		.1350
800	.4001	.2293	.1300	.2567	.3608	.1277
760	.3891	.2192	.1246	.2455	.3490	.1205
720	.3801	.2099	.1196	.2347	.3406	.1147
680	.3685	.2009	.1163	.2255	.3267	.1090
640	.3612	.1932	.1113	.2180	.3171	.1039
600	.3532	.1850	.1023	.2097	.3078	.0995
580	.3468	.1783	.0964			.0990
540	.3361	.1693	.0921			.0947
500	.3289	.1600	.0890			.0912
460	.3190	.1511	.0885			.0877
420	.3049	.1420	.0880			.0868
400	.2919	.1352	.0885			.0855
380	.2888	.1342	.0898			.0860
360	.3034	.1395	.0948			.0890
340	.3153	.1453	.0997			.0940
320	.3224	.1482	.1004			.0980
300	.3233					.1000
280						.0995

Table (C-2)

Oxide Weight Vs. Emittance Data

Sample	Crystal	Oxide Weight ($\mu g/cm^2$)	*Oxide Emittance 800°C	600°C
SE#1	(110) Semi-Elem.	4.8	.1659	.1266
SE#2	"	37.0	.2743	.2018
SE#3	"	29.1	.2315	.1665
SE#4	"	78.6	.3450	.2780
OSC#2	(110) Res. Cry. Inc.	82.8	.345	.2891
OSC#5	"	68.8	.3486	.2887
OSC#8	"	48.1	.3177	.2446
OSC#9	"	18.96	.1886	.1380
SE#5	(100) Semi-Elem.	12.7	.1639	.1278
SE#6	"	21.8	.2180	.1626
SE#7	"	46.6	.3552	.2690
SE#8	"	37.0	.2751	.2070
OSC#1	(100) Res. Cry. Inc.	38.4	.2628	.1943
OSC#3	"	29.4	.2414	.1765
OSC#4	"	77.2	.3533	.2998
OSC#6	"	13.5	.1921	.1454
OSC#7	"	62.4	.3069	.2586
SE#9	(111) Semi-Elem.	9.0	.1756	.1322
SE#10	"	33.3	.2787	.2007
SE#11	"	57.6	.3513	.2791
SE#12	"	20.4	.2320	.1696
O#1	Thin Polycrystalline	81	.3525	.3077
O#2	"	120.8	.4001	.3532
O#3	"	25.8	.2293	.1850
O#4	"	3.25	.1300	.1064
O#16	"	27.6	.2567	.2097
O#23	"	65.2	.3608	.3078
O-#15-10W1x5	Thick Poly. with Heat Sinks	43.1	.2662	.2133
O-#16-10W2x1	"	55.6	.2976	.2356

*Oxide values are adjusted using following bare metal emittances of SE#3 as a baseline.

	800°C	600°C
ϵ_{bare}	.1277	.0995

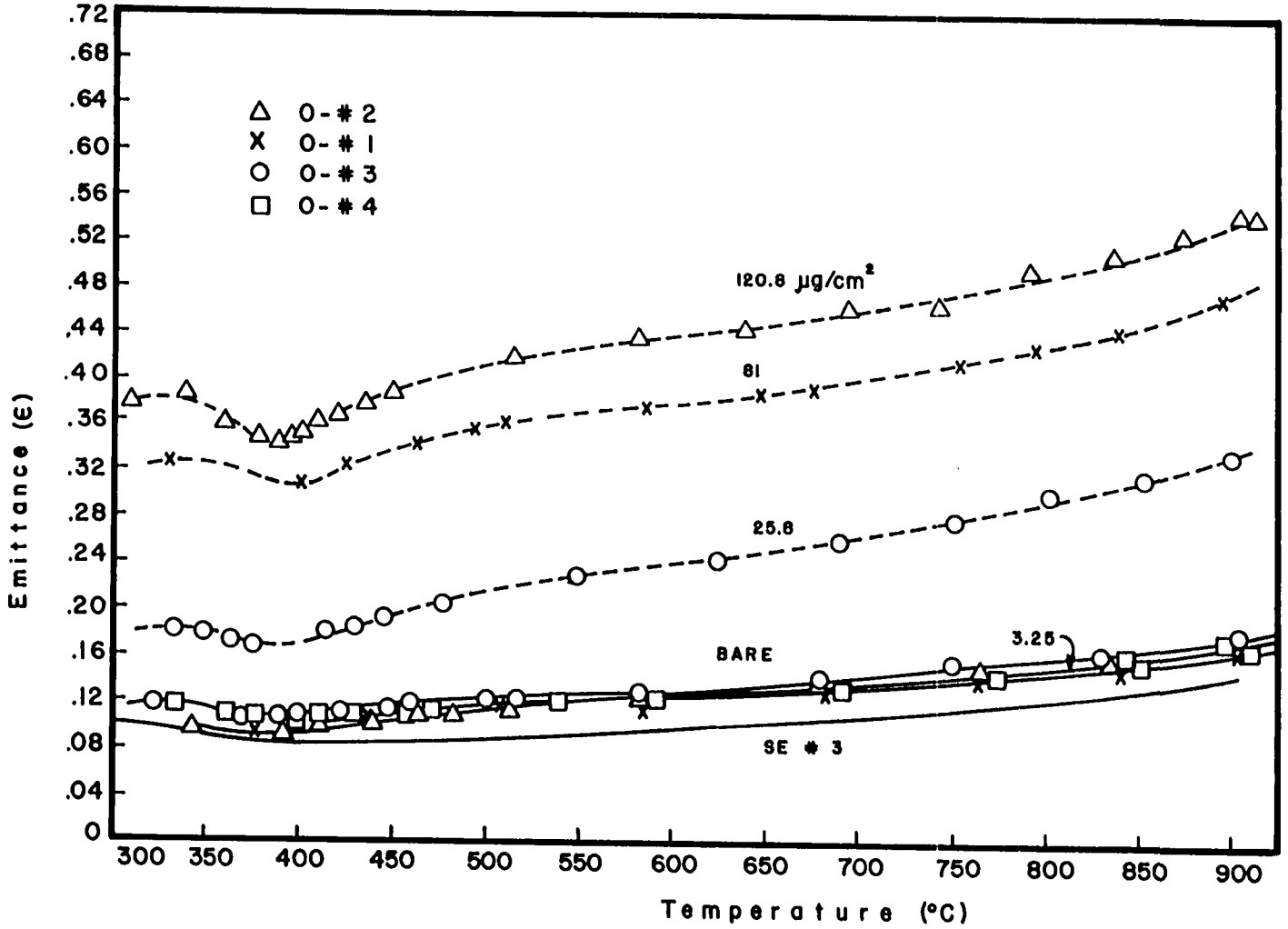

FIGURE C-I EMITTANCE vs. TEMPERATURE - EFFECT OF OXIDE THICKNESS FOR POLYCRYSTALLINE NICKEL (NO CORRECTION)

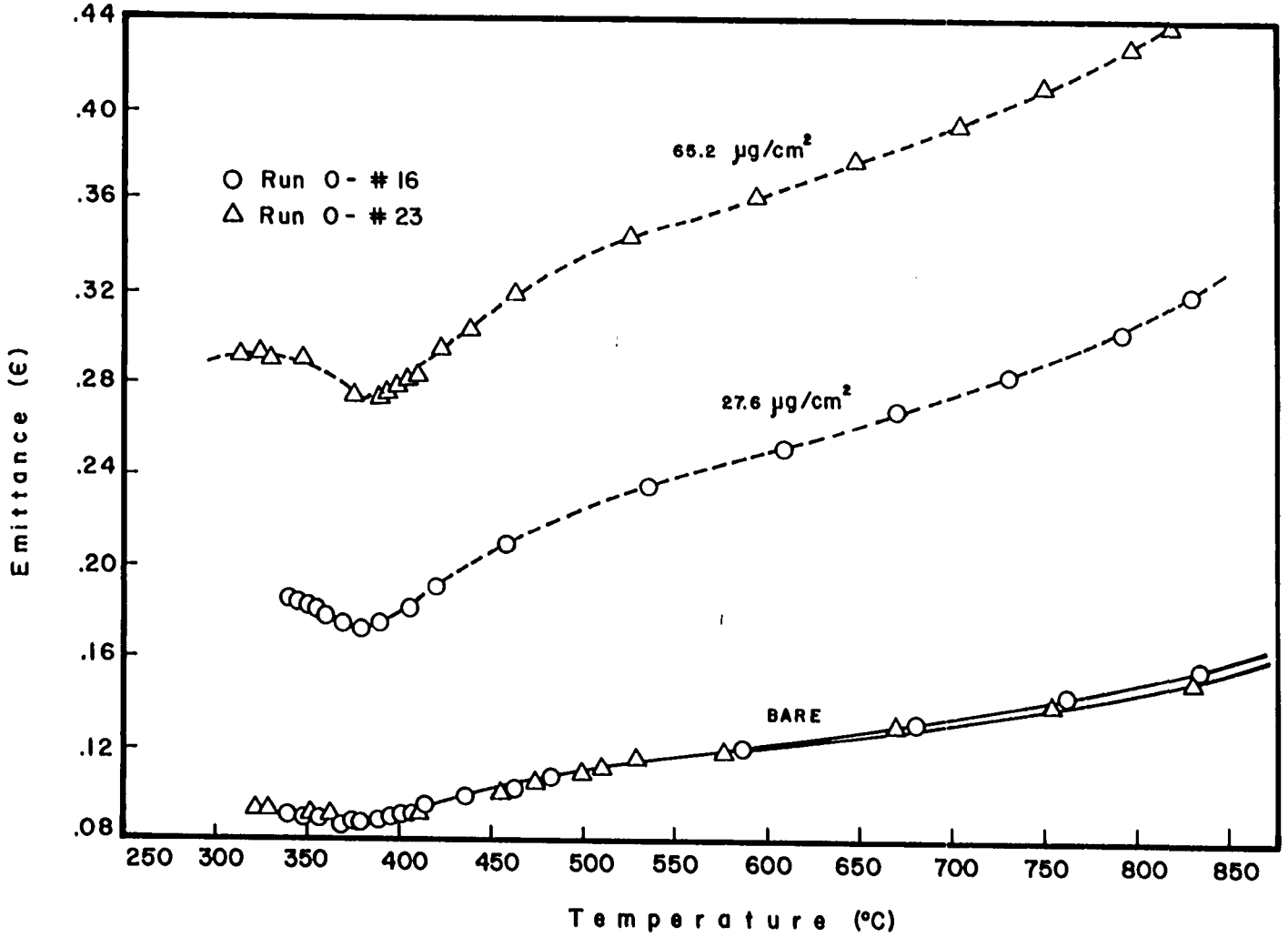

FIGURE C-II EMITTANCE vs. TEMPERATURE-EFFECT OF OXIDE THICKNESS FOR LONG (6") POLYCRYSTALLINE NICKEL SAMPLES

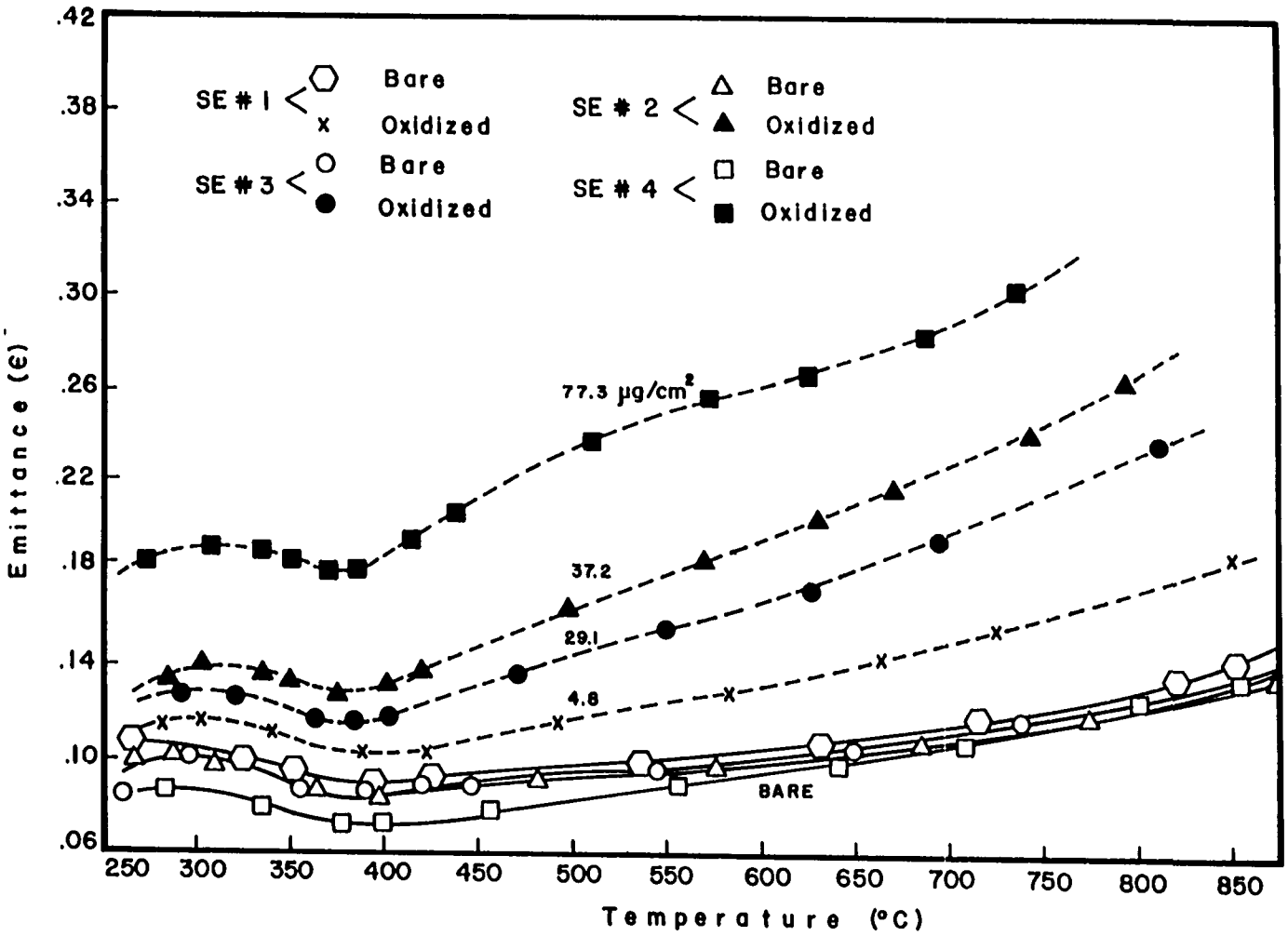

FIGURE C-III EMITTANCE vs. TEMPERATURE-EFFECT OF OXIDE THICKNESS FOR (110) SEMI-ELEMENTS SINGLE CRYSTALS OF NICKEL (NO CORRECTION)

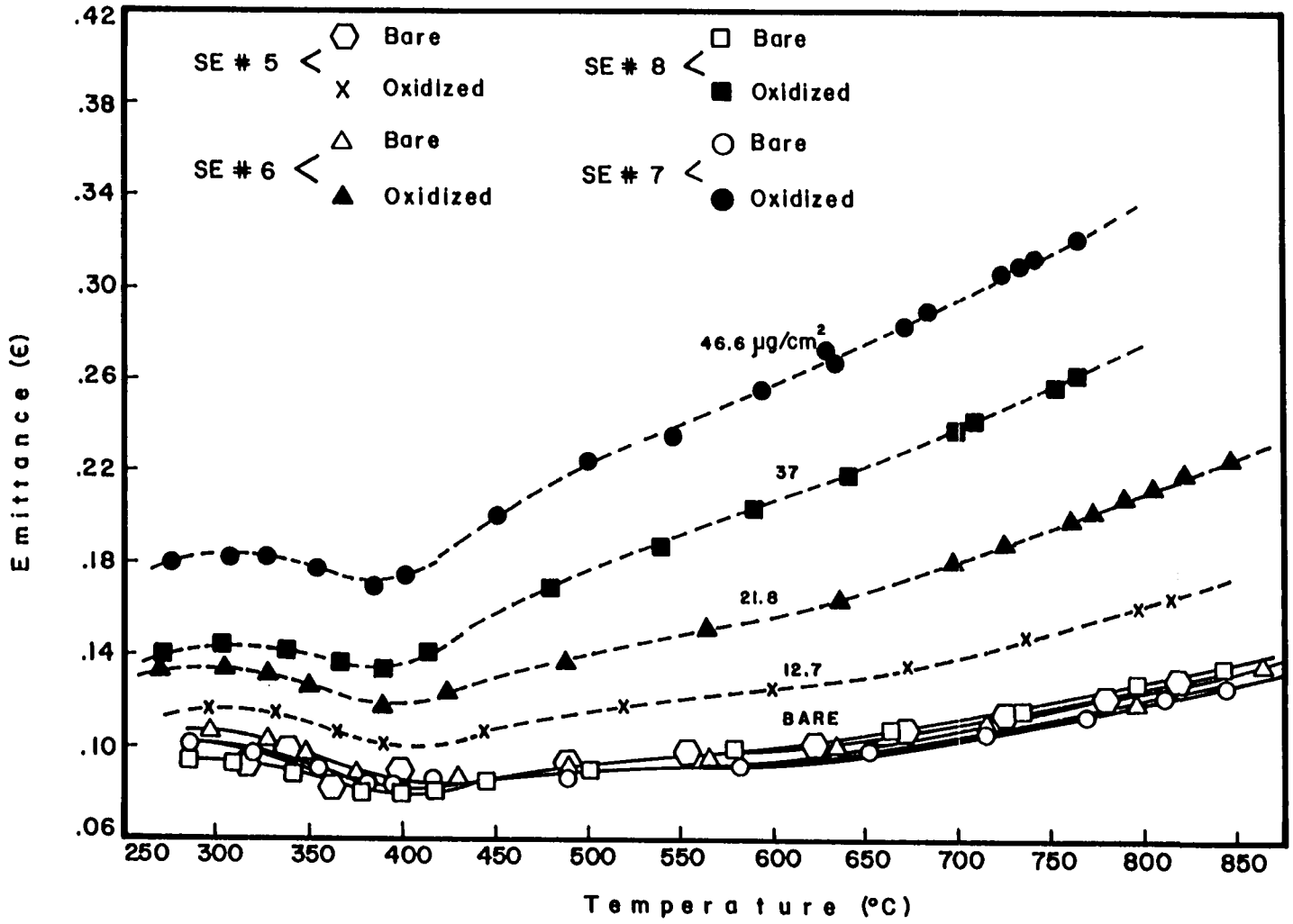

FIGURE C-IV EMITTANCE vs. TEMPERATURE - EFFECT OF OXIDE THICKNESS FOR (100) SEMI-ELEMENTS NICKEL CRYSTALS (NO CORRECTION)

PLC-7

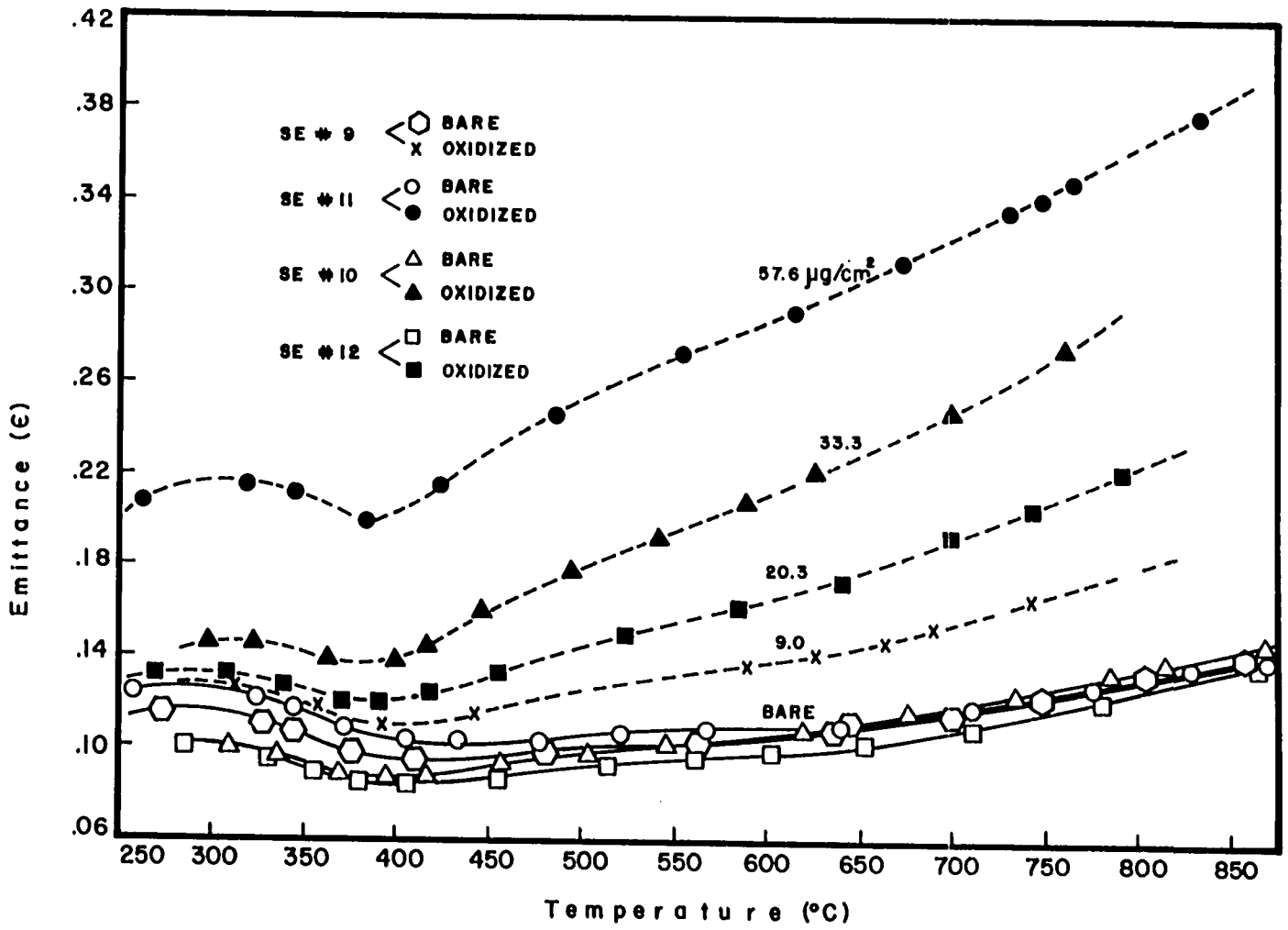

FIGURE C-V EMITTANCE vs. TEMPERATURE - EFFECT OF OXIDE THICKNESS FOR (III) SEMI-ELEMENTS NICKEL CRYSTALS (NO CORRECTION)

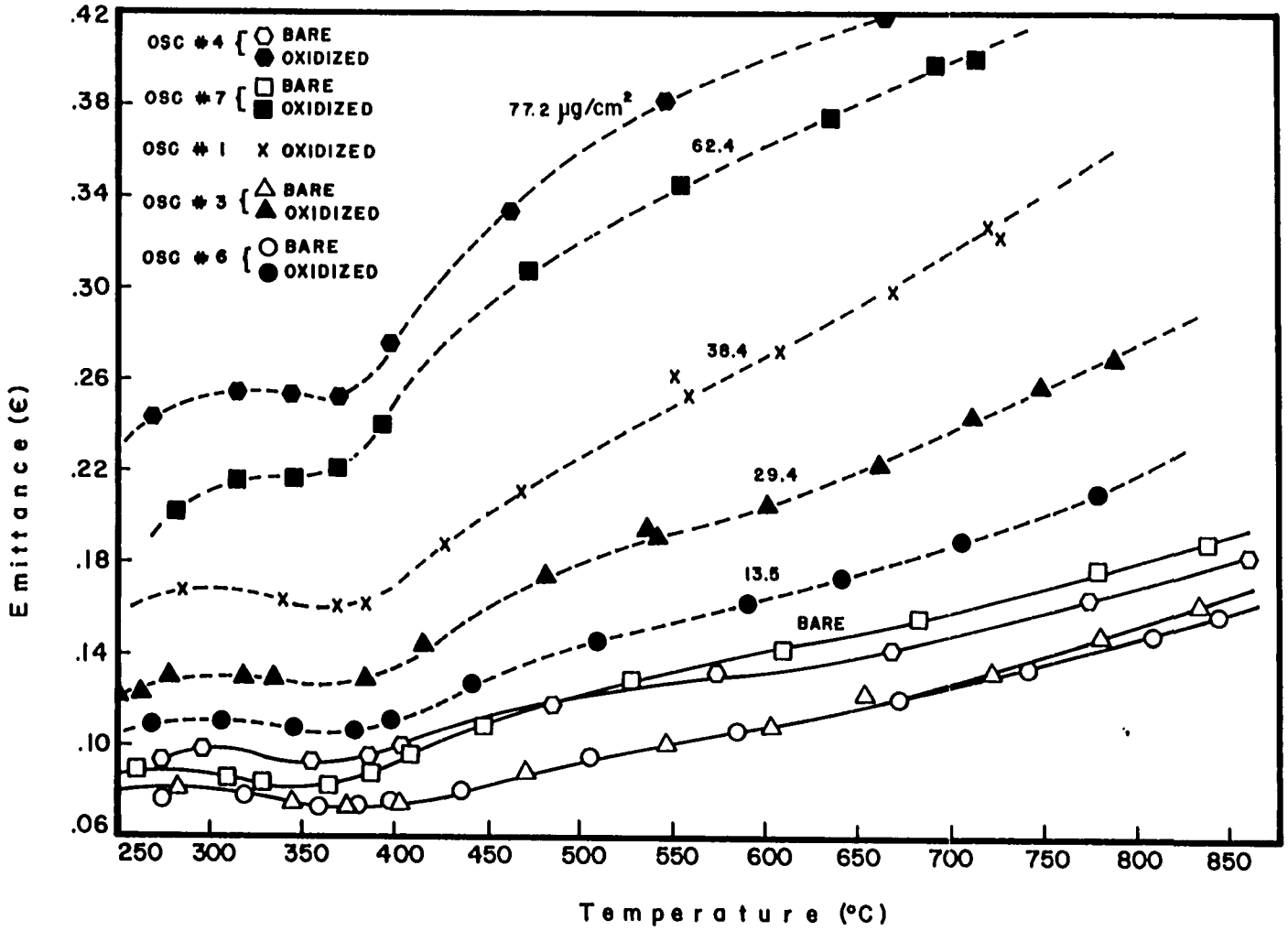

FIGURE C-VI EMITTANCE vs. TEMPERATURE - EFFECT OF OXIDE THICKNESS FOR (100) R.C.I. NICKEL CRYSTALS (NO CORRECTION)

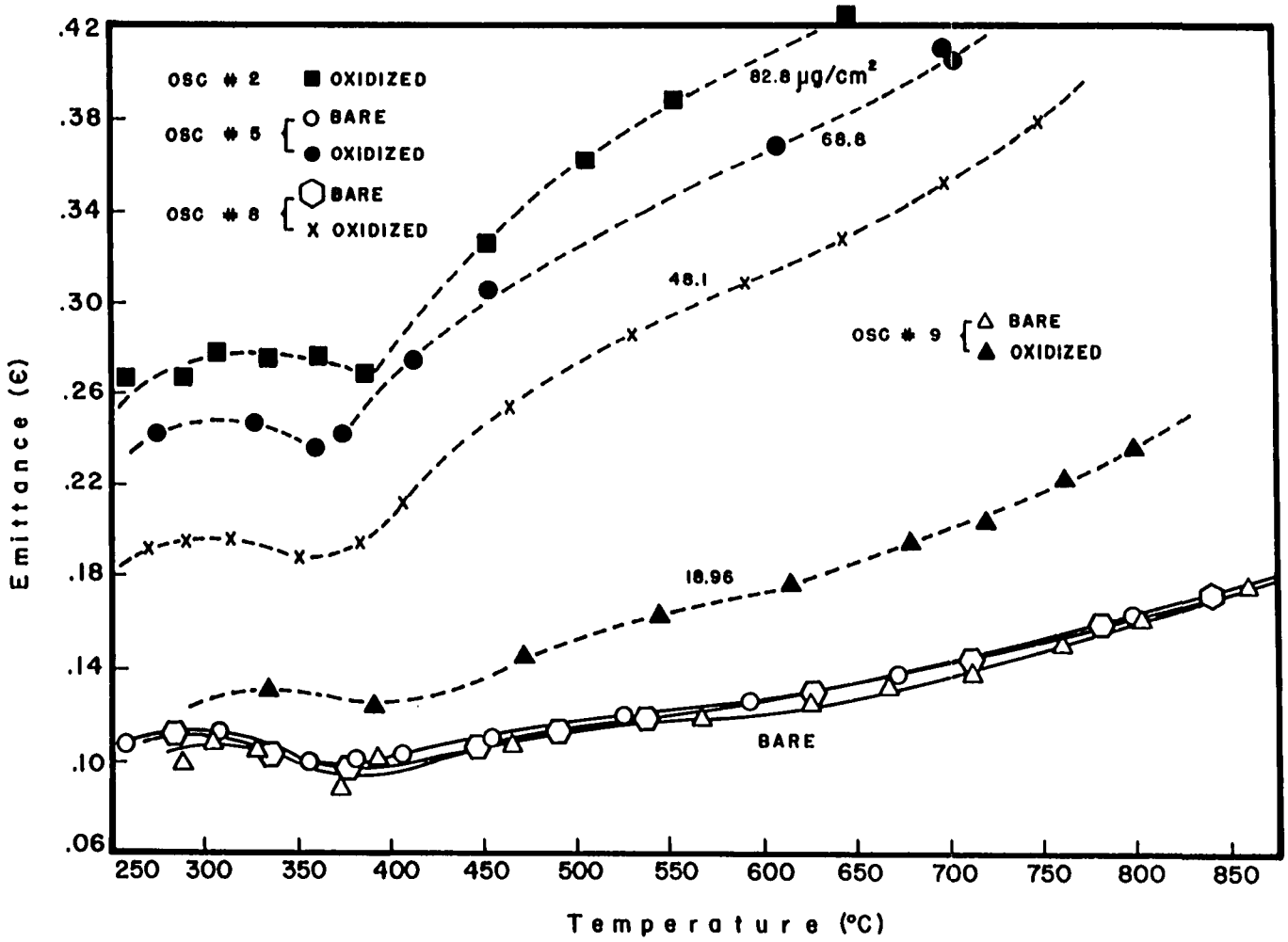

FIGURE C-VII EMITTANCE vs. TEMPERATURE - EFFECT OF OXIDE THICKNESS FOR (110) R.C.I. NICKEL CRYSTALS (NO CORRECTION)

EMITTANCE

Table (C-3)

Sample O#1 Information, Emittance Data and Calculated Values

Type Crystal--Thin Polycrystalline-3"

A. Sample Dimensions

Length (in.)	Width (in.)	Thickness (in.)	Area (cm^2)	$\frac{\text{Sample (mils)}}{\text{Heat Sink (mils)}}$	Area Factor
.485	.170	.00045	1.064	No Heat Sink	.8076

B. Emittance Runs: Bare Sample and 81 $\mu g/cm^2$ of oxygen

Sample Condition	Voltage V (volts)	Current I (amps)	Power P/A ($watts/cm^2$)	Resistance R (ohms)	R Ratio R/R_{30} (ohms/ohm)	Temperature T ^oC	Temperature T ^oK	Emittance ϵ
Bare	.26795	2.578	.6492	.1039	5.35	685	958	.137
R_{30} = .01943 ohms	.41487	3.600	1.4036	.1152	5.93	840	1113	.162
	.48908	4.082	1.8762	.1198	6.17	903	1176	.1736
$p = 1.45 \times 10^{-7}$ Torr	.33539	3.058	.9639	.1097	5.65	766	1039	.147
	.19701	2.040	.0955	.0755	3.89	373	646	.1014
	.087617	1.160	.1458	.08337	4.29	432	705	.1076
	.151766	1.681	.2398	.09028	4.65	505	778	.118
	.19701	2.040	.3777	.0966	4.97	584	857	.125
Oxidized	.89780	6.964	5.8759	.12892	6.29	934	1207	.490
R_{30} = .020502 ohms	.81680	6.4845	4.9777	.12596	6.14	895	1168	.4736
	.74496	6.050	4.2357	.12313	6.01	860	1133	.455
$p = 5.7 \times 10^{-7}$ Torr	.70476	5.804	3.8442	.12143	5.92	837	1110	.449
	.64006	5.398	3.2470	.11857	5.78	800	1073	.4345
	.56366	4.906	2.5988	.11489	5.60	750	1023	.421
	.48627	4.392	2.0071	.11072	5.40	698	971	.402

Table (C-3)
(Continued)

Sample Condition	Voltage V (volts)	Current I (amps)	Power P/A ($watts/cm^2$)	Resistance R (ohms)	R Ratio R/R_{30} (ohms/ohm)	Temperature T ^oC	Temperature T ^oK	Emittance ϵ
Oxidized	.45402	4.172	1.7801	.10883	5.31	675	948	.3925
R_{30} = .020502 ohms	.42178	3.950	1.5658	.10678	5.21	648	921	.388
	.35475	3.4725	1.1577	.10216	4.98	587	860	.379
$p = 5.7 \times 10^{-7}$ Torr	.29930	3.059	.8604	.09784	4.77	533	806	.366
	.27928	2.908	.7633	.09604	4.68	511	784	.364
	.26356	2.7875	.6904	.09455	4.61	495	768	.358
	.23475	2.562	.5652	.09163	4.47	466	739	.343
	.19925	2.280	.4269	.08739	4.26	427	700	.326
	.17194	2.064	.3335	.08330	4.06	396	669	.306
	.13438	1.856	.2344	.07240	3.53	332	605	.328

EMITTANCE

Table (C-4)

Sample O#2 Information, Emittance Data and Calculated Values

Type Crystal--Thin Polycrystalline-3"

A. Sample Dimensions

Length (in.)	Width (in.)	Thickness (in.)	Area (cm^2)	Sample (mils) / Heat Sink (mils)	Area Factor
.490	.1698	.00045	1.075	No Heat Sink	.8045

B. Emittance Runs: Bare Sample and 120.8 $\mu g/cm^2$ of oxygen

R_{30} = .019916 ohms

p = 2.3×10^{-7} Torr

Sample Condition	Voltage V (volts)	Current I (amps)	Power P/A ($watts/cm^2$)	Resistance R (ohms)	R Ratio R/R_{30} (ohms/ohm)	Temperature T ^oC	Temperature T ^oK	Emittance ϵ
Bare	.50347	4.096	1.9183	.12292	6.172	903	1176	.1776
	.57907	4.558	2.4552	.12704	6.378	958	1231	.1892
	.41895	3.556	1.3858	.11781	5.915	836	1109	.1624
	.34363	3.052	.9756	.11259	5.633	766	1039	.1486
	.26980	2.540	.6375	.10622	5.333	680	953	.1376
	.20501	2.062	.3932	.09942	4.992	590	863	.1268
	.13123	1.476	.1802	.088909	4.464	465	738	.1101
	.10441	1.254		.083262	4.181	414	687	
	.105016	1.2585	.1229	.083445	4.190	415	688	.1004
	.076880	1.0585	.0757	.072631	3.647	344	617	.0975
	.154773	1.6684	.2402	.092767	4.691	514	787	.1128
	.137636	1.5294	.1958	.089993	4.551	483	756	.1084
	.114911	1.3410	.1434	.085691	4.333	440	713	.1009
	.091512	1.1474	.0976	.079756	4.033	392	665	.09186
	.055362	.9316		.059427	3.005	282	555	.0975

Table (C-4)
(Continued)

Sample Condition	Voltage V (volts)	Current I (amps)	Power P/A (watts/cm^2)	Resistance R (ohms)	R Ratio R/R_{30} (ohms/ohm)	Temperature T ^oC	Temperature T ^oK	Emittance
Oxidized	.93877	7.0025	6.1149	.13406	6.206	913	1186	.5471
R_{30} = .02159 ohms	.92584	6.931	5.9688	.13358	6.184	906	1179	.5469
	.85508	6.528	5.1923	.13099	6.064	874	1147	.5314
$p = 9 \times 10^{-8}$ Torr	.77551	6.065	4.3752	.12787	5.920	837	1110	.5108
	.69356	5.579	3.5993	.12432	5.755	792	1065	.4964
	.60770	5.052	2.8558	.12029	5.569	743	1016	.4761
	.53320	4.582	2.2726	.11637	5.387	694	967	.4625
	.45556	4.072	1.7256	.11188	5.179	639	912	.4450
	.38626	3.604	1.2949	.10718	4.962	582	855	.4338
	.31348	3.088	.9005	.10152	4.700	516	789	.4184
	.24473	2.580	.5873	.094857	4.391	451	724	.3883
	.22848	2.456	.5220	.093029	4.307	435	708	.3785
	.21385	2.344	.4663	.091233	4.224	421	694	.3672
	.20365	2.268	.4330	.089793	4.157	410	683	.3644
	.19412	2.193	.3960	.088518	4.098	402	675	.3500
	.18913	2.1565	.3794	.087702	4.060	396	669	.3480
	.18360	2.117	.3616	.086726	4.015	389	662	.3465
	.16657	2.0305	.3146	.082034	3.798	360	633	.3638
	.15410	1.976	.2833	.077986	3.610	340	613	.3752
	.155973	2.002	.2905	.077909	3.607	339	612	.3874
	.17556	2.068	.3377	.084894	3.930	378	651	.3472
	.13236	1.859	.2289	.071200	3.296	309	582	.3784

EMITTANCE

Table (C-5)

Sample O#3 Information, Emittance Data and Calculated Values

Type Crystal--Thin Polycrystalline-3"

A. Sample Dimensions

Length (in.)	Width (in.)	Thickness (in.)	Area (cm^2)	Sample (mils) / Heat Sink (mils)	Area Factor
.513	.1698	.00044	1.1252	No Heat Sink	.7773

B. Emittance Runs: Bare Sample and 25.8 $\mu g/cm^2$ of oxygen

R_{30} = .020905 ohms

$p = 1.8 \times 10^{-7}$ Torr

Sample Condition	Voltage V (volts)	Current I (amps)	Power P/A ($watts/cm^2$)	Resistance R (ohms)	R Ratio R/R_{30} (ohms/ohm)	Temperature T ^oC	Temperature T ^oK	Emittance ϵ
Bare	.60541	4.554	2.75704	.13294	6.558	952	1225	.1925
	.54017	4.172	2.25359	.12947	6.193	908	1181	.1823
	.43866	3.5565	1.56009	.12334	5.899	831	1104	.1655
	.35920	3.052	1.09628	.11704	5.598	751	1024	.1574
	.28584	2.564	.7329	.11148	5.332	680	953	.1406
	.21301	2.052	.4371	.10381	4.965	583	856	.1295
	.17230	1.7525	.3020	.098317	4.703	517	790	.1240
	.16258	1.678	.2728	.096889	4.634	501	774	.1218
	.13978	1.5045	.2103	.092908	4.444	461	734	.1168
	.13277	1.4455	.1919	.091504	4.377	448	721	.1147
	.11993	1.3535	.1623	.088607	4.238	423	696	.1123
	.107838	1.2605	.1359	.085552	4.090	400	673	.1081
	.102630	1.2205	.1253	.084088	4.022	390	663	.1060
	.094740	1.1710	.1109	.080905	3.870	370	643	.1067
	.079915	1.1110	.0888	.071931	3.440	323	596	.1178

Table (C-5)
(Continued)

Sample Condition	Voltage V (volts)	Current I (amps)	Power P/A ($watts/cm^2$)	Resistance R (ohms)	R Ratio R/R_{30} (ohms/ohm)	Temperature T ^oC	Temperature T ^oK	Emittance
Oxidized	.88405	6.562	5.8011	.13472	6.456	979	1252	.3711
R_{30} = .020835 ohms	.80461	6.104	4.9113	.131816	6.317	942	1215	.3544
	.72081	5.608	4.0423	.128532	6.160	900	1173	.3360
$p = 2.9 \times 10^{-7}$ Torr	.63500	5.088	3.2309	.124803	5.981	853	1126	.3165
	.55611	4.600	2.5581	.12089	5.794	803	1076	.3008
	.47666	4.082	1.9457	.116771	5.596	751	1024	.2793
	.39906	3.562	1.4215	.112032	5.369	690	963	.2614
	.32698	3.058	.9999	.106926	5.124	625	898	.2440
	.25798	2.554	.6589	.101010	4.841	550	823	.2291
	.19537	2.068	.4040	.094472	4.528	478	751	.2042
	.17054	1.871	.3191	.091149	4.368	446	719	.1929
	.15808	1.7705	.2799	.08928	4.279	430	703	.1857
	.14789	1.6895	.2499	.087335	4.195	416	689	.1802
	.12265	1.497	.1836	.081928	3.926	377	650	.1688
	.11791	1.476	.1740	.079881	3.828	365	638	.1730
	.11167	1.448	.1617	.077120	3.696	349	622	.1789
	.10465	1.413	.1479	.074062	3.549	334	607	.1815

EMITTANCE

Table (C-6)

Sample O#4 Information, Emittance Data and Calculated Values

Type Crystal--Thin Polycrystalline-3"

A. Sample Dimensions

Length (in.)	Width (in.)	Thickness (in.)	Area (cm^2)	Sample (mils) / Heat Sink (mils)	Area Factor
.542	.1698	.00045	1.191	No Heat Sink	.8309

B. Emittance Runs: Bare Sample and 3.25 μ g/cm^2 of oxygen

R_{30} = .021983 ohms

p = 4.5 x 10^{-7} Torr

Sample Condition	Voltage V (volts)	Current I (amps)	Power P/A (watts/cm^2)	Resistance R (ohms)	R Ratio R/R_{30} (ohms/ohm)	Temperature T ^oC	Temperature T ^oK	Emittance ϵ
Bare	.64149	4.553	2.4522	.14089	6.409	967	1240	.1835
	.55543	4.076	1.9008	.13627	6.199	911	1184	.1712
	.47250	3.602	1.4289	.13118	5.967	849	1122	.1598
	.38014	3.048	.9728	.12472	5.674	772	1045	.1448
	.30220	2.5575	.6489	.11816	5.375	691	964	.1337
	.22427	2.0425	.3846	.10980	4.995	591	864	.1235
	.19230	1.8220	.2942	.10554	4.801	540	813	.1210
	.18151	1.7460	.2661	.10396	4.729	523	786	.1193
	.16702	1.6420	.2303	.10172	4.627	499	772	.1170
	.15058	1.5240	.1927	.09881	4.495	471	744	.1139
	.14247	1.4630	.1750	.09738	4.430	458	731	.1112
	.12755	1.3580	.1454	.09392	4.272	429	702	.1092
	.11859	1.2940	.1288	.09164	4.169	412	685	.1071
	.11118	1.2430	.1160	.08945	4.069	400	673	.1038
	.103165	1.1950	.1035	.08633	3.927	377	650	.1071
	.097686	1.1670	.0957	.08371	3.808	362	635	.1092
	.088565	1.1340	.0843	.07810	3.553	334	607	.1164
	.083931	1.1155	.0785	.07524	3.423	321	594	.1189

Table (C-6)
(Continued)

Sample Condition	Voltage V (volts)	Current I (amps)	Power P/A ($watts/cm^2$)	Resistance R (ohms)	R Ratio R/R_{30} (ohms/ohm)	Temperature T ^oC	Temperature T ^oK	Emittance
Oxidized	.64650	4.609	2.5018	.14026	6.380	959	1232	.1921
R_{30} = .021985 ohms	.55065	4.067	1.8803	.13539	6.158	899	1172	.1765
	.47157	3.608	1.4285	.13070	5.945	843	1116	.1632
$p = 1.2 \times 10^{-7}$ Torr	.38291	3.079	.9899	.12436	5.657	767	1040	.1502
	.29991	2.5535	.6430	.11713	5.328	679	952	.1394
	.22474	2.0495	.3867	.109656	4.988	589	862	.1253
	.19405	1.838	.2995	.10558	4.802	541	814	.1225
	.18013	1.739	.2630	.10358	4.711	519	792	.1203
	.16697	1.645	.2306	.10150	4.617	497	770	.1184
	.14649	1.496	.1840	.097921	4.454	463	736	.1118
	.13875	1.440	.1678	.096354	4.383	450	723	.1115
	.124686	1.3385	.1401	.093153	4.237	423	696	.1090
	.119006	1.3005	.1300	.091554	4.164	411	684	.1087
	.109270	1.2355	.1134	.088442	4.023	390	663	.1079
	.09749	1.1715	.0959	.083216	3.785	360	633	.1109
	.09190	1.1500	.0887	.079913	3.635	342	615	.1159
	.08636	1.1290	.0819	.076492	3.479	327	600	.1188

HIGH TEMPERATURE EMITTANCE

Table (C-7)

Sample O#5 Information, Emittance Data and Calculated Values

Type Crystal--Thin Polycrystalline-3"

A. Sample Dimensions

Length (in.)	Width (in.)	Thickness (in.)	Area (cm^2)	$\frac{\text{Sample (mils)}}{\text{Heat Sink (mils)}}$	Area Factor
.450	.1698	.00045	.9889	No Heat Sink	

B. Emittance Runs: Bare Sample

R_{30} = .017794 ohms

$p = 2.9 \times 10^{-7}$ Torr

Sample Condition	Voltage V (volts)	Current I (amps)	Power P/A ($watts/cm^2$)	Resistance R (ohms)	R Ratio R/R_{30} (ohms/ohm)	Temperature T ^oC	Temperature T ^oK	Emittance ϵ
Bare	.90885	6.933	6.3716	.13109	7.395	1230	1503	.2204
	.83755	6.542	5.5406	.12803	7.222	1185	1458	.2165
	.76352	6.098	4.7081	.12521	7.063	1143	1416	.2068
	.68107	5.595	3.8533	.12173	6.867	1088	1361	.1984
	.60270	5.095	3.1052	.11829	6.673	1037	1310	.1864
	.52431	4.581	2.4288	.11445	6.456	979	1252	.1748
	.37713	3.559	1.3572	.105965	5.978	853	1126	.1496
	.31439	3.093	.9833	.101645	5.733	787	1060	.1382
	.24552	2.547	.6323	.096396	5.417	702	975	.1245
	.18402	2.0455	.3806	.089963	5.056	612	885	.1134
	.160838	1.8515	.3011	.080039	4.498	561	834	.1116
	.149892	1.7575	.2664	.085287	4.793	538	811	.1106
	.138220	1.656	.2315	.083466	4.691	514	787	.1087
	.117938	1.4735	.1757	.080039	4.498	472	745	.1033
	.110055	1.4085	.1567	.078136	4.391	451	724	.1036
	.107640	1.3855	.1508	.077690	4.366	446	719	.1026

Table (C-7)
(Continued)

Sample Condition	Voltage V (volts)	Current I (amps)	Power P/A ($watts/cm^2$)	Resistance R (ohms)	R Ratio R/R_{30} (ohms/ohm)	Temperature T ^oC	Temperature T ^oK	Emittance
Bare	.102096	1.3380	.1381	.076305	4.288	432	705	.1019
R_{30} = .017794 ohms	.097977	1.3030	.1291	.075193	4.226	422	695	.1011
	.093991	1.2680	.1205	.074125	4.166	412	685	.1002
$p = 2.9 \times 10^{-7}$ Torr	.092775	1.2530	.1176	.074042	4.161	411	684	.0984
	.091512	1.2410	.1148	.073741	4.144	408	681	.0978
	.088695	1.2195	.1094	.072780	4.090	400	673	.0979
	.089549	1.2304	.1114	.072731	4.087	400	673	.0997
	.086618	1.2070	.1057	.071763	4.033	392	665	.0994
	.0848573	1.1920	.10227	.071189	4.001	388	661	.0986
	.083693	1.1820	.1000	.070806	3.979	385	658	.0983
	.083353	1.1790	.09938	.070702	3.973	384	657	.0983
	.082654	1.1745	.09816	.070314	3.952	380	653	.0996
	.081500	1.1670	.09617	.069837	3.925	377	650	.0995
	.079669	1.1564	.09316	.068894	3.872	370	643	.1009
	.077460	1.1475	.08988	.067503	3.794	360	633	.1039
	.075066	1.1360	.08623	.066079	3.714	351	624	.1059
	.072288	1.1240	.08216	.064313	3.614	340	613	.1088
	.070216	1.1150	.07917	.062974	3.539	333	606	.1104

HIGH TEMPERATURE EMITTANCE

Table (C-8)

Sample O#8 (2-3) c.c. Information, Emittance Data and Calculated Values

Type Crystal--Polycrystalline-6"

A. Sample Dimensions

Length (in.)	Width (in.)	Thickness (in.)	Area (cm^2)	$\frac{\text{Sample (mils)}}{\text{Heat Sink (mils)}}$	Area Factor
	.1687	.0025	.8969	No Heat Sinks	

B. Emittance Runs: Bare Sample

Sample Condition	Voltage V (volts)	Current I (amps)	Power P/A ($watts/cm^2$)	Resistance R (ohms)	R Ratio R/R_{30} (ohms/ohm)	Temperature T ^oC	Temperature T ^oK	Emittance ϵ
Bare	.62410	9.8346	5.5052	.063459	7.137	1161		.2299
	.50773	8.4052	3.8278	.060406	6.794	1068		.2092
R_{30} = .0088095 ohms	.38749	6.8351	2.3756	.056691	6.376	957		.1836
	.33795	6.1429	1.8620	.055015	6.188	907		.1700
$p = 2.1 \times 10^{-7}$ Torr	.27878	5.3218	1.3307	.052384	5.892	829		.1600
	.22386	4.4791	.89935	.049978	5.621	757		.1419
	.16241	3.5153	.51208	.046201	5.196	643		.1297

HIGH TEMPERATURE EMITTANCE

Table (C-8)
(Continued)

Sample O#21 Information, Emittance Data and Calculated Values

Type Crystal--Polycrystalline-3"

A. Sample Dimensions

Length (in.)	Width (in.)	Thickness (in.)	Area (cm^2)	$\frac{\text{Sample (mils)}}{\text{Heat Sink (mils)}}$	Area Factor
	.1698	.00045	.9549	No Heat Sink	

B. Emittance Runs: Bare Sample

Sample Condition	Current I (amps)	Voltage V (volts)	Power P/A ($watts/cm^2$)	Resistance R (ohms)	R Ratio R/R_{30} (ohms/ohm)	Temperature T ^oC	Temperature T ^oK	Emittance ϵ
Bare	6.522	.96633	6.0182	.14816	7.216	1183	1456	.2365
	6.023	.86905	4.9982	.14428	7.027	1132	1405	.2266
R_{30} = .020532 ohms	5.542	.78866	4.1736	.14050	6.843	1081	1354	.2194
	5.015	.68340	3.4724	.13624	6.636	1026	1299	.2032
$p = 6.6 \times 10^{-7}$ Torr	4.525	.59754	2.5819	.13205	6.432	972	1245	.1901
	4.026	.51294	1.9720	.12741	6.205	912	1185	.1770
	3.522	.43086	1.4491	.12233	5.958	846	1119	.1638
	3.019	.35224		.11667	5.683	774	1047	.1500
	2.514	.27703		.11019	5.367	690	963	.1376

EMITTANCE

Table (C-9)

Sample O#16 Information, Emittance Data and Calculated Values

Type Crystal--Thin Polycrystalline-3" and 6"

A. Sample Dimensions

Length (in.)	Width (in.)	Thickness (in.)	Area (cm^2)	$\frac{\text{Sample (mils)}}{\text{Heat Sink (mils)}}$	Area Factor
.496	.1657	.00045		none	.8322

B. Emittance Runs: Bare Sample and 27.6 $\mu g/cm^2$ of oxygen

$1/R_{30} = 52.50$ 1/ohms

$p = 1.1 \times 10^{-7}$ Torr

Sample Condition	Voltage V (volts)	Current I (amps)	Power P/A ($watts/cm^2$)	Resistance R (ohms)	R Ratio R/R_{30} (ohms/ohm)	Temperature T ^oC	Temperature T ^oK	Emittance ϵ
Bare	1.4109	3.5395	1.3261	.11262	5.913	834	1107	.1565
	.99386	3.041	.93413	.10747	5.642	763	1036	.1440
	.6535	2.536	.6142	.10162	5.335	680	953	.1326
	.39263	2.035	.36903	.094811	4.978	586	859	.1213
	.20721	1.547	.19476	.086581	4.545	482	755	.1084
	.17383	1.436	.16338	.084631	4.443	461	734	.1021
	.14647	1.3355	.13767	.082123	4.311	435	708	.09982
	.12248	1.240	.11512	.079659	4.182	414	687	.09455
	.11343	1.201	.10661	.078639	4.129	406	679	.09193
	.10817	1.179	.10167	.077818	4.085	400	673	.09097
	.10305	1.155	.096857	.077248	4.056	395	668	.08940
	.097467	1.130	.091609	.076331	4.007	388	661	.08836
	.092879	1.1085	.092879	.075587	3.968	383	656	.08691
	.087553	1.0855	.082291	.074304	3.901	373	646	.08737
	.083389	1.0654	.078377	.073465	3.857	368	641	.08598
	.079665	1.0560	.074877	.071439	3.751	355	628	.08953
	.076345	1.0420	.071757	.070315	3.692	348	621	.08997
	.072653	1.0290	.068287	.068615	3.602	339	612	.09107

Table (C-9)
(Continued)

Sample Condition	Voltage V (volts)	Current I (amps)	Power P/A ($watts/cm^2$)	Resistance R (ohms)	R Ratio R/R_{30} (ohms/ohm)	Temperature T ^oC	Temperature T ^oK	Emittance
Oxidized	.56901	5.0160	2.6829	.11344	5.898	831	1104	.3202
R_{30} = .019237 ohms	.50079	4.5475	2.1407	.11012	5.724	785	1058	.3032
	.42970	4.0445	1.6336	.10624	5.523	732	1005	.2846
$p = 4.8 \times 10^{-7}$ Torr	.35940	3.5280	1.1919	.10187	5.296	670	943	.2685
	.29686	3.0495	.85095	.097347	5.060	608	881	.2524
	.23295	2.5360	.5553	.091857	4.775	534	807	.2353
	.17240	2.0240	.3280	.085178	4.428	458	731	.2084
	.14361	1.7705	.2390	.081113	4.216	419	692	.1905
	.133479	1.6820	.2110	.079357	4.126	406	679	.1819
	.122425	1.5865	.1826	.077167	4.012	389	662	.1750
	.116775	1.5420	.1693	.075730	3.937	379	652	.1729
	.115646	1.5332	.1667	.075428	3.921	376	649	.1736
	.113084	1.520	.1616	.074397	3.867	370	643	.1750
	.109852	1.5035	.1553	.073064	3.798	361	634	.1783
	.107996	1.4950	.1518	.072238	3.755	355	628	.1815
	.105429	1.480	.1467	.071236	3.703	349	622	.1827
	.103710	1.4705	.1434	.070527	3.666	345	618	.1835
	.101016	1.456	.1383	.069379	3.607	339	612	.1844

EMITTANCE

Table (C-10)

Sample O#23 Information, Emittance Data and Calculated Values

Type Crystal--Thin Polycrystalline-3"

A. Sample Dimensions

Length (in.)	Width (in.)	Thickness (in.)	Area (cm^2)	$\frac{\text{Sample (mils)}}{\text{Heat Sink (mils)}}$	Area Factor
.494	.1698	.00045	1.086	none	.8410

B. Emittance Runs: Bare Sample and 65.2 μ g/cm^2 of oxygen

$1/R_{30}$ = 53.385 1/ohms

$p = 8.8 \times 10^{-8}$ Torr

Sample Condition	Voltage V (volts)	Current I (amps)	Power P/A (watts/cm^2)	Resistance R (ohms)	R Ratio R/R_{30} (ohms/ohm)	Temperature T ^oC	Temperature T ^oK	Emittance
Bare	.25093	2.528	.58425	.099260	5.299	670	943	.1316
	.31727	3.016	.88132	.105195	5.616	755	1028	.1401
	.39074	3.5355	1.2724	.11052	5.900	831	1104	.1518
	.25165	2.529	.58616	.099505	5.312	683	956	.1249
	.31727	3.016	.88132	.105195	5.616	755	1028	.1401
	.18701	2.020	.34793	.092579	4.942	577	850	.1193
	.16378	1.829	.29955	.089546	4.780	535	808	.1163
	.154431	1.746	.24834	.088448	4.722	521	794	.11245
	.14253	1.6445	.21588	.08667	4.627	499	772	.10965
	.129868	1.5355	.18366	.084577	4.515	475	748	.1062
	.118754	1.437	.15717	.08264	4.412	455	728	.1016
	.107828	1.3415	.13322	.080378	4.291	432	705	.0983
	.100381	1.2735	.11774	.07882	4.208	418	691	.0944
	.096000	1.234	.10910	.077795	4.153	410	683	.0918
	.091655	1.196	.1009623	.0766346	4.091	400	673	.0903
	.085295	1.1415	.089675	.0747218	3.989	385	658	.08815

Table (C-10)
(Continued)

Sample Condition	Voltage V (volts)	Current I (amps)	Power P/A (watts/cm^2)	Resistance R (ohms)	R Ratio R/R_{30} (ohms/ohm)	Temperature T ^oC	Temperature T ^oK	Emittance ϵ
Bare	.081564	1.1125	.083573	.073316	3.914	375	648	.0875
	.07548	1.0815	.075184	.069792	3.726	352	625	.0917
	.070469	1.0528	.0683302	.066935	3.573	336	609	.0930
	.066307	1.0264	.0626825	.064602	3.449	323	596	.0935
	.078606	1.0992	.079579	.071512	3.818	363	636	.9021
	.25166	2.530	.58641	.09947	5.310	673	946	.1304
Oxidized	.66225	5.7595	3.5130	.114983	5.856	819	1092	.4380
	.62575	5.5185	3.1805	.113391	5.775	798	1071	.4283
$1/R_{30} = 50.928$ 1/ohms	.55102	5.0115	2.54336	.109951	5.600	751	1024	.4108
	.48465	4.546	2.02923	.10661	5.429	705	978	.3945
	.34993	3.5575	1.14656	.098364	5.009	594	867	.3629
$p = 7.9 \times 10^{-8}$ Torr	.41230	4.0255	1.5286	.102422	5.216	648	921	.3788
	.28115	3.0205	.782147	.093080	4.740	526	799	.3452
	.22184	2.5355	.51805	.087493	4.456	463	736	.3201
	.19841	2.338	.42725	.084863	4.322	438	711	.3043
	.18417	2.2175	.37614	.083052	4.230	422	695	.2944
	.17276	2.122	.33764	.081413	4.146	409	682	.2834
	.16892	2.0885	.32492	.08088	4.119	404	677	.2836
	.16595	2.0635	.315388	.080421	4.096	401	674	.2804
	.16300	2.038	.30596	.07998	4.073	397	670	.2789
	.15930	2.009	.29475	.079293	4.038	392	665	.2772
	.15570	1.979	.28379	.078676	4.007	388	661	.2737
	.147763	1.921	.26144	.076919	3.917	375	648	.2740
	.134575	1.8585	.230356	.0724105	3.688	347	620	.2907
	.127078	1.8175	.21272	.069919	3.561	335	608	.2917
	.120787	1.780	.19802	.067857	3.456	324	597	.2935
	.113858	1.736	.18205	.065586	3.340	313	586	.2922

EMITTANCE

Table (C-11)

Sample O-#15-10W1x5 Information, Emittance Data and Calculated Values

Type Crystal--Thick Polycrystalline with Heat Sinks

A. Sample Dimensions

Length (in.)	Width (in.)	Thickness (in.)	Area (cm^2)	Sample (mils) / Heat Sink (mils)	Area Factor
.5141	.1751	.010	1.2276	2.0	.8142

B. Emittance Runs: Bare Sample and 43.1 $\mu g/cm^2$ of oxygen

R_{30} = .00088317 ohms

$p = 1.4 \times 10^{-7}$ Torr

Sample Condition	Voltage V (volts)	Current I (amps)	Power P/A ($watts/cm^2$)	Resistance R (ohms)	R Ratio R/R_{30} (ohms/ohm)	Temperature T ^oC	Temperature T ^oK	Emittance ϵ
Bare	.100635	18.9847	1.5563	.0053008	.003	859	1132	.1679
	.074461	15.0401	.91227	.0049508	5.006	753	1026	.1462
	.086042	16.8093	1.17816	.0051187	5.796	803	1076	.1559
	.062856	13.1907	.67539	.00476517	5.396	697	970	.1357
	.051626	11.3652	.47795	.0045424	5.144	630	903	.1283
	.040993	9.56131	.319279	.00428738	4.855	554	827	.1225
	.030395	7.71485	.191017	.0037398	4.461	464	737	.1174
	.017900	5.9487	.086739	.00300906	3.407	319	592	.1333
	.025868	6.93276	.14608	.00373127	4.225	421	694	.1150
	.109703	20.2757	1.81191	.00541056	6.127	891	1164	.1748
	.121224	21.8848	2.1611	.00553918	6.273	930	1203	.1826
	.138524	24.2407	2.73536	.0057145	6.471	983	1256	.1944
	.150508	25.8348	3.1674	.00582578	6.579	1011	1284	.2061

Table (C-11)
(Continued)

Sample Condition	Voltage V (volts)	Current I (amps)	Power P/A ($watts/cm^2$)	Resistance R (ohms)	R Ratio R/R_{30} (ohms/ohm)	Temperature T ^oC	Temperature T ^oK	Emittance ϵ
Oxidized	.090533	19.0483	1.4048	.0047541	5.378	692	965	.2883
	.077114	16.8422	1.0579	.004578617	5.179	639	912	.2728
R_{30} = .00088325 ohms	.066485	15.0305	.814032	.00442334	5.004	593	866	.2589
	.056360	13.2578	.608677	.00425108	4.809	541	814	.2490
$p = 1.2 \times 10^{-7}$ Torr	.046266	11.4317	.430841	.00404716	4.578	488	761	.2321
	.036242	9.55591	.282116	.0037926	4.290	430	703	.2106
	.024980	7.71485	.156987	.0032379	3.663	345	618	.2009
	.012100	5.89656	.058120	.00205204	2.321	222	495	.1937
	.018860	6.971113	.107099	.0027054	3.060	287	560	.2092
	.0067272	4.56371	.025009	.00147406	1.667	169	442	.1466
	.018634	6.96572	.10573	.0026751	3.026	285	558	.2097
	.098162	20.2673	.162063	.00484336	5.479	719	992	.2973
	.108666	21.91178	.19396	.0049592	5.601	752	1025	.3121
	.124977	24.3887	.24829	.0051243	5.797	803	1076	.3285
	.090417	19.0147	1.4005	.004755	5.377	691	964	.2886
	.150508	28.1374	3.4497	.005349	6.051	871	1144	.3568
	.07065	19.0327	1.09536	.0047628	5.387	694	967	.2229
	.16894	30.7563	4.2326	.0054928	6.21	913	1186	.3787

EMITTANCE

Table (C-12)

Sample O-#16-10W2x1 Information, Emittance Data and Calculated Values

Type Crystal--Thick Polycrystalline with Heat Sinks

A. Sample Dimensions

Length (in.)	Width (in.)	Thickness (in.)	Area (cm^2)	$\frac{\text{Sample (mils)}}{\text{Heat Sink (mils)}}$	Area Factor
.5037	.1751	.010	1.2033	5.0	.8153

B. Emittance Runs: Bare Sample and 55.6 μ g/cm^2 of oxygen

$\frac{1}{R_{30}} = 1141$

$p = 1.3 \times 10^{-7}$ Torr

Sample Condition	Voltage V (volts)	Current I (amps)	Power P/A (watts/cm^2)	Resistance R (ohms)	R Ratio R/R_{30} (ohms/ohm)	Temperature T ^oC	Temperature T ^oK	Emittance ϵ
Bare	.062959	13.3285	.6973496	.0047236	5.403	699	972	.1390
	.051590	11.4072	.4890527	.0045225	5.173	638	911	.1267
	.041003	9.53674	.3249578	.00429947	4.918	569	842	.1158
	.031168	7.71065	.19971532	.0040422	4.624	499	772	.1014
	.027153	6.93156	.1564084	.0039173	4.481	468	741	.0940
	.021710	5.86599	.105831	.00370099	4.234	422	695	.0828
	.014495	4.5667	.0550087	.00317406	3.631	342	615	.0719
	.018675	5.26069	.0816422	.0035499	4.061	396	669	.0749
	.0063736	3.29438	.0174489	.00193468	2.213	215	488	.0633
	.062940	13.3207		.00472497	5.405	699	972	
	.074148	15.1288	.0932213	.00490111	5.606	753	1026	.1494
	.085690	16.9112	.120425	.005067	5.796	803	1076	.1593
	.094018	18.1529	.14183	.00517923	5.924	837	1110	.1656
	.063119	13.3069	.697988	.0047433	5.426	704	977	.1363

Table (C-12)
(Continued)

Sample Condition	Voltage V (volts)	Current I (amps)	Power P/A ($watts/cm^2$)	Resistance R (ohms)	R Ratio R/R_{30} (ohms/ohm)	Temperature T ^oC	Temperature T ^oK	Emittance ϵ
Oxidized	.084195	18.383	1.28622	.004580	5.237	654	927	.3105
	.099779	20.947	1.73689	.0047634	5.446	711	984	.3295
$\frac{1}{R_{30}} = 1140.6$	.068809	15.7341	.899702	.0043732	5.000	593	866	.2861
	.055059	13.2476	.606145	.00415615	4.752	529	802	.2635
	.044019	11.1471	.407768	.0039489	4.515	475	748	.2357
$p = 3.4 \times 10^{-7}$ Torr	.030839	8.50174	.21788	.00362737	4.147	408	681	.1856
	.016248	5.88278	.0794317	.00276195	3.158	296	569	.1448
	.037401	9.84538	.306004	.0037988	4.344	442	715	.2130
	.024564	7.24380	.147868	.00339103	3.877	370	643	.1601
	.0096493	4.58168	.0367394	.00210606	2.408	231	504	.1148
	.019985	6.5426	.108659	.00305459	3.493	328	601	.1565
	.0049540	3.28718	.13533	.00150706	1.723	173	446	.0758
	.027594	7.85628	.180153	.0035123	4.016	389	662	.1726
	.022537	6.94594	.130088	.0032446	3.710	350	623	.1609

EMITTANCE

Table (C-13)

Sample SE#1 Information, Emittance Data and Calculated Values

Type Crystal-(110) Semi-Element

A. Sample Dimensions

Length (in.)	Width (in.)	Thickness (in.)	Area (cm^2)	$\frac{\text{Sample (mils)}}{\text{Heat Sink (mils)}}$	Area Factor
.4909	.1659	.0104	1.114	3.5	.9589

B. Emittance Runs: Bare Sample and 4.8 $\mu g/cm^2$ of oxygen

R_{30} = .0010030 ohms

$p = 2.7 \times 10^{-7}$ Torr

Sample Condition	Voltage V (volts)	Current I (amps)	Power P/A ($watts/cm^2$)	Resistance R (ohms)	R Ratio R/R_{30} (ohms/ohm)	Temperature T ^oC	Temperature T ^oK	Emittance ϵ
Bare	.104904	17.039	1.7875	.0061567	6.139	894	1167	.1532
	.092670	15.468	1.2865	.0059911	5.974	851	1124	.1428
	.082669	14.164	1.0509	.0058366	5.820	810	1083	.1355
	.082602	14.156	1.0495	.0058351	5.818	809	1082	.1358
	.062255	11.362	.6348	.0054792	5.463	715	988	.1185
	.048286	9.3432	.4049	.0051680	5.153	632	905	.1077
	.035563	7.4122	.2366	.0047979	4.784	536	809	.0993
	.023930	5.603	.1203	.0042709	4.258	426	699	.0920
	.020969	5.1672	.09725	.0040581	4.046	394	667	.0903
	.019737	4.9826	.08826	.0039612	3.950	380	653	.0896
	.018052	4.8310	.07827	.0037367	3.726	352	625	.0955
	.0158389	4.569	.06495	.0034666	3.457	325	598	.0956
	.0120305	4.267	.04607	.0028194	2.811	265	538	.1073

Table (C-13)
(Continued)

Sample Condition	Voltage V (volts)	Current I (amps)	Power P/A (watts/cm^2)	Resistance R (ohms)	R Ratio R/R_{30} (ohms/ohm)	Temperature T ^oC	Temperature T ^oK	Emittance ϵ
Oxidized	.106023	17.691	1.6834	.0059930	5.972	851	1124	.1869
R_{30} = .0010035 ohms	.073095	13.2255	.8676	.0055268	5.507	726	999	.1548
	.06065	11.4407	.6228	.0053012	5.283	667	940	.1421
$p = 1.5 \times 10^{-7}$ Torr	.046215	9.2790	.3849	.0049806	4.963	582	855	.1289
	.046215	9.2790	.3849	.0049806	4.963	582	855	.1289
	.033724	7.3115	.2213	.0046124	4.596	492	765	.1167
	.02519	5.9361	.1342	.0042435	4.229	422	695	.1051
	.021778	5.4165	.1059	.0040207	4.007	388	661	.1021
	.018479	5.0941	.08448	.0036275	3.615	341	614	.1111
	.0155647	4.8184	.06731	.0032303	3.219	302	575	.1172
	.0136814	4.558	.05591	.0030016	2.991	281	554	.1146

EMITTANCE

Table (C-14)

Sample SE#2 Information, Emittance Data and Calculated Values

Type Crystal-(110) Semi-Element

A. Sample Dimensions

Length (in.)	Width (in.)	Thickness (in.)	Area (cm^2)	$\frac{\text{Sample (mils)}}{\text{Heat Sink (mils)}}$	Area Factor
.5000	.1661	.0075	1.1359	2.5	1.035

B. Emittance Runs: Bare Sample and 37.0 μ g/cm^2 of oxygen

R_{30} = .00122415 ohms

p = 3.5 x 10^{-7} Torr

Sample Condition	Voltage V (volts)	Current I (amps)	Power P/A (watts/cm^2)	Resistance R (ohms)	R Ratio R/R_{30} (ohms/ohm)	Temperature T ^oC	Temperature T ^oK	Emittance ϵ
Bare	.079876	11.4755	.8069	.0069606	5.686	774	1047	.1192
	.107393	14.4271	1.3640	.0074438	6.081	879	1152	.1372
	.079723	11.4569	.8041	.0069585	5.684	774	1047	.1188
	.061345	9.3581	.5054	.0065552	5.355	686	959	.1064
	.043977	7.2666	.2813	.00605196	4.944	577	850	.0965
	.032065	5.7575	.1625	.0055692	4.549	482	755	.0904
	.022726	4.5661	.09135	.0049771	4.066	396.5	669.5	.0835
	.016323	4.0501	.05820	.0040303	3.292	309	582	.0962
	.020184	4.3108	.07660	.0046822	3.825	364	637	.0863
	.0130775	3.7888	.04362	.0034516	2.820	267	540	.0999
	.014835	3.9512	.05160	.0037545	3.067	288	561	.1000

Table (C-14)
(Continued)

Sample Condition	Voltage V (volts)	Current I (amps)	Power P/A (watts/cm^2)	Resistance R (ohms)	R Ratio R/R_{30} (ohms/ohm)	Temperature T ^oC	Temperature T ^oK	Emittance ϵ
Oxidized	.073620	11.680	.75695	.0063031	5.144	630	903	.2032
R_{30} = .0012254 ohms	.105509	15.466	1.4365	.0068220	5.567	743	1016	.2395
	.123476	17.502	1.9024	.0070550	5.757	793	1066	.2614
$p = 3.3 \times 10^{-7}$ Torr	.084365	12.995	.9651	.0064921	5.298	671	944	.2165
	.059106	9.8388	.5119	.0060074	4.9024	566	839	.1852
	.045716	8.0738	.3249	.0056623	4.621	498	771	.1659
	.031760	6.1573	.17215	.0051581	4.209	419	692	.1372
	.016939	4.5649	.06807	.0037107	3.028	285	558	.1351
	.025655	5.3632	.1211	.0047835	3.904	374	647	.1276
	.028916	5.7725	.1469	.0050093	4.088	400	673	.1315
	.022183	5.0857	.09931	.0043618	3.560	335	608	.1362
	.019094	4.8196	.08101	.0039617	3.233	303	576	.1401
	.023636	5.2008	.1082	.0045447	3.709	350	623	.1338

EMITTANCE

Table (C-15)

Sample SE#3 Information, Emittance Data and Calculated Values

Type Crystal-(110) Semi-Element

A. Sample Dimensions

Length (in.)	Width (in.)	Thickness (in.)	Area (cm^2)	$\frac{\text{Sample (mils)}}{\text{Heat Sink (mils)}}$	Area Factor
.5257	.1622	.0096	1.1681	3.2	1.000

B. Emittance Runs: Bare Sample and 29.1 μ g/cm^2 of oxygen

R_{30} = .0011043 ohms

p = 1.35 x 10^{-7} Torr

Sample Condition	Voltage V (volts)	Current I (amps)	Power P/A (watts/cm^2)	Resistance R (ohms)	R Ratio R/R_{30} (ohms/ohm)	Temperature T ^oC	Temperature T ^oK	Emittance ϵ
Bare	.070372	11.483	.6918	.0061284	5.550	738	1011	.1177
	.104154	15.560	1.3874	.0066937	6.061	874	1147	.1420
	.070228	11.4569	.6888	.0061297	5.551	738	1011	.1177
	.053482	9.2868	.4252	.0057589	5.215	649	922	.1049
	.038470	7.2306	.2381	.0053204	4.818	544	817	.0960
	.027095	5.618	.1303	.0048229	4.367	446	719	.0886
	.018972	4.5811	.0744	.0041414	3.750	355	692	.0867
	.012299	4.0171	.0423	.0030618	2.773	262	664	.0848
	.024316	5.2283	.1088	.0046508	4.211	419	628	.0890
	.021570	4.8526	.0896	.0044450	4.025	391	569	.0848
	.014915	4.2850	.0547	.0034807	3.152	296	535	.1010

Table (C-15)
(Continued)

Sample Condition	Voltage V (volts)	Current I (amps)	Power P/A (watts/cm^2)	Resistance R (ohms)	R Ratio R/R_{30} (ohms/ohm)	Temperature T ^oC	Temperature T ^oK	Emittance ϵ
Oxidized	.117445	18.234	1.8333	.0064410	5.826	811	1084	.2354
R_{30} = .0011056 ohms	.081831	13.722	.9613	.0059635	4.394	696	969	.1940
	.064653	11.407	.6314	.0056678	5.126	626	899	.1726
$p = 5.1 \times 10^{-7}$ Torr	.064604	11.403	.6307	.0056655	5.124	625	898	.1731
	.050127	9.3605	.4017	.0053552	4.844	551	824	.1564
	.036487	7.3475	.2295	.0049659	4.491	470	743	.1364
	.026699	5.8804	.1344	.0045403	4.107	402	675	.1188
	.024788	5.6125	.1191	.0044166	3.995	386	659	.1163
	.022534	5.3440	.1031	.0042167	3.814	363	636	.1169
	.019292	5.0803	.08391	.0037974	3.435	322	595	.1262
	.016542	4.8190	.0682	.0034326	3.105	292	565	.1283

EMITTANCE

Table (C-16)

Sample SE#4 Information, Emittance Data and Calculated Values

Type Crystal-(110) Semi-Element

A. Sample Dimensions

Length (in.)	Width (in.)	Thickness (in.)	Area (cm^2)	$\frac{\text{Sample (mils)}}{\text{Heat Sink (mils)}}$	Area Factor
.5034	.1659	.0108	1.1424	3.6	1.049

B. Emittance Runs: Bare Sample and 78.6 μ g/cm^2 of oxygen

R_{30} = .00088534 ohms

p = 6 x 10^{-8} Torr

Sample Condition	Voltage V (volts)	Current I (amps)	Power P/A (watts/cm^2)	Resistance R (ohms)	R Ratio R/R_{30} (ohms/ohm)	Temperature T ^oC	Temperature T ^oK	Emittance ϵ
Bare	.055447	11.519	.55929	.0048135	5.437	708	981	.1074
	.086111	16.254	1.2252	.0052978	5.984	854	1127	.1346
	.074221	14.4756	.9405	.0051273	5.791	801	1074	.1254
	.045033	9.8010	.3864	.0045947	5.190	642	915	.0983
	.055416	11.5192	.5588	.0048108	5.434	707	980	.1077
	.033929	7.8833	.2342	.0043039	4.861	555	828	.0894
	.023357	5.96788	.1220	.0039137	4.420	456	729	.0784
	.014348	4.5625	.5730	.00314467	3.552	334	607	.0791
	.018374	5.0779	.8167	.0036184	4.087	299.5	672.5	.0733
	.016784	4.8208	.7083	.0034816	3.932	377	650	.0733
	.011391	4.2802	.4268	.0026613	3.006	283	556	.0860

Table (C-16)
(Continued)

Sample Condition	Voltage V (volts)	Current I (amps)	Power P/A (watts/cm^2)	Resistance R (ohms)	R Ratio R/R_{30} (ohms/ohm)	Temperature T ^oC	Temperature T ^oK	Emittance ϵ
Oxidized	.048147	11.628	.4901	.0041406	4.670	509	782	.2362
R_{30} = .00088659 ohms	.085819	18.0570	1.3565	.0047527	5.361	688	961	.2831
	.060343	13.8020	.7290	.0043721	4.931	573	846	.2549
	.035555	9.2796	.2888	.0038315	4.322	438	711	.2058
$p = 1.7 \times 10^{-7}$ Torr	.070918	15.6095	.9691	.0045433	5.124	625	898	.2661
	.023687	7.2018	.1493	.0032890	3.710	350	623	.1847
	.015750	6.1297	.0845	.0025695	2.898	273.5	546.5	.1837
	.031611	8.5323	.2361	.0037049	4.179	414	687	.1939
	.027228	7.7131	.1838	.0035301	3.982	385	658	.1807
	.019440	6.6834	.1137	.0029087	3.281	307.5	580.5	.1901
	.022370	7.0790	.1387	.0031601	3.564	335.5	608.5	.1895
	.025763	7.4865	.1689	.0034413	3.881	371	644	.1817
	.099407	20.2415	1.7614	.0049110	5.539	736	1009	.3020

EMITTANCE

Table (C-17)

Sample SE#5 Information, Emittance Data and Calculated Values

Type Crystal-(100) Semi-Element

A. Sample Dimensions

Length (in.)	Width (in.)	Thickness (in.)	Area (cm^2)	$\frac{\text{Sample (mils)}}{\text{Heat Sink (mils)}}$	Area Factor
.4914	.1688	.0096	1.1303	3.2	1.018

B. Emittance Runs: Bare Sample and 12.7 μ g/cm^2 of oxygen

R_{30} = .0011032 ohms

$p = 3.55 \times 15^{-7}$ Torr

Sample Condition	Voltage V (volts)	Current I (amps)	Power P/A ($watts/cm^2$)	Resistance R (ohms)	R Ratio R/R_{30} (ohms/ohm)	Temperature T ^oC	Temperature T ^oK	Emittance ϵ
Bare	.109866	16.134	1.5682	.0068092	6.172	903	1176	.1452
	.086400	13.402	1.0244	.0064468	5.844	817	1090	.1287
	.077324	12.292	.8409	.0062906	5.702	779	1052	.1218
	.065882	10.859	.6329	.0060670	5.499	725	998	.1134
	.056375	9.6290	.48025	.0058547	5.307	673	946	.1068
	.048217	8.5419	.3644	.0056448	5.117	623	896	.1009
	.038885	7.2564	.2496	.0053587	4.857	554	827	.09575
	.030685	6.0913	.1654	.0050375	4.566	486	759	.09005
	.023084	5.0062	.1022	.0046111	4.180	414	687	.0840
	.019304	4.5820	.07825	.0042130	3.819	363	671	.08395
	.021707	4.8256	.09267	.0044983	4.077	398	636	.0887
	.016439	4.3731	.06360	.0037591	3.407	320	611	.0949
	.017806	4.4841	.07064	.0039709	3.599	338	593	.0970
	.013745	4.1348	.05028	.0033242	3.013	283.5	556.5	.1009

Table (C-17)
(Continued)

Sample Condition	Voltage V (volts)	Current I (amps)	Power P/A ($watts/cm^2$)	Resistance R (ohms)	R Ratio R/R_{30} (ohms/ohm)	Temperature T ^oC	Temperature T ^oK	Emittance
Oxidized	.099474	15.162	1.3343	.0065607	5.933	840	1113	.1519
1st Oxidation	.086801	13.647	1.0480	.0063604	5.752	792	1065	.1429
R_{30} = .0011032 ohms	.075176	12.213	.8123	.0061554	5.567	743	1016	.1338
	.064083	10.802	.6124	.0059325	5.365	689	962	.1257
p = 2×10^{-7} Torr	.051005	9.0699	.4093	.0056235	5.086	614	887	.1165
	.039610	7.4925	.2626	.0052866	4.781	535	808	.1090
	.030548	6.1878	.1672	.0049368	4.465	465	738	.1011
	.024202	5.2739	.1129	.0045890	4.150	409	682	.0945
	.021500	4.6797	.07578	.0039114	3.537	332.5	652.5	.1050
	.018304	4.9320	.09381	.0043593	3.943	379.5	605.5	.0955
	.015740	4.4503	.06197	.0035368	3.199	300	573	.1096
2nd Oxidation	.092854	14.553	1.1955	.0063804	5.770	797	1070	.1618
R_{30} = .0011057 ohms	.097965	15.166	1.3144	.0064595	5.842	816	1089	.1657
	.077550	12.642	.8674	.0061343	5.548	738	1011	.1475
p = 4.4×10^{-7} Torr	.063595	10.844	.6101	.0058645	5.304	673	946	.1357
	.050622	9.1046	.4078	.0055600	5.029	600	873	.1255
	.039054	7.4847	.2586	.0052178	4.719	521	794	.1171
	.029131	6.0452	.1558	.0048189	4.358	444	717	.1072
	.023194	5.2094	.1069	.0044523	4.027	391	664	.1012
	.018871	4.8290	.0806	.0039078	3.534	332	605	.1129
	.015760	4.5431	.0633	.0034690	3.137	295	568	.1164
	.021264	5.0130	.0943	.0042418	3.836	365	638	.1055

EMITTANCE

Table (C-18)

Sample SE#6 Information, Emittance Data and Calculated Values

Type Crystal-(100) Semi-Element

A. Sample Dimensions

Length (in.)	Width (in.)	Thickness (in.)	Area (cm^2)	$\frac{\text{Sample (mils)}}{\text{Heat Sink (mils)}}$	Area Factor
.5115	.1690	.0075	1.2114	2.5	1.007

B. Emittance Runs: Bare Sample and 21.8 $\mu g/cm^2$ of oxygen

R_{30} = .0012405 ohms

p = 2.65 x 10^{-7} Torr

Sample Condition	Voltage V (volts)	Current I (amps)	Power P/A ($watts/cm^2$)	Resistance R (ohms)	R Ratio R/R_{30} (ohms/ohm)	Temperature T ^oC	Temperature T ^oK	Emittance ϵ
Bare	.087305	12.202	.8794	.0071550	5.768	796	1069	.1195
	.107093	14.325	1.2664	.0074760	6.026	864	1137	.1343
	.070051	10.324	.5970	.0067853	5.470	717	990	.1105
	.054868	8.5605	.3877	.0064094	5.167	636	909	.1013
	.044205	7.2666	.2652	.0060833	4.904	567	840	.0955
	.034649	6.0722	.1737	.0057062	4.600	493	766	.0911
	.027512	5.1690	.1174	.0053225	4.290	431.5	704.5	.0868
	.022654	4.6400	.08676	.0048823	3.936	377	650	.0898
	.016709	4.2603	.05876	.0039220	3.162	297	570	.1063
	.019250	4.4485	.07069	.0043273	3.488	328	601	.1018
	.020875	4.5477	.07837	.0045902	3.700	349	622	.0976

Table (C-18)
(Continued)

Sample Condition	Voltage V (volts)	Current I (amps)	Power P/A (watts/cm^2)	Resistance R (ohms)	R Ratio R/R_{30} (ohms/ohm)	Temperature T ^oK	Temperature T ^oC	Emittance ϵ
Oxidized	.093120	13.647	1.0490	.0068235	5.500	725	998	.1880
R_{30} = .0012405 ohms	.104021	14.881	1.2778	.0069902	5.635	760.5	1033.5	.1989
	.108110	15.332	1.3683	.0070513	5.684	774	1047	.2021
$p = 1.75 \times 10^{-7}$ Torr	.114035	15.995	1.5057	.0071294	5.747	791	1064	.2084
	.119464	16.586	1.6357	.0072027	5.806	807	1080	.2132
	.125245	17.224	1.7808	.0072715	5.862	822	1095	.2196
	.134245	18.153	2.0117	.0073952	5.961	848	1121	.2258
	.104416	14.930	1.2869	.0069937	5.638	761	1034	.1999
	.085396	12.753	.8991	.0066961	5.398	697	970	.1807
	.070073	10.928	.6321	.0064122	5.169	637	910	.1645
	.056019	9.1921	.4251	.0060943	4.913	569	842	.1516
	.041814	7.3631	.2542	.0056789	4.578	488.5	761.5	.1366
	.031800	6.0398	.1586	.0052651	4.244	424	697	.1227
	.023874	5.1924	.1023	.0045979	3.706	350	623	.1265
	.027229	5.4713	.1230	.0049767	4.012	389	662	.1179
	.019488	4.8410	.07788	.0040256	3.245	304.5	577.6	.1332
	.015904	4.4935	.05899	.0035393	2.853	269.5	542.5	.1328
	.021737	5.0390	.09042	.0043138	3.477	326.5	599.5	.1317

EMITTANCE

Table (C-19)

Sample SE#7 Information, Emittance Data and Calculated Values

Type Crystal-(100) Semi-Element

A. Sample Dimensions

Length (in.)	Width (in.)	Thickness (in.)	Area (cm^2)	Sample (mils) / Heat Sink (mils)	Area Factor
.4912	.1675	.0075	1.1249	2.5	1.057

B. Emittance Runs: Bare Sample and 46.6 μ g/cm^2 of oxygen

R_{30} = .0010292 ohms

p = 2.2 x 10^{-7} Torr

Sample Condition	Voltage V (volts)	Current I (amps)	Power P/A (watts/cm^2)	Resistance R (ohms)	R Ratio R/R_{30} (ohms/ohm)	Temperature T ^oC	Temperature T ^oK	Emittance ϵ
Bare	.080493	13.415	.95985	.0060002	5.830	812	1085	.1228
	.088074	14.376	1.1255	.0061265	5.953	845	1118	.1277
	.070599	12.114	.7602	.0058279	5.662	769	1042	.1145
	.060388	10.737	.57635	.0056243	5.465	716	989	.1071
	.049940	9.2808	.4120	.0053810	5.228	653	926	.0999
	.040155	7.8581	.2805	.0051100	4.965	583	856	.0935
	.029603	6.2759	.1651	.0047169	4.583	490	763	.0880
	.022488	5.2070	.1041	.0043188	4.196	416	689	.0845
	.018095	4.6967	.075545	.0038527	3.743	354	627	.0909
	.0135668	4.3185	.05208	.0031416	3.052	287	560	.1017
	.020666	4.9426	.09080	.0041812	4.062	396	669	.0833
	.015848	4.5251	.06375	.0035022	3.403	320	593	.0973
	.019736	4.8266	.08468	.0040890	3.973	383	656	.0843

Table (C-19)
(Continued)

Sample Condition	Voltage V (volts)	Current I (amps)	Power P/A (watts/cm^2)	Resistance R (ohms)	R Ratio R/R_{30} (ohms/ohm)	Temperature T ^oC	Temperature T ^oK	Emittance ϵ
Oxidized	.078010	14.719	1.0207	.0052999	5.149	631	904	.2728
R_{30} = .0010292 ohms	.092346	16.769	1.3765	.0055069	5.351	685	958	.2909
	.104363	18.441	1.7107	.0056593	5.499	725	998	.3065
p = .7 x 10^{-7} Torr	.107252	18.824	1.7946	.0056976	5.536	734	1007	.3101
	.110075	19.202	1.8788	.0057325	5.570	743.5	1016.5	.3126
	.117564	20.194	2.1103	.0058217	5.656	766	1039	.3215
	.088576	16.212	1.2765	.0054636	5.308	673	946	.2839
	.078033	14.699	1.0196	.0053087	5.158	634	907	.2688
	.068650	13.309	.8122	.0051582	5.012	595	868	.2559
	.057611	11.624	.5953	.0049562	4.815	548	821	.2352
	.048959	10.258	.4464	.0047728	4.637	501	774	.2244
	.039456	8.7163	.3057	.0045267	4.398	452	725	.2010
	.030746	7.2768	.1989	.0042252	4.105	402.5	675.5	.1752
	.020405	6.0458	.1097	.0033751	3.279	308	581	.1826
	.025315	6.5696	.1478	.0038534	3.744	354	627	.1780
	.028288	6.8980	.1735	.0041009	3.984	385.5	600.5	.1700
	.022609	6.3047	.1267	.0035861	3.484	327.5	581	.1832
	.016982	5.6233	.0849	.0030199	2.934	276.5	549.5	.1801

EMITTANCE

Table (C-20)

Sample SE#8 Information, Emittance Data and Calculated Values

Type Crystal-(100) Semi-Element

A. Sample Dimensions

Length (in.)	Width (in.)	Thickness (in.)	Area (cm^2)	$\frac{\text{Sample (mils)}}{\text{Heat Sink (mils)}}$	Area Factor
.5072	.1634	.00975	1.135	3.25	.993

B. Emittance Runs: Bare Sample and 37.0 $\mu g/cm^2$ of oxygen

R_{30} = .0012054 ohms

$p = 1.5 \times 10^{-7}$ Torr

Sample Condition	Voltage V (volts)	Current I (amps)	Power P/A ($watts/cm^2$)	Resistance R (ohms)	R Ratio R/R_{30} (ohms/ohm)	Temperature T ^oC	Temperature T ^oK	Emittance ϵ
Oxidized	.077992	12.475	.8571	.0062519	5.187	642	915	.2181
	.097129	14.811	1.2673	.0065579	5.440	709	982	.2424
	.110741	16.398	1.5998	.0067533	5.603	753	1026	.2564
	.115140	16.912	1.7154	.0068081	5.648	765	1038	.2624
	.094351	14.469	1.2027	.0065209	5.410	700	973	.2387
	.065794	10.921	.6330	.0060245	4.998	591	864	.2032
	.054605	9.4498	.4546	.0057784	4.794	539	812	.1879
	.043232	7.8928	.3006	.0054774	4.544	481	754	.1682
	.031450	6.2364	.1728	.0050430	4.184	414	687	.1419
	.022879	5.2751	.1063	.0043372	3.598	338	611	.1428
	.027979	5.7572	.1419	.0048598	4.032	391	664	.1343
	.019240	4.9362	.0837	.0038977	3.234	303.5	576.5	.1441
	.025714	5.4791	.1241	.0046391	3.849	367	640	.1370
	.015740	4.5535	.06314	.0034567	2.868	270.5	543.5	.1406

Table (C-20)
(Continued)

Sample Condition	Voltage V (volts)	Current I (amps)	Power P/A ($watts/cm^2$)	Resistance R (ohms)	R Ratio R/R_{30} (ohms/ohm)	Temperature T ^oC	Temperature T ^oK	Emittance ϵ
Bare	.098261	13.743	1.11896	.0071499	5.946	843.5	1116.5	.1355
R_{30} = .0012024 ohms	.086026	12.406	.9402	.0069342	5.766	796	1069	.1277
$p = 3.2 \times 10^{-7}$ Torr	.071837	10.787	.6827	.0066596	5.538	735	1008	.1175
	.057987	9.1454	.4672	.0063406	5.273	663	936	.1085
	.044330	7.4452	.2908	.0059542	4.952	579	852	.0988
	.033890	6.0817	.1816	.0055725	4.634	501	774	.0913
	.027255	5.1926	.1247	.0052488	4.365	446	719	.0848
	.024191	4.7864	.1020	.0050541	4.203	418	691	.0818
	.020606	4.3545	.07905	.0047321	3.935	378	673	.0813
	.015972	4.0248	.05663	.0039684	3.300	309	651	.0936
	.022389	4.5591	.08992	.0049108	4.084	400	615	.0805
	.018382	4.2106	.06819	.0043656	3.630	342	582	.0891
	.014048	3.8572	.04774	.0036420	3.029	285	558	.0947

EMITTANCE

Table (C-21)

Sample SE#9 Information, Emittance Data and Calculated Values

Type Crystal-(111) Semi-Element

A. Sample Dimensions

Length (in.)	Width (in.)	Thickness (in.)	Area (cm^2)	$\frac{\text{Sample (mils)}}{\text{Heat Sink (mils)}}$	Area Factor
.48096	.16585	.009	1.0913	3.0	.9755

B. Emittance Runs: Bare Sample and 9.0 μ g/cm^2 of oxygen

R_{30} = .0010923 ohms

p = 2.5 x 10^{-7} Torr

Sample Condition	Voltage V (volts)	Current I (amps)	Power P/A (watts/cm^2)	Resistance R (ohms)	R Ratio R/R_{30} (ohms/ohm)	Temperature T ^oC	Temperature T ^oK	Emittance ϵ
Bare	.096226	14.675	1.2940	.0056837	5.203	646	919	.1114
	.082958	13.098	.9957	.0061040	5.588	747	1020	.1216
	.070269	11.512	.74125	.0065571	6.003	858	1131	.1401
	.060862	10.302	.5745	.0059078	5.409	700	973	.1140
	.052562	9.2478	.4454	.0063336	5.798	803	1076	.1318
	.050690	8.9752	.4169	.0056478	5.171	637	910	.1085
	.040304	7.5417	.2785	.0053442	4.893	563	836	.1022
	.030756	6.1988	.1747	.0049616	4.542	481	754	.0978
	.023456	5.1726	.1112	.0045347	4.152	409	682	.0941
	.0176975	4.6541	.0755	.0031507	2.884	272	545	.1156
	.018786	4.7261	.08136	.0038026	3.481	327	600	.1095
	.020745	4.8494	.09218	.0042787	3.917	375	648	.0966
	.013442	4.2665	.05255	.0039749	3.639	342.5	615.5	.1059

Table (C-21)
(Continued)

Sample Condition	Voltage V (volts)	Current I (amps)	Power P/A ($watts/cm^2$)	Resistance R (ohms)	R Ratio R/R_{30} (ohms/ohm)	Temperature T ^oC	Temperature T ^oK	Emittance ϵ
Oxidized	.095226	15.108	1.3183	.0063030	5.770	797	1070	.1784
R_{30} = .0010923 ohms	.08098	13.302	.9871	.0060878	5.573	744	1017	.1639
	.076491	12.712	.8910	.0060172	5.509	727	1000	.1584
p = 1 x 10^{-7} Torr	.068804	11.718	.7388	.0058717	5.376	691	964	.1523
	.063647	11.041	.6439	.0057646	5.278	665	938	.1482
	.050138	9.1867	.4221	.0054577	4.997	591	864	.1355
	.036900	7.2863	.2464	.0050643	4.636	501	774	.1238
	.029384	6.1800	.1664	.0047547	4.353	444	717	.1145
	.023906	5.4075	.1185	.0044209	4.051	394	667	.1100
	.021104	5.1247	.09910	.0041181	3.770	357	630	.1169
	.017660	4.8484	.07846	.0036424	3.335	313	586	.1260
	.055894	9.9800	.51115			626	899	.1397

EMITTANCE

Table (C-22)

Sample SE#10 Information, Emittance Data and Calculated Values

Type Crystal-(111) Semi-Element

A. Sample Dimensions

Length (in.)	Width (in.)	Thickness (in.)	Area (cm^2)	$\frac{\text{Sample (mils)}}{\text{Heat Sink (mils)}}$	Area Factor
.4949	.1742	.006	1.1762	3.0	.9511

B. Emittance Runs: Bare Sample and 33.3 μ g/cm^2 of oxygen

R_{30} = .00138795 ohms

p = 2.3×10^{-7} Torr

Sample Condition	Voltage V (volts)	Current I (amps)	Power P/A (watts/cm^2)	Resistance R (ohms)	R Ratio R/R_{30} (ohms/ohm)	Temperature T ^oC	Temperature T ^oK	Emittance ϵ
Bare	.101125	12.484	1.0733	.0081004	5.836	814	1087	.1363
	.11720	13.976	1.3926	.0083858	6.042	869	1142	.1450
	.093505	11.752	.9343	.0079565	5.733	785	1058	.1323
	.079826	10.403	.7060	.0076734	5.529	733	1006	.1225
	.067555	9.149	.5255	.0073839	5.320	677	950	.1149
	.056548	7.9827	.3838	.0070838	5.104	620	893	.1078
	.044813	6.6924	.2550	.0066961	4.825	546	819	.1017
	.038445	5.9622	.1950	.0064438	4.643	503	776	.0970
	.032182	5.2454	.1435	.0061353	4.420	456	729	.0922
	.027317	4.6879	.1089	.0058271	4.198	417	690	.0878
	.024986	4.4337	.0942	.0056355	4.060	396	669	.0864
	.022658	4.2266	.08142	.0053608	3.862	369	642	.0887
	.020290	4.0894	.07054	.0049616	3.575	336.5	609.5	.0957
	.018042	3.9408	.06045	.0045783	3.299	309.5	582.5	.0996

Table (C-22)
(Continued)

Sample Condition	Voltage V (volts)	Current I (amps)	Power P/A ($watts/cm^2$)	Resistance R (ohms)	R Ratio R/R_{30} (ohms/ohm)	Temperature T ^oC	Temperature T ^oK	Emittance ϵ
Oxidized	.10506	13.960	1.2469	.0075258	5.407	700	973	.2475
R_{30} = .0013919 ohms	.127751	16.274	1.7676	.0078475	5.638	761	1034	.2746
	.082282	11.521	.8060	.0071419	5.131	626	899	.2203
$p = 1.4 \times 10^{-7}$ Torr	.071888	10.363	.6334	.0069370	4.984	588	861	.2062
	.060910	9.1052	.4715	.0066896	4.806	542	815	.1919
	.050431	7.8719	.3375	.0064065	4.603	494	767	.1761
	.040880	6.7098	.2332	.0060926	4.377	446	719	.1587
	.034823	5.9670	.1767	.0058359	4.193	415.5	442.8	.1438
	.027505	5.1806	.12105	.0053092	3.814	362.5	389.8	.1378
	.020495	4.6407	.08086	.0044164	3.173	298	571	.1452
	.031856	5.6113	.1520	.0056771	4.079	399	672	.1368
	.023386	4.8864	.09716	.0047859	3.438	323	596	.1451

EMITTANCE

Table (C-23)

Sample SE#11 Information, Emittance Data and Calculated Values

Type Crystal-(111) Semi-Element

A. Sample Dimensions

Length (in.)	Width (in.)	Thickness (in.)	Area (cm^2)	$\frac{\text{Sample (mils)}}{\text{Heat Sink (mils)}}$	Area Factor
.4971	.1675	.0064	1.1381	2.1	.969

B. Emittance Runs: Bare Sample and 57.6 $\mu g/cm^2$ of oxygen

R_{30} = .0015565 ohms

$p = 1.83 \times 10^{-7}$ Torr

Sample Condition	Voltage V (volts)	Current I (amps)	Power P/A ($watts/cm^2$)	Resistance R (ohms)	R Ratio R/R_{30} (ohms/ohm)	Temperature T ^oC	Temperature T ^oK	Emittance ϵ
Bare	.11998	12.756	1.3447	.0094058	6.043	870	1143	.1396
	.093321	10.530	.8634	.0088624	5.694	776	1049	.1266
	.107925	11.770	1.1161	.0091695	5.891	828	1101	.1347
	.077300	9.1214	.6195	.0084746	5.445	711	984	.1175
	.063057	7.8191	.4332	.0080645	5.181	640	913	.1112
	.051083	6.6822	.2999	.0076446	4.911	568	841	.1074
	.038052	5.4063	.1808	.0070385	4.522	477	750	.1034
	.026264	4.3357	.10005	.0060576	3.892	372	645	.1069
	.044208	6.0126	.23355	.0073526	4.724	522	795	.1052
	.032673	4.8870	.1403	.0066857	4.295	433	706	.1029
	.015570	3.6671	.05017	.0042459	2.728	258	531	.1239
	.029583	4.5985	.1195	.0064332	4.133	406	679	.1031
	.022444	4.1662	.08216	.0053872	3.461	325	598	.1209
	.024272	4.2537	.09072	.0057061	3.666	345	618	.1161

Table (C-23)
(Continued)

Sample Condition	Voltage V (volts)	Current I (amps)	Power P/A ($watts/cm^2$)	Resistance R (ohms)	R Ratio R/R_{30} (ohms/ohm)	Temperature T ^oC	Temperature T ^oK	Emittance ϵ
Oxidized	.137739	15.955	1.9309	.0086330	5.530	733	1006	.3350
R_{30} = .0015612 ohms	.144130	16.517	2.0917	.0087262	5.589	749	1022	.3406
	.151484	17.158	2.2838	.0088288	5.655	766	1039	.3479
$p = 8.5 \times 10^{-7}$ Torr	.18325	19.852	3.1964	.0092308	5.913	834	1107	.3773
	.138206	15.979	1.9404	.0086492	5.540	736	1009	.3327
	.115428	13.915	1.4113	.0082952	5.313	674	947	.3125
	.095786	12.053	1.0144	.0079471	5.090	615.5	888.5	.2908
	.078546	10.354	.7146	.0075861	4.859	555	828	.2727
	.060721	8.5113	.4541	.0071342	4.570	487	760	.2459
	.045796	6.9148	.2782	.0066229	4.242	424	697	.2152
	.020847	4.7900	.2009	.0043522	2.788	263.5	536.5	.2069
	.029264	5.4927	.1659	.0053278	3.413	320	593	.2155
	.037674	6.0680	.1412	.0062086	3.977	384	657	.1987
	.032880	5.7431	.0877	.0057251	3.667	345.5	618.5	.2116

EMITTANCE

Table (C-24)

Sample SE#12 Information, Emittance Data and Calculated Values

Type Crystal-(111) Semi-Element

A. Sample Dimensions

Length (in.)	Width (in.)	Thickness (in.)	Area (cm^2)	$\frac{\text{Sample}}{\text{Heat Sink}}$ (mils) (mils)	Area Factor
.4948	.1686	.0095	1.1400	3.2	1.031

B. Emittance Runs: Bare Sample and 20.4 $\mu g/cm^2$ of oxygen

R_{30} = .00092587 ohms

$p = 2.1 \times 10^{-7}$ Torr

Sample Condition	Voltage V (volts)	Current I (amps)	Power P/A ($watts/cm^2$)	Resistance R (ohms)	R Ratio R/R_{30} (ohms/ohm)	Temperature T ^oC	Temperature T ^oK	Emittance ϵ
Bare	.071105	13.451	.83898	.0052862	5.709	780	1053	.1211
	.091864	16.428	1.3238	.0055919	6.039	868	1141	.1384
	.072191	13.640	.8638	.0052926	5.716	782	1055	.1214
	.057923	11.486	.5836	.0050429	5.446	711	984	.1089
	.048542	10.024	.4268	.0048426	5.230	653	926	.1017
	.036444	8.0576	.32025	.0045229	4.885	561	834	.0955
	.025083	6.1333	.2576	.0040896	4.417	455	728	.0872
	.041255	8.8493	.1967	.0046620	5.035	602	875	.0977
	.031214	7.1827	.1349	.0043457	4.693	514	787	.0923
	.020675	5.4045	.0980	.0038255	4.132	406	679	.0845
	.0158419	4.8452	.0832	.0032696	3.531	332	605	.0943
	.018619	5.0934	.0755	.0036555	3.948	380	653	.0844
	.012856	4.5549	.0673	.0028223	3.048	287	560	.1003
	.017316	4.9722	.0514	.0034826	3.761	356	629	.0897

Table (C-24)
(Continued)

Sample Condition	Voltage V (volts)	Current I (amps)	Power P/A (watts/cm^2)	Resistance R (ohms)	R Ratio R/R_{30} (ohms/ohm)	Temperature T ^oC	Temperature T ^oK	Emittance ϵ
Oxidized	.074188	14.826	.9648	.0050039	5.404	699	972	.1923
R_{30} = .00092587 ohms	.085009	16.484	1.2292	.0051571	5.570	743	1016	.2049
	.098784	18.548	1.6072	.0053259	5.752	792	1065	.2217
	.060813	12.669	.6758	.0048001	5.184	641	914	.1727
$p = 1.75 \times 10^{-7}$ Torr	.050413	10.952	.4843	.0046031	4.971	584	857	.1607
	.040885	9.3270	.3345	.0043835	4.734	524	797	.1492
	.030816	7.5440	.2039	.0040848	4.412	454	727	.1325
	.016543	5.4369	.0789	.0030427	3.286	308	581	.1314
	.022928	6.1656	.1240	.0037187	4.016	389	662	.1188
	.026117	6.7010	.1535	.0038975	4.209	418	691	.1231
	.019326	5.7428	.0974	.033653	3.634	342	615	.1272
	.013303	5.0196	.0586	.026502	2.862	270	543	.1310
	.021256	5.9242	.1105	.035880	3.875	370.5	643.5	.1192

EMITTANCE

Table (C-25)

Sample OSC#1 Information, Emittance Data and Calculated Values

Type Crystal-(100) Research Crystal Inc.

A. Sample Dimensions

Length (in.)	Width (in.)	Thickness (in.)	Area (cm^2)	$\frac{\text{Sample (mils)}}{\text{Heat Sink (mils)}}$	Area Factor
.4933	.1942	.0073	1.300	1.5	.7104

B. Emittance Runs: Bare Sample and 38.4 $\mu g/cm^2$ of oxygen

Sample Condition	Voltage V (volts)	Current I (amps)	Power P/A ($watts/cm^2$)	Resistance R (ohms)	R Ratio R/R_{30} (ohms/ohm)	Temperature T ^oC	Temperature T ^oK	Emittance ϵ
Bare	.23679	32.0268	5.8349	.0073935	7.099	1152	1425	.2499
R_{30} = .0010414 ohms	.21125	29.3935	4.7776	.0071869	6.901	1098	1371	.2389
	.18647	26.7709	3.8567	.0069654	6.688	1040	1313	.2294
$p = 5.6 \times 10^{-7}$ Torr	.16226	24.1495	3.0149	.0067190	6.452	978	1251	.2177
	.1505	22.8695	2.648	.0065808	6.319	942	1215	.2150
	.13910	21.5569	2.3071	.0064527	6.196	910	1183	.2085
	.128447	20.3194	2.008	.0063214	6.070	876	1149	.2040
	.127161	20.2187	1.9782	.0062893	6.039	867	1140	.2075
	.116278	18.9410	1.6945	.00613895	5.895	830	1103	.2030
Oxidized	.065528	13.142	.67223	.0049862	4.848	552	825	.2609
R_{30} = .0010285 ohms	.078224	15.0737	.9204	.0051894	5.046	604	877	.2781
	.114047	20.231	1.8011	.0056372	5.481	721	994	.3280
$p = 2.3 \times 10^{-7}$ Torr	.125708	21.8045	2.1397	.0057652	5.605	753	1026	.3429
	.096247	17.6759	1.3280	.0054451	5.294	670	943	.2991
	.065944	13.1499	.6769	.0050148	4.876	559	832	.2533

Table (C-25)
(Continued)

Sample Condition	Voltage V (volts)	Current I (amps)	Power P/A (watts/cm^2)	Resistance R (ohms)	R Ratio R/R_{30} (ohms/ohm)	Temperature T ^oC	Temperature T ^oK	Emittance ϵ
Oxidized	.078624	15.0863	.9259	.00521161	5.067	609	882	.2734
R_{30} = .0010285 ohms	.114443	20.2325	1.8075	.0056564	5.500	725	1008	.3239
	.065838	13.1350	.6753	.0050139	4.875	559	832	.2527
$p = 2.3 \times 10^{-7}$ Torr	.045300	9.83339	.3477	.0046068	4.479	467	740	.2101
	.029641	7.21263	.1669	.0041096	3.996	387	660	.1620
	.018317	5.87319	.8378	.0031187	3.032	285	558	.1666
	.024300	6.52044	.1237	.0037267	3.623	341	614	.1627
	.037312	8.50413	.2477	.0043875	4.266	427	700	.1882
	.027473	6.89200	.1478	.0039862	3.876	370	643	.1600

EMITTANCE

Table (C-26)

Sample OSC#2 Information, Emittance Data and Calculated Values

Type Crystal-(110) Research Crystal Inc.

A. Sample Dimensions

Length (in.)	Width (in.)	Thickness (in.)	Area (cm^2)	$\frac{\text{Sample (mils)}}{\text{Heat Sink (mils)}}$	Area Factor
.5168	.162	.006	1.113	1.2	.7104

B. Emittance Runs: Bare Sample and 82.8 $\mu g/cm^2$ of oxygen

Sample Condition	Voltage V (volts)	Current I (amps)	Power P/A ($watts/cm^2$)	Resistance R (ohms)	R Ratio R/R_{30} (ohms/ohm)	Temperature T ^oC	Temperature T ^oK	Emittance ϵ
Bare	.12244	9.3132	1.0456	.013147	5.481	721	994	.18652
R_{30} = .0024065 ohms	.15743	11.2022	1.6172	.014053	5.859	821	1094	.19607
	.18249	12.5135	2.0941	.014583	6.079	879	1152	.20627
$p = 3.9 \times 10^{-7}$ Torr	.10877	8.5401	.85181	.012736	5.31	674	947	.18476
	.09626	7.8329	.69141	.012289	5.123	625	898	.18592
	.20856	13.8427	2.6474	.015066	6.281	932	1205	.21767
	.23315	15.0635	3.2205	.015478	6.452	977	1250	.22856
	.26106	16.4162	3.9299	.015903	6.630	1025	1298	.23976
	.28791	17.6885	4.6700	.016277	6.786	1066	1339	.25146
Oxidized	.15374	12.3025	1.69884	.012497	5.196	643	916	.4304
R_{30} = .0024069 ohms	.18242	13.9758	2.28992	.0130525	5.427	705	979	.4452
	.114464	9.80582	1.008151	.011673	4.853	553	826	.3886
$p = 6.6 \times 10^{-7}$ Torr	.20054	15.0216	2.70576	.0133501	5.551	739	1012	.4583
	.21921	16.0763	3.165333	.0136356	5.669	770	1043	.4748
	.095712	8.55448	.7354158	.0111885	4.652	505	778	.3619

Table (C-26)
(Continued)

Sample Condition	Voltage V (volts)	Current I (amps)	Power P/A (watts/cm^2)	Resistance R (ohms)	R Ratio R/R_{30} (ohms/ohm)	Temperature T ^oC	Temperature T ^oK	Emittance ϵ
Oxidized	.076381	7.21443	.494949	.01058725	4.402	452	725	.3254
R_{30} = .0024069 ohms	.054482	5.66343	.277144	.00961996	4.000	387	660	.2690
	.043588	5.09409	.199437	.00855658	3.558	334	607	.2754
$p = 6.6 \times 10^{-7}$ Torr	.033653	4.55891	.1378027	.0073818	3.069	288	561	.2671
	.025834	4.05430	.09407637	.0063720	2.649	251	524	.2465
	.15460	12.3337	1.712678	.0125347	5.212	647	920	.4263
	.26138	18.363	4.311108	.014234	5.918	835	1118	.5070
	.049364	5.38775	.238886	.00916226	3.809	362	635	.2726
	.038095	4.84238	.1656914	.00786699	3.271	307	580	.2780
	.028071	4.27904	.107889	.00656011	2.727	258	531	.2664

EMITTANCE

Table (C-27)

Sample OSC#3 Information, Emittance Data and Calculated Values

Type Crystal-(100) Research Crystal Inc.

A. Sample Dimensions

Length (in.)	Width (in.)	Thickness (in.)	Area (cm^2)	$\frac{\text{Sample (mils)}}{\text{Heat Sink (mils)}}$	Area Factor
.4847	.20375	.0118	1.3369	3.9	.8653

B. Emittance Runs: Bare Sample and 29.4 $\mu g/cm^2$ of oxygen

R_{30} = .00073593 ohms

p = 1 x 10^{-7} Torr

Sample Condition	Voltage V (volts)	Current I (amps)	Power P/A ($watts/cm^2$)	Resistance R (ohms)	R Ratio R/R_{30} (ohms/ohm)	Temperature T ^oC	Temperature T ^oK	Emittance ϵ
Bare	.051155	13.240	.5065	.0038633	5.239	654	927	.1223
	.089720	20.5579	1.3795	.00436425	5.919	835	1108	.1622
	.076439	18.1338	1.0367	.00421527	5.717	782	1055	.1485
	.063132	15.5951	.7364	.00404819	5.490	723	996	.1330
	.051262	13.2416	.5077	.00387128	5.250	658	931	.1205
	.042287	11.3706	.35623	.00371897	5.044	604	877	.1087
	.034956	9.8124	.25655	.0035624	4.831	547	820	.1019
	.025686	7.7502	.14890	.0033142	4.495	471	744	.0880
	.018636	6.1441	.085643	.0030332	4.114	404	677	.0748
	.0088191	4.5577	.030065	.0019350	2.624	249	522	.0801
	.0145785	5.3878	.058750	.0027058	3.669	345	618	.0752
	.016408	5.68081	.06971	.002888	3.917	375	648	.0731
	.0107319	4.91969	.04022	.002222	3.013	283	556	.0811
	.051234	13.2404	.050739	.003869	5.247	657	930	

Table (C-27)
(Continued)

Sample Condition	Voltage V (volts)	Current I (amps)	Power P/A (watts/cm^2)	Resistance R (ohms)	R Ratio R/R_{30} (ohms/ohm)	Temperature T ^oC	Temperature T ^oK	Emittance ϵ
Oxidized	.046835	13.257	.46443	.0035329	4.790	537	810	.1939
R_{30} = .00073799 ohms	.083485	20.759	1.29627	.0040216	5.452	712	985	.2449
	.093534	22.675	1.5863	.0041250	5.592	749	1022	.2583
	.102691	24.359	.18711	.0042157	5.715	781	1054	.2691
$p = .45 \times 10^{-7}$ Torr	.046944	13.2404	.4649	.0035455	4.807	541	814	.1902
	.070508	18.1577	.95759	.00388309	5.264	662	935	.2233
	.057887	15.5741	.6743	.00371687	5.039	602	875	.2056
	.037186	11.100	.3087	.0033501	4.542	481	754	.1727
	.027074	8.7463	.1771	.0030955	4.197	416	689	.1437
	.016679	6.6757	.08329	.0024985	3.387	318	591	.1289
	.0068652	4.5757	.02349	.0015004	2.034	200	473	.0987
	.022643	7.7149	.13067	.0029350	3.979	385	658	.1284
	.010848	5.6125	.04554	.0019328	2.620	249	552	.1214
	.020246	7.1940	.10895	.0028143	3.815	263	536	.1235
	.0134252	6.150065	.061756	.00218293	2.959	278	551	.1295
	.018256	6.93995	.094764	.0026305	3.566	335	608	.12997
	.046754	13.2375	.462923	.0035319	4.788	536	809	.1942

EMITTANCE

Table (C-28)

Sample OSC#4 Information, Emittance Data and Calculated Values

Type Crystal-(100) Research Crystal Inc.

A. Sample Dimensions

Length (in.)	Width (in.)	Thickness (in.)	Area (cm^2)	$\frac{\text{Sample (mils)}}{\text{Heat Sink (mils)}}$	Area Factor
.4939	.1668	.0054	1.0947	2.7	.7486

B. Emittance Runs: Bare Sample and 77.2 μ g/cm^2 of oxygen

R_{30} = .0024947 ohms

p = 6.8×10^{-7} Torr

Sample Condition	Voltage V (volts)	Current I (amps)	Power P/A (watts/cm^2)	Resistance R (ohms)	R Ratio R/R_{30} (ohms/ohm)	Temperature T ^oC	Temperature T ^oK	Emittance ϵ
Bare	.132837	9.3414	1.1335	.014220	5.694	776	1049	.1661
	.16767	11.171	1.71102	.015009	6.010	860	1133	.1840
	.18776	12.1838	2.0897	.0154106	6.171	903	1176	.1934
	.095271	7.2216	.628496	.013193	5.283	668	941	.1428
	.071599	5.8133	.380223	.012316	4.932	574	847	.1323
	.052073	4.5709	.217432	.011392	4.562	486	759	.1184
	.036104	3.5107	.115786	.010284	4.118	404	677	.1011
	.018556	2.5512	.043245	.0072734	2.912	274	547	.0936
	.028186	3.0115	.0775398	.0093595	3.748	355	628	.0927
	.032606	3.2758	.975716	.0099536	3.986	386	659	.09530
	.021736	2.7544	.0546909	.00789137	3.160	297	570	.0989
	.132886	9.34136	1.13396	.0142255	5.696	776	1049	.1662

Table (C-28)
(Continued)

Sample Condition	Voltage V (volts)	Current I (amps)	Power P/A ($watts/cm^2$)	Resistance R (ohms)	R Ratio R/R_{30} (ohms/ohm)	Temperature T ^oC	Temperature T ^oK	Emittance ϵ
Oxidized	.113119	9.32518	.96361	.0121304	4.829	547	820	.3826
R_{30} = .0025136 ohms	.16361	12.3337	1.84336	.0132653	5.281	667	940	.4206
	.20473	14.6110	2.13256	.014012	5.578	745	1018	.4520
p = 3 x 10^{-7} Torr	.081319	7.26957	.5400	.0111862	4.453	463	736	.3337
	.058346	5.70418	.304027	.0102286	4.072	398	671	.2754
	.038534	4.57509	1.6104	.0082256	3.353	315	688	.2548
	.049450	5.09948	2.3035	.009697	3.860	369	642	.2510
	.029414	4.08366	.109726	.0072028	2.867	271	544	.2434
	.044568	4.84238	.197147	.0092037	3.664	345	618	.2523
	.24194	16.5798	3.6643	.0145924	5.809	807	1080	.4777
	.113211	9.31919	.96377	.012148	4.836	548	821	.3808
	.22158	15.5178	3.141009	.014279	5.684	774	1047	.4640

EMITTANCE

Table (C-29)

Sample OSC#5 Information, Emittance Data and Calculated Values

Type Crystal-(110) Research Crystal Inc.

A. Sample Dimensions

Length (in.)	Width (in.)	Thickness (in.)	Area (cm^2)	$\frac{\text{Sample (mils)}}{\text{Heat Sink (mils)}}$	Area Factor
.4951	.1474	.0096	1.005	3.2	.7825

B. Emittance Runs: Bare Sample and 68.8 μ g/cm^2 of oxygen

R_{30} = .0011010 ohms

p = 8.5×10^{-7} Torr

Sample Condition	Voltage V (volts)	Current I (amps)	Power P/A (watts/cm^2)	Resistance R (ohms)	R Ratio R/R_{30} (ohms/ohm)	Temperature T ^oC	Temperature T ^oK	Emittance ϵ
Bare	.076635	12.4146	.9463	.0061730	5.602	752	1025	.1522
	.088791	13.9158	1.2290	.0063806	5.790	802	1075	.1632
	.10436	15.7695	1.6368	.0066175	6.005	859	1132	.1766
	.060253	10.3104	.6179	.0058439	5.303	672	945	.1380
	.046981	8.5191	.3981	.0055148	5.005	593	866	.1266
	.037582	7.1976	.2691	.0052214	4.738	524	797	.1200
	.076612	12.4026		.00617709	5.606	753	1026	
	.028774	5.9199	.1694	.0048605	4.411	454	727	.1101
	.018808	4.5355	.0848	.0041468	3.763	357	630	.1001
	.011367	3.8158	.04314	.0029790	2.703	256	529	.1083
	.023333	5.1360	.1192	.0045430	4.123	405	678	.1034
	.015582	4.3126	.0668	.0036131	3.279	307	580	.1122
	.021026	4.8166	.1007	.0043653	3.961	381	654	.1016

Table (C-29)
(Continued)

Sample Condition	Voltage V (volts)	Current I (amps)	Power P/A (watts/cm^2)	Resistance R (ohms)	R Ratio R/R_{30} (ohms/ohm)	Temperature T ^oC	Temperature T ^oK	Emittance ϵ
Oxidized	.083639	15.0042	1.2483	.0055744	5.046	604	877	.3772
R_{30} = .0011048 ohms	.111667	18.674	2.0742	.0059798	5.413	700	973	.4117
	.122430	20.0168	2.4375	.0061164	5.536	734	1007	.4212
$p = 7.2 \times 10^{-7}$ Torr	.138533	21.968	3.0270	.0063061	5.708	780	1053	.4369
	.083946	15.0018	1.2526	.0055957	5.065	609	882	.3699
	.112006	18.6923	2.0823	.0059921	5.424	704	977	.4065
	.065378	12.4296	.8083	.0052599	4.761	794	1067	
	.047821	9.8352	.4678	.0048622	4.401	453	726	.3058
	.031655	7.3271	.2307	.0043203	3.910	375	648	.2418
	.039216	8.50054	.3316	.0046134	4.176	413	686	.2740
	.019131	5.93312	.1129	.0032244	2.919	275	548	.2425
	.025794	6.68225	.1714	.0038601	3.494	328	601	.2470
	.083894	15.0084	1.2524	.0055898	5.060	607	880	.3732
	.029340	6.99868	.2042	.0041922	3.795	360	633	.2362

EMITTANCE

Table (C-30)

Sample OSC#6 Information, Emittance Data and Calculated Values

Type Crystal-(100) Research Crystal Inc.

A. Sample Dimensions

Length (in.)	Width (in.)	Thickness (in.)	Area (cm^2)	$\frac{\text{Sample (mils)}}{\text{Heat Sink (mils)}}$	Area Factor
.5051	.02845	.0096	1.4237	3.2	.8811

B. Emittance Runs: Bare Sample and 13.5 μ g/cm^2 of oxygen

R_{30} = .00082413 ohms

$p = 1.45 \times 10^{-7}$ Torr

Sample Condition	Voltage V (volts)	Current I (amps)	Power P/A (watts/cm^2)	Resistance R (ohms)	R Ratio R/R_{30} (ohms/ohm)	Temperature T ^oC	Temperature T ^oK	Emittance ϵ
Bare	.058426	13.3615	.5483426	.0043727	5.309	673	946	.1219
	.0888405	18.5389	1.156873	.00479211	5.818	809	1082	.1497
	.098704	20.1264	1.39538	.0049042	5.951	845	1118	.1583
	.05825	13.3142	.544755	.004375028	5.309	673	946	.1211
	.072816	15.7682	.80649	.00458909	5.568	742	1015	.1350
	.043476	10.5999	.323699	.00410155	4.977	585	858	.1069
	.032652	8.49934	.194933	.0038417	4.661	507	780	.0949
	.023733	6.69663	.1116348	.00354402	4.303	434	707	.0814
	.0110437	4.60626	.0357317	.0023975	2.911	275	548	.07674
	.01999	5.9511	.0835604	.003359	4.078	398	671	.0757
	.016730	5.36138	.0630033	.00312046	3.788	359	632	.0733
	.018395	5.64245	.072905	.0032601	3.958	381	654	.0735
	.0142238	5.08510	.0508049	.00279715	3.396	319	592	.0781

Table (C-30)
(Continued)

Sample Condition	Voltage V (volts)	Current I (amps)	Power P/A (watts/cm^2)	Resistance R (ohms)	R Ratio R/R_{30} (ohms/ohm)	Temperature T ^oC	Temperature T ^oK	Emittance ϵ
Oxidized	.054633	13.255	.50865			591	864	.1633
	.098874	21.015				780	1053	.2107
R_{30} = .00082472 ohms	.079148	17.6639	.98201	.00448077	5.432	707	980	.1894
	.064485	15.0605	.68216	.0042817	5.191	642	915	.1736
$p = 6.6 \times 10^{-7}$ Torr	.054541	13.232	.5069198	.0041219	4.997	591	864	.1627
	.040805	10.5855	.303399	.0038548	4.673	509	782	.1462
	.03042	8.48316	.18128019	.0035863	4.348	442	715	.1262
	.024226	7.20664	.122632	.0033616	4.075	398	671	.1111
	.0159052	5.88337	.065727	.0027034	3.277	307	580	.1103
	.021784	6.70742	.102632	.0032477	3.937	378	651	.1055
	.0125148	5.37157	.04721889	.0023298	2.824	267	540	.1082
	.019060	6.28251	.084109	.0030338	3.678	346	619	.1069

EMITTANCE

Table (C-31)

Sample OSC#7 Information, Emittance Data and Calculated Values

Type Crystal-(100) Research Crystal Inc.

A. Sample Dimensions

Length(in.)	Width (in.)	Thickness (in.)	Area (cm^2)	$\frac{\text{Sample (mils)}}{\text{Heat Sink (mils)}}$	Area Factor
.5219	.1675	.004	1.1550	4.0	.7104

B. Emittance Runs: Bare Sample and 62.4 $\mu g/cm^2$ of oxygen

R_{30} = .0034465 ohms

p = 2×10^{-7} Torr

Sample Condition	Voltage V (volts)	Current I (amps)	Power P/A ($watts/cm^2$)	Resistance R (ohms)	R Ratio R/R_{30} (ohms/ohm)	Temperature T ^oC	Temperature T ^oK	Emittance ϵ
Bare	.16700	8.49275	1.22799	.0196638	5.705	779	1052	.1779
	.19637	9.60506	1.63307	.0204444	5.932	839	1112	.1893
	.124524	6.75836	.72866	.0184251	5.346	683	956	.1553
	.098846	5.65923	.484338	.0174663	5.068	609	882	.1430
	.074818	4.5703	.29606	.01637047	4.750	528	801	.1293
	.053188	3.52511	.162337	.0150883	4.378	448	721	.1092
	.033692	2.54585	.074266	.01323408	3.840	366	639	.0825
	.043127	3.02050	.112787	.01427809	4.143	408	681	.0961
	.019185	2.02385	.033618	.00947945	2.750	261	534	.0895
	.026049	2.29054	.0516608	.0113724	3.300	309	582	.08542
	.038154	2.76579	.091367	.01379497	4.002	388	661	.08812
	.028684	2.37205	.0589109	.0120725	3.509	329	602	.08428

Table (C-31)
(Continued)

Sample Condition	Voltage V (volts)	Current I (amps)	Power P/A ($watts/cm^2$)	Resistance R (ohms)	R Ratio R/R_{30} (ohms/ohm)	Temperature T ^oC	Temperature T ^oK	Emittance ϵ
Oxidized	.17252	9.6248	1.4376	.017925	5.167	636	909	.3757
R_{30} = .0034692 ohms	.20571	11.009	1.9607	.018686	5.386	694	967	.3990
	.21927	11.558	2.1942	.018971	5.468	716	989	.4078
$p = 7.9 \times 10^{-7}$ Torr	.17286	9.66382	1.4463	.017943	5.172	637	910	.3763
	.133238	7.90003	.911327	.0168655	4.861	556	829	.3461
	.097554	6.2388	.52094	.015637	4.507	473	746	.3080
	.064451	4.5937	.256336	.014030	4.044	393	676	.2396
	.034551	3.32015	.0993198	.010406	2.999	282	555	.2018
	.049058	3.89188	.165305	.012605	3.633	346	619	.2159
	.056278	4.18315	.203826	.0134535	3.878	370	643	.2207
	.043028	3.67374	.13686019	.0117123	3.376	316	589	.2149

EMITTANCE

Table (C-32)

Sample OSC#8 Information, Emittance Data and Calculated Values

Type Crystal-(110) Research Crystal Inc.

A. Sample Dimensions

Length (in.)	Width (in.)	Thickness (in.)	Area (cm^2)	$\frac{\text{Sample (mils)}}{\text{Heat Sink (mils)}}$	Area Factor
.5042	.1321	.010	.9246	3.3	.7865

B. Emittance Runs: Bare Sample and 48.1 μ g/cm^2 of oxygen

R_{30} = .0011905 ohms

$p = 4.5 \times 10^{-7}$ Torr

Sample Condition	Voltage V (volts)	Current I (amps)	Power P/A ($watts/cm^2$)	Resistance R (ohms)	R Ratio R/R_{30} (ohms/ohm)	Temperature T ^oC	Temperature T ^oK	Emittance ϵ
Bare	.083324	12.2600	1.1048	.00679641	5.709	780	1053	.1595
	.112564	15.4668	1.88289	.00727778	6.113	887	1160	.1842
	.098934	13.9956	1.49748	.0070689	5.938	840	1113	.1730
	.083470	12.2696	1.10761	.006680299	5.714	781	1054	.1593
	.067537	10.4111	.760439	.006487018	5.449	711	984	.1442
	.051978	8.50773	.47825	.0061095	5.132	627	900	.1301
	.038923	6.82488	.28729	.0057031	4.790	537	810	.1199
	.032516	5.96907	.209908	.0054474	4.576	488	761	.1131
	.022165	4.5685	.109513	.0048517	4.075	398	671	.0992
	.017292	4.07287	.0761679	.0042456	3.566	335	608	.1045
	.027359	5.26969	.155923	.00519176	4.361	445	718	.1067
	.020226	4.32159	.094532	.00468022	3.931	377	650	.0978
	.0135747	3.79060	.055649	.00358114	3.008	283	556	.1122

Table (C-32)
(Continued)

Sample Condition	Voltage V (volts)	Current I (amps)	Power P/A ($watts/cm^2$)	Resistance R (ohms)	R Ratio R/R_{30} (ohms/ohm)	Temperature T ^oC	Temperature T ^oK	Emittance ϵ
Oxidized	.102573	15.9205	1.7661	.00644282	5.402	699	972	.3520
R_{30} = .0011923 ohms	.120210	18.0091	2.34131	.00667495	5.596	750	1023	.3797
	.086037	13.8937	1.29279	.00619252	5.192	643	916	.3275
p = 6×10^{-8} Torr	.073179	12.2690	.97100	.00596454	5.001	593	866	.3088
	.058853	10.3770	.66049	.0056715	4.755	529	802	.2871
	.045269	8.49814	.416055	.0053269	4.466	465	738	.2543
	.032900	6.70862	.238702	.00490413	4.112	403	676	.2097
	.025025	5.64305	.152726	.00443465	3.718	351	624	.1876
	.029225	6.17464	.19516	.00473306	3.968	383	656	.1943
	.018785	5.0857	.1033209	.00369369	3.097	291	564	.1957
	.016475	4.8244	.085959	.0034149	2.863	270	543	.1922
	.021355	5.34640	.123477	.00399427	3.350	314	587	.1968

EMITTANCE

Table (C-33)

Sample OSC#9 Information, Emittance Data and Calculated Values

Type Crystal-(110) Research Crystal Inc.

A. Sample Dimensions

Length (in.)	Width (in.)	Thickness (in.)	Area (cm^2)	$\frac{\text{Sample (mils)}}{\text{Heat Sink (mils)}}$	Area Factor
.5128	.1360	.0121	.9662	2.4	.8026

B. Emittance Runs: Bare Sample and 18.96 μ g/cm^2 of oxygen

R_{30} = .00099638 ohms

p = 0.8 x 10^{-7} Torr

Sample Condition	Voltage V (volts)	Current I (amps)	Power P/A (watts/cm^2)	Resistance R (ohms)	R Ratio R/R_{30} (ohms/ohm)	Temperature T ^oC	Temperature T ^oK	Emittance ϵ
Bare	.061923	11.454	.73409	.0054062	5.453	712	985	.1387
	.082589	14.377	1.2289	.0057445	5.794	803	1076	.1626
	.096861	16.271	1.6312	.0059530	6.005	859	1132	.1760
	.072388	12.9594	.9709	.0055857	5.634	761	1034	.1508
	.054295	10.362	.58229	.00523982	5.285	667	940	.1329
	.047367	9.3252	.45716	.0050795	5.124	625	898	.1255
	.039197	8.0666	.32725	.0048592	4.901	566	839	.1184
	.027359	6.1890	.1752	.0044206	4.459	464	737	.1077
	.017683	4.5841	.08389	.0038575	3.891	372	645	.0896
	.020385	5.0941	.10747	.0040017	4.036	392	665	.1011
	.012254	4.0273	.051077	.0030427	3.069	288	561	.0990
	.0140122	4.3689	.06336	.0032073	3.235	303.5	576.5	.1091
	.0155715	4.4978	.07249	.0034620	3.492	328	601	.1044

Table (C-33)
(Continued)

Sample Condition	Voltage V (volts)	Current I (amps)	Power P/A (watts/cm^2)	Resistance R (ohms)	R Ratio R/R_{30} (ohms/ohm)	Temperature T ^oC	Temperature T ^oK	Emittance ϵ
Oxidized	.067730	12.8323	.89955	.00527809	5.334	680	953	.1942
	.088255	15.7977	1.4430	.00558657	5.646	763	1036	.2224
R_{30} = .00099064 ohms	.098773	17.2498	1.76345	.0057260	5.787	800	1073	.2360
	.076269	14.0789	1.111366	.0054172	5.475	719	992	.2039
$p = 2.3 \times 10^{-7}$ Torr				.0052783	5.334	680	953	
	.054660	10.8594	.61435	.0050334	5.087	615	888	.1765
	.043163	9.0543	.40448	.00476712	4.817	544	817	.1630
	.032495	7.30612	.24572	.0044476	4.495	471	744	.1452
	.022364	5.62747	.130257	.003974	4.016	391	664	.1233
	.017814	5.07731	.093612	.0035085	3.546	333	606	.1302
	.020476	5.34220	.113215	.00383287	3.873	370	643	.1226
	.0152779	4.83159	.0764001	.003162	3.195	300	573	.1351
	.019463	5.21635	.105079	.00373115	3.771	357	630	.1240
	.0129777	4.57509	.061452	.0028365	2.867	271	544	.1363

APPENDIX D

OXIDATION RATE DATA AND RESULTS

This appendix contains a summary of the oxidation rate results. It also includes oxidation rate data taken during certain runs, while attempting to obtain a specific emittance value.

The oxidation data was subdivided into three classes:

1. "nuclei formation region"
2. "intermediate oxide region," and
3. "heavy oxide region."

The rate data for these three regions are tabulated in this appendix.

Finally, Appendix D contains a summary of the oxidation rate data.

Table (D-1)

Summary of Oxidation Rate Results

Sample	Oxidation Time θ (minutes)	Oxide Weight W ($\mu g/cm^2$)	Oxidation Temperature $T_{average}$ (^oC)	$T_{maximum}$ (^oC)	$1/T_{ave}$ x 10^4	$1/T_{max}$ x 10^4	Oxidation Rate Constant k($\mu g/cm^2$-min.)	Type of Crystal
SE#1	3	4.8	522	527	1.258	1.250	1.6	(110)
SE#2	2.5	37	643	659	1.092	1.073	14.8	(110)
SE#3	3	29.1	592	615	1.156	1.126	9.7	(110)
SE#4	96.5	78.6		664		1.067		(110)
SE#5	11.0	12.7	512.5	521	1.272	1.258	1.15	(100)
SE#6	19.0	21.8		622	1.1476	1.117	1.15	(100)
SE#7	22.0	46.6		747	1.110	.980	2.12	(100)
SE#8	25.0	37.0		654	1.174	1.079	1.48	(100)
SE#9	7.5	9.0		575	1.237	1.161	1.20	(111)
SE#10	3.5	33.3	638	673	1.098	1.057	9.5	(111)
SE#11	14.0	57.6			1.091		4.11	(111)
SE#12	4.5	20.4	612	645	1.130	1.089	4.53	(111)
OSC#1	3.0	38.4	743	764	.984	.964	12.8	(100)
OSC#2	4.5	82.8			.894	.854	18.4	(110)
OSC#3	13.5	29.4	664	700	1.067	1.028	2.18	(100)
OSC#4	20.0	77.2	696	735	1.032	.992	3.86	(100)
OSC#5	12.0	68.8	656	686	1.076	1.043	5.73	(110)
OSC#6	3.0	13.5			1.046	1.022	4.5	(100)
OSC#7	76.5	62.4	576	652	1.178	1.081	.816	(100)
OSC#8	9.5	48.1			1.083		5.06	(110)
OSC#9	2.5	18.96	559.5	573	1.201	1.182	7.6	(110)
O-#15-PHS	4.0	43.1	765	807	.954	.926	10.8	Poly.
O-#16-PHS	19.5	55.6	615	664	1.126	1.067	2.85	Poly.

Table (D-2)

Oxidation Data During Runs

Run	Crystal	Oxidation Time θ (minutes)	Oxide $\mu g/cm^2$	T_{av}	T_{max}	$1/T_{av} \times 10^4$	$1/T_{max} \times 10^4$	Oxidation Rate ($\mu g/cm^2$-min.)
	(110)SE	3.5	30.5	626	655	1.112	1.078	8.7
	"	2.5		597	604	1.149	1.140	
SE#4	"	1.5	3.5	658	664	1.074	1.067	
	"	10.0	15	627.5	646	1.110	1.088	
	"	9.0	4	635	642	1.101	1.093	
	"	100.5	23.6	639	656	1.096	1.076	
	Total	127.0	78.6					
	(110)RCI	1.5	34.5	708	737	1.019	.990	23.0
	"	1.0		661	670	1.071	1.060	
OSC#8	"	1.0		645	653	1.089	1.080	
	"	5.0		633	640	1.104	1.095	
	"	1.0	___	651	658	1.082	1.074	
	Total	9.5	48.1					
SE#5	(100)SE	3.5	5.5	513	521	1.272	1.258	1.57
	"	7.5	7.2	512	515	1.272	1.269	
	Total	11.0	12.7					
	(100)SE	4.5	8	584	594	1.167	1.153	1.78
	"	6	6	609	622	1.134	1.117	
SE#6	"	3.5	4	606	612	1.138	1.130	
	"	5.0	3.8	594	600	1.153	1.145	
	Total	19.0	21.8					

Table (D-2)
(Continued)

Run	Crystal		Oxidation Time θ (minutes)	Oxide $\mu g/cm^2$	T_{av}	T_{max}	$1/T_{av} \times 10^4$	$1/T_{max} \times 10^4$	Oxidation Rate ($\mu g/cm^2$-min.)
SE#7	(100)SE		13.5	45	644	747	1.091	.980	3.45
	"		8.5	1.6	604	612	1.140	1.130	
		Total	22.0	46.6					
SE#8	(100)SE		3.5	22	630	654	1.107	1.079	6.3
	"		5.5	4	581	589	1.171	1.160	
	"		8	6	564	569	1.195	1.188	
	"		8	5	570.5	576	1.185	1.178	
		Total	25.0	37.0					
SE#9	(111)SE		4.5	3.8	510	521	1.277	1.259	.84
	"		3	5.2	575	588	1.178	1.161	
		Total	7.5	9.0					
SE#11	(111)SE		3.5	36.8	673	744	1.057	.983	10.5
	"		3		602.6	610	1.142	1.133	
	"		4.5	13.2	642	657	1.093	1.075	
	"		3	7.6	656	663	1.076	1.068	
		Total	14.0	57.6					

Table (D-3)

"Nuclei Formation Region" Data

Sample	Crystal	$1/T_{av}$	Oxidation Time θ (min.)	Oxide Thickness ($\mu g/cm^2$)	Oxidation Rate ($\mu g/cm^2$-min.)
OSC#9	(110)	1.201×10^{-4}	2.5'	18.96	7.6
SE#1	(110)	1.258×10^{-4}	3 '	4.8	1.6
SE#5 (1st.)	(100)	1.272×10^{-4}	3.5'	5.5	1.57
"	(100)	1.272×10^{-4}	11.0'	12.7	1.15
SE#6 (1st.)	(100)	1.167×10^{-4}	4.5'	8	1.78
" (1st. and 2nd.)	(100)	1.15×10^{-4}	10.5'	14	1.33
OSC#6	(100)	1.046×10^{-4}	3 '	13.5	4.5
SE#9 (1st.)	(111)	1.277×10^{-4}	4.5'	3.8	.844
"	(111)	1.237×10^{-4}	7.5'	9.0	1.20
SE#12	(111)	1.130×10^{-4}	4.5'	20.4	4.53
O#4	Poly thin	1.318×10^{-4}	3 '	3.25	1.083
J#35	"	1.29×10^{-4}	10 '	6.6	.66
J#36	"	1.217×10^{-4}	1 '	15.9	1.59
Hansen	"	1.008×10^{-4}	1 '	11.9	11.9

Table (D-4)

"Intermediate Oxide Region" Data

Sample	Crystal	$1/T_{av.}$	Oxidation Time θ (min.)	Oxide Thickness (μ g/cm^2)	Oxidation Rate (μ g/cm^2-min.)
OSC#8(1st.)	(110)	1.019×10^{-4}	1.5'	34.5	23
OSC#9	(110)	1.201×10^{-4}	2.5'	18.96	7.6
SE#2	(110)	1.092×10^{-4}	2.5'	37	14.8
SE#3	(110)	1.156×10^{-4}	3 '	29.1	9.7
SE#8(1st.)	(100)	1.107×10^{-4}	3.5'	22	6.3
OSC#3	(100)	1.067×10^{-4}	13.5'	29.4	2.18
OSC#1	(100)	$.984 \times 10^{-4}$	3	38.4	12.8
SE#8	(100)	1.174×10^{-4}	25 '	37	1.48
SE#10	(111)	1.098×10^{-4}	3.5'	33.3	9.5
SE#11(1st.)	(111)	1.057×10^{-4}	3.5'	36.8	10.5
Hansen	Poly	1.008×10^{-4}	2 '	20.5	10.25
"	"	"	3 '	26.1	8.70
"	"	"	4 '	32.3	8.08

Table (D-5)

"Heavy Oxide Region" Data

Sample	Crystal	$1/T_{av.}$	Oxidation Time θ (min.)	Oxide Thickness ($\mu g/cm^2$)	Oxidation Rate ($\mu g/cm^2$-min.)
OSC#2	(110)	$.894 \times 10^{-4}$	4.5'	82.8	18.4
OSC#5	(110)	1.076×10^{-4}	12 '	68.8	5.73
OSC#8	(110)	1.083×10^{-4}	9.5'	48.1	5.06
OSC#7	(100)	1.178×10^{-4}	76.5'	62.4	.816
OSC#4	(100)	1.032×10^{-4}	20 '	77.2	3.86
SE#7	(100)	1.110×10^{-4}	22 '	46.6	2.12
SE#11	(111)	1.091×10^{-4}	14 '	57.6	4.11
O-#15-10W1x5(6")	Poly-HS	$.954 \times 10^{-4}$	4 '	43.1	10.8
O-#16-10W2x1(6")	"	1.126×10^{-4}	19.5'	55.6	2.85
Hansen	Poly	1.008×10^{-4}	6 '	42.9	7.15
"	"	"	9 '	54.3	6.03

Table (D-6)

Oxidation Data

Thin Polycrystalline Samples — Oxidation Pressure 1000 Microns of Air

Oxidation Time θ (min.)	Voltage V (volts)	Current I (amps)	Resistance R (ohms)	R Ratio R/R_{30} (ohms/ohm)	Temperature T (°C)	Emittance Check ε
			Sample O#1			
After 0	.6613	5.737	.11527	5.93	839	
" 83'	.6720	5.736	.11715	5.72	783	
Total 83'						
			Sample O#2			
After 0	.72075	6.064	.11886	5.97	850	
" 35.5'	.75396	6.064	.12433	5.756	793	
Total 35.5'						
			Sample O#3			
After 0	.46267	4.101	.11282	5.4	699	
" 8.5'	.44820	4.101	.10929	5.219	649	
Total 8.5'						
			Sample O#4			
After 0	.26480	2.644	.10015	4.556	484	
" 3'	.26630	2.644	.10072	4.568	487	
Total 3'						
			Sample O#6			
After 0	.45223	4.046	.11177	5.522	731	
" 4.5'	.43167	"	.10553	5.199	645	
Total 4.5'						
			Sample O#16			
After 0					780	
" 15.5'					648	
Total 15.5'						
			Sample O#23			
After 0					833	
" 32'					694	
Total 32'						

Table (D-7)

Oxidation Data

Sample O-#15-10W1x5(6")

Polycrystalline

Oxidation Pressure
1000 Microns of Air

Oxidation Time θ (min.)	Voltage V (volts)	Current I (amps)	Resistance R (ohms)	R Ratio R/R_{30} (ohms/ohm)	Temperature T (^{o}C)	Emittance Check ϵ
After 1'	.11696	22.817	.0051260	5.805	807	
" 2'	.11942	23.710	.0050367	5.704	780	
" 3'	.11692	23.692	.0049350	5.489	749	
" 4'	.11596	22.368	.0048965	5.545	739	
" 4.5'	.11518	22.368	.0048636	5.508	728	
Total 4'						

Table (D-8)

Oxidation Data

Sample O-#16-10W2x1(6")

Polycrystalline

Oxidation Pressure
1000 Microns of Air

Oxidation Time θ (min.)	Voltage V (volts)	Current I (amps)	Resistance R (ohms)	R Ratio R/R_{30} (ohms/ohm)	Temperature T (^{o}C)	Emittance Check ϵ
After 2'	.085483	18.517	.0046165	5.269	664	
" 12'	.081250	18.517	.0043879	5.008	594	
" 21'	.081003	18.531	.0043712	4.989	588	
Total 19.5'						

Table (D-9)

Oxidation Data

Sample SE#1

(110) Semi-Elements

Oxidation Pressure
1000 Microns of Air

Oxidation Time θ (min.)	Voltage V (volts)	Current I (amps)	Resistance R (ohms)	R Ratio R/R_{30} (ohms/ohm)	Temperature T (°C)	Emittance Check ϵ
After 2'	.054631	11.477	.0047600	4.746	527	
" 3'	.054490	11.456	.0047564	4.743	527	
" 4'	.054109	11.447	.0047269	4.713	519	
" 5'	.053885	11.443	.0047090	4.695	515	
Total 3'						

Table (D-10)

Oxidation Data

Sample SE#2

(110) Semi-Elements

Oxidation Pressure
1000 Microns of Air

Oxidation Time θ (min.)	Voltage V (volts)	Current I (amps)	Resistance R (ohms)	R Ratio R/R_{30} (ohms/ohm)	Temperature T (°C)	Emittance Check ϵ
After 2'	.093852	14.591	.0064322	5.254	659	
" 2.5'	.093296	14.597	.0063915	5.216	649	
" 3'	.092754	14.582	.0063609	5.191	642	
" 3.5'	.092210	14.555	.0063353	5.170	637	
" 4'	.091875	14.539	.0063192	5.157	633	
Total 2.5'						

Table (D-11)

Oxidation Data

Sample SE#3

(110) Semi-Elements

Oxidation Pressure
1000 Microns of Air

Oxidation Time θ (min.)	Voltage V (volts)	Current I (amps)	Resistance R (ohms)	R Ratio R/R_{30} (ohms/ohm)	Temperature T (°C)	Emittance Check ϵ
After 1.5'	.074721	13.297		5.089	615	
" 2	.074226	13.285	.0055872	5.053	606	
" 2.5	.074325	13.273	.0055319	5.003	594	
" 3	.072864	13.264	.0054934	4.969	584	
" 3.5	.072520	13.258	.0054699	4.947	578	
" 4	.072230	13.254	.0054497	4.929	573	
Total 3'						

Table (D-12)

Oxidation Data

Sample SE#4

(110) Semi-Elements

Oxidation Pressure 1000 Microns of Air

Oxidation Time θ (min.)		Voltage V (volts)	Current I (amps)	Resistance R (ohms)	R Ratio R/R_{30} (ohms/ohm)	Temperature T (°C)	Emittance Check ∈
				First Oxidation			
After	2'	.072364	15.605	.0046372	5.238	655	
"	2.5	.071398	15.588	.0045803	5.174	638	
"	3	.070768	15.576	.0045340	5.121	624	
"	3.5	.070405	15.565	.0045233	5.109	621	
"	4	.070056	15.569	.0045403	5.088	615	
"	4.5	.069795	15.546	.0044896	5.071	610	
"	5	.06912	15.540	.0044795	5.060	608	
Total	3.5'						
		.049969	11.431		4.926	573	.1699
				Second Oxidation			
After	2'	.069491	15.555	.0044657	5.044	604	
"	2.5	.069318	15.546	.0044589	5.036	602	
"	3	.069168	15.537	.004518	5.028	600	
"	3.5	.069067	15.537	.0044453	5.021	598	
"	4	.069000	15.537	.0044410	5.016	596	
Total	2.5'						
		.051084	11.64	.0043887	4.945	577	.1736
				Third Oxidation			
After	1.5'	.085324	18.229	.0046807	5.274	664	
"	2	.085100				663	
"	2.5	.085335	18.260	.0046733	5.266	662	
Total	1.5'						
		.049110	11.379	.0043158	4.863	556	.1806
				Fourth Oxidation			
After	6'	.080839	17.504	.0046183	5.204	646	
"	7	.079783	17.480	.0045642	5.143	630	
"	7.5	.079674	17.472	.0045601	5.138	629	
"	8	.079589	17.46	.0045584	5.136	628	
"	9	.079474	17.45	.0045544	5.132	627	
"	10	.079354	17.44	.0045501	5.127	626	
"	11	.079284	17.44	.0045461	5.122	625	
"	12	.079185	17.44	.0045404	5.116	623	

Table (D-12)
(Continued)

Oxidation Time θ (min.)	Voltage V (volts)	Current I (amps)	Resistance R (ohms)	R Ratio R/R_{30} (ohms/ohm)	Temperature T (°C)	Emittance Check ∈
			Fourth Oxidation (Cont'd)			
After 13'	.079108	17.44	.0045360	5.111	621	
" 14	.079051	17.431	.0045351	5.110	621	
" 15	.078990	17.431	.0045316	5.106	620	
Total 10'						
	.048158	11.359		4.777	534	.1972
			Fifth Oxidation			
After 3.5'	.084409		.0046077	5.192	642	
" 4	.084038	18.261	.0046020	5.185	641	
" 5	.083625	18.203	.0045940	5.176	638	
" 6	.083379	18.170	.0045888	5.171	637	
" 7	.083178	18.146	.0045838	5.165	636	
" 8	.083015	18.125	.0045801	5.161	635	
" 9	.082886	18.109	.0045771	5.157	633	
" 10	.082796	18.099	.0045746	5.155	633	
" 11	.082681	18.085	.0045718	5.151	632	
" 12	.082623	18.080	.0045699	5.149	631	
Total 9'						
	.048183	11.423	.048183	4.753	529	.2035
			Sixth Oxidation			
After 4						
" 4.5						
" 5	.085192	18.504		5.188	642	
" 6	.084915	18.466	.0045985	5.181	640	
" 8	.084691	18.435	.0045940	5.177	639	
" 15	.089031	19.135	.0046525	5.242	656	
" 15.5	.088953	19.124	.0046514	5.241	656	
" 16	.088890	19.115	.0046503	5.240	656	
" 16.5	.088860	19.114	.0046489	5.238	655	
" 31.5	.088180	19.068	.0046245	5.211	648	
" 36.5	.088056	19.063	.0046192	5.205	647	
" 100.5	.087000	19.035	.0045705	5.150	631	
Total 96.5'						

Table (D-13)

Oxidation Data

Sample SE#5

(100) Semi-Elements

Oxidation Pressure
1000 Microns of Air

Oxidation Time θ (min.)		Voltage V (volts)	Current I (amps)	Resistance R (ohms)	R Ratio R/R_{30} (ohms/ohm)	Temperature T (°C)	Emittance Check ϵ
				First Oxidation			
After	2.5'	.054090	10.685	.0050622	4.589	591	
"	3	.055323	10.660	.0051898	4.704	517	
"	3.5	.055420	10.643	.0052072	4.720	521	
"	4	.055260	10.631	.0051980	4.712	519	
"	4.5	.055128	10.622	.0051900	4.704	517	
"	5	.054992	10.614	.0051811	4.696	515	
"	5.5	.054870	10.608	.0051725	4.689	514	
"	6	.054795	10.603	.0051679	4.684	513	
Total	3.5'						
				Second Oxidation			
After	2.5'	.054966	10.850	.0050660	4.582	490	
"	3	.055996	10.827	.0051719	4.677	510	
"	3.5	.056140	10.812	.0051924	4.696	515	
"	4	.056096	10.804	.0051922	4.696	515	
"	4.5	.056062	10.796	.0051928	4.696	515	
"	5	.055995	10.790	.0051895	4.693	514	
"	5.5						
"	6	.055937	10.787	.0051856	4.690	514	
"	6.5						
"	7	.055908	10.786	.0051834	4.688	513	
"	7.5						
"	8	.055900	10.788	.0051837	4.686	513	
"	9	.055891	10.789	.0051804	4.685	513	
"	10	.055880	10.793	.0051774	4.682	513	
Total	7.5'						
				Third Oxidation			
After	0	.062391	11.637	.0053614	4.849	552	
"	.5	.062390	11.629	.0053650	4.852	552	
"	1	.062325	11.623	.0053622	4.850	552	
"	1.5	.062280	11.615	.0053620	4.849	552	
"	2	.062151	11.610	.0053532	4.841	550	
"	2.5	.062076	11.606	.0053486	4.837	549	
"	3.0	.062016	11.603	.0053448	4.834	548	

Table (D-14)

Oxidation Data

Sample SE#6

(100) Semi-Elements

Oxidation Pressure
1000 Microns of Air

Oxidation Time θ (min.)		Voltage V (volts)	Current I (amps)	Resistance R (ohms)	R Ratio R/R_{30} (ohms/ohm)	Temperature T (°C)	Emittance Check ϵ
After	5'	.072664	11.698	.0062117	5.007	594	
"	5.5	.072193	11.658	.0061926	4.992	589	
"	6	.072004	11.650	.0061806	4.982	587	
"	6.5	.071310	11.578	.0061591	4.965	583	
"	7	.071166	11.578	.0061467	4.955	580	
"	7.5	.071277	11.606	.0061414	4.951	579	
"	8	.071604	11.654	.0061442	4.953	579	
"	8.5	.071889	11.692	.0061486	4.956	581	
Total	4.5'	.075210	11.139	.0067520	5.443	706	.1377
			Second Oxidation				
After	3'	.077935	12.656	.0061580	4.964	583	
"	3.5	.080057	12.631	.0063381	5.109	621	
"	4	.080016	12.610	.0063454	5.115	622	
"	4.5	.079751	12.595	.0063320	5.104	620	
"	5	.079498	12.585	.0063169	5.092	616	
"	5.5	.079310	12.578	.0063055	5.083	614	
"	6	.079126	12.573	.0062933	5.073	611	
"	6.5	.078933	12.568	.0062805	5.063	609	
"	7	.078816	12.565	.0062727	5.056	607	
"	7.5	.078685	12.561	.0062642	5.050	606	
"	8	.078558	12.558	.0062556	5.043	604	
"	8.5	.078400	12.553	.0062455	5.035	601	
"	9	.078303	12.551	.0062388	5.029	600	
Total	6'	.070815	10.839	.0065334	5.267	663	
			Third Oxidation				
After	1.5'	.081296			5.074	612	
"	2	.081119	12.903	.0062868	5.068	610	
"	2.5	.080923	12.892	.0062770	5.060	608	
"	3	.080792	12.887	.0062693	5.054	606	
"	3.5	.080664	12.883	.0062613	5.047	605	
"	4	.080555	12.879	.0062548	5.042	604	
Total	3.5'	.079211	11.927	.0066413	5.354	686	

Table (D-14)
(Continued)

Oxidation Time θ (min.)		Voltage V (volts)	Current I (amps)	Resistance R (ohms)	R Ratio R/R_{30} (ohms/ohm)	Temperature T (°C)	Emittance Check ϵ
				Fourth Oxidation			
After	2.5'	.079214	12.983	.0061014	4.918	570	
"	3	.080890	12.957	.0062430	5.032	600	
"	3.5	.080775	12.941	.0062418	5.032	600	
"	4	.080670	12.929	.0062395	5.030	600	
"	4.5	.080534	12.921	.0062328	5.024	599	
"	5	.080400	12.914	.0062258	5.019	597	
"	5.5	.080290	12.909	.0062197	5.014	596	
"	6	.080205	12.905	.0062150	5.010	595	
"	6.5	.080126	12.902	.0062104	5.006	594	
"	7	.080053	12.901	.0062052	5.002	593	
"	7.5	.079900	12.899	.0061943	4.993	589	
Total	5'	.069221	10.828	.0063928	5.153	632	.1693

Table (D-15)

Oxidation Data

Sample SE#7

(100) Semi-Elements

Oxidation Pressure
1000 Microns of Air

Oxidation Time θ (min.)	Voltage V (volts)	Current I (amps)	Resistance R (ohms)	R Ratio R/R_{30} (ohms/ohm)	Temperature T (°C)	Emittance Check ϵ
			First Oxidation			
After 2'	.094642	16.474	.0057449	5.582	747	
" 2.5	.092219	16.435	.0056111	5.452	712	
" 3	.090732	16.415	.0055274	5.370	690	
" 3.5	.089600	16.402	.0054627	5.308	674	
" 4	.089086	16.402	.0054314	5.277	665	
" 4.5	.088516	16.385	.0054023	5.249	658	
" 5	.088126	16.385	.0053785	5.226	652	
" 5.5	.087747	16.373	.0053592	5.207	648	
" 6	.087466	16.373	.0053421	5.190	642	
" 6.5	.087253	16.373	.0053291	5.178	639	
" 7	.087051	16.365	.0053193	5.168	637	
" 7.5	.086832	"	.0053060	5.155	633	
" 8	.086688	"	.0052972	5.147	631	
" 9	.086438	"	.0052819	5.132	627	
" 10	.086236	"	.0052724	5.123	625	
" 11	.086061	"	.0052617	5.112	621	
" 12	.085898	"	.0052518	5.103	620	
" 13	.085744	"	.0052424	5.093	616	
" 14	.085626	"	.0052351	5.086	615	
" 15	.085505	"	.0052277	5.079	613	
Total 13.5'	.065121	12.787	.0050928	4.948	578	.2368
			Second Oxidation			
After 1.5'	.082974	16.541	.0050166	4.874	559	
" 2	.086088	16.481	.0052235	5.075	612	
" 2.5	.085955	16.481	.0052154	5.067	611	
" 3	.085769	16.429	.0052206	5.072	611	
" 3.5	.085569	16.406	.0052157	5.068	610	
" 4	.085445	16.395	.0052116	5.064	609	
" 4.5	.085341	16.385	.0052085	5.061	608	
" 5	.085281	16.385	.0052048	5.057	607	
" 5.5	.085170	16.371	.0052025	5.055	606	
" 6.5	.085100	16.371	.0051982	5.051	605	
" 7	.085009	16.362	.0051955	5.048	605	

Table (D-15)
(Continued)

Oxidation Time θ (min.)	Voltage V (volts)	Current I (amps)	Resistance R (ohms)	R Ratio R/R_{30} (ohms/ohm)	Temperature T (°C)	Emittance Check ∈
		Second Oxidation (Cont'd)				
After 7.5	.084952	16.362	.0051920	5.045	604	
" 8	.084863	16.350	.0051904	5.043	604	
" 8.5	.084807	16.344	.0051889	5.042	604	
" 9	.084777	16.344	.0051870	5.040	603	
" 9.5	.084720	16.339	.0051851	5.038	602	
" 10	.084676	16.339	.0051824	5.035	601	
Total 8.5'						

Table (D-16)

Oxidation Data

Sample SE#8

(100) Semi-Elements

Oxidation Pressure
1000 Microns of Air

Oxidation Time θ (min.)		Voltage V (volts)	Current I (amps)	Resistance R (ohms)	R Ratio R/R_{30} (ohms/ohm)	Temperature T (°C)	Emittance Check ϵ
			First Oxidation				
After	2'	.083256	13.228	.0062939	5.234	654	
"	2.5	.082756	13.206	.0062665	5.211	648	
"	3	.081845	13.188	.0062060	5.161	635	
"	3.5	.081230	13.180	.0061631	5.125	626	
"	4	.080796	13.173	.0061335	5.101	618	
"	4.5	.080475	13.167	.0061119	5.083	614	
"	5	.080155	13.162	.0060899	5.064	610	
Total	3.5'	.072609	11.483	.0063232	5.258	660	.1727
			Second Oxidation				
After	2'	.077146	12.871	.0059938	4.984	588	
"	2.5	.077050	12.841	.0060003	4.990	589	
"	3	.076832	12.825	.0059908	4.982	587	
"	3.5	.076648	12.816	.0059806	4.974	585	
"	4	.076520	12.812	.0059725	4.967	584	
"	4.5	.076393	12.806	.0059654	4.961	582	
"	5	.076295	12.804	.0059587	4.955	580	
"	5.5	.076191	12.804	.0059506	4.948	579	
"	6	.076112		.0059463	4.945	578	
"	6.5	.076040		.0059406	4.940	576	
"	7	.075970	12.798	.0059361	4.936	575	
Total	5.5'	.073005	11.668	.0062569	5.203	646	.1876
			Third Oxidation				
After	1.5'	.074422	12.763	.0058311	4.849	561	
"	2	.075305	12.749	.0059067	4.912	576	
"	2.5	.075292	12.737	.0059113	4.916	576	
"	3	.075195	12.729	.0059074	4.913	575	
"	3.5	.075116	12.725	.0059030	4.909	574	
"	4	.075039	12.721	.0058988	4.905	573	
"	4.5	.074972	12.718	.0058590	4.902	573	
"	5	.074919	12.717	.0058912	4.899	572	

Table (D-16)
(Continued)

Oxidation Time θ (min.)		Voltage V (volts)	Current I (amps)	Resistance R (ohms)	R Ratio R/R_{30} (ohms/ohm)	Temperature T (°C)	Emittance Check ϵ
			Third Oxidation (Cont'd)				
After	5.5'	.074870	12.716	.0058888	4.897	571	
"	6	.074825	12.715	.0058852	4.894	570	
"	6.5	.074795	12.714	.0058829	4.892	569	
"	7	.074758	"	.0058800	4.892	569	
"	7.5	.074720	"	.0058770	4.887	569	
"	8	.074690	"	.0058746	4.885	568	
"	8.5	.074652	"	.0058716	4.883	568	
"	9	.074616	"	.0058688	4.880	567	
"	9.5	.074590	"	.0058668	4.879	567	
Total	8'	.071361	11.553	.0061768	5.137	628	.1967
			Fourth Oxidation				
After	1.5'	.077582	13.209	.0058734	4.884	561	
"	2	.078361	13.192	.0059400	4.940	576	
"	2.5	.078281	13.179	.0059398	4.940	576	
"	3	.078166	13.169	.0059356	4.936	575	
"	3.5	.078083	13.164	.0059316	4.933	574	
"	4	.077992	13.159	.0059269	4.929	573	
"	4.5	.077938	13.156	.0059241	4.927	573	
"	5	.077882	13.154	.0059208	4.924	572	
"	5.5	.077823	13.151	.0059176	4.921	571	
"	6	.077777	13.151	.0059142	4.918	570	
"	6.5	.077743	13.150	.0059120	4.916	569	
"	7	.077702	13.149	.0059093	4.914	569	
"	7.5	.077670	"	.0059074	4.913	569	
"	8	.077631	"	.0059044	4.910	568	
"	8.5	.077606	"	.0059025	4.909	568	
"	9	.077570	"	.0058998	4.906	567	
"	9.5	.077540	13.148	.0058975	4.904	567	
Total	8'	.077992	12.475	.0062519	5.199	645	.2152

Table (D-17)

Oxidation Data

Sample SE#9

(111) Semi-Elements

Oxidation Pressure
1000 Microns of Air

Oxidation Time θ (min.)		Voltage V (volts)	Current I (amps)	Resistance R (ohms)	R Ratio R/R_{30} (ohms/ohm)	Temperature T (°C)	Emittance Check ϵ
			First Oxidation				
After	2.5'	.054966	10.754	.0051112	4.679	511	
"	3.5	.054980	10.661	.0051571	4.721	521	
"	4	.054571	10.620	.0051385	4.704	516	
"	5	.053900	10.553	.0051076	4.676	511	
"	6	.053433	10.505	.0050864	4.657	507	
"	7	.052854	10.438	.0050636	4.636	500	
Total	4.5'	.054553	9.6267	.0056668	5.188	642	.1225
			Second Oxidation				
After	2'	.066470	12.326	.0053927	4.937	575	
"	2.5	.066720	12.2535	.0054450	4.985	588	
"	3	.066200	12.204	.0054245	4.966	583	
"	3.5	.065620	12.154	.0053990	4.943	577	
"	4	.065246	12.131	.0053785	4.924	572	
"	4.5	.064691	12.068	.0053605	4.908	568	
"	5	.064279	12.0316	.0053425	4.891	563	
Total	3'	.055894	9.9800	.0056006	5.127	626	

Table (D-18)

Oxidation Data

Sample SE#10

(111) Semi-Elements

Oxidation Pressure
1000 Microns of Air

Oxidation Time θ (min.)	Voltage V (volts)	Current I (amps)	Resistance R (ohms)	R Ratio R/R_{30} (ohms/ohm)	Temperature T (°C)	Emittance Check ∈
After 2'	.102370	13.898	.0073658	5.303	673	
" 2.5	.100380	13.868	.0072382	5.211	648	
" 3	.099553	13.850	.0071879	5.175	638	
" 3.5	.098850	13.835	.0071449	5.144	631	
" 4	.098381	13.828	.0071146	5.122	625	
" 4.5	.098100	13.825	.0070956	5.109	621	
" 5	.097812	13.823	.007076	5.094	617	
Total 3.5'						

Table (D-19)

Oxidation Data

Sample SE#11

(111) Semi-Elements

Oxidation Pressure
1000 Microns of Air

Oxidation Time θ (min.)		Voltage V (volts)	Current I (amps)	Resistance R (ohms)	R Ratio R/R_{30} (ohms/ohm)	Temperature T (°C)	Emittance Check ∈
			First Oxidation				
After	1.5'	.120506	13.892	.0086745	5.573	744	
"	2	.115645	"	.0083246	5.348	684	
"	2.5	.113386	13.816	.0082069	5.273	664	
"	3	.112409	13.804	.0081432	5.232	653	
"	3.5	.111506	13.781	.0080913	5.199	645	
"	4	.110878	13.771	.0080516	5.173	638	
"	4.5	.110577	13.774	.0080280	5.158	633	
Total	3.5'	.059192	13.548	.0072902	4.684	512	.2003
			Second Oxidation				
After	2.5'	.10435	13.242	.0078802	5.063	610	
"	3	.10455	13.287	.0078686	5.056	607	
"	3.5	.104359	13.266	.0078667	5.054	606	
"	4	.103656	13.212	.0078456	5.041	603	
"	4.5	.103690	13.228	.0078387	5.036	602	
"	5	.103590	13.224	.0078335	5.033	600	
Total	3'						
After	6'	.121622	14.903	.0081609	5.243	657	
"	6.5	.120345	14.809	.0081265	5.221	651	
"	7	.119587	14.764	.008099	5.204	646	
"	7.5	.119040	14.732	.0080804	5.192	642	
"	8	.118696	14.713	.0080674	5.183	641	
"	8.5	.118475	14.705	.0080568	5.176	638	
"	9	.118270	14.696	.0080478	5.171	637	
"	9.5	.118269	14.716	.0080368	5.164	636	
"	10	.118300	14.716	.0080389	5.165	636	
Total	5'	.058998	13.843	.0071114	4.569	487	

Table (D-19)
(Continued)

Oxidation Time θ (min.)		Voltage V (volts)	Current I (amps)	Resistance R (ohms)	R Ratio R/R_{30} (ohms/ohm)	Temperature T (°C)	Emittance Check ϵ
				Third Oxidation			
After	1.5'	.128588	15.684	.0081987	5.267	663	
"	2	.127590	15.570	.0081946	5.265	662	
"	2.5	.126693	15.492	.0081780	5.254	659	
"	3	.125940	15.438	.0081578	5.241	656	
"	3.5	.125478	15.402	.0081469	5.234	654	
"	4	.125150	15.380	.0081372	5.228	653	
Total	3'						

Table (D-20)

Oxidation Data

Sample SE#12

(111) Semi-Elements

Oxidation Pressure
1000 Microns of Air

Oxidation Time θ (min.)		Voltage V (volts)	Current I (amps)	Resistance R (ohms)	R Ratio R/R_{30} (ohms/ohm)	Temperature T (°C)	Emittance Check ∈
After	2'	.070123	14.733	.0047596	5.140	629	
"	2.5	.070820	14.7105	.0048142	5.199	645	
"	3	.070058	14.695	.0047675	5.149	631	
"	3.5	.069420	14.685	.0047273	5.105	620	
"	4	.069000	14.676	.0047016	5.078	613	
"	4.5	.068656	"	.0046781	5.052	606	
"	5	.068350	"	.0046573	5.030	600	
"	5.5	.068101	"	.0046403	5.012	596	
"	6	.067900	"	.0046266	4.997	590	
"	6.5	.067767	14.659	.0046229	4.993	589	
Total	4.5'						

Table (D-21)

Oxidation Data

Sample OSC#1

(100) Research Crystal Inc.

Oxidation Pressure
1000 Microns of Air

Oxidation Time θ (min.)		Voltage V (volts)	Current I (amps)	Resistance R (ohms)	R Ratio R/R_{30} (ohms/ohm)	Temperature T (°C)	Emittance Check ∈
After	1.5'	.117736	20.2805	.00580537	5.575	745	
After	1'	.130504	22.1863	.00588219	5.648	764	
"	2	.125700	22.1586	.0056727	5.447	717	
Total	3'						

Table (D-22)

Oxidation Data

Sample OSC#2

(110) Research Crystal Inc. Oxidation Pressure 1000 Microns of Air

Oxidation Time θ (min.)	Voltage V (volts)	Current I (amps)	Resistance R (ohms)	R Ratio R/R_{30} (ohms/ohm)	Temperature T (°C)	Emittance ∈
After 1'	.32574	22.0904	.014746	6.149	898	
After 1'	.29012	20.2805	.014305	5.965	849	
" 1.5	.28981	20.262	.014303	5.964	849	
" 2.5	.28936	20.243	.014294	5.961	848	
" 3.5	.28863	20.231	.014267	5.949	845	
" 4.5	.28792	20.2265	.014235	5.873	824	
Total 4.5'						

Table (D-23)

Oxidation Data

Sample OSC#3

(100) Research Crystal Inc. Oxidation Pressure 1000 Microns of Air

Oxidation Time θ (min.)	Voltage V (volts)	Current I (amps)	Resistance R (ohms)	R Ratio R/R_{30} (ohms/ohm)	Temperature T (°C)	Emittance Check ∈
After 1'	.082816	20.769	.0039875	5.408	700	
" 2	.081797	20.768	.0039386	5.343	683	
" 3	.081491	20.750	.0039273	5.327	679	
" 4	.081082	20.742	.0039091	5.303	673	
" 5						
" 6						
" 7	.080235	20.740	.0038686	5.248	658	
" 8						
" 9						
" 10	.079692	20.748	.0038409	5.210	648	
" 11						
" 12						
" 13						
" 14	.079343	20.755	.0038228	5.186	642	
Total 13.5'						

Table (D-24)

Oxidation Data

Sample OSC#4

(100) Research Crystal Inc.

Oxidation Pressure
1000 Microns of Air

Oxidation Time θ (min.)	Voltage V (volts)	Current I (amps)	Resistance R (ohms)	R Ratio R/R_{30} (ohms/ohm)	Temperature T (°C)	Emittance Check ϵ
After 2'	.20136	14.577	.013814	5.535	735	
" 6	.19614	14.510	.013527	5.386	696	
" 7	.19574	"	.013490	5.371	690	
" 8	.19553	"	.013460	5.366	689	
" 9	.19538	"	.013465	5.362	688	
" 10	.19531	"	.013460	5.360	687	
" 11	.19527	"	.013458	5.359	687	
" 15	.19530	"	.013460	5.359	687	
" 16	.19543	"	.013469	5.363	689	
" 21	.19551	14.509	.013475	5.364	689	
Total 20'						

Table (D-25)

Oxidation Data

Sample OSC#5

(110) Research Crystal Inc.

Oxidation Pressure
1000 Microns of Air

Oxidation Time θ (min.)	Voltage V (volts)	Current I (amps)	Resistance R (ohms)	R Ratio R/R_{30} (ohms/ohm)	Temperature T (°C)	Emittance ϵ
After 2'	.088565	15.7317	.0056275	5.104	620	
" 3	.096894	16.9439	.0057186	5.187	641	
" 3.5						
" 4	.114424	19.380	.0059042	5.355	686	
" 5	.112901	19.344	.0058365	5.294	670	
" 6	.112180	"	.0057992	5.260	661	
" 7	.111651	"	.0057719	5.235	654	
" 14	.111441	19.306	.0057724	5.236	654	
Total 12'						

Table (D-26)

Oxidation Data

Sample OSC#6

(100) Research Crystal Inc. Oxidation Pressure 1000 Microns of Air

Oxidation Time θ (min.)	Voltage V (volts)	Current I (amps)	Resistance R (ohms)	R Ratio R/R_{30} (ohms/ohm)	Temperature T (°C)	Emittance Check ∈
After 2'	.089350				705	
After 2'	.088223	19.966	.0044187	5.362	688	
" 3	.087669		.0043909	5.328	679	
Total 3'						

Table (D-27)

Oxidation Data

Sample OSC#7

(100) Research Crystal Inc. Oxidation Pressure 1000 Microns of Air

Oxidation Time θ (min.)	Voltage V (volts)	Current I (amps)	Resistance R (ohms)	R Ratio R/R_{30} (ohms/ohm)	Temperature T (°C)	Emittance Check ∈
After 1'	.17304			5.225	652	
" 2	.16940	9.5829	.017677	5.129	626	
" 3	.16765	9.5661	.017525	5.085	614	
" 4	.16661	9.5559	.017438	5.060	608	
" 5	.16601	9.5661	.017525	5.041	603	
" 6	.16550	9.5559	.017319	5.025	599	
" 8	.16435	9.5505	.017209	4.993	589	
" 10	.16451	9.5505	.017225	4.998	591	
" 11	.16411	9.5505	.017184	4.986	588	
" 13	.16375	9.5559	.017184	4.972	584	
" 14	.16353	"	.017136	4.965	583	
" 15	.16339	"	.017113	4.961	582	
" 16	.16325	"	.017098	4.957	580	
" 17	.16314	"	.017084	4.953	579	
" 18	.16300	"	.017072	4.949	579	
" 19	.16289	"	.017057	4.946	578	
" 20	.16277	"	.017046	4.942	516	
" 22	.16258	"	.017033	4.936	575	
" 23	.16253	9.5559	.017014	4.935	574	
" 30	.16209	9.5631	.016950	4.918	570	
" 38	.16178	9.5697	.016905	4.905	567	
" 53	.16174	9.5697	.016901	4.904	567	
" 77	.16192	9.5709	.016918	4.909	568	
Total 76.5'						

Table (D-28)

Oxidation Data

Sample OSC#8

(110) Research Crystal Inc.

Oxidation Pressure 1000 Microns of Air

Oxidation Time θ (min.)	Voltage V (volts)	Current I (amps)	Resistance R (ohms)	R Ratio R/R_{30} (ohms/ohm)	Temperature T (°C)	Emittance Check ε
			First Oxidation			
After 1'	.106509	16.141	.0065987	5.543	737	
" 2	.101764	16.085	.0063266	5.314	675	
Total 1.5'	.075524	12.258	.0061612	5.175	638	.2593
			Second Oxidation			
After 1.5'	.103166	16.369	.0063025	5.294	670	
" 2	.102204	16.308	.0062671	5.264	662	
Total 1'	.074545	12.253		5.110	621	.2761
			Third Oxidation			
After 1.5'	.100707	16.181	.0062238	5.228	653	
" 2	.100246	16.145	.0062091	5.216	648	
Total 1'	.072872	12.236		4.993	589	.3125
			Fourth Oxidation			
After 1.5'	.097214	15.819	.0061454	5.162	635	
" 2	.097073	"	.0061400	5.158	634	
" 2.5	.096923	"	.0061305	5.150	632	
" 3	.096766	15.802	.0061237	5.144	631	
" 4					635	
" 4.5	.100086	16.233	.0061656	5.179	640	
" 5					637.5	
" 6	.099728	16.224	.0061469	5.163	635	
After 1.5	.106830			5.252	658	
" 2	.106556			5.250	658	
Total 6'						

Table (D-29)

Oxidation Data

Sample OSC#9

(110) Research Crystal Inc.

Oxidation Pressure
1000 Microns of Air

Oxidation Time θ (min.)		Voltage V (volts)	Current I (amps)	Resistance R (ohms)	R Ratio R/R_{30} (ohms/ohm)	Temperature T (°C)	Emittance Check ϵ
After	1.5'	.061463	12.780	.0048093	4.851	553	
"	2	.062255	12.749	.0048831	4.926	573	
"	2.5	.061903	12.729	.0048631	4.905	567	
"	3	.061453	12.711	.0048346	4.877	559	
"	3.5	.061163	12.700	.0048160	4.858	554	
"	4	.060940	12.693	.0048011	4.843	551	
Total	2.5'						

APPENDIX E

OXIDE REDUCTION DATA

This appendix includes a summary of the oxide reduction data taken during the oxide weight determination step.

Table (E-1)

Oxide Reduction Data

Run #-O#3 25.8 $\mu g/cm^2$

Time θ(min.)	T (°C)	Spring Reading (min.)	ΔSpring Reading
0	41		
4	41	36.270	
7	71	"	0
8	100	"	0
9	119	"	0
10	137	"	0
11	156	"	0
12	174	"	0
13	191	36.293	+.023
14	201	"	0
15	220	36.330	+.037
16	250	36.414	+.084
17	271	36.405	-.009
18	295	36.885	+.480
19	308	37.136	+.251
20	325	"	0
21	338	"	0
22	354	"	0
23		"	0
24	368	"	0
27	456	37.176	+.045
36	565	37.221	+.045
42	686	"	0
52	822	37.339	+.118
57	811		
67	812	37.387	+.048
100	818	37.444	+.057

Run #-O#2 120.8 $\mu g/cm^2$

Time θ(min.)	T (°C)	Spring Reading (min.)	ΔSpring Reading
0	45	40.031	
1.5	75.5		
5	116	40.032	+.001
10	214	39.986	
12	264	40.022	
13		40.357	+.335
14	300		
14.5		43.907	+.550
15.5	332		
17	350	43.910	+.003
20	404	"	0
22	448		
25.5		43.948	+.038
27	521		
29	548	43.985	+.037
30			
35	685	43.982	-.003
40	775	44.013	+.031
48	811	44.083	+.070
59	810	44.114	+.031
76	816	44.158	+.044
86	"	44.173	+.015
101	"	44.164	-.009
111	"	44.135	-.009
119	"	44.127	-.008

APPENDIX F

NICKEL SINGLE CRYSTAL PREPARATION

This appendix contains a detailed report on the preparation of the thin nickel single crystal specimens. It includes

1. ABSTRACT
2. INTRODUCTION
3. THEORY AND LITERATURE
4. EXPERIMENTAL APPARATUS AND PROCEDURE
5. DISCUSSION OF RESULTS

ABSTRACT

Thin polished nickel single crystal specimens were prepared from a purchased single crystal rod. Other polished single crystals specimens were prepared from purchased oriented crystals. Nickel crystals with (100), (110) and (111) orientations were prepared.

The finished crystals were normally 3" long by .17" wide by 5-10 mils thick. The samples were parallel and finely polished on both sides.

The single crystal preparation consisted chiefly of the following operations:

(1) spark cutting

(2) mechanical thinning

(3) fine grinding

(4) mechanical polishing

(5) chemical polishing

(6) x-ray inspection

INTRODUCTION

Nickel is a face-centered cubic structure as shown below:

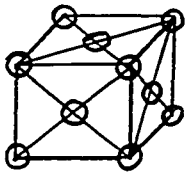

The three closest packed surfaces of nickel are the (100), (110) and (111) configurations as shown below:

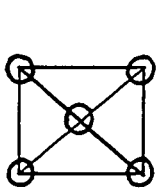

(100)

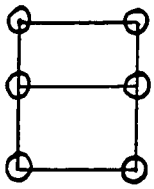

(110)

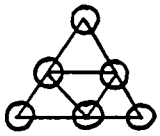

(111)

Atoms on the surface of the (111) orientation have 9 nearest neighbors, making it the most closely packed. The (100) crystal has 8 nearest neighbors whereas the (110) orientation has 7, making it the least closely packed of the three. Because of this difference, one would expect to observe separate and different chemical effects on these surfaces. This is what occurs.

Solids with small ordered regions arranged in different orientations and separated by boundaries are considered to be polycrystalline. If a body contains no grain boundaries and the atoms, ions, or groups of atoms or ions in an ordered network repeats through the body, it is said to be a single crystal.

Single crystals are grown in three principal ways with many modifications of each of these techniques (35):

(1) solidification of a pure melt of the composition to be grown,

(2) crystallization from a solution containing the crystal components,

(3) condensation of vapors having the desired composition.

All of these techniques provide means for transporting atoms, ions, molecules, or groups of atoms to a growth surface under such conditions that they find their most stable positions prior to becoming a fixed part of the solid lattice.

Most materials which melt without decomposing or without changing their crystal structure below the melting point, are grown from the melt. This method offers the greatest potential for producing large, pure, single crystals at reasonable growth rates.

There are three major types of melt-growth processes as shown below:

(1) the crucible, or temperature-gradient techniques (Bridgman-Stockbarger);

(2) vertical-pull (Czochralski) methods;

(3) floating-zone process.

In the Bridgman method, the material to be crystallized is normally melted in a cone-tipped cylindrical crucible as shown in Figure F-I. The temperature is maintained high enough to insure that all particles have been fused. The crucible is then passed through a sharp temperature-gradient region such that solidification starts at the bottom tip, A, of the crucible. Thus the restricted volume limits the

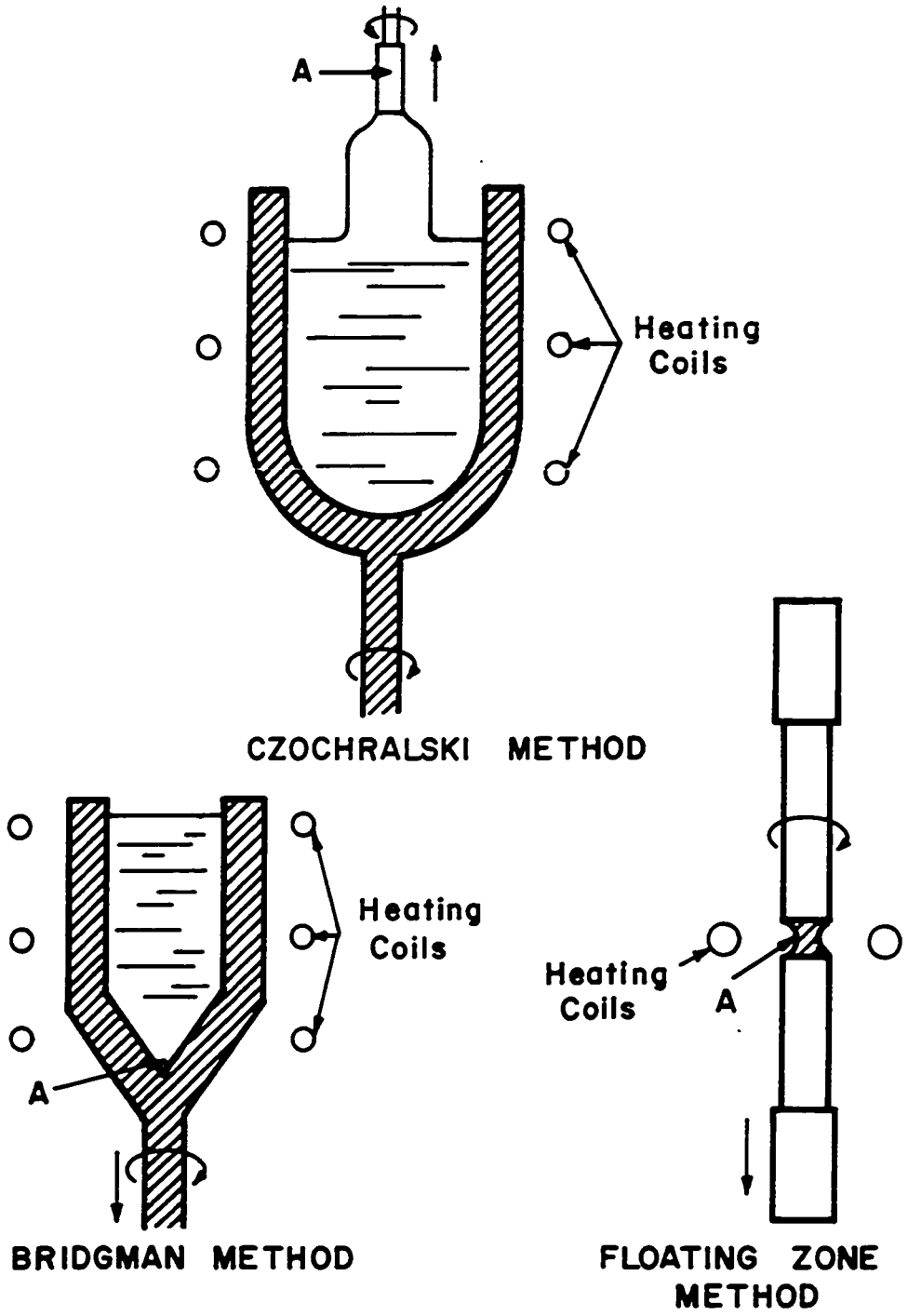

FIGURE F-I CRYSTAL GROWING [From Literature of Arthur D. Little]

number of nucleating points to one or at least to a very few. As the solidification front moves through the crucible, one crystal predominates and fills the entire container.

In the vertical-pull (Czochralski) method, a relatively cool rod or single crystal "seed" A is lowered into a melt of the material to be grown, which is held exactly at the melting temperature. The "seed" is then withdrawn slowly so that the melt at the interface is frozen and withdrawn from the melt. By proper control of the temperature and withdrawal rate, the growing mass can be constricted to insure the single crystal growth and can be widened during the withdrawal to produce single crystal cylinders several inches in diameter. This method has the advantage of resulting in less-strained crystals than those obtained by cooling in a container.

Floating zone crystal growth, as shown in Figure F-I, is another modification of these procedures. In this case only a very thin molten zone, A, is passed through a solid polycrystalline rod of the material starting from a single crystal "seed" from one end. This technique does not require a crucible so that high purities can be achieved. Comparatively high thermal gradients, however, are imposed on the crystal during this process and the crystal may contain numerous imperfections and strains.

A spark cutting technique is often used to cut large single crystal rods into smaller rectangular sections. Other methods of cutting single crystals consist of diamond saws, jeweler's saws, wire cutters, and acid saws, or a combination of these. The spark cutter

has the advantage of cutting relatively quick and also giving a nearly parallel cut. The mechanical cutters are slower for nickel and give a much deeper damage of the surface. The wire cutter is extremely slow and is not very feasible for the relatively "soft" nickel. Acid cutters give a rougher cut than the spark cutter.

In all of the cutting or cleaving operations, there is a residual surface damage, the depth of which varies with the method used. Use of an etchant is common to remove the damage. The etched surface, however, although strain-free, usually has a dull or satin finish. To obtain a highly smooth shiny surface as was desired, a polishing operation was necessary. This polishing can be accomplished either by hand, which is very tedious, or by a mechanical polisher, which results in more surface strains.

To remove surface strains or damage, it is necessary for the final step to be either chemical polishing or electrochemical polishing. With electrochemical polishing, it is very difficult to obtain uniform polishing of a large specimen. It is very easy to develop ridges, grooves, or pits in the surface of the nickel. Chemical polishing of nickel is feasible; however, the best polishing is usually accomplished with either a boiling acid solution or a potentially explosive solution.

To determine crystal orientation both before spark cutting and after the final polishing step, back reflection Laue x-ray pictures are feasible. By observing the shape of the spots, it is possible to obtain a qualitative estimate as to whether the crystal is strained

or not. Since in the normal high energy x-rays the rays also penetrate into the bulk metal, the picture obtained is not that of just the surface. A better "look" at the surface can be obtained with a Low Energy Election Diffraction (LEED) unit, in which most of the rays do not penetrate much deeper than the surface.

THEORY AND LITERATURE

A. Spark Cutting

There are many instances mentioned in the literature in which spark cutting or electro-erosion devices are used to cut metals. Wilms and Wade (34) describe the use of a spark cutter for cutting chromium, aluminum, iron and antimony. Chandrasekhar (7) describes the use of a spark cutter to cut single crystals of indium, tin, bismuth, aluminum and copper. Tibbetts and Propst (32) describe the use of an electro-erosion machine during the preparation of thin single crystal tungsten ribbons.

The spark cutter, shown in Figure F-II, produces a rapid series of spark discharges of controlled energy between the tool and the work. The sparks erode the work at a rate dependent on the energy and frequency of the discharges--high energies for fast roughing work and low energies for fine finishes. The 200-250 volt 50-60 c/s mains is rectified by a full wave bridge of silicon rectifiers and the resulting D.C. applied to the simple relaxation circuit illustrated in Figure F-II.

The condenser C charges at a rate determined by the resistor R until the dielectric breakdown voltage V is reached when a spark discharge takes place across the work gap d. C is then recharged through R and the cycle repeated. The breakdown voltage V is proportional to the work gap d which must be controlled within close limits for efficient operation. V is therefore used to control a servo system which maintains d at its optimum value.

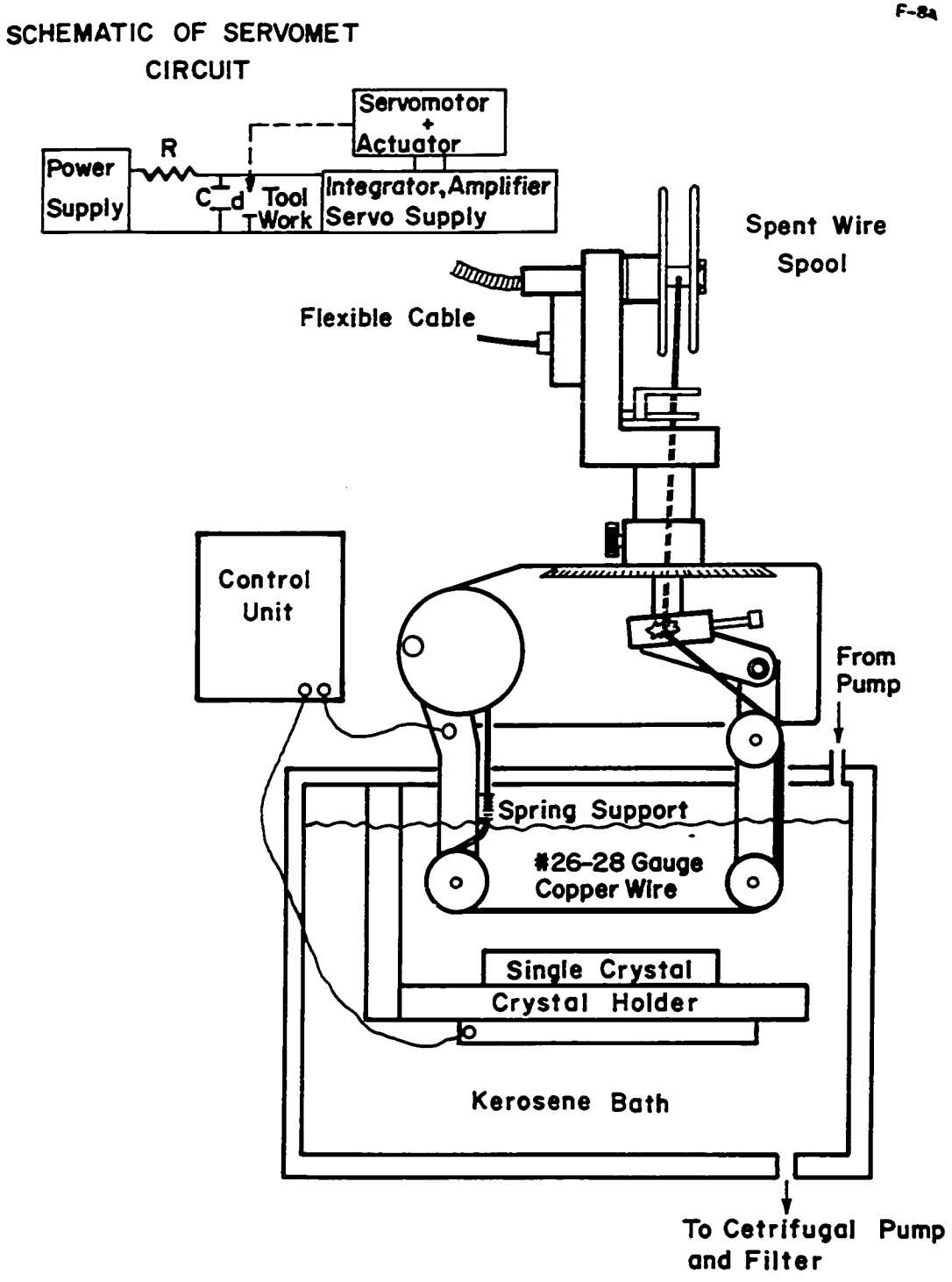

FIGURE F-II SCHEMATIC OF SERVOMET SPARK CUTTER

Some chemical contamination of the surface layer after spark cutting generally occurs and consists of tool material and carbon from decomposition of the dielectric. Contamination is confined to a very thin surface layer and can generally be removed by a light etch. Damage to the surface usually consists of a very thin melted layer (2-3 microns deep for lowest energy setting) which has frozen epitaxially. Below this is a layer subjected to thermal shock and possibly a further layer disturbed by shock waves due to cavitation. The extent and depth of surface damage depend on the work material and spark energy.

B. Polishing--Chemical (31)

Polishing of metal surfaces by immersion in a suitable solution without the application of an external potential is called "chemical" polishing as distinct from "electrolytic" polishing. The results can vary from etching, where the surface may be smoothed but not brightened to "bright dipping" where the surface is brightened but not smoothed. The results depend on the solution and operating conditions.

The functions of an ideal polishing process can be distinguished as

(a) "smoothing" by elimination of the large-scale irregularities (> a micron in size) and

(b) "brightening" by removal of the smaller irregularities (down to about a hundredth of a micron in size) without the appearance of etch pits.

As in electropolishing, it is theorized that two distinct processes occur:

(1) the formation of a viscous layer on the metal surface and

(2) the formation of a thin surface film, which provides an explanation for the absence of etched pits on polished surfaces.

Several methods have been described in the literature for chemically polishing nickel. Three of the methods are shown below:

Table (F-1)

Chemical Polishing Solutions for Nickel

Solution		Time	T (^{o}C)	Reference
30% HNO_3 10% H_2SO_4	10% Orthophosphoric 50% Glacial Acetic	$\frac{1}{2}$-1 min.	85-95	DeJong(10)
20% HNO_3 25% Acetic	55% Phosphoric 0.5% HCl	up to 5 min.	88 ^{o}C	
40% HNO_3 30% Phosphoric	30% Acetic 1% Sodium Chloride	up to 4 min.	85.5^{o}C	

C. Other Single Crystal Preparations

Rhodin (26) prepared 10 mil thick copper single crystals plates from a 6 in. x $1\frac{1}{4}$ in. cylindrical single crystal of copper grown by the standard Bridgman method. After determining the crystal orientation by the back-reflection Laue x-ray method, he cut sections 3/4 in. x 1/2 in. with an alundum cutting wheel. These were then reduced to .040 in. thickness by mechanical polishing. The plate was then reduced to a thickness of 10 mils by electropolishing.

Kruger (18) prepared single crystals of copper having (100), (110), and (111) orientations by cutting a large copper single crystal.

This was followed by mechanical polishing and electrolytic polishing.

Tibbetts and Propst (32) prepared 5 mil thick single crystal tungsten ribbons from a cylindrical tungsten crystal 1 cm. in diameter x 1 in. long. The crystal was cut initially with a spark-erosion machine. This was then followed by electropolishing to obtain an almost mirror finish along with a good back reflection Laue x-ray picture.

Harris, Ball and Gwathmey (16) prepared flat faces on copper single crystal spheres parallel to the (311), (111), and (100) planes. These were prepared by machining followed by electropolishing.

EXPERIMENTAL APPARATUS AND PROCEDURE

The apparatus used to prepare the thin polished single crystals consisted essentially of the x-ray machine, a spark cutter, automatic grinding devices, mechanical polishing wheels and chemical polishing equipment.

A large single crystal 6" long by 1/2"-3/4" in diameter was the starting material. The crystal was grown by Research Crystal Incorporated in Richmond, Virginia. The orientation was (100) along the axial direction as shown in Figure F-III-B. Since the desired crystals were 3" long, it was possible to cut crystal specimens with a (100) and (110) orientation. To obtain (111) crystals of 3" length, it was necessary to have a single crystal with a (110) orientation along the axis.

A. Cutting of Large Crystal

The large 6" long crystal was first cut with the spark cutter to give a 3" long crystal. This crystal was then sliced into four quadrants as shown in Figure F-III-C. The energy of the spark cutter could be varied with a setting of 1 to 7. The lowest reading gave the roughest but fastest cut. With a setting of 7, it was possible to have a smoother cut, but the time required for cutting was very long. Most of the cuts were made with a spark cutter setting of 5.

The crystals were glued to the sample holder with Duco cement. An attempt was made to use sealing wax; however, it was soluble in the kerosene. The glued sample was removed from the holder by acetone.

FIGURE F-III-A

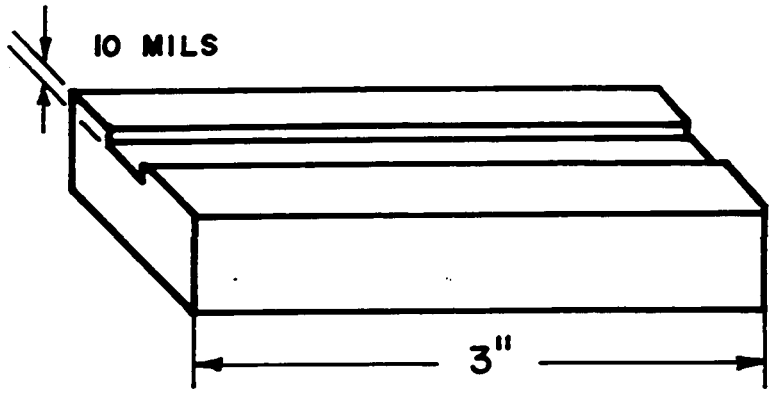

Holder For Thinning Crystal Specimens

FIGURE F-III-B

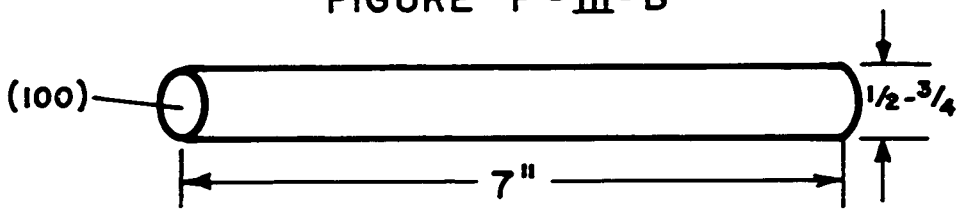

Original Nickel Crystal

FIGURE F-III-C

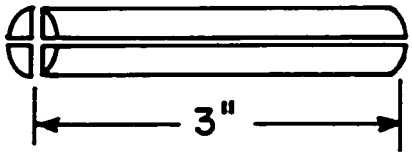

Sliced Crystal

FIGURE F-III-D

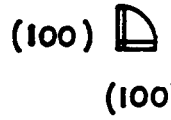

Cutting of (100) Crystals

FIGURE F-III-E

Cutting of (110) Crystals

FIGURE F-III CUTTING OF NICKEL SINGLE CRYSTAL

A #26 gauge copper wire proved to be the most feasible size of wire. Thinner wire resulted in breakage and larger wire gave too wide a cut resulting in wastage.

After cutting the large sample into four parts, one of the sections was glued to the holder and smaller slices (ca. 1/16 inch) cut as shown in Figure F-III-D. Attempts made to cut thinner sections resulted in bending of the crystal. A Laue back reflection x-ray picture was taken prior to cutting the sample into 4 parts to assure clevage along a (100) direction.

Crystals with (110) orientation were cut from the quadrants by gluing the sample in a right angle holder and cutting the crystal as shown in Figure F-III-E.

B. Thinning, Grinding and Mechanical Polishing of Single Crystal Slices

After slicing the crystals into about 1/16" thick slices with the spark cutter, the slices were then thinned to about 12 mils thick with a Buehler type belt grinder. The 1/16" thick sample was glued to the sample holder, shown in Figure F-III-A. A thin film of Duco cement was spread over one side of the crystal plate which was then placed on the holder. Pressure was applied to the sample by placing lead weights on the top of the sample. The drying period was approximately 24 hours.

After grinding the exposed surface on a 350 or 400 grit wet belt for several minutes, a parallel surface was usually attained. Following this paralleling operation, the sample was then ground on a wet 600 grit paper for about $\frac{1}{2}$-1 hour.

The sample was then polished on a Buehler-type polishing wheel using Selph cloth and .3 micron alumina. This was then followed by polishing with .05 micron alumina until a mirror smooth finish was obtained.

The sample and holder were then placed in a beaker of acetone to remove the sample. The sample usually loosened after about 15 minutes and separated from the holder. Several attempts to remove the sample by prying resulted in bent specimens.

The sample was then reglued to the holder again using lead weights to assure good contact. After drying 24 hours, the exposed side was ground on the wet 600 grit cloth until the sample was about 10 mils thick. The belt grinding step was not used at this stage, since the thin sample was very susceptible to bending. Finally, the sample was polished and removed from the holder as described previously.

Samples as thin as 4-5 mils were prepared by this technique; however, much more care and careful handling were required to obtain a polished sample.

C. Chemical Polishing of Thin Single Crystals

Prior to chemically polishing the thin sample, it was ultrasonically cleaned in benzene, then acetone, and finally in warm distilled water. The chemical polishing solution used consisted of

30% HNO_3
10% H_2SO_4
10% Orthophosphoric acid
50% Glacial acetic acid

The polishing step was carried out at a temperature of 85-95°C in a beaker agitated with a magnetic stirrer. The immersion time was approximately 7-10 seconds. The sample was held with a clamp attached to a long holder and held at the edge so that essentially all of the crystal was uniformly exposed.

Immediately after removing the sample from the hot acid solution, the sample was immersed in distilled water to remove all traces of acid.

Some unsuccessful attempts were made to electrochemically polish the large thin nickel crystal specimens. In most cases, the polishing was very poor and non-uniform.

Other types of chemical polishing solutions were also investigated, but without success.

D. Observation of Finished Crystals

Following the chemical polishing step, the crystal was mounted on a holder and a back reflection Laue x-ray picture taken on a G. E. type x-ray instrument. The x-ray was taken with a copper target with an exposure time of about 20 minutes.

The crystal orientation determination consisted of drawing hyperbolas through the spots and joining these hyperbolas on a larger scale. This plot is then compared to a standard projection to determine the orientation.

Microphotographs were also taken of some of the finished specimens to observe macroscopic surface conditions.

DISCUSSION OF RESULTS

The finished samples were normally about 3" long by 1/6" wide by about 10 mils thick with a bright polished surface on each side. Good back reflection Laue x-ray pictures were obtained for the samples.

Approximately 10 of these crystals--both (100) and (110) orientation--were prepared from the Research Crystal Inc. grown nickel single crystal. Twelve other nickel single crystals--four (100), four (110) and four (111)--were also purchased from Semi-Elements Inc. These crystals, thinned to about 10 mils by etching, had a fairly rough etched surface which had a satin appearance. These samples were also refinished to give a bright smooth appearance on each side.

In the spark cutting operation, some difficulty was encountered with the cut sample closing onto the copper wire causing breakage or sticking. When the wire was repaired or removed, the planing action of the spark cutter caused the wire to start from the beginning of the cut sometimes causing grooves on the surface.

The spark cutting operation resulted in some surface damage as mentioned earlier. A microphotograph of a spark cut surface is shown in Figure F-IV. With a setting of 5 on the spark cutter, it took approximately 3/4-1 hour to cut through a 1/4-3/8" section of the single crystal.

Extreme care was required for the thinning operation, since a coarse grit at a high rpm was used. With a 320 grit paper, approximately 2.8 mils/minute were removed. Approximately 1 hour on each side was required for the fine grinding step using 600 grit wet paper.

An additional $\frac{1}{2}$-1 hour was required on each side on the polishing wheel with .3 and .05 alumina. Pictures of the single crystals during different stages of grinding and polishing are shown in Figures F-V and VI.

In the chemical polishing step, the time of immersion was extremely important. If the polishing were continued for more than 10 seconds, extensive pitting and "blister" formation occurred. If the chemical polishing time were less than 5 seconds, some of the mechanical damage remained.

During chemical polishing of some very thin single crystals ($<$ 5 mils thick), a white substance appeared as spots on the surface. In some instances it was possible to remove these spots by rubbing vigorously with acetone on a polishing cloth.

Back reflection Laue x-ray pictures were taken at different stages of the finishing process. Some of these are shown in Figures F-VII to F-XVII.

MICROPHOTOGRAPHS DURING PREPARATION OF NICKEL SINGLE CRYSTALS

Figure F-IV 500x
Spark Cut Surface

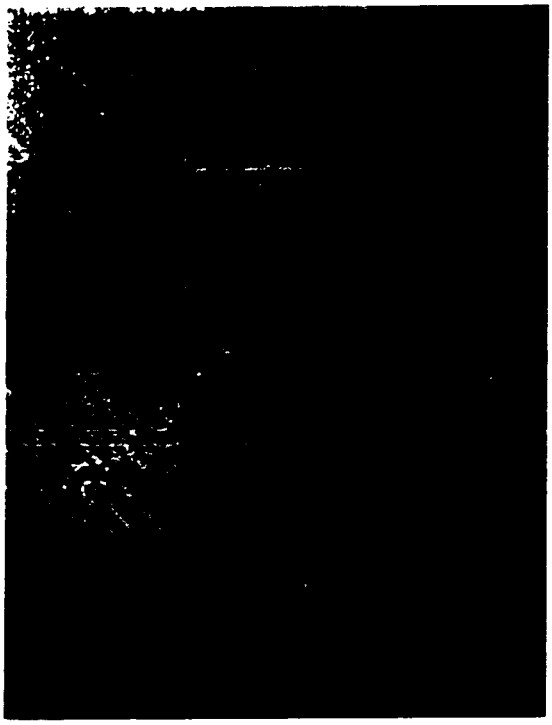

Figure F-V 1000x
Single Crystal After
Mechanical Polishing

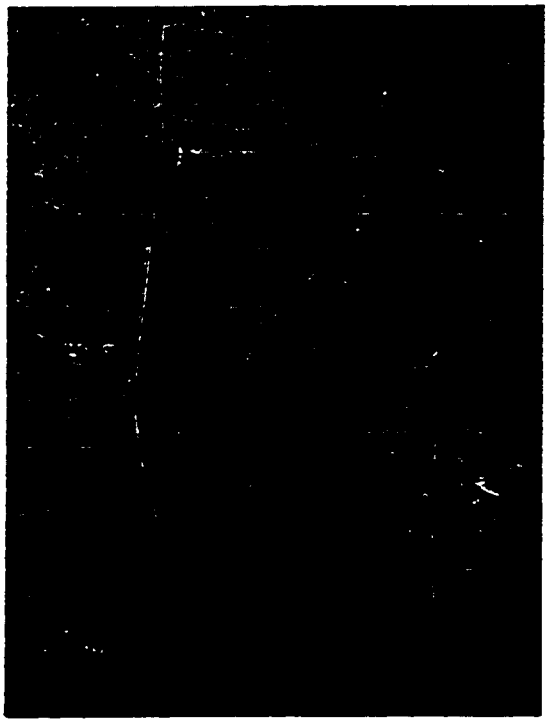

Figure F-VI 1000x
Single Crystal After
Chemical Polishing

BACK REFLECTION LAUE X-RAYS OF SEMI-FINISHED SINGLE CRYSTALS AND POLYCRYSTALLINE NICKEL

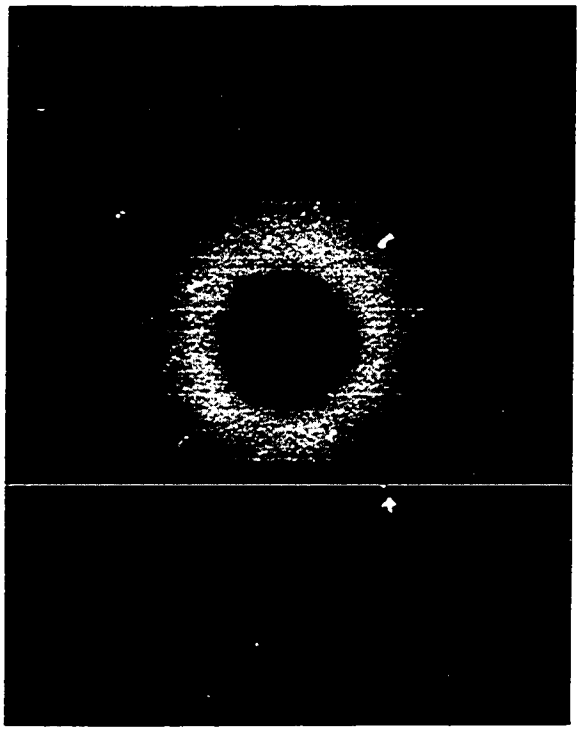

Figure F-VII Damaged Single Crystal

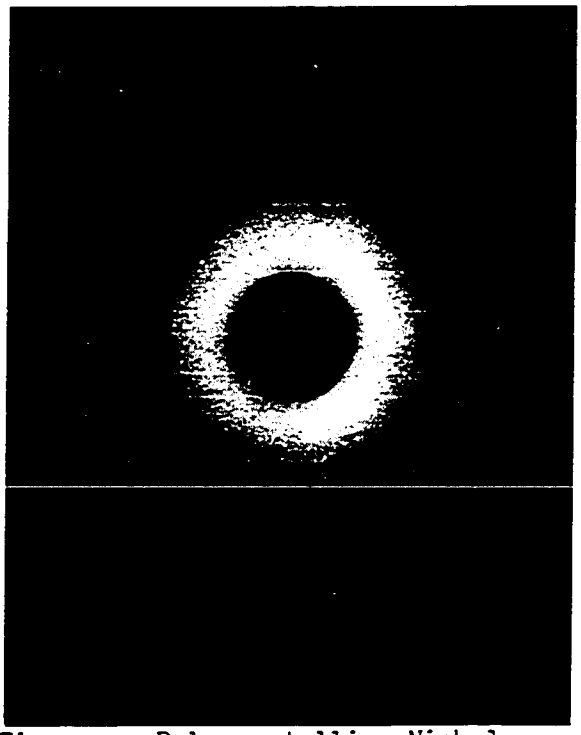

Figure F-VIII Polycrystalline Nickel After Mechanical Polishing

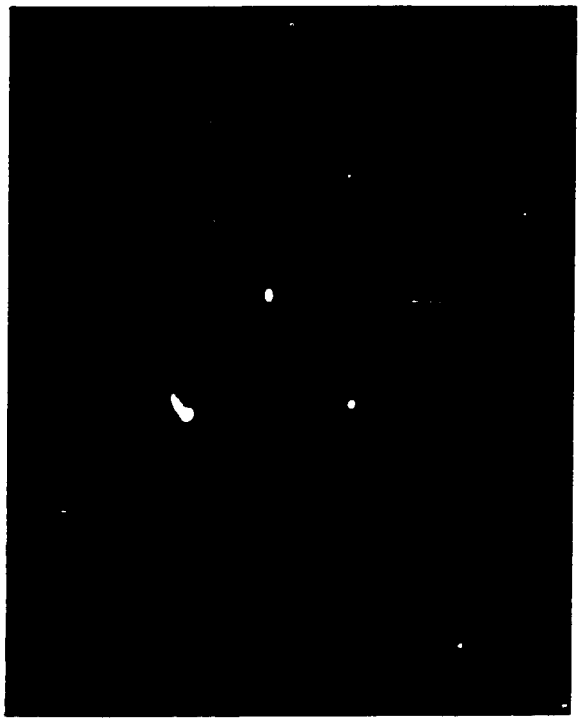

Figure F-IX Single Crystal Specimen After Mechanical Polishing Through 0.3 Micron Alumina

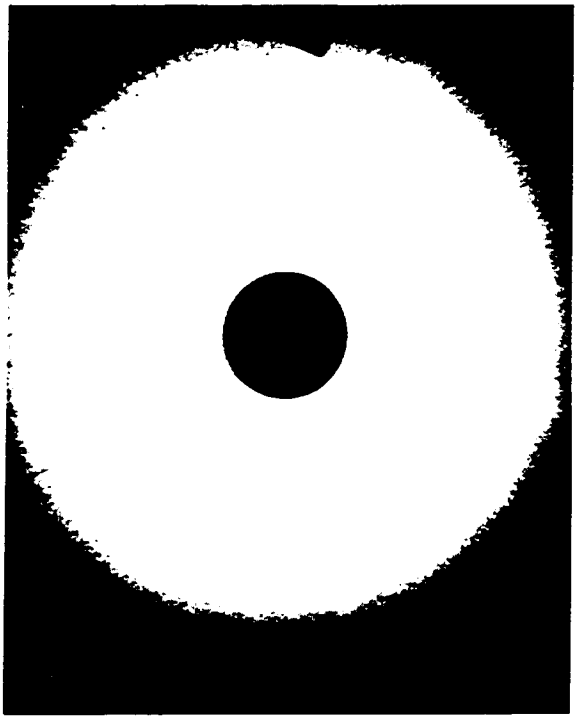

Figure F-X Single Crystal After Spark Cutting

BACK REFLECTION LAUE X-RAYS OF FINISHED NICKEL SINGLE CRYSTALS

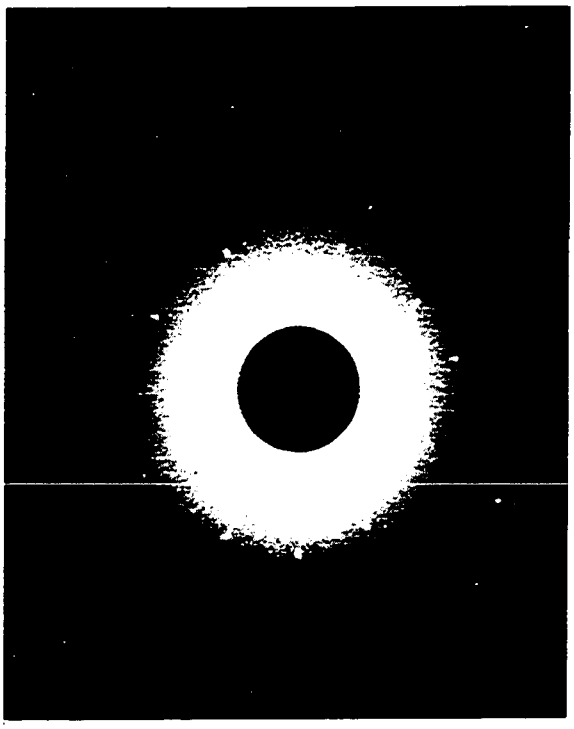

OSC#5 Figure F-XI (110)

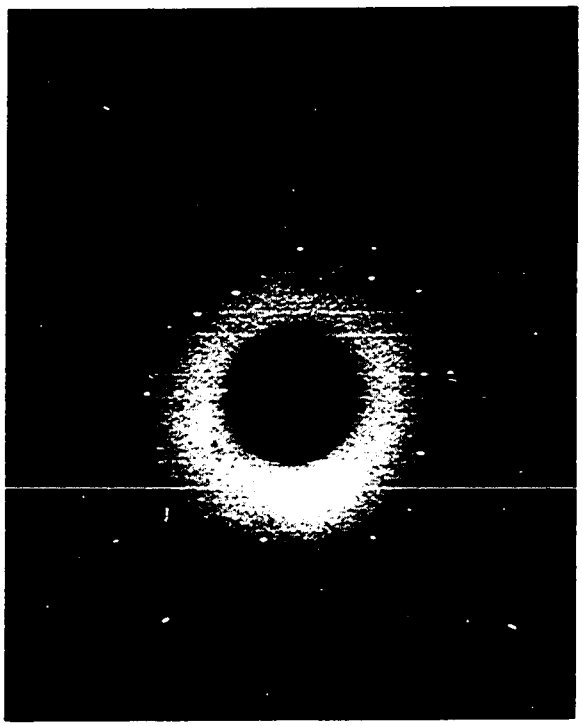

OSC#6 Figure F-XII (110)

SE#1 Figure F-XIII (110)

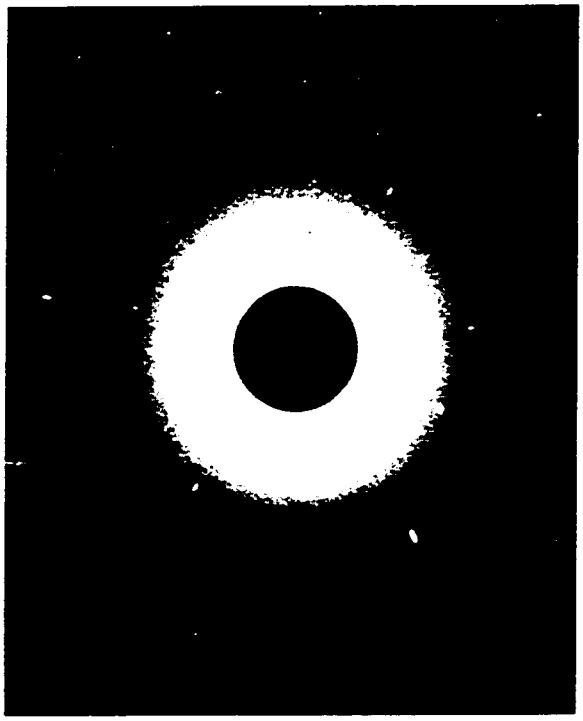

SE#10 Figure F-XIV (111)

APPENDIX G

MICROPHOTOGRAPHS

This appendix contains 46 color microphotographs taken during the various stages of oxidation of the nickel single crystals. The pictures were taken at a magnification of 50x to observe the macroscopic oxide formation and 1000x to observe microscopic oxide formation.

This appendix also includes a summarized table of the microphotographs listing exposure and development time.

Finally, this appendix contains back reflection Laue x-ray pictures of three nickel single crystals after reducing the oxide from the surface.

Table (G-1)

Description of Microphotographs

Page	Figure	Sample	Crystal	Oxide ($\mu g/cm^2$)	Magnification	Time(sec.) Exp.	Dev.
G-4	1-P	SE#5	(100)	12.7	50x	3	75
	2-P	SE#5	(100)	12.7	"	3	"
	3-P	SE#9	(111)	9.0	"		"
	4-P	SE#1	(110)	4.9	"		"
G-5	5-P	SE#12	(111)	20.3	50x		75
	6-P	SE#12	(111)	20.3	"		"
	7-P	SE#6	(100)	21.8	"	12	"
	8-P	SE#3	(110)	29.1	"		"
G-6	9-P	SE#2	(110)	37.2	50x		75
	10-P	SE#2	(110)	37.2	"		"
	11-P	SE#10	(111)	33.3	"		"
	12-P	SE#8	(100)	37.0	"	15	"
G-7	13-P	SE#7	(100)	46.6	50x	25	75
	14-P	SE#7	(100)	46.6	"	25	"
	15-P	SE#11	(111)	57.6	"	35	"
	16-P	SE#4	(110)	77.3	"		"
G-8	17-P	OSC#6	(100)	13.5	50x	1	75
	18-P	OSC#3	(100)	29.4	"		"
	19-P	OSC#1	(100)	38.1	"		"
	20-P	OSC#4	(100)	77.2	"		"
G-9	21-P	OSC#8	(110)	48.1	50x	10	75
	22-P	OSC#5	(110)	68.8	"	10	"
	23-P	OSC#2	(110)	82.8	"	20	"
	24-P	O-#15-10W1x5	Poly-crystalline	43.1	"		"
G-10	25-P	SE#1	(110)	4.9	1000x	4	75
	26-P	SE#1	(110)	4.9	"	4	"
	27-P	SE#5	(100)	12.7	"	7	"
	28-P	SE#5	(100)	12.7	"	15	"
G-11	29-P	SE#3	(110)	29.1	1000x	6	75
	30-P	SE#3	(110)	29.1	"	6	"
	31-P	SE#3	(110)	29.1	"	7	"
	32-P	SE#3	(110)	29.1	"	6	"

Table (G-1)
(Continued)

Page	Figure	Sample	Crystal	Oxide (g/cm^2)	Magnification	Time(sec.) Exp.	Dev.
G-12	33-P	SE#2	(110)	37.2	1000x	15	90
	34-P	SE#2	(110)	37.2	"	14	70
	35-P	SE#8	(100)	37.0	"	7	75
	36-P	SE#8	(100)	37.0	"	20	"
G-13	37-P	SE#6	(100)	21.8	1000x	20	75
	38-P	SE#6	(100)	21.8	"	15	"
	39-P	SE#7	(100)	46.6	"	20	"
	40-P	SE#7	(100)	46.6	"	25	"
G-14	41-P	SE#9	(111)	9.0	1000x	5	"
	42-P	SE#12	(111)	20.4	"	5	"
	43-P	SE#10	(111)	33.3	"	5	"
	44-P	SE#11	(111)	57.6	"	12	"
G-15	45-P	SE#4	(110)	77.3	1000x—	8	75
	46-P	SE#4	(110)	77.3	"	9	70

MICROPHOTOGRAPHS OF OXIDIZED NICKEL SINGLE CRYSTALS

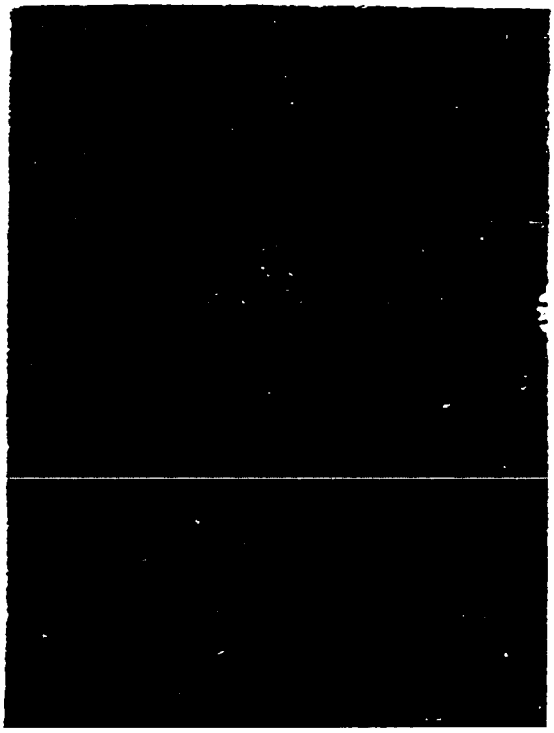

SE#5 (100) Figure 1-P 12.7 μg/cm^2 50x

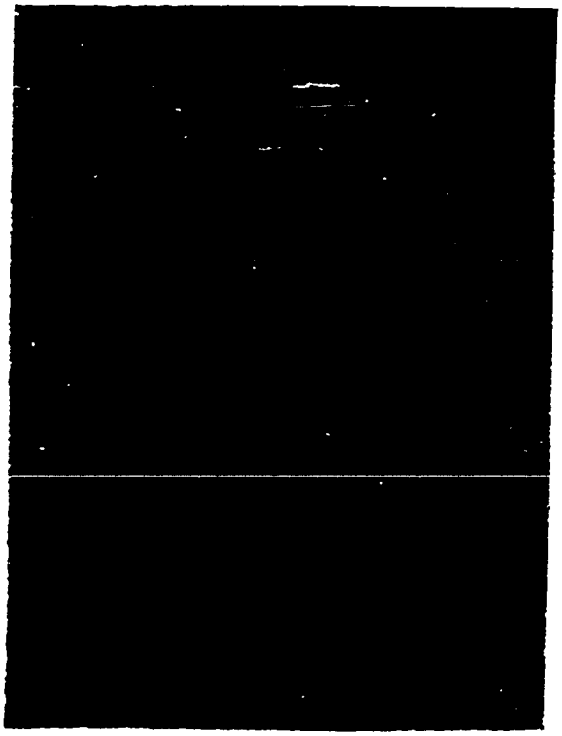

SE#5 (100) Figure 2-P 12.7 μg/cm^2 50x

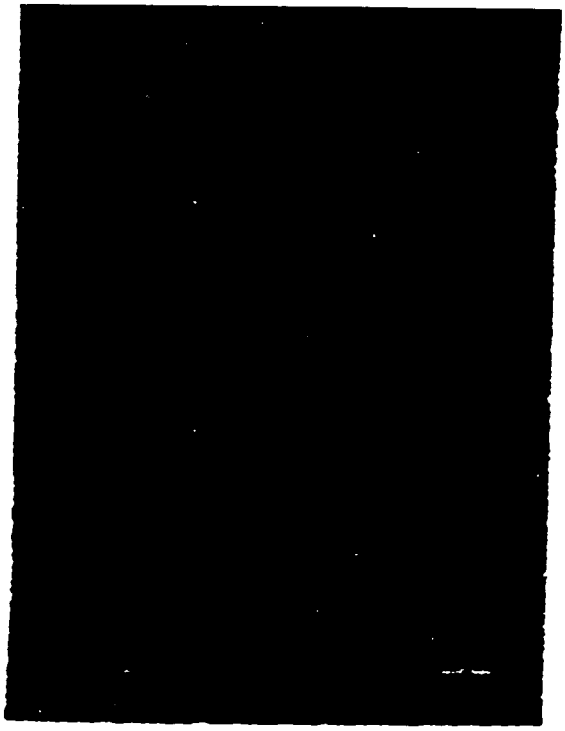

SE#9 (111) Figure 3-P 9.0 μg/cm^2 50x

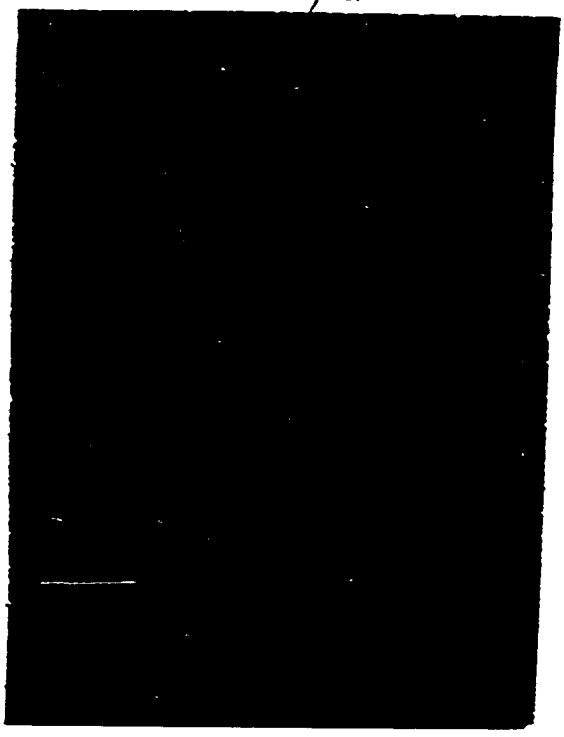

SE#1 (110) Figure 4-P 4.9 μg/cm^2 50x

MICROPHOTOGRAPHS OF OXIDIZED NICKEL SINGLE CRYSTALS

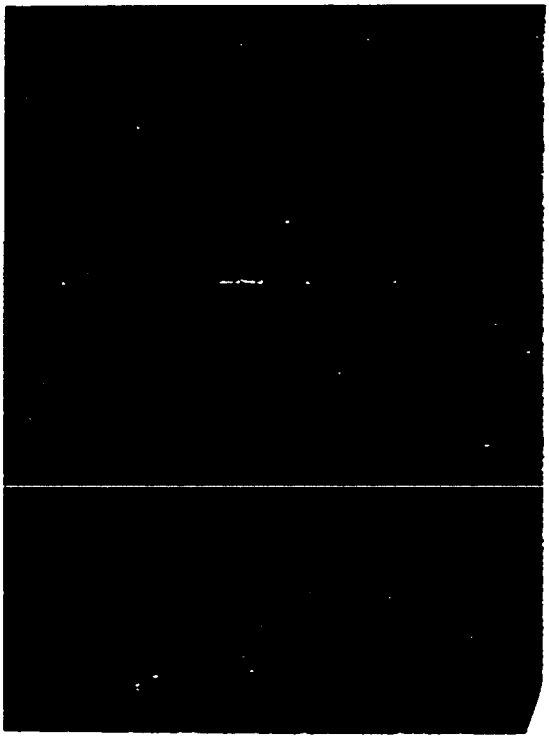

SE#12 (111) Figure 5-P 20.3 $\mu g/cm^2$ 50x

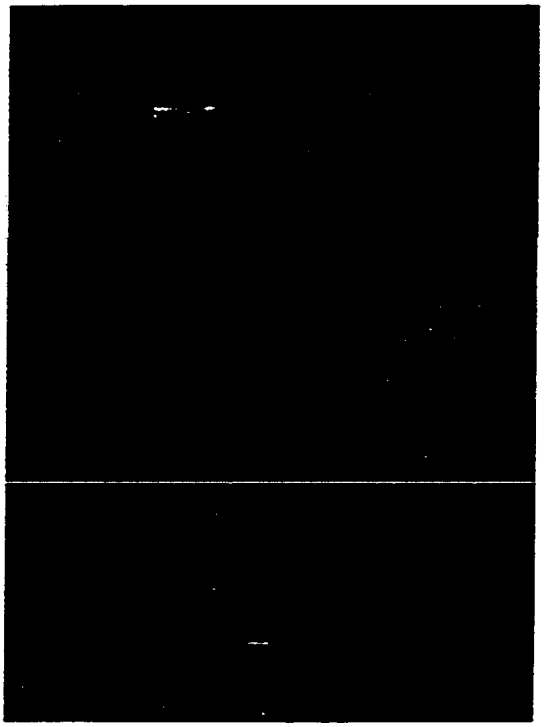

SE#12 (111) Figure 6-P 20.3 $\mu g/cm^2$ 50x

SE#6 (100) Figure 7-P 21.8 $\mu g/cm^2$ 50x

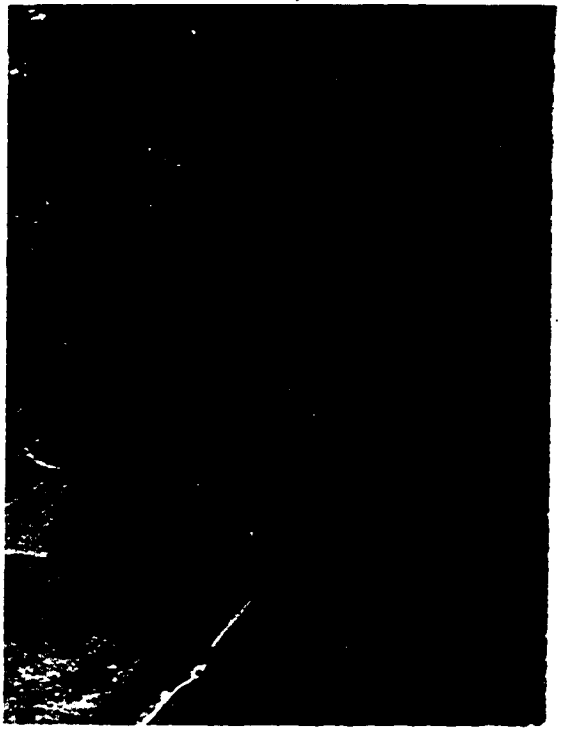

SE#3 (110) Figure 8-P 29.1 $\mu g/cm^2$ 50x

MICROPHOTOGRAPHS OF OXIDIZED NICKEL SINGLE CRYSTALS

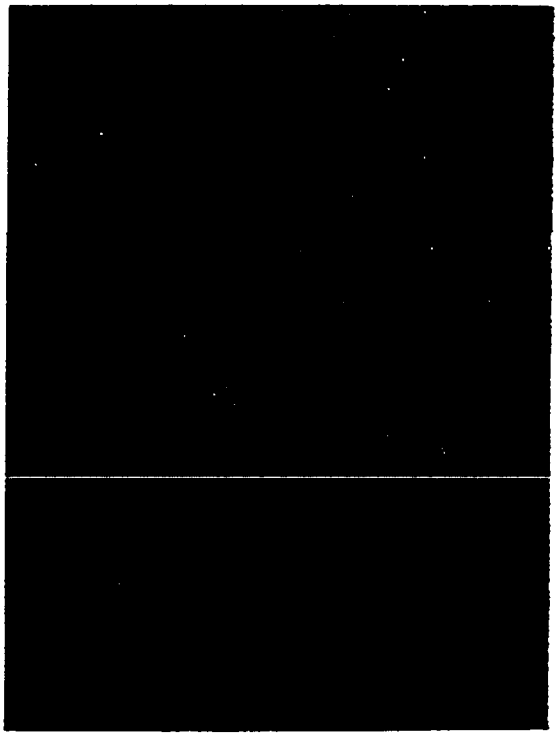

SE#2 (110) Figure 9-P 37.2 $\mu g/cm^2$ 50x

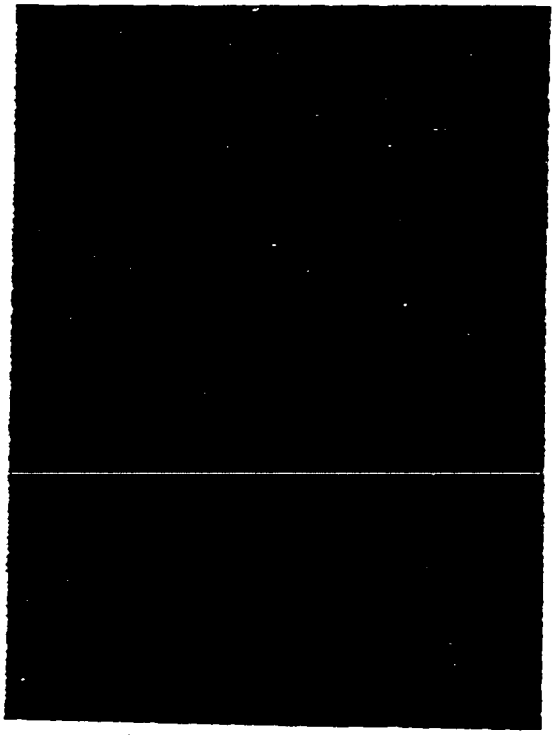

SE#2 (110) Figure 10-P 37.2 $\mu g/cm^2$ 50x

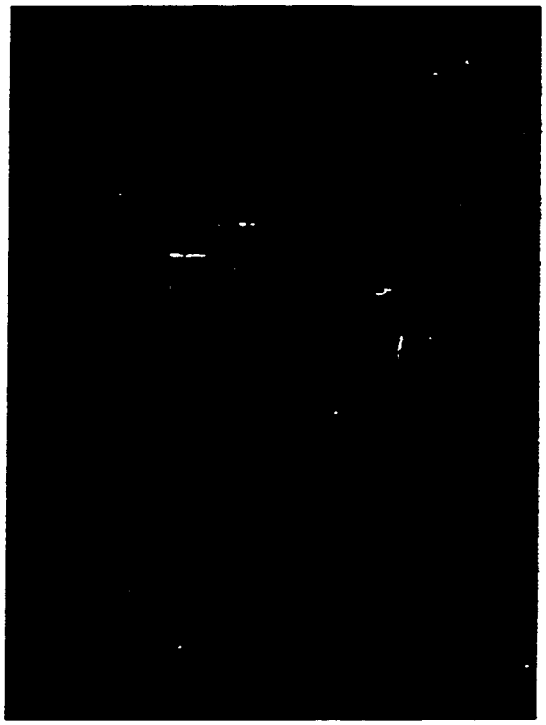

SE#10 (111) Figure 11-P 33.3 $\mu g/cm^2$ 50x

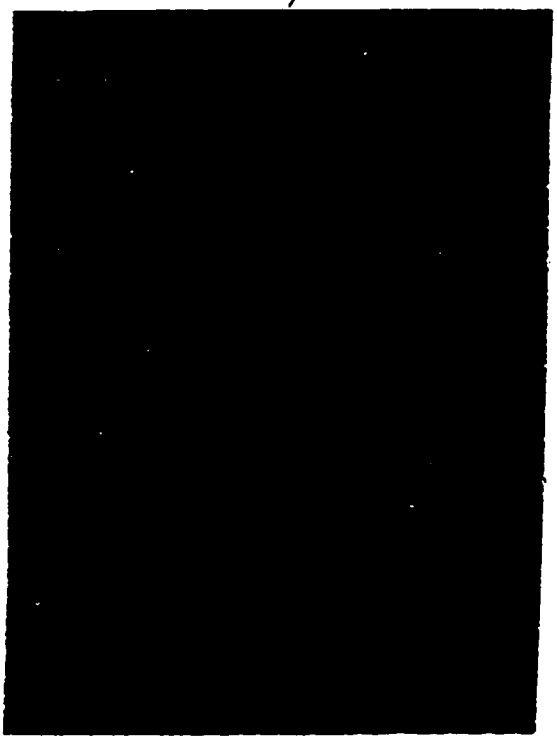

SE#8 (100) Figure 12-P 37.0 $\mu g/cm^2$ 50x

MICROPHOTOGRAPHS OF OXIDIZED NICKEL SINGLE CRYSTALS

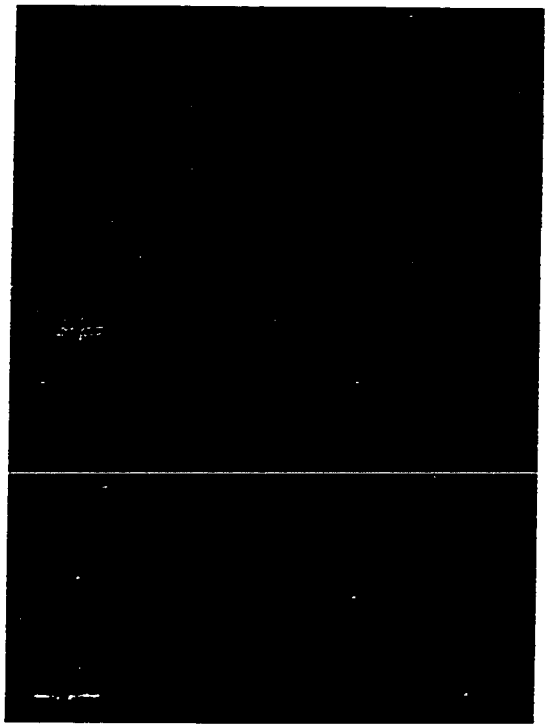

SE#7 (100) Figure 13-P 46.6 $\mu g/cm^2$ 50x

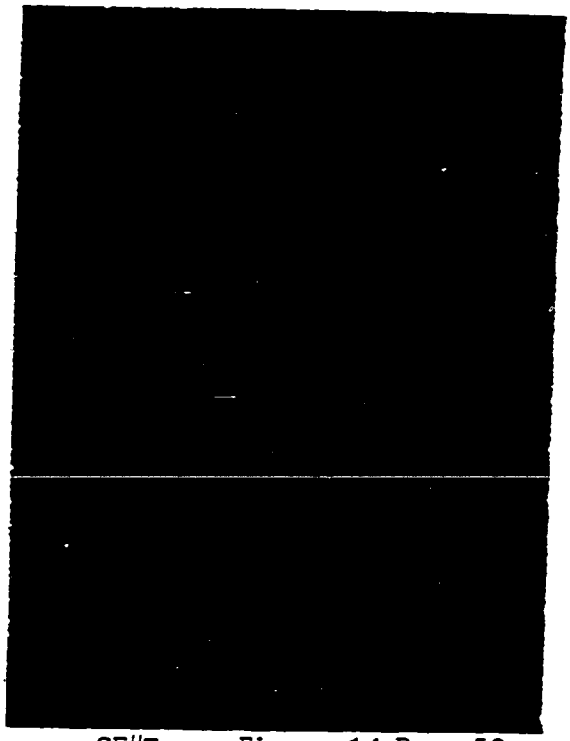

SE#7 (100) Figure 14-P 46.6 $\mu g/cm^2$ 50x

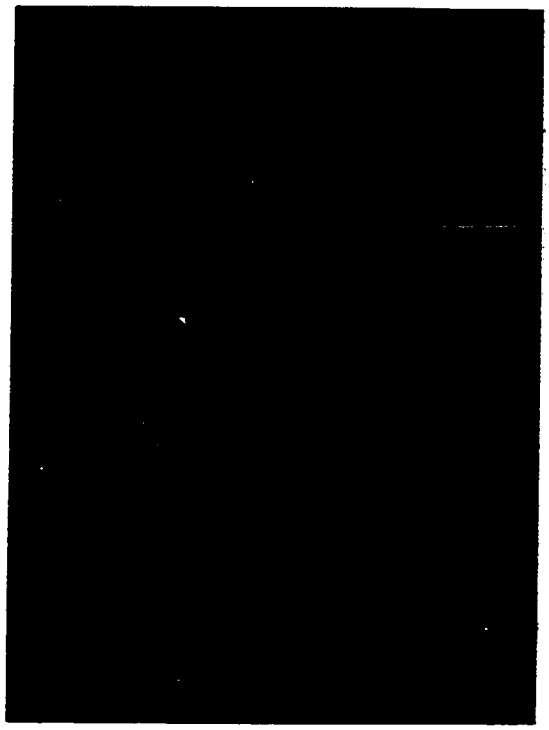

SE#11 (111) Figure 15-P 57.6 $\mu g/cm^2$ 50x

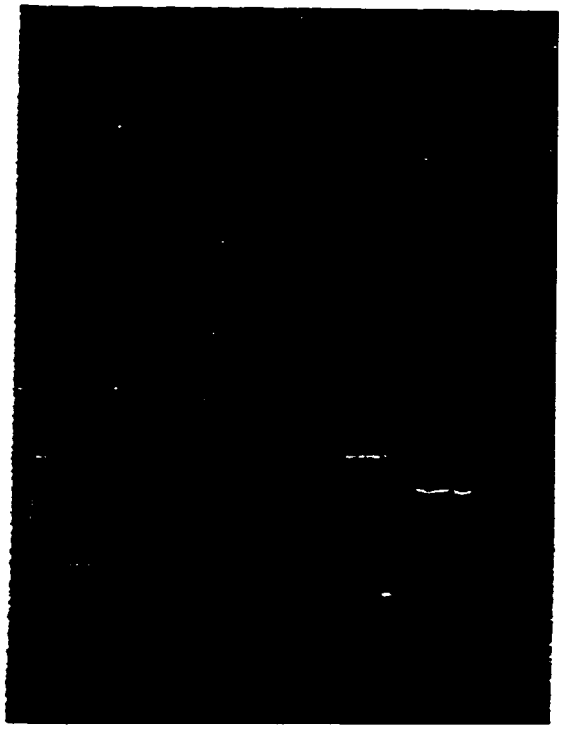

SE#4 (110) Figure 16-P 77.3 $\mu g/cm^2$ 50x

MICROPHOTOGRAPHS OF OXIDIZED NICKEL SINGLE CRYSTALS

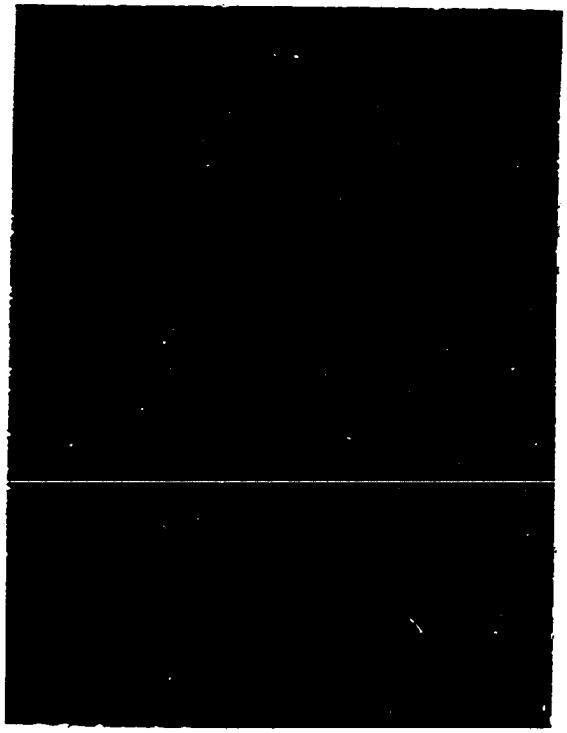

OSC#6 (100) Figure 17-P 13.5 $\mu g/cm^2$ 50x

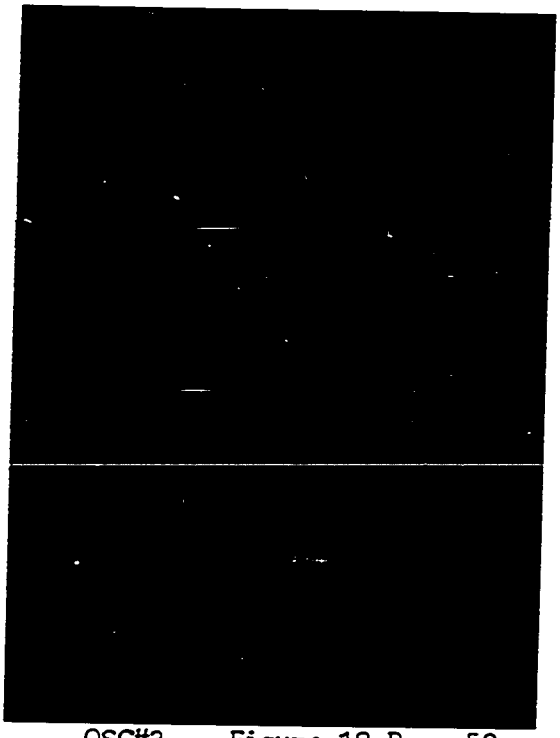

OSC#3 (100) Figure 18-P 29.4 $\mu g/cm^2$ 50x

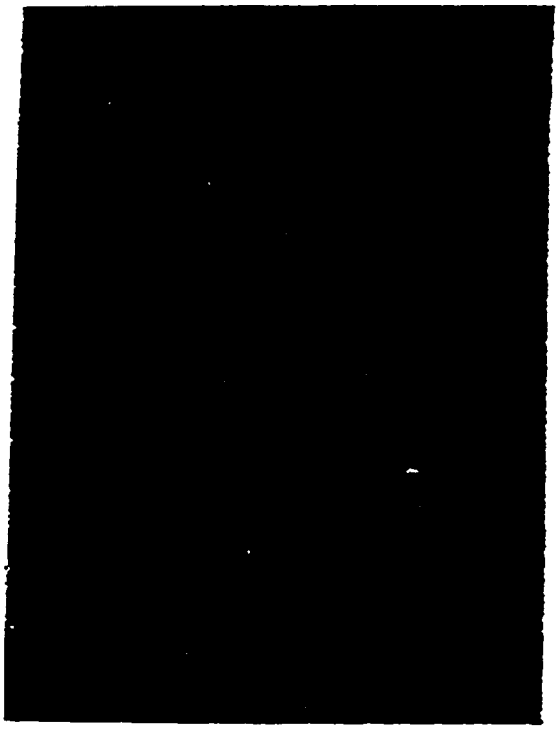

OSC#1 (100) Figure 19-P 38.1 $\mu g/cm^2$ 50x

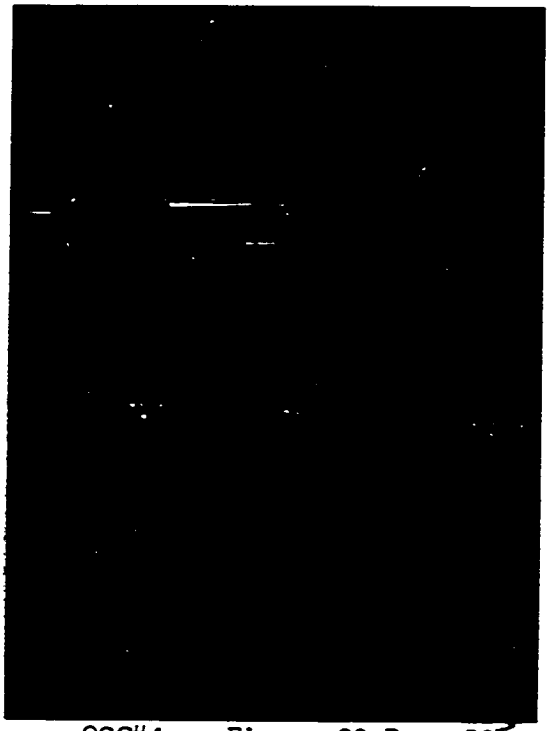

OSC#4 (100) Figure 20-P 77.2 $\mu g/cm^2$ 50x

MICROPHOTOGRAPHS OF OXIDIZED SINGLE AND POLYCRYSTALLINE NICKEL

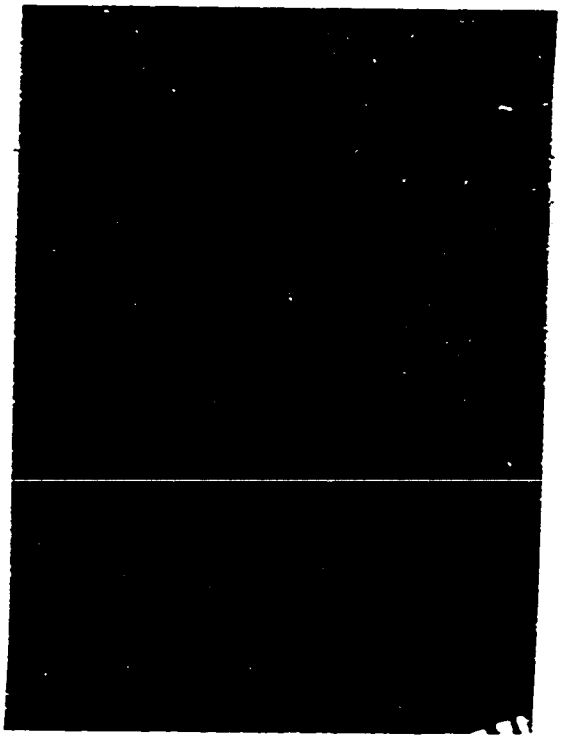

OSC#8 Figure 21-P 50x
(110) 48.1 $\mu g/cm^2$

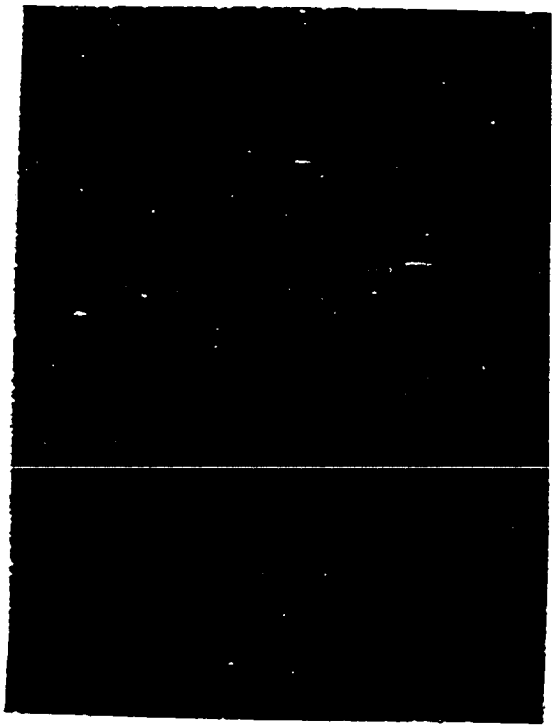

OSC#5 Figure 22-P 50x
(110) 68.8 $\mu g/cm^2$

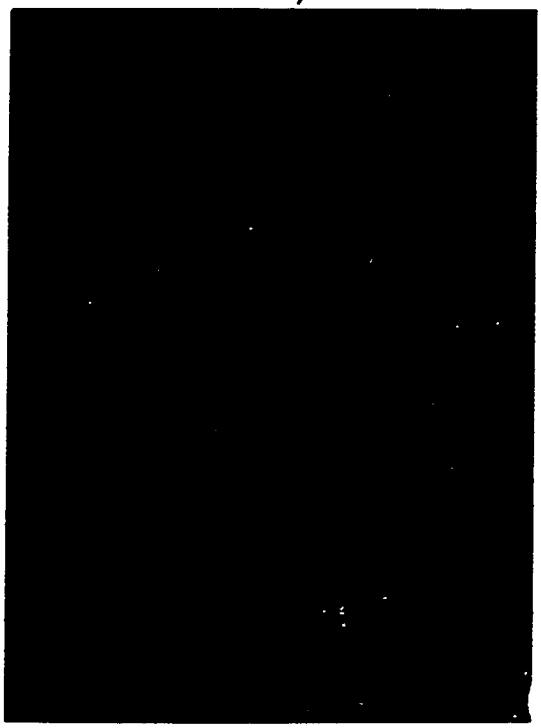

OSC#2 Figure 23-P 50x
(110) 82.8 $\mu g/cm^2$

O-#15-10W1x5 Figure 24-P 50x
Polycrystalline 43.1 $\mu g/cm^2$

MICROPHOTOGRAPHS OF OXIDIZED NICKEL SINGLE CRYSTALS

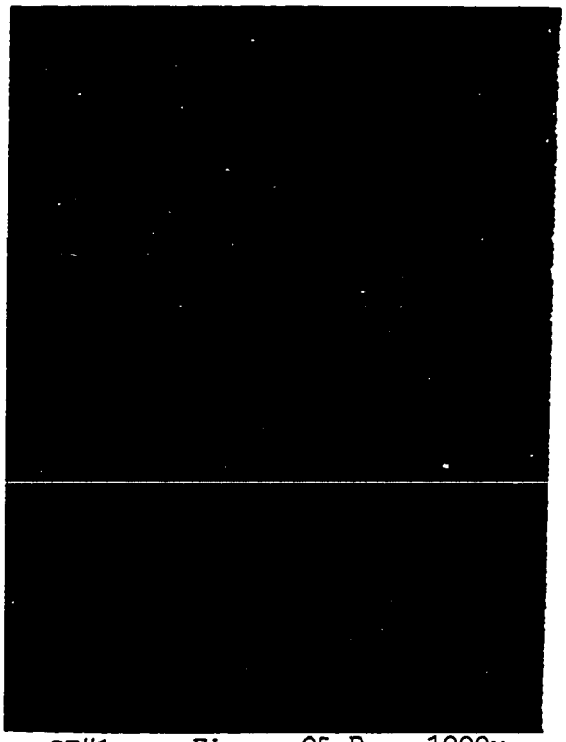

SE#1 (110) Figure 25-P 4.9 $\mu g/cm^2$ 1000x

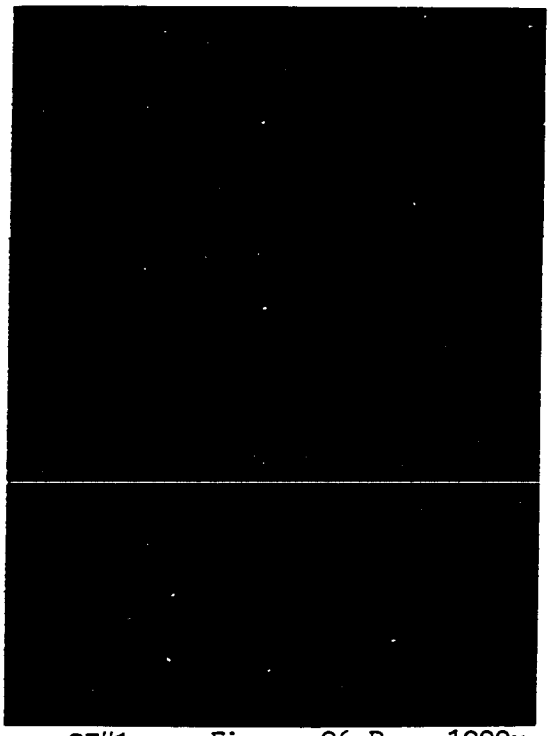

SE#1 (110) Figure 26-P 4.9 $\mu g/cm^2$ 1000x

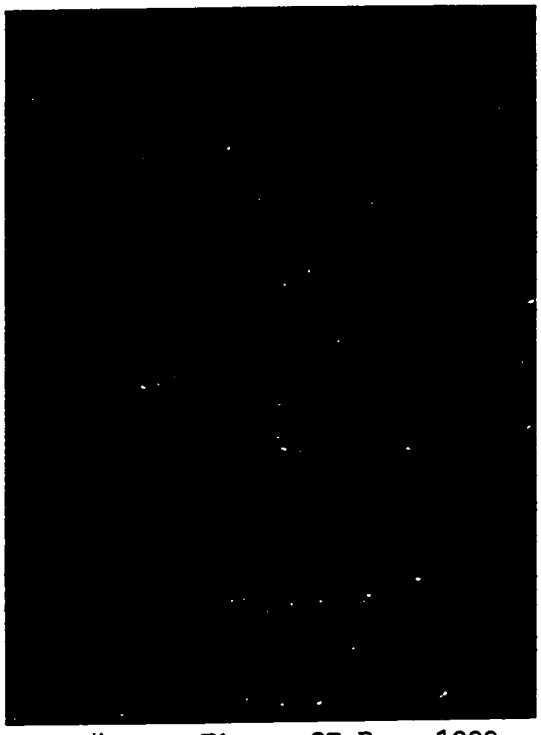

SE#5 (100) Figure 27-P 12.7 $\mu g/cm^2$ 1000x

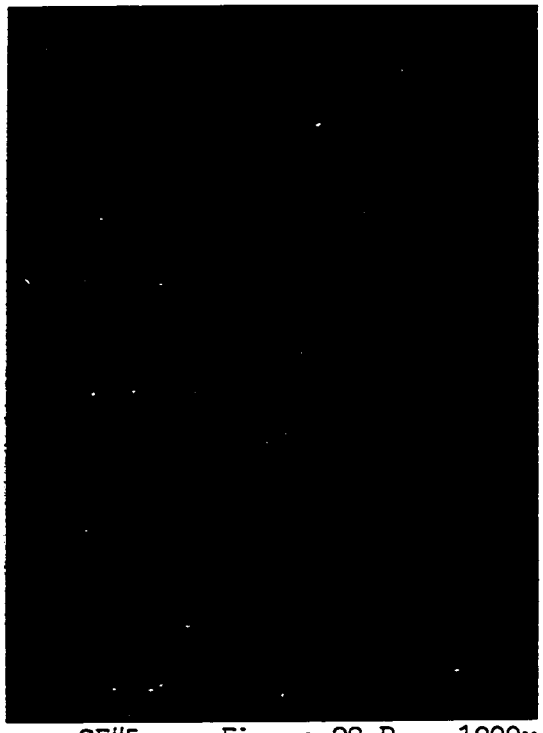

SE#5 (100) Figure 28-P 12.7 $\mu g/cm^2$ 1000x

MICROPHOTAGRAPHS OF OXIDIZED NICKEL SINGLE CRYSTALS

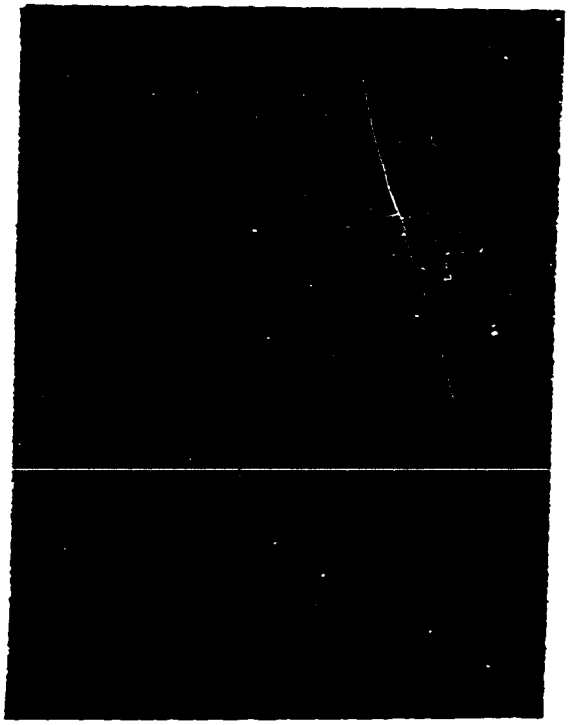

SE#3 (110) Figure 29-P 29.1 $\mu g/cm^2$ 1000x

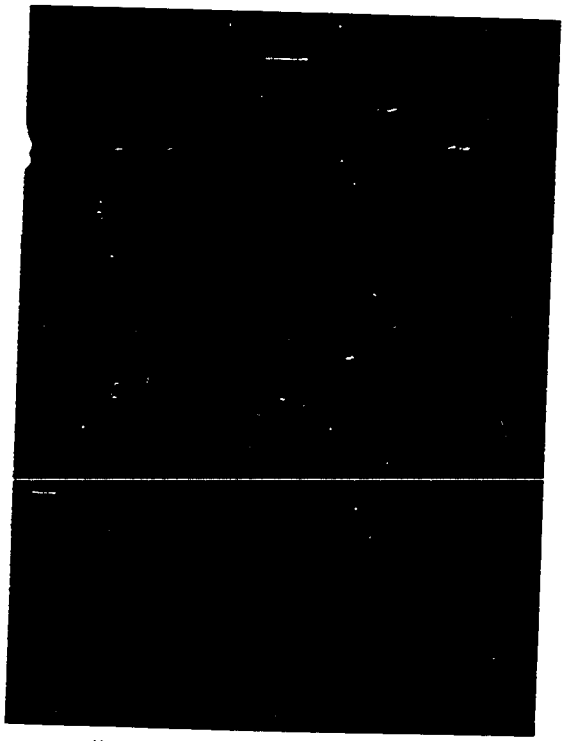

SE#3 (110) Figure 30-P 29.1 $\mu g/cm^2$ 1000x

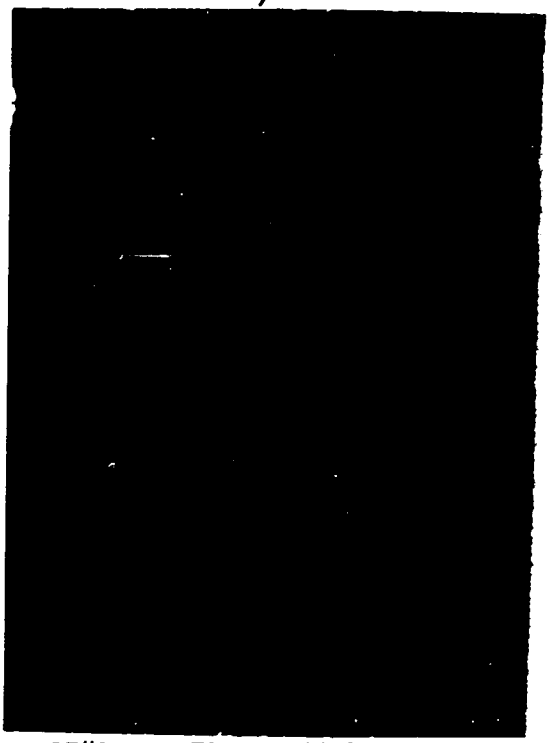

SE#3 (110) Figure 31-P 29.1 $\mu g/cm^2$ 1000x

SE#3 (110) Figure 32-P 29.1 $\mu g/cm^2$ 1000x

MICROPHOTOGRAPHS OF OXIDIZED NICKEL SINGLE CRYSTALS

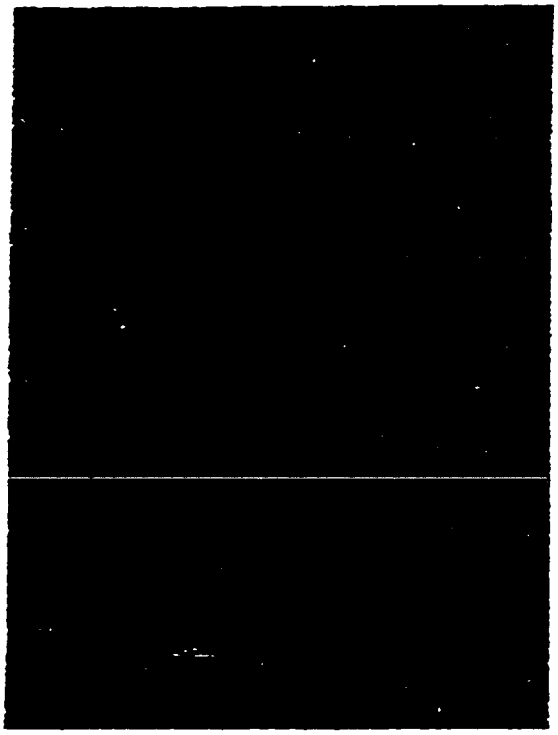

SE#2 (110) Figure 33-P 37.2 $\mu g/cm^2$ 1000x

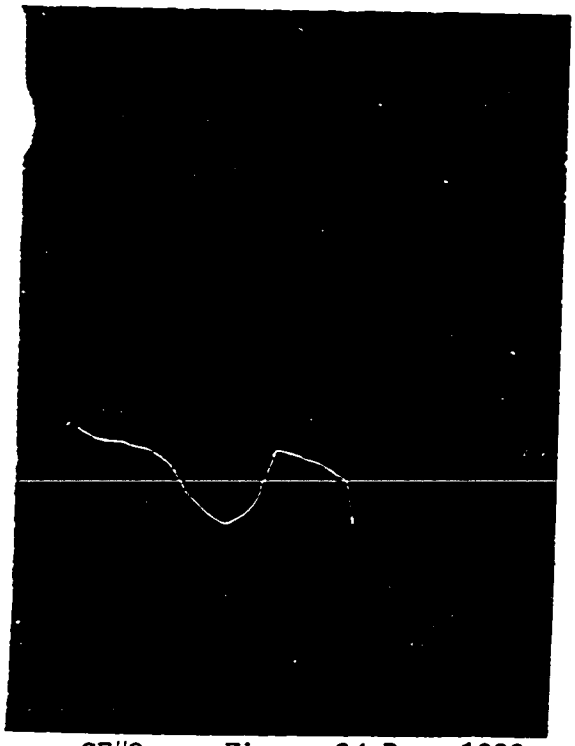

SE#2 (110) Figure 34-P 37.2 $\mu g/cm^2$ 1000x

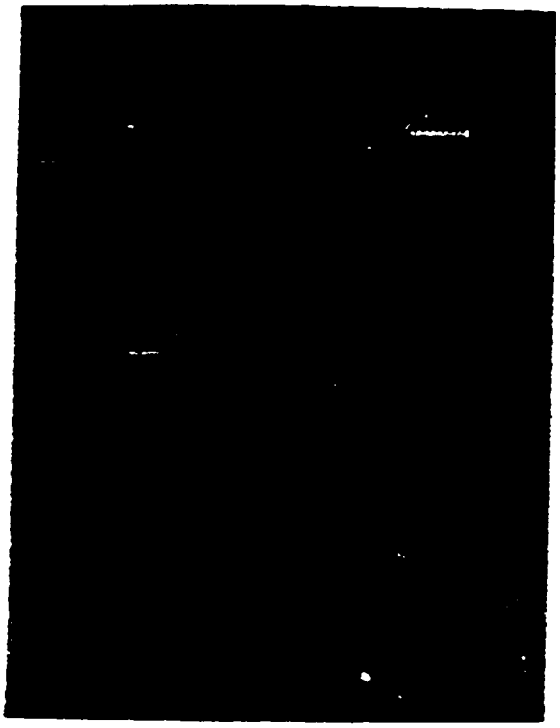

SE#8 (100) Figure 35-P 37.0 $\mu g/cm^2$ 1000x

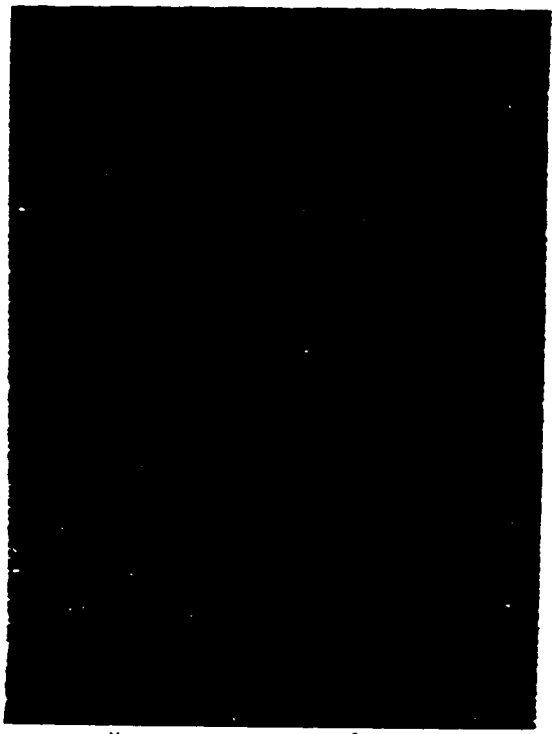

SE#8 (100) Figure 36-P 37.0 $\mu g/cm^2$ 1000x

MICROPHOTOGRAPHS OF OXIDIZED NICKEL SINGLE CRYSTALS

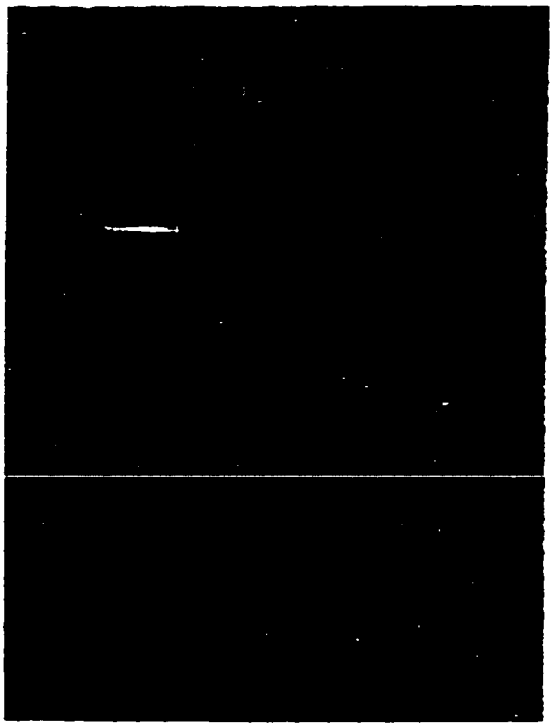

SE#6 (100) Figure 37-P 21.8 $\mu g/cm^2$ 1000x

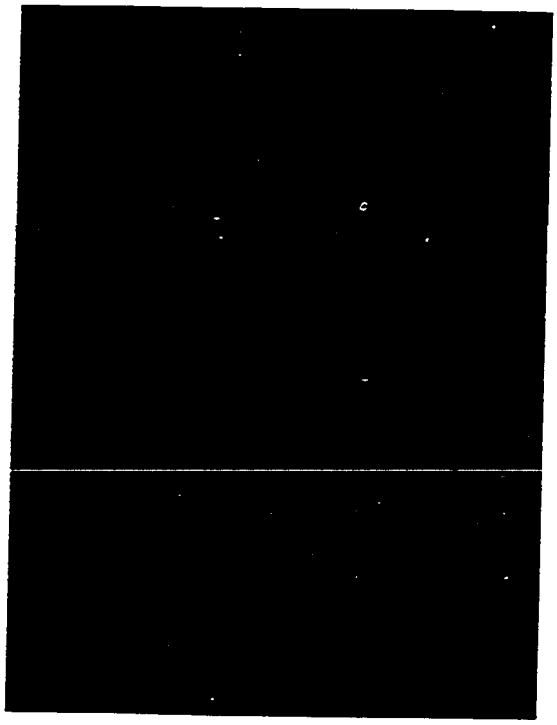

SE#6 (100) Figure 38-P 21.8 $\mu g/cm^2$ 1000x

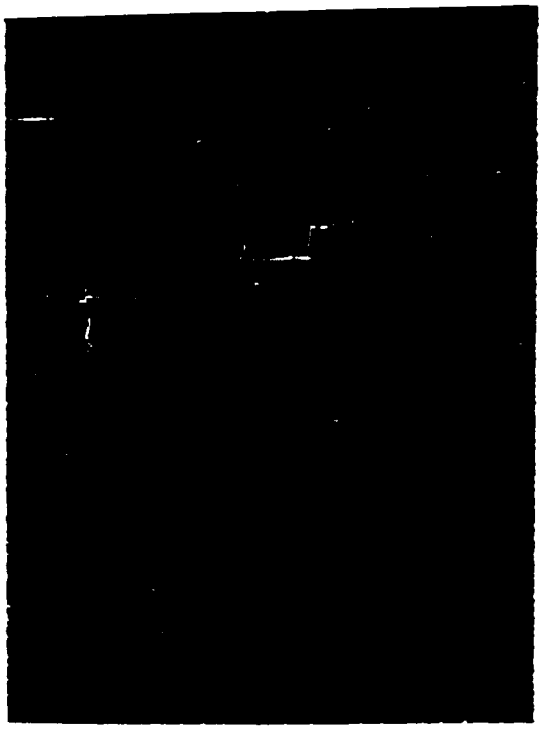

SE#7 (100) Figure 39-P 46.6 $\mu g/cm^2$ 1000x

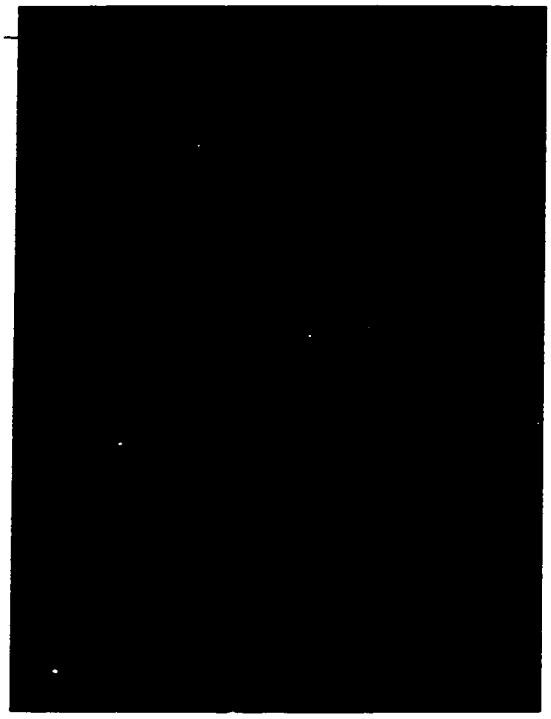

SE#7 (100) Figure 40-P 46.6 $\mu g/cm^2$ 1000x

MICROPHOTOGRAPHS OF OXIDIZED NICKEL SINGLE CRYSTALS

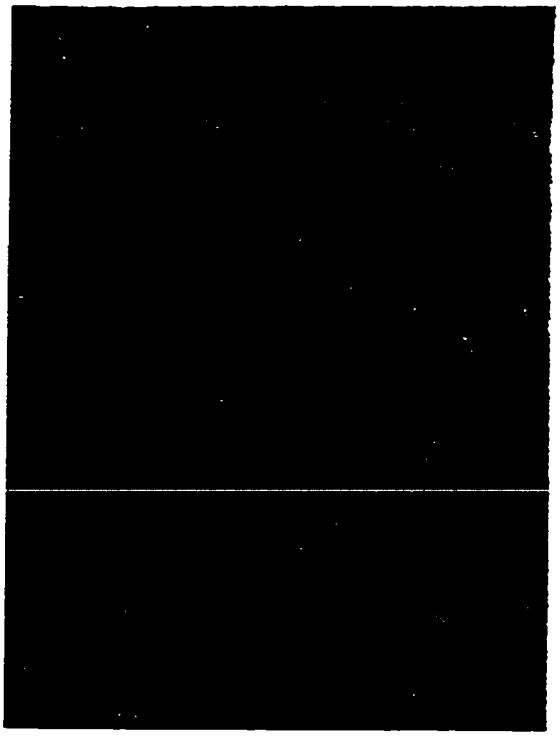

SE#9 (111) Figure 41-P 9.0 $\mu g/cm^2$ 1000x

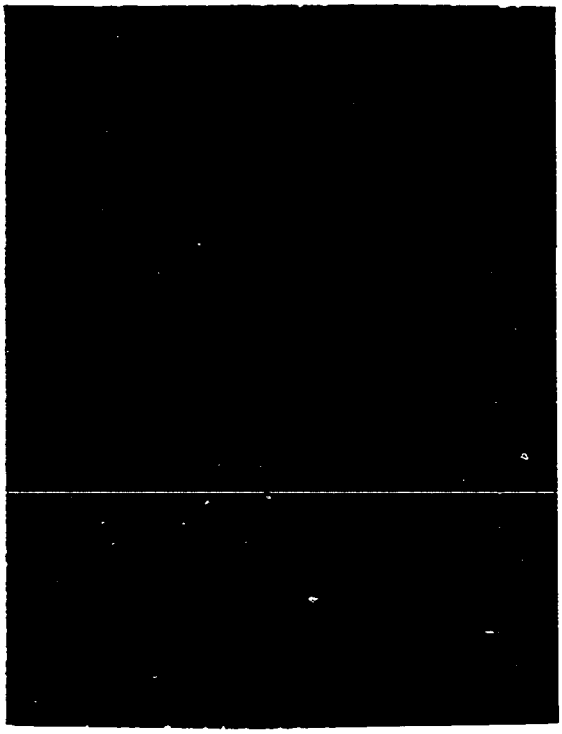

SE#12 (111) Figure 42-P 20.4 $\mu g/cm^2$ 1000x

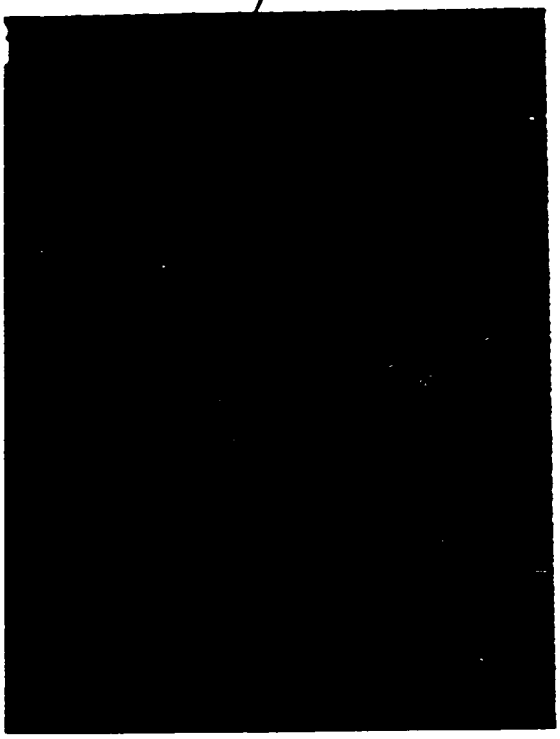

SE#10 (111) Figure 43-P 33.3 $\mu g/cm^2$ 1000x

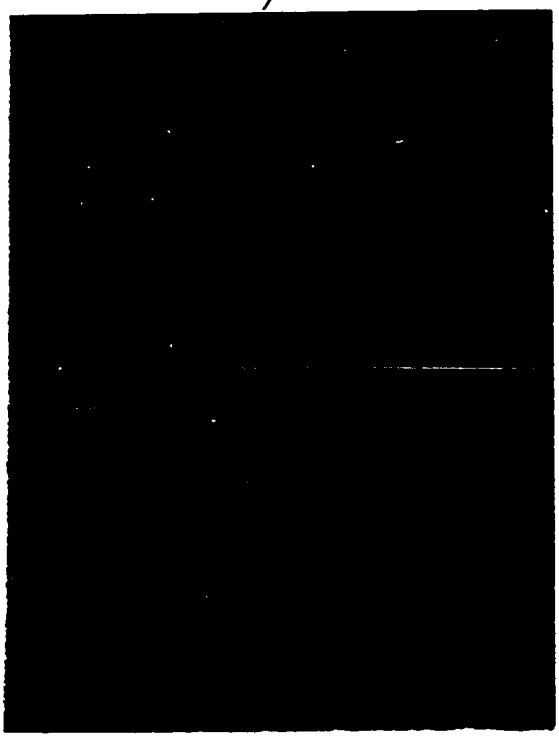

SE#11 (111) Figure 44-P 57.6 $\mu g/cm^2$ 1000x

MICROPHOTOGRAPHS OF OXIDIZED NICKEL SINGLE CRYSTALS

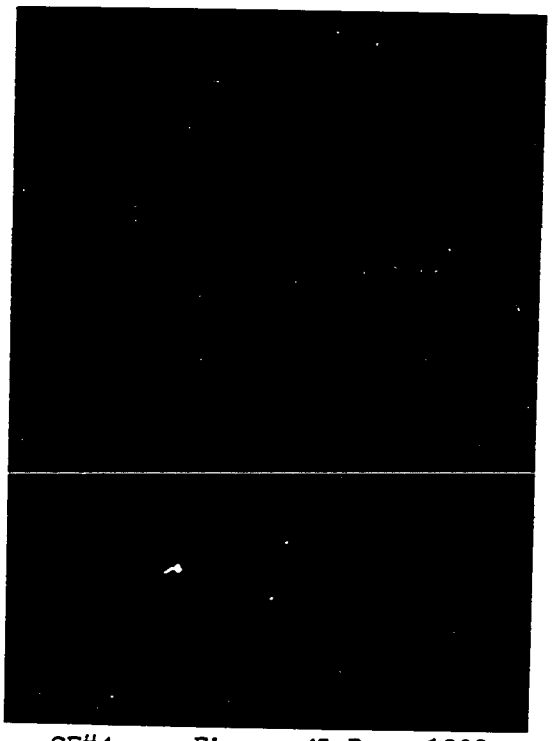

SE#4 (110) Figure 45-P 77.3 $\mu g/cm^2$ 1000x

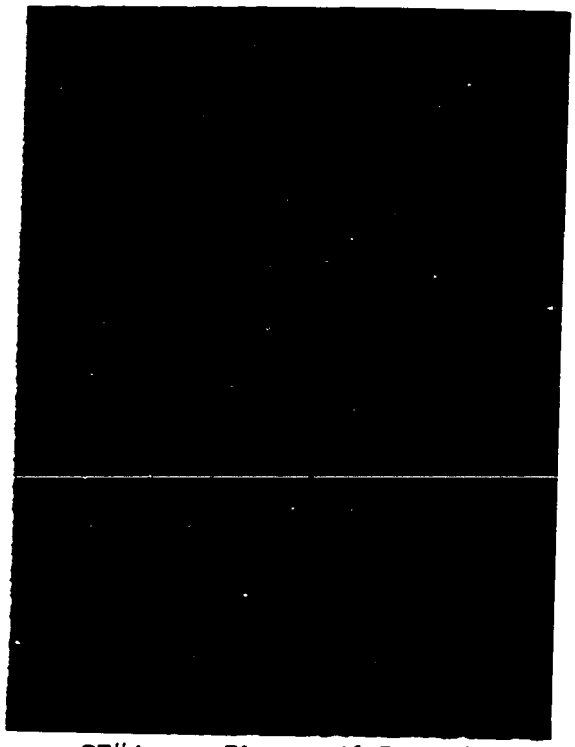

SE#4 (110) Figure 46-P 77.3 $\mu g/cm^2$ 1000x

BACK REFLECTION LAUE X-RAYS OF NICKEL SINGLE CRYSTALS
AFTER OXIDATION AND REDUCTION

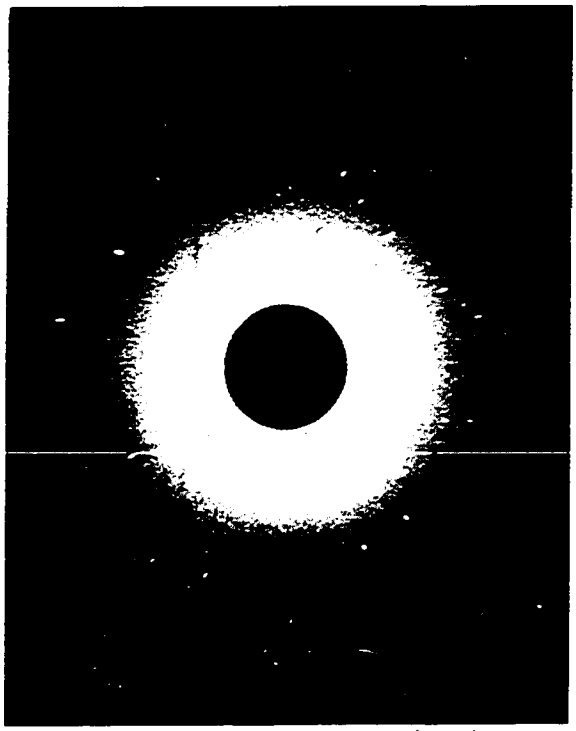

OSC#1 Figure G-I (100)
38.4 $\mu g/cm^2$ Before Reduction

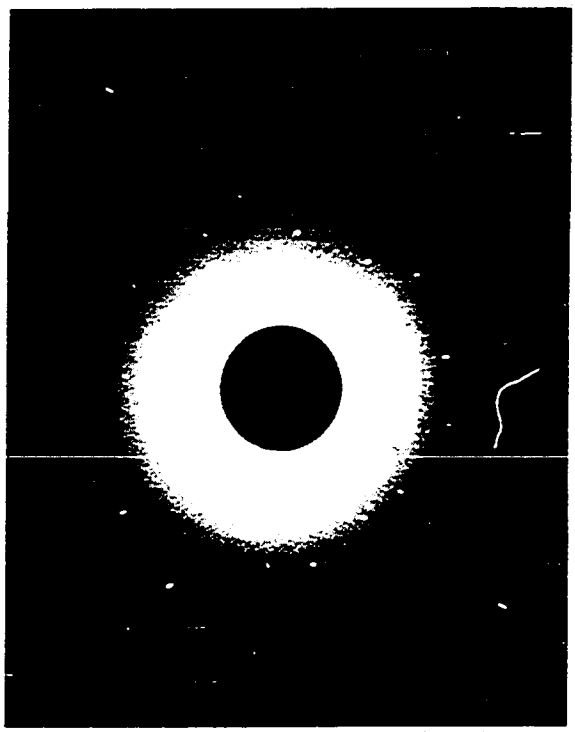

OSC#6 Figure G-II (100)
13.5 $\mu g/cm^2$ Before Reduction

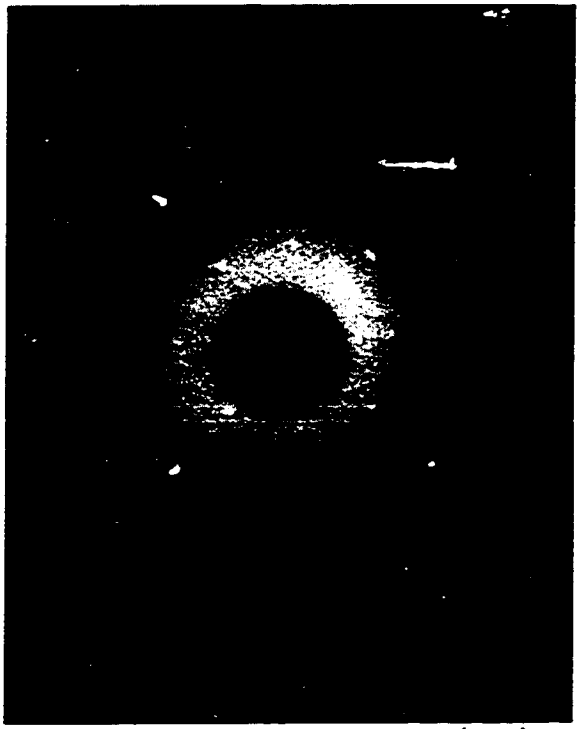

OSC#2 Figure G-III (110)
82.8 $\mu g/cm^2$ Before Reduction

BIBLIOGRAPHY

1. Barnes, B. F., Phys. Rev. 34, 1026 (1929).

2. Bauer, Bartlett, Ong, and Fussell, J. Electrochem. Soc. 110, 185, March 1963.

3. Benard, J., Acta Metallurg. 8, 272 (1960).

4. Burgess, G. K. and P. D. Foote, N. B. S. Tech. News Bull. 11, 41 (1914).

5. Campbell, D. T., "High Temperature Oxidation of Nickel in the Thin Film Region," Ph. D. Thesis, Rice University (December 1960).

6. Cennamo, F., N. Cimento 16, 147 (1939).

7. Chandrasekhar, B. S., The Rev. of Sci. Instrs., p. 368, 1961.

8. Constable, F. H., Proc. Roy. Soc. (A) 115, 570 (1927).

9. Constable, F. H., Proc. Roy. Soc. (A) 117, 376 (1929).

10. Dejong, J. J., "Chemical Polishing of Metals and Alloys," Metalen 9, 2 (1954).

11. Evans, U. R., "Metallic Corrosion, Passivity and Protection," Edward Arnold and Co., London, 1938.

12. Evans, U. R., "The Corrosion and Oxidation of Metals: Scientific Principles and Practical Applications," Edward Arnold Ltd., London, 1960.

13. Fueki, K., and H. Ishibashi, J. Electrochem. Soc., 108, 306, April 1961.

14. Gulbransen, E. A. and K. F. Andrew, J. Electrochem. Soc. 101, 128, March 1954.

15. Hansen, W. E., "Isothermal Oxidation of Nickel in the Thin Film Region at Several Oxygen Pressures," Masters Thesis, Rice University (September 1964).

16. Harris, W. W., F. L. Ball and A. T. Gwathmey, Acta Metallurgica 5, 574 (1957).

17. Hauffe, K. and H. J. Engell, Metall. 6, 285 (1952).

18. Kruger, Jerome, J. Electrochem. Soc. 106, 847, October 1959.

19. Kubaschewski, O. and B. E. Hopkins, "Oxidation of Metals and Alloys," Butterworth's, London, 1962.

20. Kubaschewski, O. and B. E. Hopkins, "Oxidation of Metals and Alloys," Butterworth's, London, 1962, pp. 182-190.

21. Lashof, T. W. and L. B. Macurdy, "Precision Laboratory Standards of Mass and Laboratory Weights," N. B. S. Circular 547, Section 1. (August 20, 1954).

22. MacRae, A. U., "Low Energy Electron Diffraction," Science 139, No. 3553 (February 1963).

23. Martius, U. M., Can. J. of Phys. 33, 466 (1955).

24. Moore, W. J., J. Chem. Phys. 18, 231 (1950).

25. Phillips, W. L., Jr., J. Electrochem. Soc. 110, No. 9, 1014.

26. Rhodin, T. N., Jr., J. Applied Physics 21, 971 (October 1950).

27. Richmond, J. C., and W. N. Harrison, Bull. Am. Ceram. Soc. 39, 668 (1960).

28. Russell, H. W., General Electric Information Series No. R59 ETR-1 (January 23, 1959).

29. Sartell, J. A. and C. H. Li, J. Instit. of Metals 90, 92 (1961-62).

30. Shelton, J. L., "The Total Hemispherical Thermal Emittance of Nickel as a Function of Oxide Thickness in the Temperature Range 400-900°C," Ph. D. Thesis, Rice University, July 1964.

31. Tegart, W. J. McG., "The Electrolytic and Chemical Polishing of Metals," Pergamon, London, etc., 1959.

32. Tibbetts, G. and F. M. Propst, The Rev. of Sci. Instrs., p. 1268, 1963.

33. Uhlig, H. H., J. Pickett, and J. MacNairn, Acta. Met. 7, 111 (1959).

34. Wilms, G. R. and J. B. Wade, Metallurgia, 263, December 1956.

35. "Growth of Single Crystal Materials," a brochure from Division 500, Arthur D. Little, Inc.